

University of Southampton Research Repository

Copyright © and Moral Rights for this thesis and, where applicable, any accompanying data are retained by the author and/or other copyright owners. A copy can be downloaded for personal non-commercial research or study, without prior permission or charge. This thesis and the accompanying data cannot be reproduced or quoted extensively from without first obtaining permission in writing from the copyright holder/s. The content of the thesis and accompanying research data (where applicable) must not be changed in any way or sold commercially in any format or medium without the formal permission of the copyright holder/s.

When referring to this thesis and any accompanying data, full bibliographic details must be given, e.g.

Thesis: Author (Year of Submission) "Full thesis title", University of Southampton, name of the University Faculty or School or Department, PhD Thesis, pagination.

Data: Author (Year) Title. URI [dataset]

University of Southampton

Faculty of Engineering and Physical Sciences

Bioengineering



Nanoparticle-based antibiotic delivery for targeting intracellular bacteria

by

Eleanor Porges

Thesis for the degree of Doctor of Philosophy

December 2020

University of Southampton

Abstract

Faculty of Engineering and Physical Sciences

Bioengineering

Thesis for the degree of Doctor of Philosophy

Nanoparticle-based antibiotic delivery for targeting intracellular bacteria

by

Eleanor Porges

Intracellular bacterial infections, such as *Burkholderia spp*, are notoriously difficult to treat, in part due to poor membrane permeability and intracellular bioavailability of antibiotics. Current treatment options involve high doses of antibiotics for sustained periods of time, therefore contributing to the issues of antibiotic resistance, and potentially causing off-target effects in the patient. In the absence of novel antibiotic compounds, intracellular targeting polymersome (PM)-encapsulated antibiotics may increase the efficacy of existing antibiotics by promoting targeted, infection-specific intracellular uptake in otherwise poorly bioavailable antibiotics. In this study it was hypothesised that PMs composed of widely available polyethylene oxide-polycaprolactone (PEO-PCL) block co-polymers could stably encapsulate antibiotics and release them intracellularly to reduce macrophage infection. PMs were generated via the nanoprecipitation method. Antibiotics doxycycline and rifampicin were retained stably for 14 days within PMs under dialysis. PM-antibiotic preparations did not inhibit the growth of free-living *B. thailandensis*, highlighting their ability to sequester their payloads until at the target intracellular niche. On uptake by murine macrophages, PMs co-localised with intracellular *B. thailandensis* and significantly reduced bacterial burden (by factors of ≈ 100 and 10 for doxycycline and rifampicin-loaded preparations respectively). It was concluded that PMs present a viable approach for the targeted treatment of persistent intracellular *B. thailandensis* infection.

Keywords: intracellular bacteria • antibiotics • drug delivery • bioweapons • nanoparticles • polymersomes

Table of Contents

Table of Contents	i
List of Tables	v
List of Figures	vii
Research Thesis: Declaration of Authorship	xi
Acknowledgements.....	xiii
Abbreviations	xiv
Chapter 1.....	1
1.1 Thesis overview.....	2
1.2 An introduction to bacteria.....	2
1.2.1 Commensals, pathogens, and the human microbiome.....	2
1.2.2 Bacteria as bioweapons	3
1.2.3 Immune response to unwanted bacteria	4
1.3 Antibiotics.....	7
1.3.1 What are they and what do they do?	7
1.3.2 Mechanisms of action	7
1.3.3 Antibiotics and the human microbiome	9
1.3.4 Antibiotic resistance.....	10
1.3.4.1 <i>How resistance arises and is spread</i>	10
1.3.4.2 <i>Mechanisms of resistance</i>	13
1.4 A background to intracellular bacteria.....	15
1.4.1 Intracellular lifestyle.....	15
1.4.2 Challenges associated with treating intracellular infections	18
1.4.3 Intracellular bacteria of interest for this project	20
1.4.3.1 <i>Burkholderia pseudomallei</i>	20
1.4.3.2 <i>Burkholderia thailandensis – model organism for this project</i>	22
1.5 Nanoparticles as intracellular drug delivery systems.....	23
1.5.1 A background to drug delivery systems.....	23
1.5.2 Types of nanoparticle delivery systems	25

Table of Contents

1.5.2.1 Liposomes	25
1.5.2.2 Polymersomes	27
1.5.3 Targeted antibiotic delivery	29
1.5.4 Environmentally responsive antibiotic delivery	30
1.5.5 Characterisation of nanoparticles.....	31
1.5.6 Examples of nanoparticles used to treat bacterial infections	36
1.6 Hypotheses and aims	40
Chapter 2	43
2.1 Materials	44
2.1.1 Polymersome production	44
2.1.2 Antibiotics	44
2.1.3 Bacterial assays	47
2.1.4 Other reagents used	47
2.1.5 Equipment.....	48
2.2 Methods	49
2.2.1 Polymersome production – encapsulation of drug cargo	49
2.2.2 Polymersome characterisation	50
2.2.2.1 PM sizing by dynamic light scattering (DLS)	50
2.2.2.2 PM sizing by transmission electron microscopy (TEM)	51
2.2.2.3 Encapsulation and release using NanoDrop	51
2.2.2.4 Encapsulation and release using high performance liquid chromatography (HPLC)...	52
2.2.2.5 Polymersome sensitivity to pH	53
2.2.2.6 Concentrating polymersomes using ultracentrifugation (UCF)	53
2.2.3 Cellular uptake assays.....	53
2.2.3.1 Cell culture.....	53
2.2.3.2 Preparing a bacterial culture.....	53
2.2.3.3 Polymersome uptake into healthy RAW 264.7 macrophages	54
2.2.3.4 Polymersome uptake into <i>B. thailandensis</i> infected RAW 264.7 macrophages, and their bacterial co-localisation	55
2.2.4 Bacterial inhibition assays.....	56
2.2.4.1 Optical density (OD) assays.....	56

2.2.4.1.1 Free antibiotic and <i>B. thailandensis</i> MIC assay	56
2.2.4.1.2 Old versus new antibiotic efficacy.....	56
2.2.4.1.3 PM-loaded antibiotic and <i>B. thailandensis</i> assay.....	57
2.2.4.1.4 Broken PM-antibiotic and <i>B. thailandensis</i> assay	57
2.2.4.2 PM-loaded antibiotic and intracellular <i>B. thailandensis</i> assay	58
Chapter 3.....	61
3.1 Introduction	62
3.2 Results	66
3.2.1 Antibiotic selection using MIC assays	66
3.2.2 Antibiotic encapsulation and stability tests	67
3.2.2.1 <i>Disrupting the PMs for more accurate payload measurement</i>	67
3.2.2.2 <i>Encapsulation of levofloxacin</i>	69
3.2.2.2.1 Determination of levofloxacin encapsulation using UV-vis analysis.....	69
3.2.2.2.2 Determination of levofloxacin encapsulation using HPLC analysis.....	71
3.2.2.2.3 Levofloxacin retained as dead volume in syringe	73
3.2.2.3 <i>Encapsulation of novobiocin</i>	74
3.2.2.4 <i>Encapsulation of doxycycline</i>	78
3.2.2.5 <i>Encapsulation of rifampicin</i>	81
3.2.2.6 <i>Comparison of novobiocin, doxycycline and rifampicin PMs</i>	85
3.2.3 Concentrating the polymersomes to increase drug concentration.....	86
3.2.4 Sizing of the polymersomes using transmission electron microscopy	90
3.3 Discussion	92
Chapter 4	103
4.1 Introduction	104
4.2 Results.....	108
4.2.1 Polymersome uptake into healthy RAW 264.7 macrophage cells.....	108
4.2.1.1 <i>Epifluorescence</i>	108
4.2.1.2 <i>Real-time polymersome uptake into RAW 264.7 cells</i>	110
4.2.1.3 <i>Coherent anti-Stokes Raman scattering (CARS)</i>	112

Table of Contents

4.2.2 Polymersome uptake into <i>B. thailandensis</i> infected RAW 264.7 cells	116
4.2.2.1 Confocal analysis of uptake.....	116
4.2.2.2 ImageStream analysis of uptake and bacterial co-localisation	118
4.3 Discussion.....	125
Chapter 5	133
5.1 Introduction.....	134
5.2 Results....	138
5.2.1 Comparison of old and new antibiotic efficacies.....	138
5.2.2 PM-antibiotic preparations did not inhibit <i>B. thailandensis</i> growing free in culture.....	140
5.2.3 Broken PM-antibiotic effect on <i>B. thailandensis</i> growth free in culture.....	142
5.2.3.1 PM disruption using DMF.....	142
5.2.3.2 PM disruption using heat	147
5.2.4 PM-antibiotic preparations are able to successfully kill intracellular <i>B. thailandensis</i>	149
5.2.5 PM-antibiotic screening assay	155
5.3 Discussion.....	160
Chapter 6	169
6.1 Summary of the main findings of the study	170
6.2 Relevance of the findings.....	172
6.3 Limitations and indications for future work.....	174
6.4 Conclusions.....	179
List of References.....	181

List of Tables

Table 1	Examples of nanoparticles used for the delivery of antibiotics to intracellular bacterial infections.....	36
Table 2	Overview of the different reagents needed for PM preparation.....	44
Table 3	Overview of the different antibiotics used for bacterial assays and PM production.....	44
Table 4	Overview of the physicochemical properties of the antibiotic used within this project.....	46
Table 5	The different materials and reagents used for various bacterial assays.....	47
Table 6	Other chemical reagents used over the course of the project.....	47
Table 7	Equipment used within the project.....	48
Table 8	Sizes and Pdl values for PM-novobiocin and control preparations.....	76
Table 9	Sizes and Pdl values for PM-doxycycline measured over a 14-day period.....	81
Table 10	Sizes and Pdl values for PM-rifampicin measured over a 14-day period.....	84
Table 11	Estimations of the expected local antibiotic concentration within PM-doxycycline and PM-rifampicin formulations.....	89
Table 12	Quantification of PM and <i>B. thailandensis</i> co-localisation within RAW 264.7 macrophage cells. Data is taken from the bacteria and PM exposed cell populations at both 3 and 21-hour incubations.....	118

List of Figures

Figure 1.1	An overview of the immune response in vertebrates.....	4
Figure 1.2	Macrophages are capable of degrading invading pathogens by mechanisms such as phagocytosis.....	5
Figure 1.3	A summary of the adaptive immune response.....	6
Figure 1.4	An overview of a small number of cellular sites which antibiotics target.....	8
Figure 1.5	An overview of the different mechanisms of HGT.....	12
Figure 1.6	A simplified illustration of the differences between the Gram-negative and Gram-positive cell walls of bacteria.....	13
Figure 1.7	An overview of some of the different mechanisms of resistance coded for by bacteria.....	14
Figure 1.8	An illustration of how intracellular bacteria can spread from cell to cell via actin polymerisation at their poles.....	18
Figure 1.9	An illustration of the liposomal class of nanoparticle drug delivery systems.....	26
Figure 1.10	Overview of the principles behind PM drug delivery systems.....	28
Figure 1.11	Schematic of the experimental setup of an HPLC machine.....	32
Figure 1.12	Schematic of the imaging flow cytometry setup.....	34
Figure 1.13	An illustration of chemical linkers being used to attach ligands to PMs, aiding their specific targeting.....	39
Figure 2.1	An overview of the PM production process.....	50
Figure 2.2	PM-antibiotic release assay schematic.....	52
Figure 2.3	An illustration of the bacterial OD assay setup.....	57
Figure 2.4	A step-by-step illustration of the intracellular killing assays.....	59
Figure 3.1	MIC assay to test free antibiotic efficacy on <i>B. thailandensis</i> free in culture medium.....	66
Figure 3.2	Assessment of PM breaking using altered pH.....	68
Figure 3.3	Assessment of PM disruption using different organic solvents.....	69
Figure 3.4	Levofloxacin absorption spectra and standard curve.....	70
Figure 3.5	Absorption measurements of levofloxacin loaded PMs.....	71
Figure 3.6	The standard curve for levofloxacin generated using HPLC.....	72
Figure 3.7	The release of levofloxacin from loaded PMs compared to the free drug control.....	73
Figure 3.8	Dead volume within syringe	74
Figure 3.9	Novobiocin absorption spectra and standard curve.....	74
Figure 3.10	Encapsulation and size characterisation of PM-novobiocin preparations.....	75
Figure 3.11	Optimal loading of novobiocin into PMs.....	77
Figure 3.12	PM-novobiocin stability over 14 days.....	78
Figure 3.13	Doxycycline absorption spectra and standard curve.....	79
Figure 3.14	Optimal loading of doxycycline into PMs.....	80

List of Figures

Figure 3.15	PM-doxycycline stability over 14 days.....	80
Figure 3.16	Rifampicin absorption spectra and standard curve.....	81
Figure 3.17	Optimal loading of rifampicin into PMs.....	83
Figure 3.18	PM-rifampicin stability over 14 days.....	84
Figure 3.19	Comparison of PM-antibiotic preparations.....	86
Figure 3.20	A schematic of the bulk PM solution, versus the PM pellet as a local concentration assessment.....	87
Figure 3.21	Investigation into UCF speeds on PMs, and their subsequent sizes.....	88
Figure 3.22	Bulk versus local PM-antibiotic concentrations.....	90
Figure 3.23	Size characterisation of empty PMs using TEM.....	91
Figure 4.1	Preparation of Dil-loaded nanoparticles.....	108
Figure 4.2	Epifluorescent images showing PM uptake into RAW 264.7 cells after a 4-hour incubation.....	109
Figure 4.3	Stills from a time-lapse video of PM-Dil uptake into RAW 264.7 macrophage cells	110
Figure 4.4	Co-localisation between PM-Dil nanoparticles and lysosomes.....	111
Figure 4.5	CARS image processing stages.....	113
Figure 4.6	CARS and TPF images alongside quantitative image analysis data.....	115
Figure 4.7	Preparation of PM-DiD-loaded nanoparticles.....	116
Figure 4.8	Confocal microscope image of PM-DiD uptake into <i>B. thailandensis</i> infected RAW 264.7 macrophage cells.....	117
Figure 4.9	A breakdown of the gating process used to select cells displaying co-localisation, and a visualisation of the detected fluorophores.....	119
Figure 4.10	Imaging flow cytometry gating for PM positive cells.....	121
Figure 4.11	Assessment of PM uptake into RAW 264.7 macrophage cells.....	122
Figure 4.12	The proportion of cells containing intracellular bacteria from the ImageStream assay.....	123
Figure 4.13	Co-localisation of <i>B. thailandensis</i> and PMs.....	124
Figure 5.1	Comparison of doxycycline and rifampicin efficacies at day 0 versus day 7.....	139
Figure 5.2	Effect of PM-antibiotic on free growing <i>B. thailandensis</i>	141
Figure 5.3	Absorbance spectra of broken PM-rifampicin nanoparticles after DMF disruption.....	143
Figure 5.4	Effect of disrupted PM-rifampicin nanoparticles on the growth of <i>B. thailandensis</i>	144
Figure 5.5	Effect of disrupted PM-doxycycline nanoparticles on the growth of <i>B. thailandensis</i>	146
Figure 5.6	Effect of breaking PM-doxycycline nanoparticles, using 98°C heat, on the growth of <i>B. thailandensis</i>	148

Figure 5.7	Effect of breaking PM-doxycycline nanoparticles, using 65°C heat, on the growth of <i>B. thailandensis</i>	149
Figure 5.8	Effect of PM-doxycycline on intracellular <i>B. thailandensis</i> at 3 and 21 hours.....	151
Figure 5.9	Intraassay variability of PM-doxycycline nanoparticles on intracellular <i>B. thailandensis</i>	153
Figure 5.10	Comparison of PM-antibiotic preparations and their equivalent free drug concentrations on the efficacy against intracellular <i>B. thailandensis</i>	155
Figure 5.11	DLS sizing data of the new PM-antibiotic preparations.....	156
Figure 5.12	MIC for kanamycin acting on free growing <i>B. thailandensis</i>	157
Figure 5.13	Effect of PM-kanamycin nanoparticles on intracellular <i>B. thailandensis</i>	158
Figure 5.14	Effect of encapsulated β -lactam or aminoglycoside antibiotics on intracellular <i>B. thailandensis</i>	159
Figure 6.1	Polymersomes for intracellular antibiotic delivery.....	179

List of Figures

Research Thesis: Declaration of Authorship

Print name:

ELEANOR PORGES

Title of thesis:

Nanoparticle-
based antibiotic
delivery for
targeting
intracellular
bacteria

I declare that this thesis and the work presented in it are my own and has been generated by me as the result of my own original research.

I confirm that:

1. This work was done wholly or mainly while in candidature for a research degree at this University;
2. Where any part of this thesis has previously been submitted for a degree or any other qualification at this University or any other institution, this has been clearly stated;
3. Where I have consulted the published work of others, this is always clearly attributed;
4. Where I have quoted from the work of others, the source is always given. With the exception of such quotations, this thesis is entirely my own work;
5. I have acknowledged all main sources of help;
6. Where the thesis is based on work done by myself jointly with others, I have made clear exactly what was done by others and what I have contributed myself;
7. None of this work has been published before submission

Signature:

Date:

Acknowledgements

I would like to firstly thank my wonderful supervisors Dr Nicholas Evans, Dr Tracey Newman, and Dr Caroline Rowland for their support and guidance throughout this project. They have all continually encouraged and inspired me during the last four years, and I will be eternally grateful for their help and advice. Thank you to Nick in particular for all of the hours spent providing thesis and presentation feedback over the years, and for reassuring me when things were tough - you have helped increase my confidence as a scientist enormously.

Thank you to all of the team at Defence Science and Technology Laboratory (DSTL). Being able to have the opportunity to work at such a fantastic organisation has been a once in a lifetime experience and I have loved every moment. Thank you to Dr Dominic Jenner for all of his imaging flow cytometry wisdom, and to Adam Taylor for all of the initial lab training and for being a good friend throughout. Thank you to John for all of the HPLC help, and to Jo, Natalie, James, and Angela for always making me feel so welcome and helping me whenever I needed it.

I would also like to thank the teams at Bone and Joint, and the Highfield Nanoneuroscience group, in particular Alan, Antonio, Jon, Kate, Rachel, Leafy, Connor, Grace, and Edo. Working with all of you has been the biggest blessing of my life. You are all the most incredible people and truly the highlight of this PhD journey. I am so grateful for everything we have been able to experience together – TERMIS was one of the greatest weeks of my life! Thank you for all of the morale boosting talks when things were hard, for all of the nights out celebrating our team successes, and for the friendship which I hope lasts a lifetime. A special thank you to Anna. I would be utterly lost without you and the endless phone calls we have – you are one in a million.

I am also extremely thankful to my new team at Public Health England for welcoming me into their group and supporting me during the final few weeks of writing. Thank you for being patient whilst I was juggling both this and learning lots about TB! I am overjoyed to be working with you all.

Finally, the biggest thanks go to my family: Mum, Dad, Kate, Nanny and Gramps. You all know you are my backbone and I am the luckiest person in the world to have you all. Thank you for all you do for me. Thank you, Dad, for all the help with stats and hard questions.

Abbreviations

AAD	Antibiotic associated diarrhoeas
AMR	Antimicrobial resistance
ANOVA	Analysis of variance
CARS	Coherent anti-Stokes Raman scattering
CCD	Charge coupled device
CFU	Colony forming units
DiD	1,1'-Dioctadecyl-3,3,3',3'-Tetramethylindodicarbocyanine, 4-chlorobenzenesulfonate salt
Dil	1,1'-Dioctadecyl-3,3,3',3'-Tetramethylindodicarbocyanine perchlorate ('Dil'; DiIC ₁₈ (3))
DLS	Dynamic light scattering
DMEM	Dulbecco's modified Eagle's medium
DMF	Dimethylformamide
DNA	Deoxyribonucleic acid
DPPC	Dipalmitoylphosphatidylcholine
DSPE	1,2-distearoyl-sn-glycero-3-phosphoethanolamine
DSTL	Defence Science and Technology Laboratory
FACS	Fluorescence activated cell sorter
FBS	Fetal bovine serum
FDA	Food and Drug Administration
GFP	Green fluorescent protein
HEMA	Hydroxyethyl methacrylate
HGT	Horizontal gene transfer
HIV	Human immunodeficiency virus
HPLC	High performance liquid chromatography
IFC	Imaging flow cytometry
IR	Infrared
LAM	Lipoarabinomannan
LM	Liposome
MDR	Multidrug resistance
MIC	Minimum inhibitory concentration
MOI	Multiplicity of infection
MRSA	Methicillin-resistant <i>Staphylococcus aureus</i>
MW	Molecular weight
MWCO	Molecular weight cut-off

NMR	Nuclear magnetic resonance
NPV	Net present value
NTA	Nanoparticle tracking analysis
OD	Optical density
OPO	Optical parametric oscillator
PAMP	Pathogen-associated molecular pattern
PBS	Phosphate buffered saline
PdI	Polydispersity index
PDMS	Poly(dimethylsiloxane)
PDPA	Poly(2-(diisopropylamino) ethyl methacrylate)
PEE	Poly(ethyleneethylene)
PEG	Poly(ethylene glycol)
PEO-PCL	Poly(ethylene oxide)-b-poly(caprolactone)
PFA	Paraformaldehyde
PI3P	Phosphatidylinositol 3-phosphate
PLGA	Poly(d-L-lactide-co-glycolide)
PLH	Poly(L-histidine)
PM	Polymersome
PMOXA	Poly(2-methyloxazoline)
PMPC	Poly(2-(methacryloyloxy) ethyl phosphorylcholine)
PNIPAM	Poly(N-isopropylacrylamide)
PRR	Pattern recognition receptor
RES	Reticuloendothelial system
RNA	Ribonucleic acid
SD	Standard deviation
TAT	Trans-activator of transcription
TDI	Time delay integration
TEM	Transmission electron microscopy
TPF	Two-photon fluorescence
UCF	Ultracentrifugation
UV-vis	Ultraviolet-visible

Abbreviations

Chapter 1: Introduction

Chapter 1: Introduction

1.1 Thesis overview

The aim of this thesis is to develop a method to deliver antibiotics to intracellular locations, using polymersome (PM) nanoparticles, in order to improve the treatment of persistent bacterial infections. Intracellular infections are challenging to treat for multiple reasons including poor intracellular antibiotic bioavailability; antibiotic resistance; and the side effects associated with the long and sustained medication courses currently used for treatment. This project aimed to encapsulate a range of antibiotics within PMs, and subsequently show their ability to be taken up by infected cells and inhibit bacterial growth once at this target location. Therefore, it is first necessary to introduce bacteria and their relevance to human health, before reviewing the literature on antibiotics and nanoparticles currently being used for drug delivery purposes.

1.2 An introduction to bacteria

1.2.1 Commensals, pathogens, and the human microbiome

Bacteria are single-celled microorganisms which are adept at surviving in every environment found on Earth, including the human body. Recent work by Sender *et al.* (2016) demonstrated that a reference human, containing approximately 30 trillion human cells, was found to play host to approximately 38 trillion bacterial cells, a ratio of around 1:1. This work highlights the large number of bacteria the body has to cope with. The human microbiome encompasses all microorganisms living inside the body, including the different bacterial species.

Harmful bacteria, those which readily cause illness and disease, are called obligate pathogens. Some have an extremely fast doubling time, for example *Escherichia coli* which doubles in as little as 20 minutes (Fossum *et al.*, 2007), whereas others take longer, for example *Mycobacterium tuberculosis* which has a doubling time of 24 hours (Ginsberg and Spigelman, 2007). These replication rates can impact the ways in which bacteria cause illness amongst people. For example, in the case of *E. coli* the fast replication time means the pathogenic bacteria can quickly (usually within a matter of days) cause illness (Lim *et al.*, 2010), whereas *M. tuberculosis* causes a much more slowly-developing illness in comparison, with the active bacteria causing detectable symptoms after months (Heemskerk *et al.*, 2015) or even years (Flynn and Chan, 2001).

However, there are also bacterial species which do not usually cause harm to their hosts. These are known as commensals, and they often have beneficial effects. An example of such a species is *Bifidobacterium*, a coloniser of the gut. This bacterium produces vitamins that the host can use, and can create a barrier preventing pathogenic bacteria from attaching to and colonising the gut surface (Picard *et al.*, 2005). Despite this, any bacteria, when given the opportunity, may cause an infection. Therefore, commensals are sometimes also referred to as being opportunistic, or facultative, pathogens – bacteria which will only cause illness in the host when the opportunity presents itself, for example through weakened host immune defences. *Staphylococcus epidermidis* is an example of such a species, as it is part of the human body's normal microbiome and naturally colonises human epithelial cells without causing harm. However, it commonly causes unpleasant infections involving medical device implants, when these become contaminated with the bacteria from the skin of the patient, or health care worker (Otto, 2009).

Additionally, aside from the large number of bacterial species within the body, there are also species that live externally in the environment which may also cause infection. Bacteria may enter our bodies through a variety of routes, for example: dirty drinking water, cuts in the skin, and inhalation, to name just a few. There is the potential for any of these situations to cause an infection, and so this highlights the constant battle our bodies face against bacteria. This being said, the balance between commensals and pathogens within the microbiome is important to ensure a healthy host, and is also fragile – numerous things can alter the composition and disrupt the balance, including antibiotics, which will be discussed in section 1.3.3.

1.2.2 Bacteria as bioweapons

In some situations, certain bacterial species can be used by humans in a detrimental way. If a species possesses the correct characteristics, it can allow for them to be cultured and used for biowarfare purposes to inflict harm on others. Some of the characteristics a bacterial species must have in order to be considered a biological threat consist of the following: the ability to be infectious even at low doses; rapid growth and short incubation periods; the ability to be mass produced; stability after release into populations; and little or no existing immunity within the population to the bacterium (Beeching *et al.*, 2002).

Due to the ease of access and widespread locations of many dangerous pathogens, for example soils, there are concerns for their use in bioterrorism. For example, *Bacillus anthracis*, the species behind the infection anthrax, is a soil-borne organism which can be found across the globe. It grows well, and quickly, on standard culture media, and it is thought that relatively little expertise

is required to generate an aerosolised, and therefore easily disseminated, form (Christian, 2013). For these reasons, there is a need for defences against these types of organisms. Whether for soldiers visiting countries where these may have been used, or for civilians caught up in on-going wars – the need for a treatment is potentially great.

1.2.3 Immune response to unwanted bacteria

Given the vast number of bacteria present within the body, and the huge array of bacterial species outside the body, it is inevitable that occasionally humans will become infected, and will need to mount an immune response to the infection. There are two arms of the immune response: the innate response, and the adaptive response (Figure 1.1).

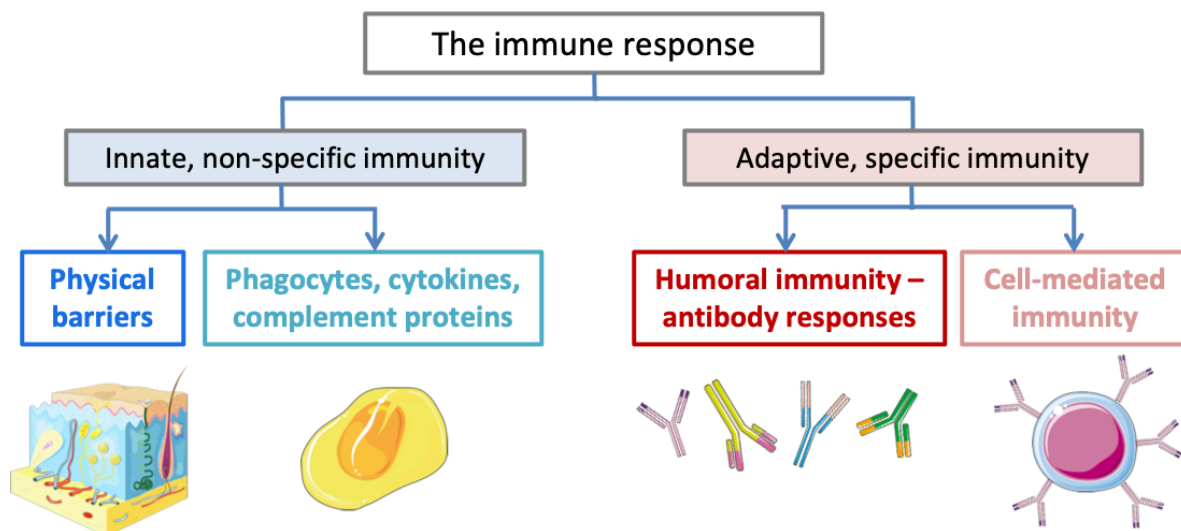


Figure 1.1 – An overview of the immune response in vertebrates. The innate response is the non-specific immunity which can act rapidly against invading pathogens, whereas the adaptive response is specific to certain pathogens, and takes much longer to activate upon first exposure to the pathogen. The adaptive response further branches into humoral immunity which involves antibody production, and cell-mediated immunity.

The first line of defence to an infection involves physical barriers. These can include anything that creates a block to the infection, such as the human body’s outer layer of skin. Chemical secretions from the body also play a role, for example the low pH of stomach acid, which is harsh enough to kill many types of pathogen. In terms of the immune system, the innate immune response tackles infection relatively quickly. It is composed of numerous types of cells and molecules, for example neutrophils, macrophages, cytokines, and proteins of the complement system, which work together to coordinate a response to protect against infection. The innate response is able to act quickly as it targets elements which are common to many types of invading pathogens, but not

found in host cells. These elements are called pathogen-associated molecular patterns (PAMPs) and are recognised by pattern recognition receptors (PRRs) on the surface of neutrophils and other phagocytic cells, such as macrophages. Once recognised as foreign, phagocytic cells will engulf the bacteria and process it, which in most cases will lead to its death (Figure 1.2). Once activated, cells of the innate immune system can also stimulate the adaptive immune response by producing signals, such as cytokines and chemokines, which will activate cells such as the T lymphocytes (Janeway *et al.*, 2001).

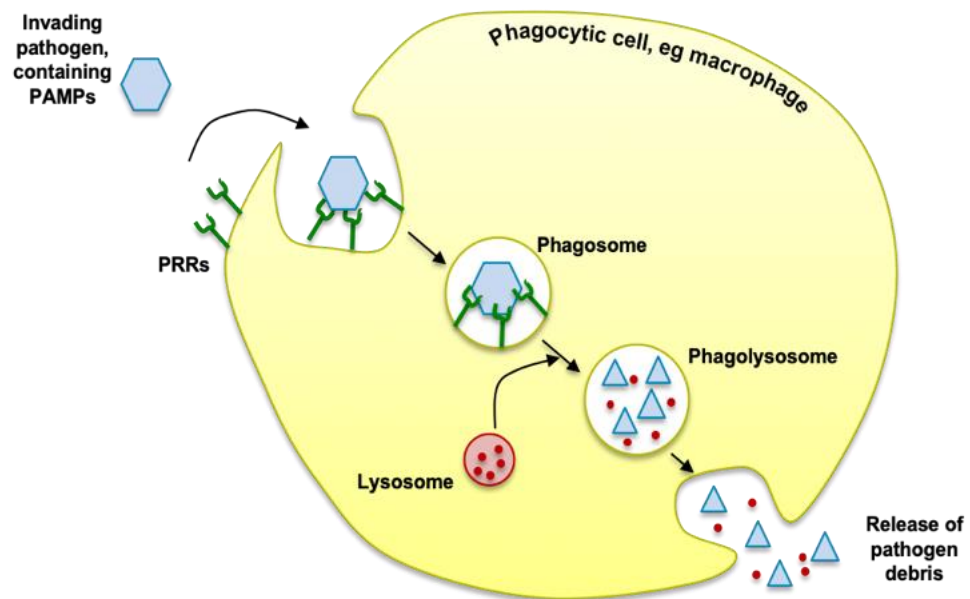


Figure 1.2 – Macrophages are capable of degrading invading pathogens by mechanisms such as phagocytosis. Phagocytic cells will recognise specific regions of the invading pathogen, called PAMPs, and will bind to these via PRRs. The pathogen will be taken up into a vesicle (phagosome) by endocytosis, and this will then fuse with a lysosome to form a phagolysosome. The lysosome contains hydrolytic enzymes which will break down and degrade the pathogen. This debris will then be released from the cell via exocytosis.

Whilst the innate system can act rapidly and recognise a wide range of pathogens in a non-specific manner, the adaptive response is specific for individual pathogenic species, and so can take longer to act if the pathogen has not been encountered by the body previously. The adaptive response is comprised of both the cell-mediated response, and the humoral response, which involves antibodies (Figure 1.3). Antibodies are synthesised, exclusively, by the B cells (Alberts *et al.*, 2002), and have specificity unique antigens. When stimulated by an antigen, or by the helper T cells, the B cells with correct specificity to the antigen will proliferate, so that multiple cells with the correct antibody are made. Some of these may then differentiate into effector B cells, the plasma cells. These are capable of secreting antibodies which go on to bind the infective agent independent of the B cell. Other B cells may differentiate into memory B cells. These are long-lived and can quickly produce antibodies to the same antigen, if encountered

again within the lifetime. This concept of immunological memory is vital to ensuring a strong, and fast, secondary immune response when the same antigen is encountered again (Reece *et al.*, 2011).

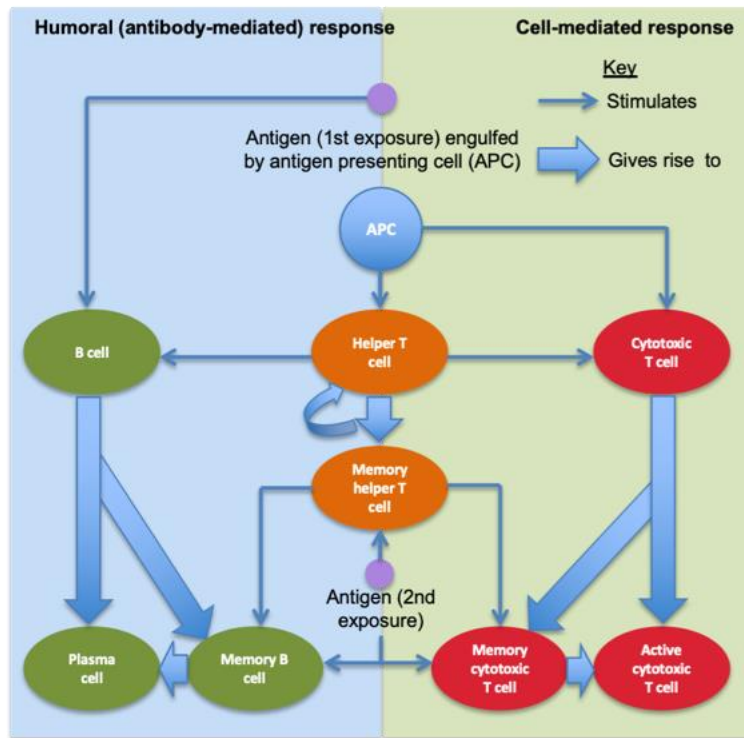


Figure 1.3 – A summary of the adaptive immune response. Includes both the humoral, antibody-mediated response, and the cell-mediated response. Figure adapted from Reece *et al.* (2011).

One interesting point is how the immune system and commensal bacteria within our bodies have built a symbiotic relationship with one another, and how the immune system does not attack these commensals. This is a subject which has remained largely unanswered, but recent work is beginning to shed some light. In short, the microorganisms present at birth, gained from the mother’s own commensal flora, help to calibrate/tune the immune system. If a newborn is not exposed to these upon birth, for example if born by caesarean, the immune system is not directed to mature in a way that tolerates commensals. This may lead to diseases such as inflammatory bowel disease, and susceptibility to allergies - conditions where the immune system mounts an inappropriate response (Cash and Hooper, 2005).

1.3 Antibiotics

1.3.1 What are they and what do they do?

The immune system constantly defends against pathogens, and efficiently keeps our bodies safe from infection for the most part. However, sometimes the immune system is unable to kill the bacteria, and as a result humans have developed medicines, specifically antibiotics, to help fight these bacterial infections. Antibiotics are compounds which can kill or inhibit bacteria. They are made naturally in the environment by microbes, however can also be synthetically generated in laboratories. As long as they are functional against bacteria the term antibiotic can be used (Davies and Davies, 2010). The benefits of antibiotics are enormous. Infections now perceived as nothing more than a minor inconvenience, could once, in a time before antibiotics, have proven fatal for a person. Indeed, in 1920 the average life expectancy of a person was around 54 years old, versus nearly 80 years old in 2015 – this will be in part due to the availability of antibiotics (Ventola, 2015).

1.3.2 Mechanisms of action

A key feature of antibiotics is that in general they are able to target bacterial cells without damaging host cells from the body. They achieve this by either targeting elements of the bacterial cell which are not present in the host, or by targeting elements which are more sensitive in bacterial cells. Different antibiotics have different modes of action, but they all work overall in one of two ways, by being either bacteriostatic or bactericidal. Bacteriostatic antibiotics inhibit bacterial cell growth, so will only affect bacteria which are dividing and multiplying. Alternatively, bactericidal antibiotics induce bacterial cell death (Kohanski *et al.*, 2010).

Figure 1.4 shows a summary, however by no means a complete list, of some of the different ways antibiotics can be used to selectively target bacterial cells. One of the most desirable targets for antibiotics is the bacterial cell wall, as it is absent in eukaryotic (and therefore human) cells. The cell wall is made up of peptidoglycan, which protects bacteria from the potential osmotic stresses of their environments; without it most cells cannot survive. Transpeptidase enzymes are responsible for the generation of new cell wall, and so are a target for a number of antibiotic groups, including the β -lactams. These antibiotics irreversibly bind to the enzymes, blocking their function, resulting in the inability to generate new cell wall and therefore for the bacterial cells to grow and divide.

Antibiotics may also target bacterial transcription, through classes of antibiotics such as the rifamycins. These work by binding to the ribonucleic acid (RNA) polymerase enzyme - inhibiting its function. This enzyme carries out RNA synthesis, leading to the production of RNA transcripts which code for protein (Campbell *et al.*, 2001). Despite the effectiveness of this mechanism, antibiotics targeting the RNA polymerase enzymes of bacteria should be used with caution due to the homology found with eukaryotic RNA polymerases. However, enough structural variation exists for the drugs to work. Hence, this is an example of a mechanism by which antibiotics target cellular machinery present in both host and bacteria, but with its effects being much more potent in the latter.

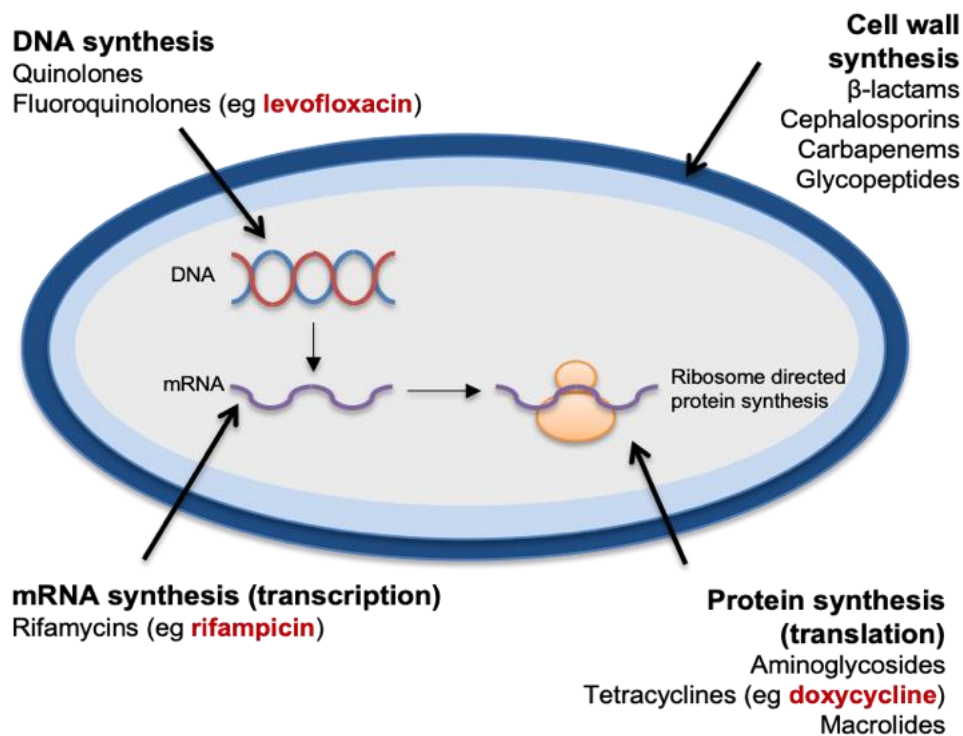


Figure 1.4 – An overview of a small number of cellular sites which antibiotics target. Different antibiotics work in different ways, targeting different components of the bacterial cell. The following list gives examples, but there are many others which exist and work in similar ways. The β -lactams prevent new cell wall forming leaving bacteria vulnerable to osmotic stress; quinolones act upon DNA gyrase to prevent the synthesis of new DNA, rendering the cell unable to replicate and divide; transcription may also be targeted, for example by rifampicin, which binds to and inhibits a subunit of RNA polymerase rendering it unable to synthesise new mRNA; protein synthesis may also be halted by classes of antibiotics such as the aminoglycosides, which work by binding to the ribosome and inhibiting its function. Figure adapted from Brown (2015).

Deoxyribonucleic acid (DNA) gyrase is the bacterial enzyme responsible for introducing negative supercoils into the DNA, and regulating the level of supercoiling throughout essential cell processes such as DNA synthesis, replication, and transcription. The process of introducing a negative supercoil involves cleaving the DNA and then later resealing. Antibiotics such as the quinolones and fluoroquinolones function by binding to DNA gyrase and preventing the resealing of the DNA strands after the cleavage has been performed. This ultimately leads to the DNA replication machinery stalling, resulting in a blockage of DNA synthesis. This is what causes the cells to die (Kohanski *et al.*, 2010).

1.3.3 Antibiotics and the human microbiome

Although antibiotics target bacterial cells, they can still indirectly cause damage to the host by disrupting the balance between pathogenic and commensal bacteria. Although this topic is complex and beyond the scope of this thesis a general description is useful to understand the limitations of antibiotics in human disease.

Commensal microorganisms offer the host a range of benefits – discussed previously in section 1.2.1. However, regardless of whether they are beneficial or not, many of these commensals are bacteria, and will therefore possess the same targets for antibiotics as pathogens. The importance of having a healthy microbiome can be seen even from the point of birth. Babies born naturally are exposed to the birth canal microflora which contains, for example, the *Lactobacillus* species – bacteria known to be present as commensals in a healthy gut flora. In contrast, babies born by caesarean are initially exposed to skin resident bacteria, from the mother's skin, including species such as *Staphylococcus*. Although this may not necessarily cause infection, it may alter the make-up of the microflora of the children born by caesarean, compared to by natural birth. Furthermore, antibiotics are commonly administered to the mothers during a caesarean section birth, and this is likely to cause an imbalance in the microflora of these babies (Langdon *et al.*, 2016). Indeed, the gut microflora of babies born by caesarean has been associated with increased risk of immunological disorders such as asthma (Roudit *et al.*, 2009), type 1 diabetes (Bonifacio *et al.*, 2011), and even more worryingly with methicillin-resistant *Staphylococcus aureus* (MRSA) infections, in which up to 82% of reported cases in newborns stem from babies born by caesarean versus from natural births (Centers for Disease Control and Prevention, 2006).

These effects are not limited to newborn babies. There is evidence that many antibiotics alter the adult gut microbial composition, some even permanently (Dethlefsen and Relman, 2011). For example, ciprofloxacin, a fluoroquinolone, lowers the general bacterial diversity of the gut, and

also lowers the numbers of bacterial species which produce the short-chain fatty acids which the host can exploit - indicating the indirect negative effect antibiotics can have on the host (Langdon *et al.*, 2016). Antibiotics can also eliminate commensal bacteria from colonising body regions, such as the gut, which allows pathogenic bacteria to take over and colonise these surfaces, leaving the host potentially susceptible to secondary infections, for example antibiotic associated diarrhoeas (AAD) (Francino, 2016). The use of probiotics to alleviate some of the side effects caused by antibiotics is a possible approach, as they may help to maintain a healthy microbiome and prevent symptoms such as AAD (Angelakis *et al.*, 2013). Furthermore, antibiotics create a selection pressure for resistant bacteria. Bacteria which have survived the dose of antibiotics will multiply and pass on their resistance genes, in turn increasing the number of bacteria possessing such genes (Zaman *et al.*, 2017). All of the above reasons suggest that the ultimate goal for antibiotic use should be to use them for the shortest duration at the lowest efficacious dose.

1.3.4 Antibiotic resistance

1.3.4.1 How resistance arises and is spread

Before the discovery of antibiotics, and their use in the clinic, infectious diseases resulted in the deaths of up to 25% of England's population in the early 1900s. By 1928, Alexander Fleming had discovered the well-known β -lactam antibiotic, penicillin, and by 1945 this was being mass produced and distributed for medical use. As a result, by the mid-1900s the number of deaths in England due to infectious diseases had dropped to less than 1% (Aminov, 2010). However, bacteria are able to develop resistance to antibiotics with relative speed, and in the case of penicillin as early as the 1950s resistance was so prominent that other antibiotic alternatives needed to be developed. As it stands, resistance has been observed against nearly every antibiotic available in use today (Ventola, 2015). Global deaths as a result of multidrug resistance are rising, and as of 2019 it was thought that over 33,000 deaths yearly in Europe were a direct consequence of antibiotic resistant infections (da Cunha *et al.*, 2019). The World Health Organisation has warned that without antibiotics there will be increased incidences of infections, and furthermore that people may die as a result of seemingly minor injuries (Zaman *et al.*, 2017).

The issue of antimicrobial resistance (AMR) is complex and multifaceted, however it is exacerbated by the overuse and misuse of the drugs, from increased international travel, from the release of antibiotics into the environment, and elements such as poor sanitation (Aslam *et al.*, 2018). Antibiotic compounds are produced by microorganisms as defence mechanisms against bacteria in order to reduce resource competition. Therefore, bacteria have naturally evolved resistance genes to overcome this. However, the sheer quantity of antibiotic drugs now present in

the environment as a result of human activity, has created a huge selection pressure for any bacteria which do possess these resistance genes. This, coupled with the fact that bacteria have an extremely fast doubling time, has led to the rapid spread of these genes throughout the bacterial population (Zaman *et al.*, 2017). There is also a serious lack of new antibiotic drug development and discovery, which largely stems from reduced economic incentives. In fact, fifteen out of eighteen large pharmaceutical companies have completely withdrawn from the field of antibiotic research, contributing to the reality that a new class of antibiotic has not been discovered for 40 years (Bartlett *et al.*, 2013). It is estimated that the cost of developing a new antibiotic from research to the point of commercialisation is between \$700 million to \$1.1 billion, and can take over 10 years (Renwick *et al.*, 2016). However, with risk of resistance arising at any point, and the fact that many newly discovered antibiotics are kept as a last resort, there is a substantially lower return on this investment when compared to other drugs (da Cunha *et al.*, 2019). For example, London School of Economics reported that the net present value (NPV) of an antibiotic project was +\$50 million, whereas the NPV for musculoskeletal drugs was estimated to be around +\$1.15 billion (Renwick *et al.*, 2016). Alongside these economic factors, there are also basic barriers to research, and a 2007 study concluded that when using high intensity throughput antibiotic screening for antibiotic discovery, the success rate of an antibiotic progressing from screening to Phase 1 clinical trials was only 2.6% (Payne *et al.*, 2007). Overall, these statistics highlight the challenges faced with novel antibiotic discovery, and the large reduction in such advancement in recent years.

Resistance may initially arise through spontaneous mutation, whereby a DNA change is introduced to a certain gene which may then give rise to a more resistant form of the bacteria. These genetic changes will then be passed on to daughter cells when the bacteria undergo replication. Indeed, work has been performed which shows a positive correlation between mutation rate and antibiotic resistance. Oliver *et al.* (2000) used mutator and non-mutator isolates from the bacteria *Pseudomonas aeruginosa* to show that there was a significant difference in the resistance to various antibiotics tested; mutator isolates showed approximately double the frequency of resistance to their non-mutator counterparts.

Another method through which resistance can arise is via horizontal gene transfer (HGT). HGT is the process by which bacteria can share genetic information with one another, in a way which differs from the standard transfer of information between parent and offspring. Although there are various ways it can take place, the general pattern is that DNA is transferred from one bacterium into another, where it then homologously recombines with the new bacterium's DNA to be incorporated as its own. Assuming the recombination process is not deleterious for the

bacterium, it can benefit from the acquired DNA – for example if resistance genes have been obtained. The main mechanisms by which HGT operates are via processes called transformation, transduction, and conjugation (Figure 1.5) (Von Wintersdorff *et al.*, 2016).

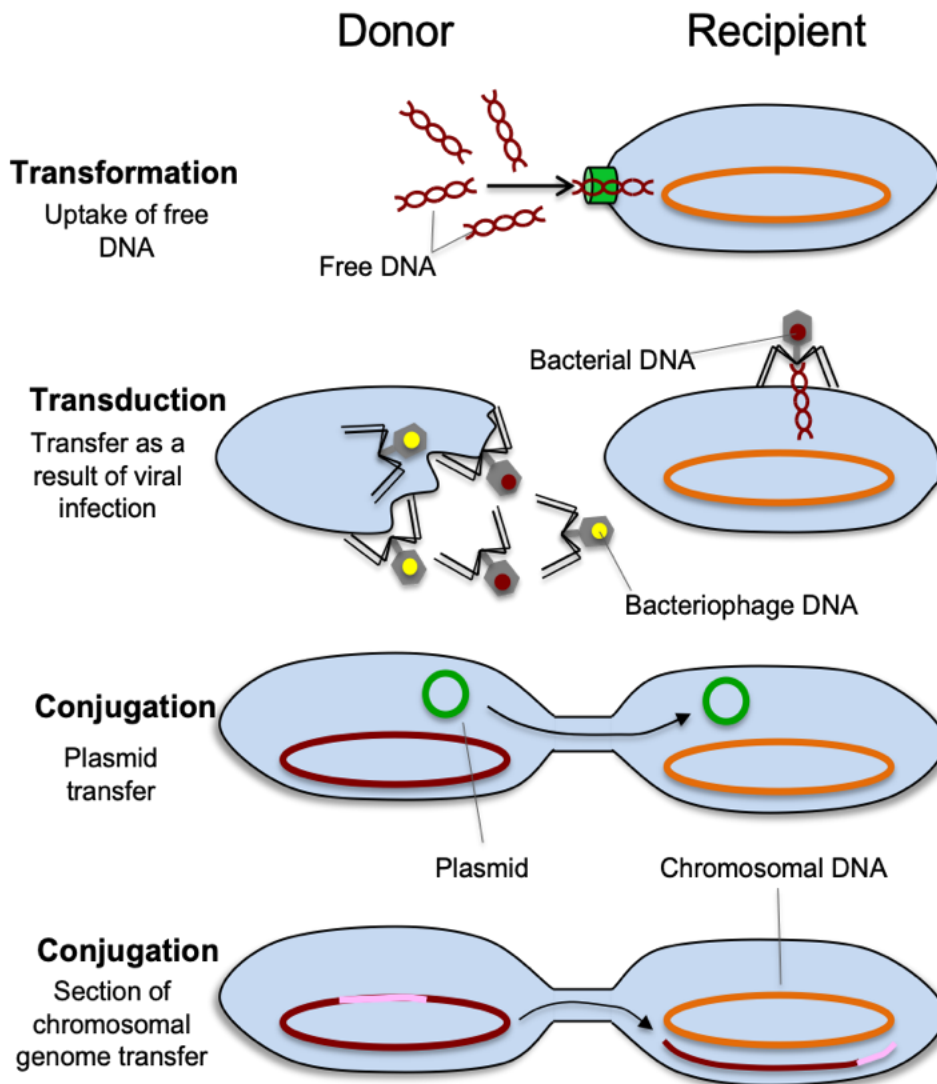


Figure 1.5 – An overview of the different mechanisms of HGT. Transformation – some bacteria are naturally competent, meaning they can take up free DNA from the environment around them. **Transduction** - bacteriophages can infect cells, fragment the bacterial DNA, and during the process of repackaging their own newly replicated genome can incorrectly package bacterial DNA instead. They can then transfer this to a newly infected cell upon lysing of the old cell. **Conjugation** - some bacteria contain mobile elements, such as plasmids, which can move themselves from one bacteria to another, often via surface appendages such as pili. They commonly contain antibiotic resistance genes. The transfer can involve conjugative plasmids alone, or whole sections of chromosomal DNA if the conjugative plasmid has incorporated itself into the main genome. Figure adapted from von Wintersdorff *et al.* (2016).

1.3.4.2 Mechanisms of resistance

So far it has been shown some of the ways in which resistance genes can be spread. Perhaps more interestingly is how these genes give rise to the phenotypic effect of antibiotic resistance, which is determined by the properties of the proteins they encode. One mechanism bacteria have evolved is to reduce intracellular drug concentration by increasing cellular efflux or by limiting cellular permeability. Gram-negative bacteria are far more resistant to antibiotics than Gram-positive bacteria, due to the extra layer of barrier protection offered from their outer membrane (Figure 1.6). However, despite this, antibiotics can still enter the cell via outer membrane porin proteins. Bacteria can increase resistance to certain antibiotics by down-regulating these porin proteins, thereby reducing the level of antibiotics gaining access into the cell. Similarly, if drugs do enter the cell, the bacteria can cope by increasing the efflux of these compounds. Resistance can arise when these pumps become up-regulated and allow high levels of the drug to be removed from the cell (Blair *et al.*, 2014).

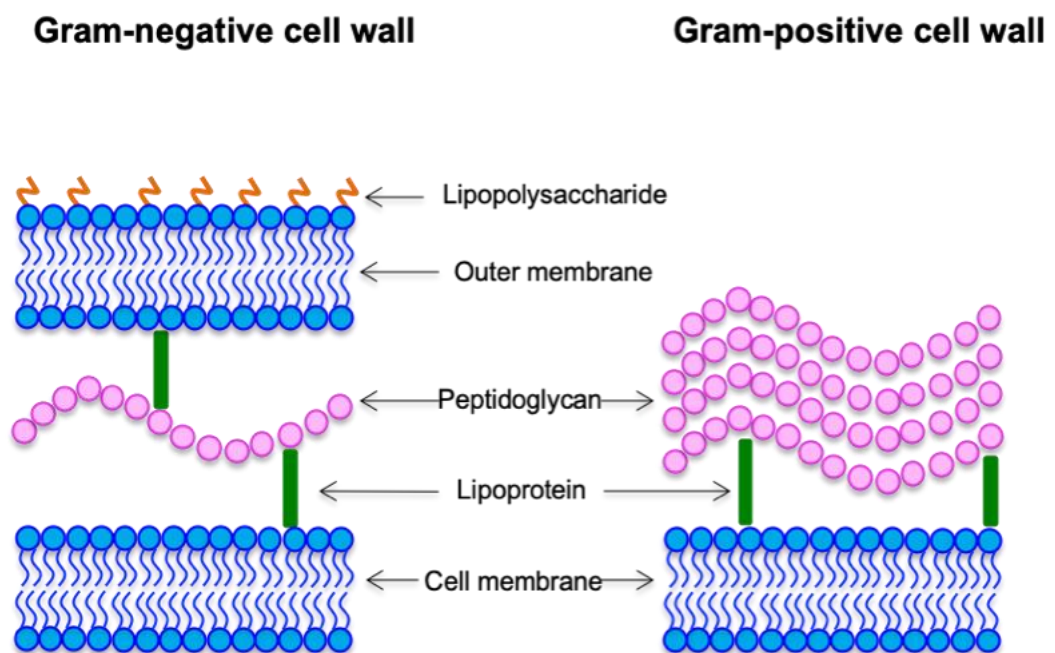


Figure 1.6 – A simplified illustration of the differences between the Gram-negative and Gram-positive cell walls of bacteria. One notable difference includes the presence of a second membrane in Gram-negative bacteria, which offers additional protection against incoming antibiotics, for example. The peptidoglycan layer common to both types is far thicker in Gram-positive bacteria, perhaps also creating protection for these organisms.

Another resistance mechanism evolved by bacteria is to produce novel proteins that fulfil equivalent roles to those targeted and inhibited by the antibiotic. One such example involves MRSA. Methicillin is a β -lactam antibiotic which, (as shown in section 1.3.2), functions by preventing transpeptidase enzymes from synthesising new bacterial cell wall. Methicillin resistance in MRSA arises from the bacteria encoding a new, unique, transpeptidase called penicillin binding protein 2a. This protein is able to compensate for the inhibition of the original transpeptidase, but is sufficiently different so that it is not targeted by methicillin, or any other β -lactam for that matter (Tenover, 2006).

A final example of a mechanism which causes antibiotic resistance is the modification, or complete breakdown, of the antibiotic itself. Many bacteria contain enzymes which are capable of breaking down and destroying the incoming antibiotics. An example is in the case of β -lactams and β -lactamases (Blair *et al.*, 2014). Figure 1.7 below illustrates all of the mechanisms discussed within this section.

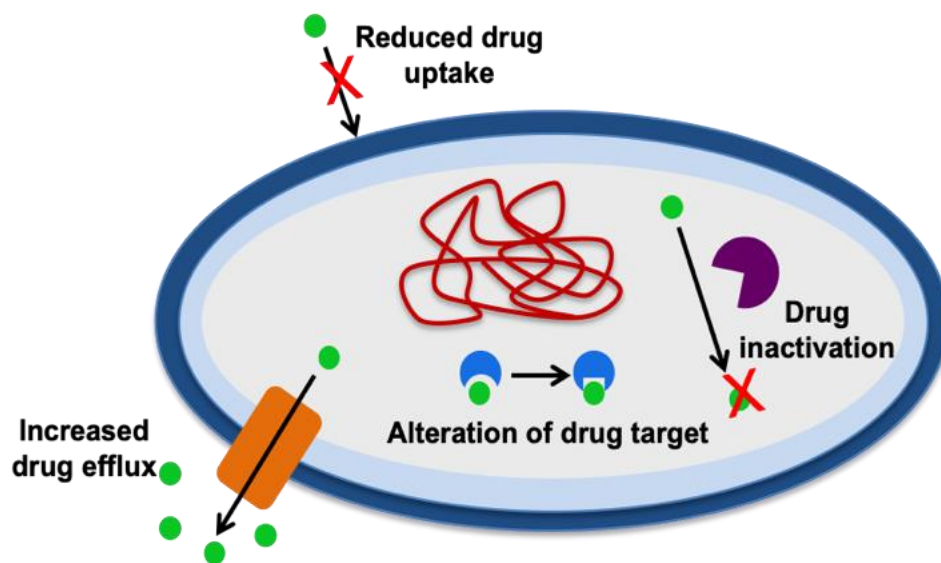


Figure 1.7 – An overview of some of the different mechanisms of resistance coded for by bacteria. Multiple methods are used by bacteria to increase resistance to antibiotics. They may have a reduced uptake of the drug due to their cell wall, or due to down-regulation of influx proteins in the membrane. Bacteria can also increase efflux of any drug which does enter the cell by up-regulating efflux proteins. The antibiotic may be broken down via enzymes, and the drug target itself may be altered to result in an inhibition of antibiotic functioning at the desired location. Figure adapted from Allen *et al.* (2010).

1.4 A background to intracellular bacteria

1.4.1 Intracellular lifestyle

Commensals are generally limited to colonising areas such as the surface of the skin, or the gastrointestinal and respiratory tracts, leaving internal tissues as sterile environments in most cases. However, some pathogens have evolved to overcome these host barriers and invade into deeper tissues, causing serious, and sometimes fatal, infections.

If commensal opportunistic pathogens invade tissues they will encounter an immune response against them. These bacteria do not always possess the ability to survive intracellularly, i.e. to invade specific host cells and persist within them, and so in most cases are extracellular niche species. These bacteria will be taken up by cells of the innate immune response and digested so that they no longer pose a threat (see section 1.2.3). This process of internalisation and digestion usually takes place within fifteen to thirty minutes (Ernst *et al.*, 1999). Intracellular species however are capable of penetrating these host cells, residing within them, and benefiting from the conditions intracellular living brings. This section will focus on what these benefits are, and how bacterial species can achieve this.

Epithelial cell boundary layers, such as those in the gut, are covered with a protective mucus layer. This layer contains components, such as antimicrobial peptides, which are designed to prevent bacteria from penetrating into the tissues below. Intracellular bacteria, and even in some cases extracellular bacteria such as *E. coli*, have developed mechanisms to penetrate this mucus layer. Some may produce proteases which are capable of breaking down the mucus to allow entry to deeper layers (Ribet and Cossart, 2015). *Vibrio cholerae* is one such example, which secretes a metalloprotease called vibriolysin to degrade the intestinal mucosa (Benitez and Silva, 2016).

Cells commonly infected by intracellular pathogens are the phagocytic cells as these cells are specialised to take up foreign particles. However, as discussed above, the purpose of these cells is to destroy internalised bacteria, and so the intracellular bacteria, unlike extracellular species, must have mechanisms to block this action. One method of evading destruction involves preventing the formation of phagolysosomes inside phagocytic cells. These contain the degradative enzymes which destroy the bacteria. *M. tuberculosis* is an example of a pathogen which prevents phagolysosome formation. Within the membrane of the host cells is a component called phosphatidylinositol 3-phosphate (PI3P). PI3P is essential to the host for the generation of the destructive phagolysosomes – it is thought to work as an attachment site for other proteins involved in the maturing process of phagosomes into phagolysosomes. *M. tuberculosis* overcomes

Chapter 1: Introduction

this process by inhibiting activity of the PI3 kinase hVp34, which generates PI3P, and in return prevents generation of PI3P on the phagosomal membrane, inhibiting phagolysosome biosynthesis. *M. tuberculosis* glycolipid lipoarabinomannan (LAM) is thought to be responsible for this survival mechanism, as purified LAM was sufficient to prevent lysosome fusion with the phagosomes (Pieters, 2008).

Another survival mechanism is bacterial tolerance of acidic and enzyme-rich environments. If a bacterial species fails to prevent phagolysosome formation, or finds itself in another acidic intracellular compartment, it may survive by tolerating the conditions found there. Work performed by Vandal *et al.* (2008) used *M. tuberculosis* to illustrate this example. The study showed that *in vitro*, *M. tuberculosis* was able to survive at a pH of 4.5. This was further supported in a cellular model showing that the bacteria could survive, and maintain their intrabacterial pH of approximately pH 7, when taken up by macrophages. This survival mechanism has important ramifications in the context of antibiotic delivery. As will be later discussed in section 1.5.4, some types of drug delivery systems can be targeted to environmental stimuli, such as pH/acidity. If these bacteria can reside in acidic environments, and antibiotics can be solely targeted to these areas, the benefits may be significant. Intracellular environments not only pose a challenge for bacteria from acidic conditions, but also from enzymes such as lysozyme, which is a degradative enzyme produced by lysosome organelles. Bacteria have evolved three main mechanisms to resisting this including modifying their cell wall peptidoglycan to leave it resistant to lysosomal hydrolysis; changing the charge and integrity of their cell wall and membrane; and releasing lysosomal inhibitors (reviewed by Ragland and Criss, 2017).

Intracellular bacteria are also capable of forcing non-phagocytic cells, such as epithelial cells, to engulf them. Bacteria can achieve this through a range of molecular mechanisms, but usually the end result of these is the triggering of a signalling cascade to reorganise the host cell's actin cytoskeleton in order to engulf the bacteria into the cell. A number of bacterial species display this behaviour to gain entry into non-phagocytic cells, including *Listeria monocytogenes* and *Salmonella* species (Ribet and Cossart, 2015).

Aside from the obvious need for survival methods inside macrophages, these bacteria have also found ways of more general intracellular survival, which can apply to life within non-phagocytic cells. For example, some *Chlamydia* species can prevent the onset of apoptosis, by degrading pro-apoptotic proteins, in turn inhibiting the clearance of infection by the host. Alternatively, some bacterial species, such as *Salmonella*, maintain the activation of anti-apoptotic factors (Ashida *et al.*, 2011).

Autophagy is another mechanism with which intracellular bacteria must cope. Autophagy means 'eating of self' and is a self-degradative process whereby components of the cell can be broken down and recycled, via lysosome fusion. Autophagy is split into several subsets, and the term 'xenophagy' is used to specifically describe the process of destroying invading bacteria. Intracellular pathogens can trigger xenophagy via a number of routes, including from the damage created upon exit of the phagosome into the cell cytosol, and through the detection of bacterial proteins. Some intracellular bacteria, for example *Burkholderia spp.*, have evolved to combat these defence mechanisms in a number of ways, including blocking the xenophagic machinery, camouflaging themselves in host protein, or by altering/destroying the targets which trigger xenophagy. Some of the bacteria even benefit from autophagy processes, as they are known to use autophagy breakdown products as a source of nutrients (Steele *et al.*, 2015).

The benefit of living in an intracellular environment is the increased protection from the host's immune system – intracellular bacteria are far more shielded from blood-borne defence mechanisms such as antibodies (Leon-Sicairos *et al.*, 2015). As antibodies are generally unable to penetrate host cell membranes, this component of the immune system is mostly inactive against intracellular organisms, thereby presenting a challenge in terms of combatting these pathogens. Additionally, host cells contain high concentrations of nutrients, from metabolic breakdown processes, which the bacteria can exploit. An example of this is the *Legionella* species of bacteria. This bacterium uses effector proteins to recruit vesicles to the phagosome membrane and fuse with it, potentially acting as a rich nutrient source to the bacteria within (Bhavsar *et al.*, 2007).

Additionally, once a bacterium has entered the host cell, many are capable of moving from one cell to another without ever having to leave this protective environment. Many species, including *Burkholderia*, *Listeria* and *Shigella* groups, are able to induce actin polymerisation at the surface of one of their poles, and can use this force to drive them forward within the host cell (Goldberg, 2001). It can also propel them through the cellular membrane into the neighbouring cell, highlighted in Figure 1.8 (Carlsson and Brown, 2006).

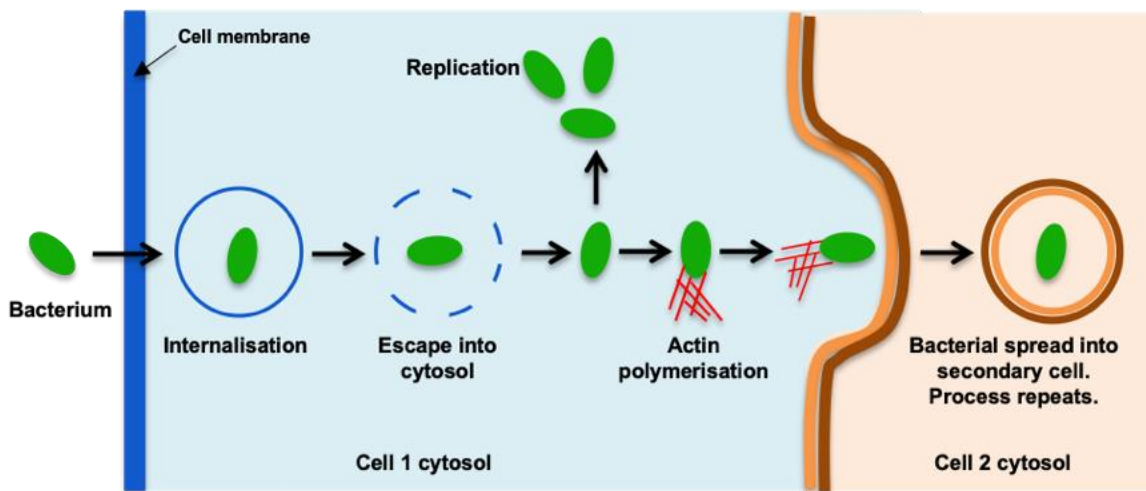


Figure 1.8 – An illustration of how intracellular bacteria can spread from cell to cell via actin polymerisation at their poles. After internalisation into the host cell the bacteria can leave the phagosome, or general vacuole, vesicle structures and become free within the cytosol. Here they can replicate, as well as initiating actin formation at their poles to push and propel them through the cytosol and also through the membrane into new host cells. This way, the bacteria never have to leave the protective environment of the host cell. Figure adapted from Ray *et al.* (2009).

Overall, there are benefits to living intracellularly, and multiple ways in which these species ensure their survival. Knowing how these species survive, and the kinds of cells they are capable of infecting, is essential for antibiotic delivery. As previously stated, the ability to selectively target antibiotics only to infected regions has enormous benefit, and understanding the lifestyle of these bacteria provides further ammunition to potentially achieve this in the future. Another possible avenue of research could involve combining antibiotic treatment with compounds that might trigger the intracellular killing processes, such as xenophagy, to result in a potentially collective effect alongside the antibiotics.

1.4.2 Challenges associated with treating intracellular infections

As previously discussed, the main challenge associated with combatting intracellular bacteria is the inability of antibodies or antibiotics to penetrate the membranes of host cells. In addition, the pathogenic bacteria may be successful in exploiting the host cells to gain access to a rich supply of nutrients while inhibiting the host defence mechanisms of programmed cell death or autophagy.

Multiple factors contribute to whether a drug can be taken up by a host cell. If a drug is lipid soluble it may be able to more easily passively diffuse across the membrane, active transport using pumps may enable uptake, and in some cell cases the drug may be taken up by endocytosis. Antibiotics such as the aminoglycosides and β -lactams penetrate cells much less easily compared

to groups like the macrolides and azolides, which have better intracellular penetration (McOrist, 2000). Despite this, even antibiotics that can cross the host cell membrane must be able to localise to the correct intracellular location in order to be effective against the invading bacteria. For example, the macrolides have been shown to spread evenly through the cell cytosol and cellular compartments once inside, whereas azolides are much more limited to cellular compartments, such as phagosomes, meaning bacteria within the cytosol could escape unharmed. Therefore, ensuring the correct localisation of drug to bacterium is important (McOrist, 2000).

The variability in host cell permeability to antibiotics depends partly on the chemical structure of the drug, and partly on any interactions with active transport pumps found in eukaryotic cells. These pumps recognise substrates based on factors such as their degree of hydrophobicity or potential for hydrogen bonding. In the case of tetracycline, a drug which can penetrate host cells, the multidrug resistance (MDR)1 efflux transporter recognises it as a substrate, and will pump it out of cells faster than it can accumulate (Van Bambeke *et al.*, 2003).

Another factor is the observation that some antibiotics, which can successfully enter into host cells, appear to show a loss of antimicrobial activity once there. Nguyen *et al.* (2006) demonstrated how the efficacy of fluoroquinolone antibiotics decreases in the intracellular environment. The group studied the effect of fluoroquinolone levofloxacin on *Staphylococcus aureus* growing intracellularly within monocytes. Although levofloxacin was able to kill intracellular *S. aureus*, it was shown to be 20 times less potent than when applied extracellularly, with some intracellular bacteria able to persist. The reasons for this may include co-localisation of drug with bacteria intracellularly not being achieved, intracellular pH levels being too acidic for optimal drug efficacy (levofloxacin is known to display a reduced activity at a pH of ≈ 5), or even the binding of the drug to cell macromolecules – upon ultrafiltration Nguyen and colleagues found that $\approx 20\%$ of the levofloxacin was bound to cellular structures. All of these reasons could contribute to reducing the intracellular effect.

Overall, the struggle of treating intracellular infections using antibiotics stems from the limited number of antibiotics available for such infections. Of all the antibiotics in clinical use, only some will be able to be taken up into host cells. Of those, not all will belong to the correct class of antibiotic for the specific infection, and of the ones which are, the bacteria may have grown resistant. This highlights how there is a large reduction in the antibiotic options available for treating these bacteria.

In terms of current treatment options for intracellular infections, generally high and sustained levels of antibiotics are necessary. For example, *M. tuberculosis* requires a 6-month treatment period consisting of four different types of antibiotics. In the case of multidrug-resistant TB, this course can extend for 20 months or longer (Caño-muñiz *et al.*, 2018). *Bacillus anthracis* infections, causing anthrax, require antibiotic courses that can last for up to 2 months (Spencer, 2003). *Brucella spp.* infections which cause the common zoonotic disease brucellosis, require combination therapy for a minimum of 6 weeks (Alavi and Alavi, 2013). For comparison, *Pseudomonas aeruginosa* is an example of a species considered to be solely extracellular, and infection in this case usually requires treatment lasting only a maximum of 2 weeks (Bassetti *et al.*, 2018). There are several drawbacks to lengthy and highly dosed treatment regimes. Patient compliance may be poor, and antibiotic course incompleteness can lead to resistance due to persisting bacteria. Another problem is the side effects upon the patient from taking such drug doses. As seen in section 1.3.3, the use of antibiotics can alter the commensal make-up of the host, which brings with it its own problems. Taking antibiotics for so long may lead to temporary, or even permanent, changes in the host's health. Additionally, the more drugs being taken the higher the chance of the patient being allergic to one or more of them (Ladavière and Gref, 2015).

Overall, treating intracellular infections poses many challenges. This is largely due to the limitations in antibiotic availability, but also that current treatment options, although sometimes effective, have issues with patient compliance and unpleasant side effects. Therefore, there is a strong need for new methods which can be used to treat these infections.

1.4.3 Intracellular bacteria of interest for this project

1.4.3.1 *Burkholderia pseudomallei*

This PhD project will focus around the species *Burkholderia pseudomallei*. This is an intracellular bacterial species which has the potential to be misused for biowarfare purposes, as introduced in section 1.2.2.

B. pseudomallei is an intracellular pathogen which is classed as being highly endemic to areas of the world such as north-east Thailand and northern Australia, however sporadic cases have also been reported elsewhere. This pathogen is able to persist in the environment and can be found living in areas such as soil, rice paddies, or stagnant water, from which it can be cultured with relative ease (Allwood *et al.*, 2011). It can enter host bodies in a range of ways, via inhalation, ingestion, or most commonly by cutaneous routes, and it is a species which is infectious even at

low doses (Gilad *et al.*, 2007). Once in the body *B. pseudomallei* usually initially infects phagocytic cells such as the macrophages, although it is also able to infect non-phagocytic cells as well. It is able to survive intracellularly due to the prevention of phagolysosome formation after uptake into the phagosome (Willcocks *et al.*, 2016). It can exit the phagosome in as little as 15 minutes (Cheng and Currie, 2005), where it can then replicate and survive in the host cell cytosol (Ozanic *et al.*, 2015). *B. pseudomallei* possesses a variety of characteristics which contribute to its virulence and disease-causing ability. One of these is the presence of a capsule, which aids survival in the host's blood by preventing opsonisation of specific complement proteins which act as a mark for immune degradation (Reckseidler-Zenteno *et al.*, 2005). *B. pseudomallei* also possess a Type III secretion system which is thought to contribute towards the ability to invade non-phagocytic cells and replicate intracellularly within host organisms by escaping from endocytic vacuoles (Stevens *et al.*, 2002, 2003). The species also secretes a protein, called BimA, which aids the mobility of a bacterium through actin reorganisation and the formation of actin tails. This type of mobility contributes to this pathogen's capability of achieving cell-to-cell intracellular spread (see Figure 1.8) (Stevens *et al.*, 2005). *B. pseudomallei* also contains drug resistance genes within its genome which encode for features such as efflux pumps and β -lactamases which contribute towards its ability to evade killing by antibiotics, and therefore highlight the challenges faced with its treatment (Larsen and Johnson, 2009).

B. pseudomallei is the causative agent of the infection melioidosis. This disease can elicit symptoms such as septicaemia, pneumonia, and in some rare cases neurological effects can occur in the form of brainstem encephalitis (Limmathurotsakul and Peacock, 2011). Chronic melioidosis is where the infection can last for longer than two months, and this was found to occur 11% of the time, based on data from a 20 year-long Australian study. Additionally, *B. pseudomallei* is also capable of becoming a latent infection, with infection only becoming apparent many years after initial exposure. It is thought that 4% of all melioidosis cases are the result of an activated latent infection (Currie *et al.*, 2010; Wiersinga *et al.*, 2019). *B. pseudomallei* infections often require a combination of antibiotics and a lengthy period of treatment. Typically, this involves intravenously delivered initial antibiotics, followed by oral antibiotics for up to 6 months (Limmathurotsakul and Peacock, 2011). As previously discussed, these heavy treatment plans lead to issues with patient compliance, and also the detrimental side effects antibiotics can have on the body. Antibiotic resistance is another concern. Isolates resistant to the antibiotics are not uncommon (Gilad *et al.*, 2007), and so new, and more effective, treatment options must be investigated before there are no antibiotics left which are capable of killing the infection.

Despite being highly infectious, person-to-person transmission has largely not been reported

(Gilad *et al.*, 2007). As a putative bioweapon, this relative lack of human-to-human transmission has both advantages and drawbacks. Human-to-human spread has the potential to lead to the uncontrolled spread of disease amongst not only the intended victims, but also the weapon's users. Conversely, a lack of person-to-person transmission may result in a lower impact at a target area. Disease progression is also key, and the time taken for a specific bacterial infection to become symptomatic within a host should be considered. A fast-acting infection has the potential to cause short-term disruptions, but could be argued that early diagnosis helps containment of the disease. Slower disease progressions may cause a large-scale spread of the disease, if able to go undetected for a period of time. This may eventually cause significant disruption to the population of a target area, but would not be the preferred choice of agent if a fast response was needed. For *B. pseudomallei* the incubation period can be highly variable. In one study, 25% of patients experienced an incubation period of between 1-21 days (Currie *et al.*, 2000; Limmathurotsakul and Peacock, 2011), however it can also have a very slow onset, with the largest period of time between exposure to development of clinical symptoms being recorded as 62 years (Wiersinga *et al.*, 2006). The slow onset of infection may also be due to this species' ability to hide away inside host cells where they remain protected from immune responses and antibiotic treatment.

1.4.3.2 *Burkholderia thailandensis* – model organism for this project

B. pseudomallei is a dangerous pathogen and requires Category 3 containment facilities. In order to be able to perform preliminary laboratory tests with ease, models of the organism were used. Work for this project began with using *Burkholderia thailandensis*, a model of *B. pseudomallei*, which requires only Category 2 containment. *B. thailandensis* and *B. pseudomallei* are found in similar environments, however *B. thailandensis* is not a recognised human pathogen. Despite this, 85% of the species' genetic information is conserved, making *B. thailandensis* an excellent model (Majerczyk *et al.*, 2014).

The intracellular lifestyles of *B. thailandensis* and *B. pseudomallei* are very similar. They can passively penetrate phagocytic cells, such as macrophages, or they can make use of their Type IV pilli appendages, and Type III secretion systems, to stimulate uptake into non-phagocytic cells, such as epithelial cells of the lung (Li *et al.*, 2015). They are able to escape from their original endocytic compartments, crucially, before phagolysosomal fusion occurs, and migrate into the cytoplasm where they can replicate (Willcocks *et al.*, 2016). Once in the cytoplasm, they enable actin polymerisation at one of their poles, and this enables them to propel themselves forward in the cell. Such forces can create membrane protrusions which can be phagocytosed by

neighbouring cells, allowing cell-to-cell spread. This kind of movement ensures these bacteria never have to leave the protective environment of the cell (Wiersinga *et al.*, 2006). They also employ a range of mechanisms to survive intracellularly, including inhibiting the production of antimicrobial free radical species, such as nitric oxide, which cells such as macrophages are usually able to eliminate infecting pathogens with (Allwood *et al.*, 2011).

An interesting question raised is that, if these bacterial species are so similar, and survive intracellularly in much the same way, then why is *B. pseudomallei* so much more pathogenic than *B. thailandensis*? This answer to this remains largely unknown but is thought to depend on differences in the virulence genes expressed by both species. For example, in order to generate the actin tails and allow spread *B. thailandensis* produces an effector protein, known as BimA, which mimics the host cell's own actin polymerase complex (Arp 3/3). However, the orthologous BimA effector protein from *B. pseudomallei* works to achieve the same function, but by a different mechanism involving mimicking a much more efficient complex (Ena/VASP), resulting in greater numbers of actin tails being produced. This in turn will allow greater levels of cell-to-cell spread and transmission of infection (Willcocks *et al.*, 2016). Therefore, this is just one possible example of why *B. pseudomallei* is more pathogenic than its close relative *B. thailandensis*.

1.5 Nanoparticles as intracellular drug delivery systems

1.5.1 A background to drug delivery systems

As seen previously the efficacy of conventional antibiotic therapy for intracellular infections is fundamentally limited by several factors, including poor intracellular drug bioavailability and off-target side effects. Furthermore, the lack of new antibiotics being developed creates a limited treatment choice for bacterial infections. One avenue being explored to help combat these struggles is the repackaging of currently available antibiotics using nanoparticles. The idea is that rather than attempting to develop new antibiotics, existing ones can be made more effective through incorporation with nanoparticles (Schalk, 2018; Dassonville-Klimpt and Sonnet, 2020). Many antibiotics, including those primarily from the β -lactam and aminoglycoside classes, are less able to penetrate host cell membranes leaving the bacteria shielded (McOrist, 2000). There has been evidence in the literature that many different β -lactams and aminoglycosides are effective against *B. thailandensis in vitro*, and free growing, but once the bacteria reside intracellularly they become ineffective (Thibault *et al.*, 2004; Thamlikitkul and Trakulsomboon, 2010; Kovacs-Simon *et al.*, 2019). Therefore, if these drugs could be delivered to intracellular locations, they would be

Chapter 1: Introduction

able to take effect thereby increasing the number of antibiotic treatment options for these types of infections without the challenges associated with developing new antibiotics from scratch.

In recent decades research into the areas of nanoscience and nanotechnology, for the benefit of applications to medicine, has increased rapidly. The use of nanosystems for drug delivery provides multiple advantages and has the potential to overcome some of the conventional route limitations faced. Some key examples include:

- Increase in the drug half-life
- Improvements in the solubility of certain drugs
- Reduced clearance of the drug by natural bodily processes
- Potential to allow targeted delivery to site of infection only
- Potential for co-loading of multiple drug types into one particle, thereby allowing co-delivery of drugs to cells
- In some cases encapsulation allows antibiotics which would not normally be able to traverse the host membrane to do so (Fierer *et al.*, 1990; Shi *et al.*, 2010).

These nanoparticle delivery systems are now accepted to be $\leq 100\text{nm}$ in size, although not all systems will adhere to this, and may be larger (De Jong and Borm, 2008). Nanoparticles have a higher cellular uptake than microparticles, and so increasing the system size may reduce the efficiency with which they are taken up intracellularly. Drugs of interest can be incorporated with nanoparticles in various ways. For example, the drug may be adsorbed onto the surface, dissolved into the nanoparticle structure, or even encapsulated within aqueous cores of some carriers. Depending on the drug, and the desired style of delivery and release, different nanoparticles with different characteristics can be constructed to fulfil these requirements (Singh and Lillard, 2009).

Although these drug delivery systems have huge potential, there are considerations to be taken when designing the systems depending on what their route of uptake into the host will be, how they will end up at their desired target location, and challenges they may encounter along the way, starting from the point of administration. If administered orally, the nanoparticle delivery systems must be able to retain stability upon exposure to the harsh gastric environments, for example the low pH and enzymatic pressures in the stomach. Polymeric nanoparticles tend to be an advantageous material of choice for this, as they have been shown to withstand these elements. One group used polymeric nanospheres for orally delivered insulin, and found the nanospheres increased the stability of insulin, compared to free drug, and resisted proteolytic enzyme degradation *in vitro* (Damgé *et al.*, 1997). Similarly, nanoparticles may enter the gastrointestinal tract where they will encounter the mucosa. This structure efficiently entraps

nanoparticles and removes them as it is shed, decreasing the residence time of the particles (Ensign *et al.*, 2012). Intravenous delivery into the bloodstream is another route of administration. Once in the circulation nanoparticles are subject to all of the blood components, such as blood cells, platelets and serum proteins. These serum proteins can opsonise the nanoparticles leading to increased host immune recognition, and clearance from the bloodstream (Longmire *et al.*, 2008). If the delivery systems are able to spread through the blood system, or via the oral route, without being cleared, they still need to reach their target. This involves crossing endothelial layers to access the target tissues and cells below, and in the case of vascular endothelium especially, this generally has low permeability to nanoparticles. If they make it through this layer, they must traverse many layers of extracellular matrix to reach target tissues, and once there must be taken up, frequently via endocytosis. This results in the nanosystems being encapsulated themselves within endosomal vesicles. Very often the drug target, i.e. intracellular bacteria, may be residing within the cytosol, leading to the required release of the delivery system from the endosomes (Mitragotri *et al.*, 2014). These are factors which must be considered when designing drug delivery systems, and in the context of what they will be used for, which chemical-physical characteristics are most essential for them to possess in order to overcome these hurdles.

1.5.2 Types of nanoparticle delivery systems

There are many different types of nanoparticles under investigation for drug delivery, and their compositions can vary greatly. This report will focus on two of the more widely researched organic varieties, liposomes and polymersomes.

1.5.2.1 Liposomes

Liposomes (LMs) have been used for drug delivery since the 1960s (Shi *et al.*, 2010). LMs are made up of amphiphilic phospholipids. Amphiphilic describes a compound which has hydrophobic and hydrophilic regions; in the case of phospholipids this corresponds to their hydrophobic fatty acid tail groups, and hydrophilic headgroups. Due to this, these phospholipids will self-assemble in an aqueous solution, and in the case of LMs will form a spherical vesicle with a lipid bilayer similar to that of a cell membrane (Monteiro *et al.*, 2014) (Figure 1.9).

LMs are the most well-studied drug delivery system, and arguably the most successful and widely used to date. This is largely due to the fact that they are biocompatible, pharmacologically inactive, and minimally toxic all due to being composed of natural phospholipids. Hydrophobic drugs can be packaged into the non-aqueous bilayer membrane, and hydrophilic drugs into the

aqueous cores (Sercombe *et al.*, 2015). This increases the availability of drugs for medical use, as it enables drugs which would not normally be soluble within the body to be used in treatments.

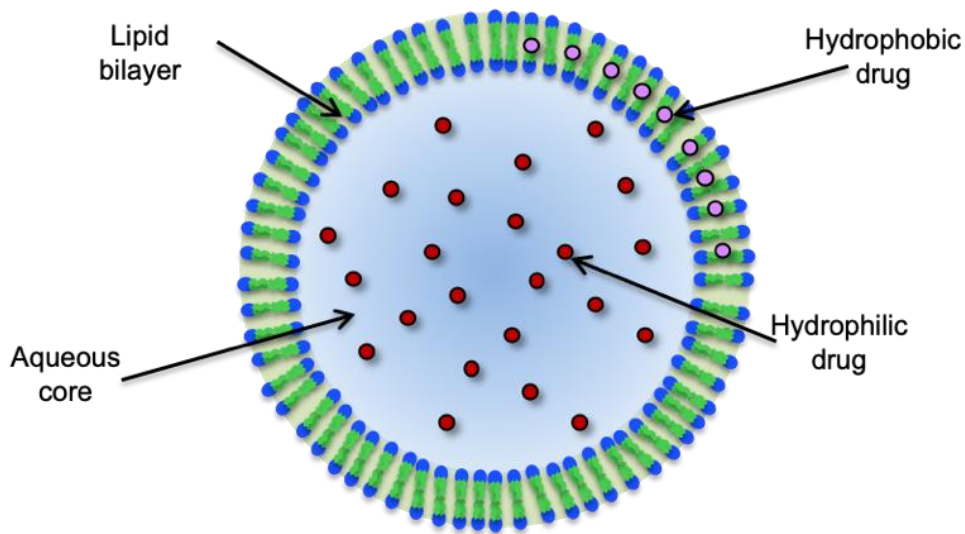


Figure 1.9 – An illustration of the liposomal class of nanoparticle drug delivery systems. LMs are made up from a lipid bilayer, and are spherical in shape, creating a vesicle type structure. Liposomal membranes are hydrophobic and therefore can incorporate hydrophobic drug molecules, whereas the centre core is aqueous, meaning hydrophilic drugs can also be encapsulated. Often LMs can be conjugated with the polymer PEG (not shown) and this increases the circulation time within the host. Figure adapted from Sercombe *et al.* (2015).

One limitation LMs have is that they are relatively short-lived within the body. Upon intravenous administration into the host blood stream they are rapidly cleared by the reticuloendothelial system (RES). This is essentially all of the immune phagocytic cells located in the blood, and primarily within organs such as the liver, spleen and kidneys. This uptake reduces the levels of drug-loaded LMs reaching target cells. In the past attempts were trialed to evade this uptake route by saturating macrophages with empty LMs, and essentially blocking them from the further uptake of active drug loaded LMs. However, this created uncertainty as to whether macrophage saturation would lead to a reduced immune response, and therefore a trigger for increased risk of infection. Instead, the circulation time of LMs, and their tendency to be removed by the RES, can be improved by conjugating the polymer poly(ethylene glycol) (PEG) to the LM surface. The addition of PEG allows for the steric hindrance of electrostatic and hydrophobic reactions with serum proteins and cells in the blood. This reduces the level of liposomal opsonisation and uptake of cells by the RES (Allen and Cullis, 2013; Sercombe *et al.*, 2015).

1.5.2.2 Polymersomes

PMs are vesicles made up of amphiphilic block co-polymers. They are similar to LMs structurally, in that they have a bilayer surrounding an aqueous core. Due to the amphiphilic nature of the polymers of which they are composed, and the way they self-assemble in solution, PMs have both hydrophobic (the membrane shell) and hydrophilic (the aqueous core) regions to them (Figure 1.10A). Therefore, both hydrophilic and hydrophobic drugs can be loaded within PMs, into the aqueous core, or the shell membrane, respectively (Lee and Feijen, 2012).

The material composition of PMs gives them an advantage over LMs. Studies performed by Discher *et al.* (1999) compared the bilayer sizes of LMs composed of typical phospholipids, and PMs composed from the block co-polymer polyethyleneoxide-polyethylethylene (PEO-PEE). The polymer had a length approximately 10 times longer than the phospholipid. Upon hydration and vesicle formation the PEO-PEE PMs had a hydrophobic region thickness of approximately 8 nm, versus the liposomal hydrophobic region of approximately 3 nm (Figure 1.10B). Further studies by Discher and colleagues evaluated the permeability of PM and LM membranes. They found that LM membrane permeability was at least 10 times greater, but up to as much as 60 times greater, than that of PMs. This relative lack of PM permeability is most likely a direct result of their thick bilayer membrane, allowing them to have a lower intrinsic leakiness than LMs. This is useful when considering using PMs for drug loading.

Another benefit of using PMs is that they have been found to be more stable in circulation. LMs are rapidly cleared by the RES, and whilst this can be moderately improved via the conjugation of PEG molecules, the results still do not compare to PMs which contain much higher levels of PEG, and PEG-like molecules, due to their hydrophilic domains being entirely composed of them. Aside from reduced permeability and increased membrane thickness as a result of long PEG length, circulation time is also increased due to PEG conferring greater resistance to deposition of serum proteins from the blood. These findings are supported by fluorescent techniques which show bare LMs present in rat circulation for 4 hours, compared to an increased circulation time of 10-15 hours when conjugated with small levels of PEG. When PMs composed of varying PEG chain length were injected into rat circulation, they circulated for between approximately 15-25 hours. This approximate 2-fold longer circulation time is another factor behind PMs being a more attractive drug delivery system than LMs (Photos *et al.*, 2003). This characteristic of increased circulation time due to PEGylation comes as both a benefit and also a potential challenge. Many bacteria reside intracellularly within phagocytic cells, the very cells which make up the RES, and so targeting to these areas may prove challenging if the chosen nanoparticle possesses high PEG

levels. In fact, there have been multiple examples within the literature where nanoparticle PEGylation has been demonstrated to hinder macrophage uptake (Qie *et al.*, 2016; Behzadi *et al.*, 2017). Therefore, it is important when choosing the material composition of nanoparticles that a balance is struck between minimal clearance from the circulation, whilst also achieving good uptake into the target cell.

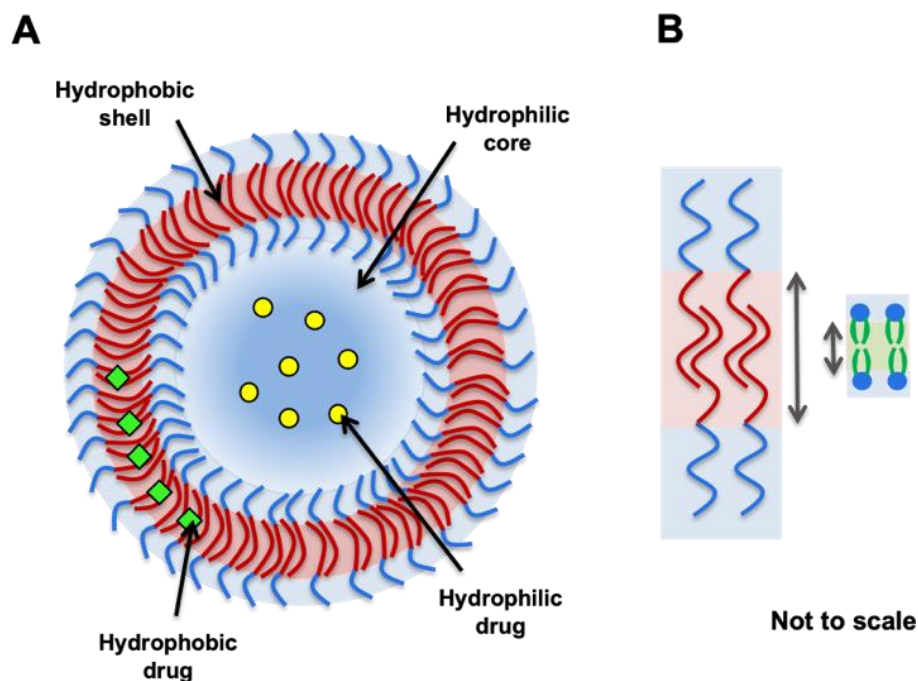


Figure 1.10 – Overview of the principles behind PM drug delivery systems. (A) PMs are composed of amphiphilic block co-polymers which will self-assemble in aqueous solution to generate both hydrophobic and hydrophilic regions. As a result both polar and non-polar drugs can be loaded within these nanoparticles. (B) Illustration comparing the lengths of polymers versus phospholipids. Due to the longer lengths of polymers, much thicker hydrophobic regions can be achieved in PMs, compared to LMs. The grey arrows display these hydrophobic regions. Figure adapted from Messenger *et al.* (2014) and Discher *et al.* (1999).

Despite all of the benefits of PMs over other nanosystems, the translation from bench to clinic has been slow, and clinical investigations are still on-going. There are currently no Food and Drug Administration (FDA) approved PM formulations (Anselmo and Mitragotri, 2019), compared to 15 approved LM-based products available for clinical use as of 2018 (Fatima *et al.*, 2018). With all of the benefits they have this highlights their exciting future in medical applications, and the potential to dominate the marketplace in years to come.

1.5.3 Targeted antibiotic delivery

One of the most fundamental aims for the use of nanoparticles is the enhanced delivery of drugs to their target area. In the context of antibiotics, this would be the delivery of the drugs to the sites of bacterial infection. Increasing targeting to only these areas has the potential to reduce the level of free drug distributed to the rest of the body, and to achieve high and sustained levels of cell drug concentrations. In turn, this reduces chances of commensal bacterial death, and encouraging resistance within these populations.

A key challenge comes with finding differences between diseased, or infected, tissues and those which are healthy. Often this is achieved through targeting cell surface markers which are overexpressed in unhealthy cells. Antibodies are excellent at specific targeting, however due to their large sizes can detrimentally influence the behaviours of the nanocarriers once in the host. Others, such as peptides, sugars, and hormones, can be used at a reduced cost, but are not as specific to target areas as antibodies (Larson and Ghandehari, 2012).

Passive targeting to bacterial infection sites can sometimes be achieved. Bacterial infections are known to increase permeability of the vasculature as a result of their production of compounds such as proteases. Similarly, the inflammatory response itself causes leakiness in vasculature to allow for immune response cells, such as the macrophages, to gain access to the infection site. This increased permeability allows any circulating nanoparticles loaded with antibiotic to accumulate at these sites easily and take effect (Gao *et al.*, 2014). Other ideas centre around the fact that bacteria possess an overall net negative charge on their cell wall surfaces (Dickson and Koohmaraie, 1989). Nanoparticles with a positive surface charge may be able to target bacteria via electrostatic interactions.

Active targeting has also been investigated. By conjugating ligands, with the capability of binding to pathogens, onto the surface of nanoparticles, they can be actively directed to infection sites. Some peptides, such as the human immunodeficiency virus (HIV) trans-activator of transcription (TAT), possess the ability to penetrate cells, and are usually utilised by pathogens to gain access to intracellular environments. TAT has been frequently used on nanoparticles to increase uptake of chemotherapeutic payloads into tumour cells (Dehaini *et al.*, 2016). This suggests it could also be a key player in targeting nanoparticles to intracellular environments where bacteria are residing. Macrophages by nature passively take up nanoparticles, through processes such as endocytosis, however uptake could be enhanced through the addition of targeting moieties specific to

macrophage surface markers. A range of ligands including, mannose and O-steroyl amylopectin, have been shown to enhance nanosystem uptake (Gao *et al.*, 2014).

1.5.4 Environmentally responsive antibiotic delivery

Another approach taken to try and maximise targeted delivery, is to utilise environmentally responsive nanosystems. This method aims to release payloads from nanosystems in a more controlled way, by keeping the nanosystems largely inactive until at their target location (Gao *et al.*, 2014). This is being achieved by using environmentally sensitive polymers to give PMs, and even modified LMs, these characteristics.

The first example is of nanoparticles being triggered to degrade and release their payloads in response to an alteration in pH. pH within the cytosol is approximately 7, whilst intracellular compartments such as endosomes and lysosomes are approximately 6 and 4.5, respectively. One particular copolymer of interest is poly(2-(methacryloyloxy) ethyl phosphorylcholine)-b-poly(2-(diisopropylamino) ethyl methacrylate), or PMPC-b-PDPA. This block copolymer generates pH sensitive PMs (Meng *et al.*, 2012). The PMs generated are stable at physiological pH, but will dissociate below a pH of 6, highlighting their use for delivery to intracellular and acidic compartments. Whilst much research has so far focused around using these types of pH sensitive nanocarriers to deliver anti-cancer therapies (Shen *et al.* 2008), the same mechanisms could apply to target intracellular bacterial pathogens.

The second environmental stimulus to be considered is temperature. The rationale for this approach comes from the observation that frequently diseased tissue regions often display higher temperatures than their healthy counterparts (Larson and Ghandehari, 2012). Some polymers are capable of becoming soluble upon cooling, for example poly(N-isopropylacrylamide) (PNIPAM), whereas others are capable of becoming soluble upon heating, for example polyacrylamide. PMs formed from copolymers including PNIPAM will self-assemble at temperatures above 30°C, but cooled to below this temperature they will disassemble. On the other hand, PMs formed from copolymers including polyacrylamide will self-assemble at temperatures below 25°C, but when heated above this they will disassemble (Gandhi *et al.*, 2015). With this in mind, it may be possible to heat or cool specific areas of the body, externally and noninvasively, to treat infection using these temperature sensitive PMs. A similar example comes from Gannon *et al.* (2008) who showed that, *in vitro*, intracellular gold nanoparticles can be externally induced, using radiofrequency, to release heat which can kill nanoparticle containing cancer cells. This method of

application may however be better suited to infections that are localised to one area, rather than systemically across the body.

Despite both pH and temperature being two sophisticated mechanisms of achieving release at the target site, there have been other examples within the literature which achieve the same result without the need for complex chemistries. Scarpa *et al.* (2016) investigated the delivery of PEO-PCL PMs to intracellular locations within mammalian L929 fibroblast cells. The group reported that although these PMs had no specific environmentally responsive mechanism, such as pH and temperature sensitivity, they were able to release their payloads and measure an accumulation within the cell cytoplasm. This was measured using fluorescence detection of fluorescein, a hydrophilic dye which remains quenched under high concentrations, and therefore only fluoresces once released from the PM. These findings suggest that endosomal escape of PMs is possible without the need for intricate chemical alterations of the polymer.

1.5.5 Characterisation of nanoparticles

Nanoparticles are now commonly researched for a variety of applications, however one of the largest fields is their use in nanomedicine. As a result, different information about their properties is required, ranging from details such as their size, to the concentration of payload they might contain. There are many different analytical techniques available to achieve this, but in this section some key examples which were used within this project will be discussed.

The analytical technique most commonly used to assess nanoparticle size is dynamic light scattering (DLS). A beam of light is shone onto the suspension of nanoparticles, which scatter the light (Rayleigh scattering) and as a result alter the direction and intensity of this beam. As the nanoparticles are measured in solution, they have an element of random movement associated with them (Brownian motion) which causes changes to this direction and intensity over time. This variation over time, therefore, contains information on the random movement of the nanoparticles which is used to determine the diffusion coefficient. From this diffusion coefficient, and by using various mathematical equations, the hydrodynamic radius of these spherical nanoparticles can then be established (Lim *et al.*, 2013). The DLS technique is also able to generate a value for the polydispersity index (PDI) of the sample. This reflects the particle size distribution of nanoparticles within a sample. A value between 0.0 and 1.0 is given. The closer to 0.0 the PDI is, the more monodisperse a sample is, and the closer to 1.0, the more polydisperse it is (Cruz. *et al.*, 2005). In simple terms it is a measure of how many of the particles within a sample share the same size as one another. DLS is widely used within the nanoparticle field for size

measurement, however limitations do exist. DLS is a low-resolution method meaning that it cannot distinguish between two nanoparticle populations of similar size. This can lead to incorrect PDI readouts where a sample appears to be more uniform in size than it truly is. Furthermore, large aggregates, or particles, can skew the measurements to give a larger average particle population size (Stetefeld *et al.*, 2016). For this reason a variety of sizing techniques, including perhaps transmission electron microscopy (TEM) would be preferable for when characterising nanoparticle size.

Another method commonly used for the characterisation of PMs, specifically for measuring encapsulated drug load, is high performance liquid chromatography (HPLC). This method is able to separate components of a sample and quantify their amounts. It differs from conventional chromatography as samples are injected through the column under high pressure, rather than relying on gravity alone (Thammana, 2016). The column (stationary phase) composes immobilised hydrophobic ligands, and the mobile phase consists of hydrophilic, aqueous, buffers. When the sample is injected through the column, in association with the mobile phase, the more hydrophobic compounds will interact with the hydrophobic stationary phase, whereas hydrophilic compounds will associate with the mobile phase. As a result, the more hydrophilic compounds will have faster elution times, showing how different elements can be separated according to their level of hydrophobicity. After elution through the column the compounds pass through a detector, often UV-vis, to generate a series of peaks relating to each sample component, and also reflect the quantity present (Aguilar, 2004) (Figure 1.11).

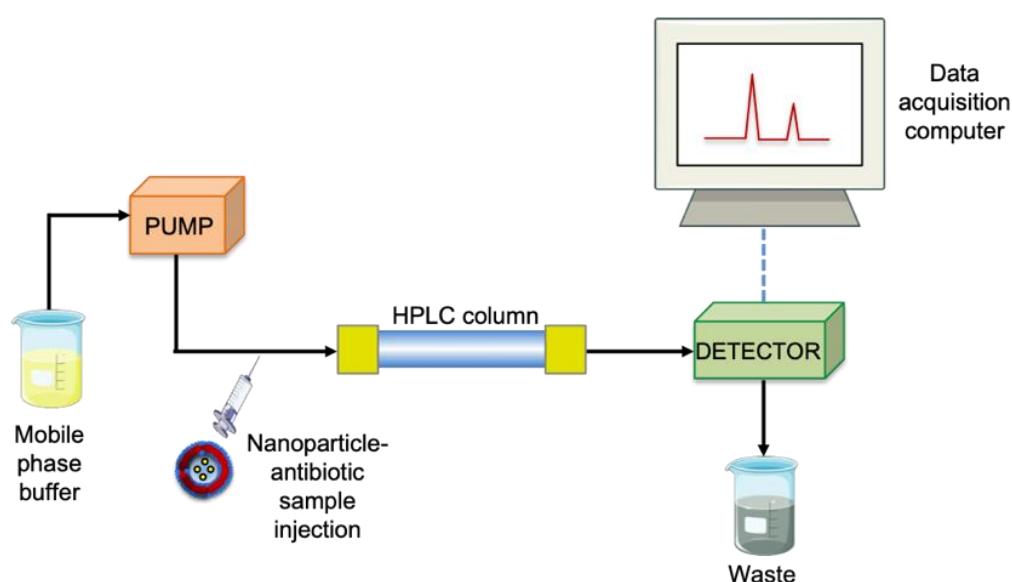


Figure 1.11 – Schematic of the experimental setup of an HPLC machine. A mobile phase solvent buffer and a stationary phase HPLC column are used together to separate chemical compounds based on their level of hydrophobicity. After samples have passed through the HPLC column they are picked up by a detector, usually UV-vis, and the concentrations present can be determined from the chromatogram produced on a receiving computer.

The main benefit of using HPLC for concentration assessment, rather than other methods such as UV-vis spectrophotometry, is its high sensitivity. One paper reported that when assessing the concentration of antibiotic levofloxacin using both UV-vis and HPLC techniques, the lower limits were 2.5 µg/ml and 0.05 µg/ml, respectively (Wang *et al.*, 2019). This sensitivity is key for nanoparticle payload analysis as in many cases the expected encapsulation of antibiotics would be low. Despite this, HPLC is a relatively complex technique and requires optimisation of mobile phase buffers for each new compound. Therefore, methods like UV-vis spectrophotometry are still sometimes preferred for initial experiments and during assay optimisation.

Another avenue of nanoparticle research explores the localisation of nanoparticles within cells. Nanoparticles are often labelled, using a fluorescent marker for example, allowing for their tracking. A common technique used for quantifying the amount of a fluorescence within a cell population is flow cytometry. Samples can be prepared for fluorescence detection in a variety of ways including staining with a dye, expression of a protein (for example green fluorescent protein, GFP), or through the conjugation of antibodies. The cells are then suspended in a buffer, in flow, and analysed using laser excitation on a single cell basis (McKinnon, 2018). One particular type of flow cytometer, a fluorescence activated cell sorter (FACS) is able to go further and sort cells from a mixed population, depending on their fluorescence signalling (Adan *et al.*, 2017). However, one particular shortfall of traditional flow cytometry is the inability to image cells as they pass through machine detectors. Imaging would allow the collection of information on sub-cellular distribution of fluorescent dyes. In 2005, the first imaging flow cytometry (IFC) machine, ImageStream, was developed which was able to image cells in a high-throughput fashion (Barteneva *et al.*, 2012). IFC works in much the same way as a normal flow cytometer, but with some key differences. When cells pass through the fluidics in a stream, they are illuminated so that brightfield images can be captured. Upon exposure to a variety of different lasers the emitted fluorescence is captured by a microscope and also then broken down by a spectral decomposition component into defined regions of wavelength, which are detected by a charge coupled device (CCD) camera with six channels (Figure 1.12). The CCD camera maintains a high level of resolution and sensitivity, even when cellular events are being acquired at 100 per second, due to the presence of time delay integration (TDI) mode. This feature allows the detector to track object motion, and avoid image streaking, thereby preserving image quality even with fast movement from cells (George *et al.*, 2004; Voronin *et al.*, 2020).

The ability of the IFC to breakdown collected cell images spectrally into subimages, including both fluorescence and brightfield, provides the basis to the benefits of using imaging flow cytometers over traditional flow cytometers. For one, it allows quantification of separate signals coming from

overlapping cellular regions, and this allows information such as co-localisation of fluorescence to be collected and analysed. Additionally, due to the collection of the brightfield images of cells, IFC also allows for extensive morphological features to be gathered, for example the area of cells, perimeter details and spot count information (Zuba-Surma *et al.*, 2007). Furthermore, the ability to visualise cells from the brightfield images allows for the differentiation of internalised components, versus components only bound to the walls of cells. This is crucial when using IFC for nanoparticle cellular uptake studies (Phanse *et al.*, 2012).

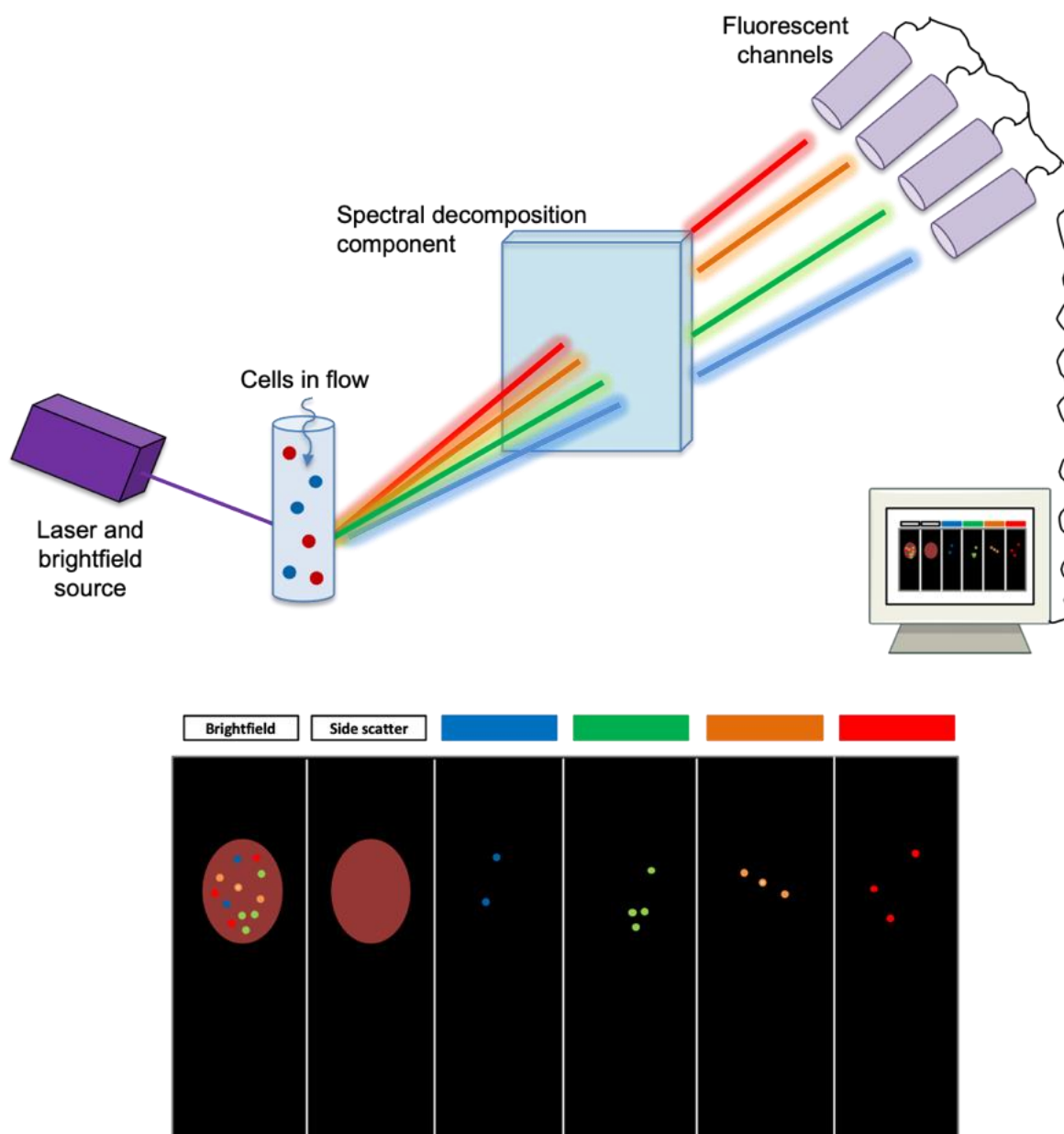


Figure 1.12 – Schematic of the imaging flow cytometry setup. Cells in flow are excited using one or more lasers, and illuminated for the purpose of brightfield microscopy. The fluorescence is captured, and broken down by a spectral decomposition component, into defined regions. A charge coupled device camera, containing six channels, captures these and allows for images to be collected. Figure adapted from Voronin *et al.* (2020).

Many examples exist within the literature of groups who have attempted to characterise nanoparticle uptake into cells. However, in most of these cases, unless the nanoparticles have an intrinsic fluorescence, they are labelled using fluorescent dyes as a means to track their movement. A paper by Münter *et al.* (2018) looking into fluorescently labelled LMs perfectly highlights the challenges this type of labelling can raise. By imaging the fluorescence signal coming from a labelled nanoparticle, it relies on the assumption that the fluorescent tag remains associated with the nanoparticle. However, it has been suggested that in fact the fluorescent tag might become dissociated from the nanoparticle, with this group reporting that between 10% - 75% of dye dissociated, of those tested. The result of this is that any image collected from the nanoparticles may be of dissociated dye, rather than of a true image of the nanoparticle itself. Furthermore, the dye may go on to bind to other types of non-specific membrane, causing false positive results (Takov *et al.*, 2017).

A solution to this problem would be to find a method that is capable of imaging nanoparticles without the need for pre-labelling them. Raman spectroscopy is an imaging platform that allows this. When a light photon interacts with a substance, it can be temporarily excited to a higher energy state. The relaxation, and return to ground energy state, can happen in one of two ways: elastically, or inelastically. During elastic light scattering, such as Rayleigh scattering, no energy is transferred to the substance, and so the wavelength of light remains unchanged. This means no information can be gathered about the substance under investigation. However, during inelastic light scattering, such as Raman scattering, there is a transfer of energy between the incident light and the substance which in turn causes a change in frequency and wavelength of detected light (Ember *et al.*, 2017). The scattered spectrum obtained, i.e. the Raman spectrum, is dependent on the substance itself, as each type of molecule has characteristic molecular vibrations due to its chemical structure (Kumamoto *et al.*, 2018).

Two types of Raman scattering exist: Stokes and anti-Stokes. Stokes scattering occurs when energy is transferred from the incident light photon to the substance which results in a scattered photon of reduced energy and therefore frequency. During anti-Stokes scattering the opposite is true, and energy is transferred from the substance to the incident photon, which occurs if the substance was in a higher energy state than the incident photon initially (Ember *et al.*, 2017). Coherent anti-Stokes Raman scattering (CARS) involves using multiple incident photons to simultaneously interact with the substance of interest, which generates far stronger signals than the standard spontaneous Raman spectroscopy - typically 10^6 times greater (Jones *et al.*, 2019). Importantly, CARS can be tuned to detect specific bonds of interest, for example carbon-hydrogen

bonds within molecules (Masihzadeh *et al.*, 2013), and specifically, in many types of nanoparticles.

1.5.6 Examples of nanoparticles used to treat bacterial infections

So far, this report has addressed challenges associated with intracellular bacteria, current treatment options and their limitations, and has also underlined the prominent mark nanotherapeutics are making on modern medicine. The types of nanoparticles that are available for use in drug delivery is far more extensive than what is possible to cover within this report, however Table 1 highlights some examples of nanoparticles which have been employed as potential delivery systems to intracellular bacterial infections.

Table 1: Examples of nanoparticles used for the delivery of antibiotics to intracellular bacterial infections.

Nanoparticle	Use	Reference
Solid lipid nanoparticles	Intracellular delivery of antibiotic enrofloxacin to RAW 264.7 macrophages infected with <i>Salmonella spp.</i>	Xie <i>et al.</i> , 2017
Gold (Au) nanoparticles	Intracellular delivery of gentamicin to RAW 264.7 macrophages infected with <i>P. aeruginosa</i> and <i>L. monocytogenes</i>	Mu <i>et al.</i> , 2016
Silver (Ag) nanoparticles	Investigated the antimicrobial effect of silver nanoparticles on <i>Brucella melitensis</i> residing intracellularly within murine peritoneal macrophages	Alizadeh <i>et al.</i> , 2013
Silica xerogel nanoparticles	Used for gentamicin delivery for <i>in vivo</i> reduction of <i>Salmonella enterica</i> in the livers and spleens of mice	Seleem <i>et al.</i> , 2009
Polymeric nanoparticles	Intracellular delivery of gentamicin using poly(lactic-co-glycolic acid) nanoparticles to <i>B. melitensis</i> infected THP-1 macrophages	Imbuluzqueta <i>et al.</i> , 2013
Polymer-drug conjugates	Intracellular delivery of penicillin, bound to a polymer backbone, to <i>S. aureus</i> infected RAW 264.7 macrophages.	Abed <i>et al.</i> , 2015

The remainder of this section will focus on research on the use of LMs and PMs to encapsulate antibiotics to target these kinds of infections. The use of LMs for antibiotic encapsulation has been well documented. This may be due to the fact that many LM types are FDA approved and already clinically in use, giving an incentive to use them in drug delivery research. Many different classes of antibiotic have successfully been encapsulated within LMs for *in vivo* effect, including: β -lactams, aminoglycosides and fluoroquinolones (Pinto-Alphandary *et al.*, 2000).

In 1985, Bakker-Woudenberg and colleagues showed that encapsulating antibiotics within LMs could improve antibiotic efficacy. The team demonstrated that liposomal encapsulated ampicillin was more effective than the same dose of free drug when used to treat intracellular *L.*

monocytogenes. The primary target organs for *L. monocytogenes* infections are the liver and spleen. Mice were infected with the bacteria, and then administered ampicillin at various timepoints. LM encapsulated ampicillin was administered in 2 doses (at 0.27 mg), totalling 0.54 mg, whereas free drug was administered in 8 doses (at 6 mg), totalling 48 mg. One control sample received empty LMs, while the other received 2 doses of free ampicillin at 0.27 mg, the same as used in the LM encapsulated samples. By the end of the study it was found that the liver and spleen were free of bacteria, after 0.54 mg of liposomal ampicillin and after 48 mg of free ampicillin. Empty LMs had no effect on the infection progress. Importantly, the levels of bacteria cultured from mice treated with 0.54 mg of free ampicillin were not significantly different from mice which received no treatment. This study displays how encapsulation of the antibiotic ampicillin increases the efficacy by around 90-fold (Bakker-Woudenberg *et al.*, 1985). Not only does this study highlight how less antibiotic can be used if encapsulated, it also demonstrates how they can be used at lower doses, 2 doses compared to 8. This is positive in terms of potential future patient compliance, as it means fewer doses may have to be administered.

Since those early liposomal studies, a number of FDA approved formulations are being used in the clinic. Largely, these are for the treatment of cancers, however there are antibiotic options in the pipeline. One example is Arikace[®], which as of 2018 was granted FDA approval for its clinical use (Fatima *et al.*, 2018). The preparation is made from DPPC lipids and cholesterol, and encapsulates the antibiotic amikacin, an aminoglycoside. Arikace[®] is being used to treat patients with bacterial lung infections caused by non-tuberculosis *Mycobacteria* (Shirley, 2019). The LM-amikacin preparations were found to achieve a five- to eight-fold increase in alveolar macrophage uptake of amikacin, compared to administration of free amikacin (Zhang *et al.*, 2018). Furthermore, the LMs were found to allow sustained release of amikacin in the lungs, without displaying a systemic exposure to the antibiotic – highly important for limiting resistance (Griffith *et al.*, 2018). The LM-encapsulated antibiotic also possesses a longer half-life within the body than the free drug counterparts, useful for achieving lower doses of the drug (Clancy *et al.*, 2013).

Multiple other studies over the years have investigated the use of LMs for the delivery of antibiotics to intracellular infections. Fierer *et al.* (1990) demonstrated that LM-encapsulated gentamicin could be used to treat *Salmonella dublin* infections. It was found that eight out of ten infected mice survived after a single injection of the LM formulation, whereas no infected mice survived when given the same dosing of free gentamicin. Similarly, Vitas *et al.* (1997) showed that gentamicin loaded into positively charged LMs produced a protective effect on *Brucella abortus* infected mice. Infected mice treated with free gentamicin, or negatively charged gentamicin LMs, did not see this protective result. It is known that aminoglycosides, like gentamicin, are poorly

effective at crossing the host cell membrane barrier usually. The results from these studies are exciting, as they highlight how LMs, and potentially other nanoparticles, can be used to deliver drugs to intracellular locations, which may not have the ability to in free form. Furthermore, this has the potential to work for a range of other antibiotics, and ultimately increase the number of antibiotics available to treat intracellular pathogens.

Another avenue of liposomal research being undertaken is the use of these nanoparticles to achieve co-delivery of drugs. Eloy *et al.* (2016) used DSPE and cholesterol based LMs to encapsulate the drugs paclitaxel and rapamycin, with the aim of using them for breast cancer treatment. Results demonstrated that the co-loaded LMs were more cytotoxic to 4T1 breast cancer cells than the free drugs. The drugs acted more synergistically when delivered together in LMs, compared to when delivered together in free form. These results are promising as although they focused on drugs for cancer treatment, there is nothing to say the same principle cannot be applied to a bacterial scenario. In fact, this has already been shown using the co-delivery of antibiotics in other types of systems, namely polymer based PLGA nanoparticles. Here, Toti *et al.* (2011) loaded azithromycin and rifampin into the nanoparticles to treat intracellular *Chlamydia trachomatis* infection. Similar to other studies the results showed that the nanoparticle encapsulated antibiotics were more effective at reducing bacterial growth than their combined free counterparts.

PMs have been shown to be able to be functionalised to better target them to desired locations. Egli and colleagues in 2011 showed how active targeting could be achieved by adding chemical groups onto the PM surfaces. They used poly(dimethylsiloxane)-block-poly(2-methylloxazoline) (PDMS-b-PMOXA) copolymers to form the PMs. This copolymer contains secondary amine groups at the hydrophilic terminus, allowing surface-exposed amine groups upon PM formation. These amine groups allow the polymer to be modified via the attachment of a succinimidyl 4-formylbenzoate (NHS-4FB) group. Similarly, the ligand intended for conjugation is modified via the attachment of a succinimidyl 6-hydrazinonicotinate acetone hydrazone (NHS-HyNic) group. The two groups, NHS-4FB and NHS-HyNic, are complementary reactive parts, and so can join together to result in a linkage between the PMs and the desired ligand (Egli *et al.*, 2011) (Figure 1.13). In this example, the linkers were used to attach antibodies which directed the PMs towards human breast cancer cells, however the same principles could be applied to the targeting of bacterial infected cells.

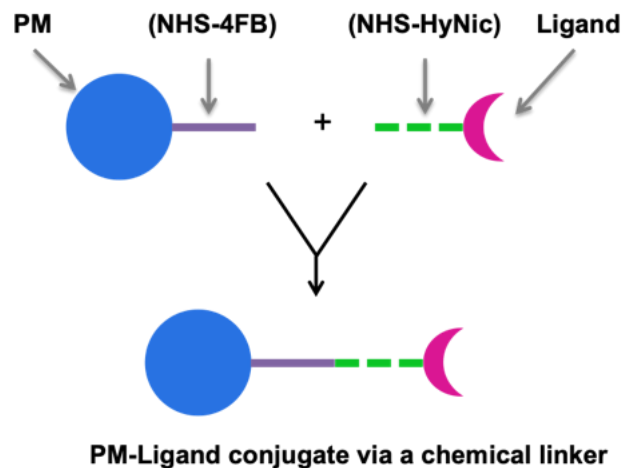


Figure 1.13 – An illustration of chemical linkers being used to attach ligands to PMs, aiding their specific targeting. Here, chemical group NHS-4FB was used to modify the PM, whilst NHS-HyNic modified the ligand. These groups are reactive complements to one another, and so can be joined to bring the PM into association with the ligand. This final conjugate can be used to better aid the PMs to reach their desired target destination, as the ligands will display affinity for target host cell receptors. Figure adapted from Egli *et al.* (2011).

The remainder of this section will focus on the use of PMs to deliver antibiotics to intracellular bacterial infections. Wayakanon and colleagues, in 2013, investigated *Porphyromonas gingivalis*, which can invade oral epithelial cells and cause periodontitis. Multiple antibiotics are effective at killing these bacteria *in vitro*, but due to limitations in traversing the cell membrane, are less effective at *in vivo* killing. This team used PMs composed of poly[2-(methacryloyloxy)ethyl phosphorylcholine] (PMPC) and poly[2-(di-isopropylamino)ethyl methacrylate] (PDPA) block copolymers, and packaged antibiotics metronidazole and doxycycline. The PMPC component allowed interaction with endocytosis-associated receptors on the host membrane, whilst the PDPA component was sensitive to pH – a decrease in pH below 6.4 caused the PMs to dissociate. As the pH within early endosomes is ≈ 6.2 , this caused the PMs to dissociate once inside these compartments. It is believed that the event of the PMs dissociating causes enough of an osmotic shock within the compartments to temporarily disrupt the membrane integrity and allow the PM payload to be released into the cell cytoplasm. The results from this study followed the pattern of previously described papers, in that the PM-encapsulated antibiotics studied had significantly more of an effect on reducing bacterial burden than their free counterparts, or control tests used. Similar also to the work conducted using LMs, this study demonstrates how PMs can be used to successfully deliver certain types of antibiotics intracellularly which would not normally have access to these sites (Wayakanon *et al.*, 2013).

Chapter 1: Introduction

Other examples of using PMs for intracellular antibiotic delivery include using pH-sensitive block copolymers for targeting macrophage-residing *B. thailandensis*, similarly to this project (Lane *et al.*, 2015). More recently, another variation of pH-sensitive PMs were used to load a range of different antibiotics for the targeting of *S. aureus* and *M. tuberculosis* in both *in vitro* and *in vivo* settings (Fenaroli *et al.*, 2020). These key papers are discussed in greater detail in Chapter 5. Whilst the work reported from these groups shows a large overlap with the aims of this project, some limitations to their work exist. The seemingly sophisticated pH-sensitive PMs used rely on complex polymer chemistry, which translates to complicated, and often time-consuming, nanoparticle synthesis using materials that in many cases have yet to obtain FDA approval. There is a need for PMs made from simple, FDA-approved polymers, which are straightforward to produce.

The end goal of using nanoparticles for antibiotic delivery would be to enable the repurposing, through the repackaging, of antibiotics which are currently otherwise rendered useless for intracellular infections due to poor bioavailability. If this could be achieved the number of antibiotic treatment options 'on the shelf' would increase, whilst simultaneously offering a more targeted approach, protecting commensal host bacteria from the antibiotic's effects, and limiting resistance selection pressures.

For this PhD project the use of PMs for antibiotic loading and drug delivery to intracellular infection sites was investigated. PMs were composed of the block copolymer poly(ethylene oxide-*b*-caprolactone) (PEO-PCL). It was hypothesised that these PMs, made from simple and FDA-approved materials, would be able to stably encapsulate antibiotics and deliver them to the specific intracellular locations. It was reasoned that the intracellular acidic and enzymatic conditions would be sufficient for antibiotic release without the need for complex polymer chemistries. This thesis provides, for the first time, evidence of intracellular targeting and killing of *B. thailandensis* as a result of PEO-PCL PM antibiotic delivery.

1.6 Hypotheses and aims

The overarching hypothesis of this project was that nanoparticles, specifically PMs, can be used to deliver antibiotics intracellularly within mammalian macrophage cells, and reduce the levels of *Burkholderia thailandensis*, with a view to applying this in the future to the potential biothreat pathogen *B. pseudomallei*. Future delivery of PMs will likely follow the intravenous administration route.

The project, over the course of the three years, tested three different hypotheses with target objectives for each:

Hypothesis One

- PEO-PCL PMs can successfully encapsulate antibiotics
 - ❖ Objectives
 - To assess the minimum inhibitory concentration (MIC) of a range of different antibiotics against *B. thailandensis*, to determine viable antibiotics for encapsulation. Performed using optical density (OD) as a bacterial growth measurement
 - To determine the optimal loading of antibiotics into PMs using UV-vis
 - To determine the retention of these drugs by the PMs, using UV-vis and high-performance liquid chromatography (HPLC) methods
 - To assess the sizes of the PM-antibiotic formulations using both dynamic light scattering (DLS) and transmission electron microscopy (TEM) methods.

Hypothesis Two

- PEO-PCL PMs can be taken up intracellularly, into cells such as RAW 264.7 macrophages
 - ❖ Objectives
 - Use dye-labelled nanoparticles to visualise uptake into both healthy and *B. thailandensis* infected RAW 264.7 macrophages, using epifluorescence and confocal microscopy imaging techniques
 - To assess the level of direct intracellular co-localisation observed between green fluorescent protein (GFP) tagged *B. thailandensis*, and dye-labelled PMs, using ImageStream imaging flow cytometry
 - To use coherent anti-Stokes Raman spectroscopy (CARS) technology to assess PM uptake into healthy RAW 264.7 cells without a need for prior PM labelling.

Hypothesis Three

- PEO-PCL PMs can inhibit the growth of intracellular *B. thailandensis*
 - ❖ Objectives
 - To assess whether PM-antibiotic preparations can inhibit the growth of free growing *B. thailandensis*, using OD as a readout
 - To determine whether PM-antibiotic preparations can be broken, using a variety of methods, in order to release their antibiotic payload

Chapter 1: Introduction

- To assess whether PM-antibiotic preparations can inhibit the growth of *B. thailandensis* growing intracellularly within RAW 264.7 macrophages, using colony forming unit (CFU) counts as a readout
- To select a range of antibiotics which are unable to penetrate host cells, encapsulate them within PMs, and assess whether their intracellular killing is improved through PM encapsulation.

Chapter 2: Materials and Methods

Chapter 2: Materials and Methods

2.1 Materials

2.1.1 Polymersome production

Table 2: Overview of the different reagents needed for PM preparation.

Reagent	Description	Supplier
Poly(ethylene oxide(5000)-b-caprolactone(18,000))	The amphiphilic block copolymer used to form the PMs. Assembles once dropped into solution.	Polymer Source Inc., Canada
Dimethylformamide (DMF)	Used to dissolve the polymer.	Sigma-Aldrich, UK
Phosphate buffered saline (PBS)	Solution the PMs are dropped into. Makes up the aqueous core component of the PMs.	Oxoid, UK
Dialysis tubing (10,000 MWCO)	Allows for the filtration of DMF from the PM mix. DMF harmful to cells and so must be removed. Allows for removal of any un-encapsulated drug left in solution, but not incorporated within PMs.	Sigma-Aldrich, UK
DiD	A lipophilic membrane dye used to stain PMs for fluorescence tracking purposes.	Fisher Scientific, UK
Dil	A lipophilic membrane dye used to stain PMs for fluorescence tracking purposes.	Fisher Scientific, UK
Fluorescein	Used to visualise payload release from PMs.	Sigma-Aldrich, UK
Ferrocene	Loaded into PMs used for transmission electron microscopy (TEM) analysis.	Sigma-Aldrich, UK

2.1.2 Antibiotics

Table 3: Overview of the different antibiotics used for bacterial assays and PM production.

Reagent	Description	Supplier
Levofloxacin	Varying concentrations were used, either dissolved in PBS or DMF. Used to assess encapsulation into PMs.	Sigma-Aldrich, UK
Doxycycline hyclate	Varying concentrations used, with the antibiotic dissolved in PBS or DMF. Used to assess encapsulation into PMs.	Sigma-Aldrich, UK
Rifampicin	Varying concentrations used, with the antibiotic dissolved in DMF. Used to assess encapsulation into PMs.	Sigma-Aldrich, UK
Novobiocin sodium salt	Varying concentrations used, with the antibiotic dissolved in PBS or DMF. Used to assess encapsulation into PMs.	Sigma-Aldrich, UK
Gentamicin sulphate salt	Used at a PM loading concentration of	Sigma-Aldrich, UK

	50 mg/ml, with the antibiotic dissolved in PBS. Used to test encapsulation of antibiotics with poor intracellular bioavailability.	
Piperacillin sodium salt	Used at a PM loading concentration of 50 mg/ml, with the antibiotic dissolved in PBS. Used to test encapsulation of antibiotics with poor intracellular bioavailability.	Sigma-Aldrich, UK
Biapenem	Used at a PM loading concentration of 5 mg/ml, with the antibiotic dissolved in PBS. Used to test encapsulation of antibiotics with poor intracellular bioavailability.	Sigma-Aldrich, UK
Tobramycin sulphate salt	Used at a PM loading concentration of 50 mg/ml, with the antibiotic dissolved in PBS. Used to test encapsulation of antibiotics with poor intracellular bioavailability.	Sigma-Aldrich, UK
Sisomicin sulphate salt	Used at a PM loading concentration of 50 mg/ml, with the antibiotic dissolved in PBS. Used to test encapsulation of antibiotics with poor intracellular bioavailability.	Sigma-Aldrich, UK
Kanamycin sulphate	Used at a PM loading concentration of 100 mg/ml, with the antibiotic dissolved in PBS. Used to test encapsulation of antibiotics with poor intracellular bioavailability.	Sigma-Aldrich, UK
Kanamycin solution	Stock solution at 50 mg/ml and stored in the fridge at 4°C. Used at a concentration of 1 mg/ml. Antibiotic used within assays to kill extracellular bacteria.	Sigma-Aldrich, UK
Chloramphenicol	Stock solution at 50 mg/ml and stored in the freezer at -22°C. Used at a concentration of 50 µg/ml. Antibiotic applied to bacterial broth culture to ensure <i>B. thailandensis</i> E555 GFP retains its GFP gene, encoded for on a plasmid containing chloramphenicol resistance.	Sigma-Aldrich, UK

Table 4: Overview of the physicochemical properties of the antibiotics used within this project.

Antibiotic	logP	pKa	Water solubility	Intracellular bioavailability	References
Levofloxacin	-0.02 to 0.7	6.3	Soluble, 1.44 mg/ml reported	✓	Drugbank
Doxycycline hyclate	-3.3 to -0.3	3.5 to 9.5	Soluble, 50 mg/ml reported	✓	Drugbank Sigma-Aldrich (Jantratid <i>et al.</i> , 2010)
Rifampicin	2.7 to 3.9	6.9 to 7.5	Soluble, 2.5 mg/ml reported	✓	Drugbank Sigma-Aldrich
Novobiocin sodium salt	1.4 to 3.5	-3.3 to 11.1	Soluble, 0.02 mg/ml reported	✓	Drugbank (Mattern and Scudiero, 1981; Zhao <i>et al.</i> , 2003)
Gentamicin sulphate salt	-4 to -2.2	9.9 to 12.6	Soluble, 50 mg/ml reported	Poorly	Drugbank Sigma-Aldrich
Piperacillin sodium salt	-0.3 to 1.2	-4.3 to 3.5	Soluble, 50 mg/ml reported	Poorly	Drugbank Sigma-Aldrich
Biapenem	-6.1 to -2	-1.6 to 3.5	Soluble, 5 mg/ml reported	Poorly	Drugbank Sigma-Aldrich
Tobramycin sulphate salt	-6.5 to -3	9.8 to 12.5	Soluble, 50 mg/ml reported	Poorly	Drugbank Sigma-Aldrich
Sisomicin sulphate salt	-4.3 to -2	9.9 to 12.6	Soluble, 20 mg/ml reported	Poorly	Drugbank MedChemExpress
Kanamycin sulphate	-7.1 to -3.1	9.8 to 12.1	Soluble, 50 mg/ml reported	Poorly	Drugbank Sigma-Aldrich
Kanamycin solution	-7.1 to -3.1	9.8 to 12.1	Soluble, 50 mg/ml	Poorly	Drugbank Sigma-Aldrich
Chloramphenicol	0.9 to 1.2	-2.8 to 7.5	Soluble, 2.5 mg/ml reported	✓	Drugbank Sigma-Aldrich (Jacobs and Wilson, 1983)

2.1.3 Bacterial assays

Table 5: The different materials and reagents used for various bacterial assays.

Reagent	Description	Supplier
<i>Burkholderia thailandensis</i> E555 pBHR4-groS-eGFP	Category 2 bacterial model organism. GFP tagged strain. Grown in the presence of 50 µg/ml chloramphenicol to ensure plasmid maintenance. Bacterial stocks were stored at -80°C until use, or streaked onto agar plate seed stocks and once grown left in the fridge at 4°C. The bacterial strain was supplied by the University of Exeter, but plasmid construction details remain unpublished.	Exeter University
RAW 264.7 macrophages	Cell model chosen for investigating intracellular infections.	Public Health England, Porton Down
Luria broth (L-broth)	Used to culture the bacteria.	Defence Science and Technology Laboratory, Porton Down
Dulbecco's modified Eagle's medium (DMEM) (+ 10% inactivated foetal calf serum and 2mM L-glutamine)	Used to culture the RAW 264.7 macrophages.	Gibco, UK
Trypan blue	Used in the process of counting cells.	Sigma-Aldrich, UK
L-15 media	Used as culture medium for infection assays	Gibco, UK
PBS (x10 dilution from stock)	Used largely as a vector control.	Gibco, UK
10% sodium hypochlorite	All bacterial work was performed on a cloth soaked with sodium hypochlorite.	Sychem, UK

2.1.4 Other reagents used

Table 6: Other chemical reagents used over the course of the project so far.

Reagent	Description	Supplier
Potassium dihydrogen phosphate	HPLC mobile phase buffer A component. Stored at room temperature.	Fisher Scientific, UK
Potassium hydroxide	HPLC mobile phase buffer A component. Stored at room temperature.	Sigma-Aldrich, UK
Acetonitrile	HPLC mobile phase buffer B component. Also used to assess possible PM disruption. Stored at room temperature.	Fisher Scientific, UK
Methanol	HPLC mobile phase buffer B component. Stored at room temperature.	Fisher Scientific, UK
Hydrochloric acid	Used for pH adjustments.	Sigma-Aldrich, UK
Sodium hydroxide	Used for pH adjustments.	Sigma-Aldrich, UK

0.5% paraformaldehyde (PFA)	Used to fix cells before imaging.	Sigma-Aldrich, UK
Hoechst 33342	Nuclear marker.	Fisher Scientific, UK
Lysotracker	Lysosomal marker.	Fisher Scientific, UK

2.1.5 Equipment

Table 7: Equipment used within the project

Equipment	Description	Supplier
Syringe pump	Used in the production of PMs	World Precision Instruments, UK
NanoDrop 2000c	A UV-vis spectrophotometer used to assess antibiotic payload concentrations within PMs	Thermo Fisher, UK
Optima Max-XP Ultracentrifuge	Used to pellet PMs	Beckman Coulter, USA
Zetasizer Nano ZS ZEN3600	A dynamic light scattering machine used to assess PM hydrodynamic size	Malvern, UK
ImageStream [®] X MkII	Imaging flow cytometer used within PM and <i>B. thailandensis</i> co-localisation assays.	Amnis, USA
Zeiss LSM 710	A confocal microscope used to assess the uptake of PMs into RAW 264.7 macrophage cells.	Zeiss, Germany
Zeiss Axio Imager.M2m	An epifluorescence microscope used to assess the uptake of PMs into RAW 264.7 macrophage cells.	Zeiss, Germany
Nanoimager S	A super resolution microscope used to assess the real-time uptake of PMs into RAW 264.7 macrophage cells.	Oxford, UK
Coherent anti-Stokes Raman scattering (CARS) imager	A label-free imaging method used to assess PM uptake into RAW 264.7 macrophage cells.	Southampton, UK
Agilent HPLC machine	Used to assess the retention of antibiotic levofloxacin within PMs over a one-week period.	Agilent, USA
FluoroMax-4 fluorometer	Used to measure the levels of fluorescein as an indication of PM disruption.	Horiba Scientific, UK
Multiskan [™] FC OD plate reader	Used to assess the growth of <i>B. thailandensis</i> over 24-hour periods.	Thermo Fisher, UK
Genesys 10 UV scanning spectrophotometer	Used to assess the optical density of <i>B. thailandensis</i> , and subsequently dilute to appropriate titres for experimental assays.	Thermo Fisher, UK

2.2 Methods

2.2.1 Polymersome production – encapsulation of drug cargo

PMs were made by first dissolving 6 mg of polyethylene oxide(5k)-b-polycaprolactone(18k) (PEO-PCL) in 0.4 ml of dimethylformamide (DMF). The solution was then sonicated for \approx 20-30 minutes to aid dissolution. The resulting solution was added dropwise using a syringe driver at 0.75 ml/min (\approx 1 drop every 8 seconds), under stirring, to a vial containing 1.6 ml of phosphate-buffered saline (PBS) (Fisher Scientific, UK). The final 2 ml solutions were then placed into sealed dialysis tubing (10,000 MWCO), and dialysed in excess PBS (500 ml). Solutions were left dialysing for a minimum of 48 hours, and included at least 3 PBS changes. Samples collected after this process were stored at 4°C until ready to be used. For antibiotic or lipophilic membrane dye loaded PMs, the reagents were dissolved into either the aqueous (PBS) or solvent (DMF) fractions at concentrations stated within the results section. Throughout this thesis, reagents dissolved into the aqueous PBS fraction are referred to as 'core loaded', and those in the solvent DMF fraction as 'shell loaded' (Figure 2.1).

PEO and PCL were chosen as the constituent polymers in this project primarily due to their FDA approval, as mentioned on page 40. The molecular weights chosen, 5k and 18k respectively, were due to the effects of molecular weight ratios on the resulting nanoparticle structures that can form. A review by Blanazs *et al.* (2009) highlights how as the ratio between hydrophilic and hydrophobic blocks changes, the resulting nanoparticle shapes also change. A range of different structures can be formed including spherical micelles, cylindrical micelles and PMs. It has been noted in the literature that increasing the size of the hydrophobic block causes formation of PM vesicles as opposed to the other structures (Oltra *et al.*, 2014). Work carried out during previous PhD projects within our research group found that this particular combination of polymers, at the stated molecular weights, resulted in the most stable preparations with the most reliable sizing.

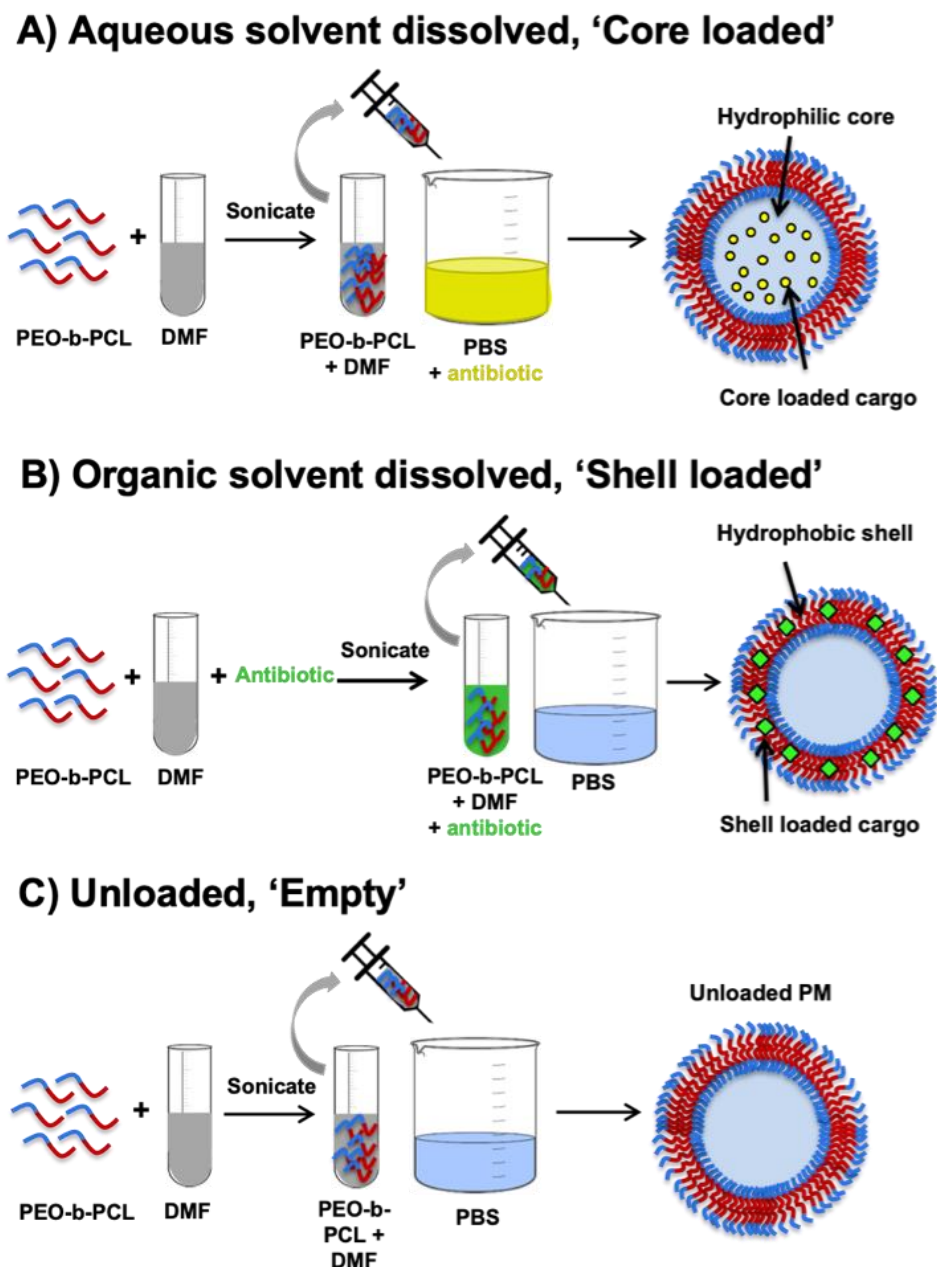


Figure 2.1 – An overview of the PM production process. (A) Core loaded preparation, (B) shell loaded preparation, and (C) unloaded PMs.

2.2.2 Polymersome characterisation

2.2.2.1 PM sizing by dynamic light scattering (DLS)

A DLS machine (Zetasizer Nano ZS ZEN3600, Malvern, UK) was used to determine the nanoparticle size and polydispersity. The nanoparticle solution was diluted 1:10 in PBS before being measured. Samples were placed into a disposable sizing cuvette, at a volume of at least 1 ml. Measurements were carried out at 25°C. Light was detected at a scattering angle of 173°. The instrument was set

up to take 10 data recordings per sample, with an acquisition of 10 seconds for each. Each sample measurement was repeated in triplicate.

2.2.2.2 PM sizing by transmission electron microscopy (TEM)

PMs were made as described in section 2.2.1, with the addition of ferrocene dissolved in the DMF organic solvent fraction to a concentration of 1 mg/ml. After the usual dialysis period, PMs were diluted 1:50 with PBS, and 5 μ l of sample placed onto a copper grid and allowed to air dry. PMs were then imaged by the University of Southampton Biomedical Imaging Unit on a Hitachi HT7700 transmission electron microscope.

2.2.2.3 Encapsulation and release using NanoDrop

The concentration of antibiotic incorporated into the PMs was determined by measuring the UV absorbance of samples on the NanoDrop 2000c UV-vis spectrophotometer (Thermo Scientific, UK). Absorbance was measured at wavelengths between 190 nm and 840 nm to determine the absorbance spectrum of the free, unencapsulated antibiotic. Multiple antibiotic samples of known concentrations were measured, and then used to construct standard curves. PM samples were diluted appropriately for the NanoDrop analysis, to ensure measured absorbance peaks fell within the linear ranges of the standard curves being used for interpolation. All NanoDrop readings were performed using black-sided quartz cuvettes. In some cases PM preparations were mixed with a 1:1 ratio of DMF to ensure PM disruption to reduce interference from nanoparticle Rayleigh scattering. To assess release of antibiotic from the nanoparticles samples were left to continuously dialyse in 500 ml PBS at room temperature, with at least seven buffer changes, over a 14-day period. At a series of timepoints, 200 μ l of the PM-antibiotic sample was taken from within the dialysis membrane, and the volume not replaced. These timepoint samples were measured using UV-vis to assess changes in antibiotic concentration within the nanoparticles over time (Figure 2.2). In all cases of PM-antibiotic concentration assessments, PM-empty samples were used as controls and the absorbance spectra of these deducted from the PM-antibiotic preparations to minimise signal interference from the polymer. To determine the presence of any remaining, un-dialysed antibiotic in the preparations, approximately 400 μ l of PM sample was spun through a centrifugal spin filter (Fisher Scientific, UK) at 14,000 x g for 10 minutes to filter PMs from their surrounding buffer. This buffer filtrate was then measured on the NanoDrop to assess for residual antibiotic signals.

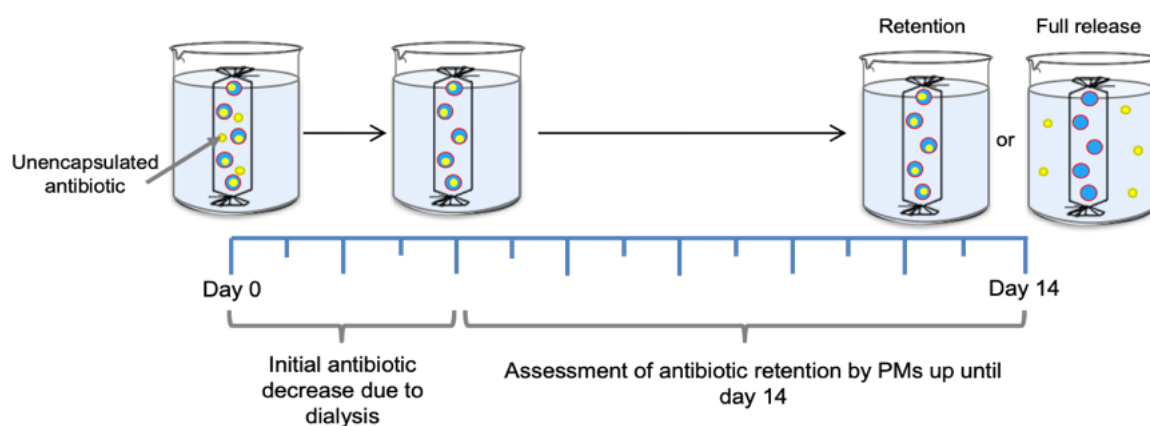


Figure 2.2 – PM-antibiotic release assay schematic. An illustration of the assay used to assess PM retention of the antibiotic over a 14-day period. Samples were left to dialyse for 14 days, with regular antibiotic concentration reading timepoints. Measurements were taken using the Nanodrop 2000c UV-vis spectrophotometer.

2.2.2.4 Encapsulation and release using high performance liquid chromatography (HPLC)

HPLC was an alternative method used to determine encapsulation and release of antibiotics from the nanoparticles, due to its high sensitivity. Nanoparticle samples, loaded with 20 mg/ml levofloxacin, were dialysed into 300 ml of PBS solution, at room temperature and under continuous stirring. At a series of timepoints over the course of 7 days, 500 μ l of the dialysate solution was removed and stored in an Eppendorf in the fridge at 4°C until further use. The volume of PBS buffer dialysate was not replaced after each removal. Dialysate samples, containing only levofloxacin which had dialysed from the dialysis bag into the buffer solution, were then taken to be analysed by HPLC (Agilent 1100). Samples were run through a reverse phase C18 stationary phase column (Agilent, US). The mobile phase was composed of 60% phosphate buffer (pH = 12.2), and 40% acetonitrile:methanol (15:25). 10 μ l of each sample was injected into the HPLC machine, and each sample was measured in triplicate. The elution peak of levofloxacin was detected by UV absorbance at 287 nm. The corresponding concentration of levofloxacin present was determined by referring to a levofloxacin standard curve, also generated using the HPLC. HPLC assays were performed using facilities at Defence Science and Technology Laboratory (DSTL), Porton Down.

2.2.2.5 Polymersome sensitivity to pH

Hydrophilic fluorescent dye, fluorescein, was included in the aqueous fraction of the PMs at a concentration of 88 μ M, and samples dialysed as described in section 2.2.1. PM-fluorescein were mixed with 100 mM hydrochloric acid until a pH of 4.5 was achieved. Samples were visually assessed for any colour changes, indicating the release of fluorescein dye from the PMs, and also measured on the NanoDrop as described in section 2.2.2.3, to detect whether a reduction in nanoparticle Rayleigh scattering was seen. PM samples were also measured using a FluoroMax-4 fluorometer to assess changes in fluorescence signal. Samples were diluted with PBS as appropriate and analysed over a range of wavelengths (increment of 0.5 nm from 480 nm to 648 nm).

2.2.2.6 Concentrating polymersomes using ultracentrifugation (UCF)

PMs were made and dialysed as described in section 2.2.1 and then transferred into balanced 1.5 ml microfuge tubes (Beckman Coulter, USA) before being loaded into an Optima MAX-XP ultracentrifuge (Beckman Coulter, USA). PM samples were spun for 2 hours at 186,000 \times g (55,000 RPM).

2.2.3 Cellular uptake assays

2.2.3.1 Cell culture

The murine mouse line RAW 264.7 macrophages were maintained in Dulbecco's modified Eagle's medium (DMEM), supplemented with 10% (v/v) inactivated fetal bovine serum (FBS) and 2 mM L-glutamine. The cells were incubated at 37°C and 5% CO₂. If cells were incubated in a non-CO₂ environment, they were switched to L-15 media supplemented in the same manner. RAW cells were subcultured by scraping at \approx 80% confluence. Cells were seeded at varying densities as described in the following sections.

2.2.3.2 Preparing a bacterial culture

B. thailandensis E555 pBHR4-groS-eGFP was grown in 50 ml of Luria broth (L-broth), or on Luria agar (L-agar) plates, both supplemented with 50 μ g/ml chloramphenicol. Broth cultures were incubated for 16-18 hours at 37°C with orbital shaking at 180 rpm. Plates were incubated at 37°C for 48 hours to allow countable colonies.

2.2.3.3 Polymersome uptake into healthy RAW 264.7 macrophages

Epifluorescence analysis: RAW 264.7 macrophage cells were seeded into a glass-bottom culture dish at a density of 42,000 cells/cm² and left overnight incubating at 37°C. Dil was dissolved into the organic phase fraction of PMs at a loading concentration of 50 µM, and after a 48-hour period of dialysis possessed an encapsulated concentration of 6.9 µM. PM-Dil were then applied to macrophage cells at 1:4 dilution to a final concentration of 1.7 µM Dil. PM-Dil and RAW 264.7 cells were left to incubate for 4 hours at 37°C. Cells were then fixed in 4% (v/v) PFA before Hoechst stain was added for 10 minutes at 1 µg/ml. Cells were imaged on a Zeiss Axio Imager.M2m at a 63x oil immersion objective. The DAPI (Hoechst) excitation filter used was: FF01-357/44-25 with an emission filter of FF01-460/80-25; the rhodamine (Dil) excitation filter used was: FF01-536/40-25 with an emission filter of FF01-593/40-25.

Nanoimager analysis: Cells were seeded as with the epifluorescence method, and PM-Dil applied at a 1:16 dilution to a final concentration of 0.4 µM, with cells in DMEM media containing LysoTracker dye to a final concentration of 75 nM. Cells were live imaged for a period of 25 minutes on a Nanoimager S super resolution microscope (Oxford Nanoimaging Ltd, Oxford, UK). The microscope was fitted with Olympus UPlanSApo 100x immersion objective (1.49 NA).

CARS analysis: RAW 264.7 macrophage cells were seeded into chambered glass coverslips at 50,000 cells/cm², using phenol-red-free DMEM media. Following a night incubating at 37°C, fresh phenol-red-free DMEM media was applied alongside PM preparations. PM-doxycycline was applied to a final antibiotic concentration of 4.5 µg/ml. Negative controls included PM-empty nanoparticles, and an untreated cell control. Positive controls included free doxycycline applied to a final concentration of 4.5 µg/ml and 20 µg/ml. Cells were left to incubate at 37°C for 21 hours. Three replicate cultures were produced.

For CARS imaging, a custom in-house built system was used. A fundamental infrared (IR) fibre laser (1031 nm, 2 picosecond, 80 MHz, Emerald Engine, APE) was coupled into a Nikon Ti eclipse inverted microscope with a 40x water immersion objective (1.15 NA). A portion of the 1031 nm IR laser was frequency doubled and used to synchronously pump an optical parametric oscillator (OPO) (APE, Levante Emerald, 650-950 nm). This created a tunable pump beam. Excitation wavelengths of 1031 nm (Stokes) and 797.2 nm (pump) were used. This made for a CARS imaging frequency of 2845 cm⁻¹ (C-H stretch). CARS signal was collected using a bandpass filter (643 ± 20 nm) and PMT (Hamamatsu H10722-20). Total power at the sample was 120 mW (80 mW pump, 40 mW Stokes). Cells were imaged live using a ChamLide TC live cell chamber with CU-109

incubation and FC-5 automatic CO₂/air mixer at 37°C and 5% CO₂. ScanImage (Vidrio Technologies) software was utilised for image acquisition. Images were acquired using a 3 by 3 tile scan, with 50% offset. This covered an area of approximately 0.1 mm². Three different points were imaged for each culture. Image tiles were stitched together in post-processing using the MIST plugin within ImageJ. CARS images were analysed to count the number and total area of white puncta present. Only the area within cell boundaries was analysed. In order to count and analyse the CARS puncta, a spot detection plugin within Icy was utilised. All CARS image collection and processing was performed by PhD student James Harrison.

2.2.3.4 Polymersome uptake into *B. thailandensis* infected RAW 264.7 macrophages, and their bacterial co-localisation

Confocal assay: RAW 264.7 cells were seeded at a density of 1.25×10^5 cells/cm² (2.5×10^5 cells/ml) and incubated overnight at 37°C to ensure the following day cell density was 2.5×10^5 cells/cm² (5×10^5 cells/ml). To infect cells with *B. thailandensis* bacteria were diluted in L-15 medium to a concentration of 5×10^7 bacteria/ml, measured using a Genesys 10 uv scanning spectrophotometer (Thermo Fisher, UK), and applied to cells for a period of 1 hour (multiplicity of infection (MOI) = 100). Following this, media was changed and kanamycin added at a concentration of 1 mg/ml to kill extracellular bacteria. DiD was loaded into PMs at a loading concentration of 50 µM, and after dialysis had an encapsulated concentration of 7.2 µM. PM-DiD were then added to the infected cell culture at a 1:10 dilution to give a final concentration of 0.72 µM. Cells and PMs were incubated for 3 hours, and then fixed using 0.5% (v/v) PFA, prior to imaging. Cells were imaged with a Zeiss LSM 710 confocal microscope (Zeiss, Germany), at a x63 objective. Confocal assays were performed using facilities at DSTL, Porton Down.

Imaging flow cytometry (ImageStream): RAW 264.7 macrophages were seeded into a 24-well plate at 2.5×10^5 cells/cm² (5×10^5 cells/ml) and left overnight to incubate at 37°C to ensure a cell density of 5×10^5 cells/cm² (1×10^6 cells/ml) by the following day. *B. thailandensis* culture was diluted, using L-15 media, to a concentration of 1×10^8 bacteria/ml (MOI = 100). This was added to the cells and left to incubate for 1 hour, to allow bacterial infection of the cells. The media was then removed, and a kanamycin (1 mg/ml)/L-15 solution added to the wells, before cells were left to incubate for a further 3 hours. PM-DiD were applied at a 1:10 dilution to a final concentration of 0.72 µM. Cells were left to incubate for 3 or 21 hours before being fixed in 0.5% (v/v) PFA and collected for imaging flow cytometry analysis. Control groups included infected cells in the absence of PMs, and cells containing PMs but with no prior bacterial infection. Imaging was performed using an ImageStream[®]X MkII (ISX, Amnis, Seattle, USA). Cells were imaged at a 60x

magnification with an image resolution of 0.3 $\mu\text{m}/\text{pixel}$, and a 2.5 μm optical slice image of cells. 10,000 cellular events were acquired for each sample set. Data was collected from the relevant channels, including Channel 01 (brightfield camera), Channel 02 (488 nm laser power: 100 mW, for *B. thailandensis* eGFP visualisation), and Channel 11 (642 nm laser power: 150 mW, for DiD visualisation). Single stain controls were used to calculate and apply a compensation matrix to all collected data presented. Presented images are all displayed using the same imaging parameters. Data was analysed using IDEAS[®] version 6.2 software (Luminex, USA). Of the cells acquired, only those in focus were selected, and PM positive cells were defined by gating relative to untreated cells. Imaging flow cytometry assays were performed using facilities at DSTL, Porton Down.

2.2.4 Bacterial inhibition assays

2.2.4.1 Optical density (OD) assays

A culture of *B. thailandensis* was prepared, as described in section 2.2.3.2, and then diluted in L-broth to a concentration of 1×10^6 bacteria/ml, using a Genesys 10 UV scanning spectrophotometer (Thermo Fisher, UK). 100 μl of this bacterial culture was added to the wells of a 96-well plate, alongside L-broth and the antibiotic, or PM-antibiotic sample, being tested for its efficacy against *B. thailandensis*, to give final well volume of 200 μl . The plate was left in a Multiskan[™] FC optical density (OD) plate reader (Thermo Fisher Scientific, UK) for 24 hours at 37°C, with OD readings being taken every 15 minutes (Figure 2.3). Each antibiotic, or PM-antibiotic, condition was performed with three technical repeats. Optical density bacterial inhibition assays were performed using facilities at DSTL, Porton Down.

2.2.4.1.1 Free antibiotic and *B. thailandensis* MIC assay

The OD assay plate was set up as described in section 2.2.4.1. Antibiotics were serially diluted along the plate to final concentrations between 0 – 100 $\mu\text{g}/\text{ml}$.

2.2.4.1.2 Old versus new antibiotic efficacy

Rifampicin and doxycycline were made up to a concentration of 1 mg/ml; one assay used samples made fresh, day 0, and the other compared the bacterial inhibition efficacy of samples at day 7. Day 7 samples were stored in the fridge at 4°C until use. Antibiotics were serially diluted along the plate so that final concentrations of 0 – 6.25 $\mu\text{g}/\text{ml}$ of doxycycline and 0 – 50.0 $\mu\text{g}/\text{ml}$ of rifampicin were tested. These concentration ranges were chosen based on data from the MIC assays conducted. A negative control of L-broth media only, and positive control of *B. thailandensis* minus any antibiotic were also included.

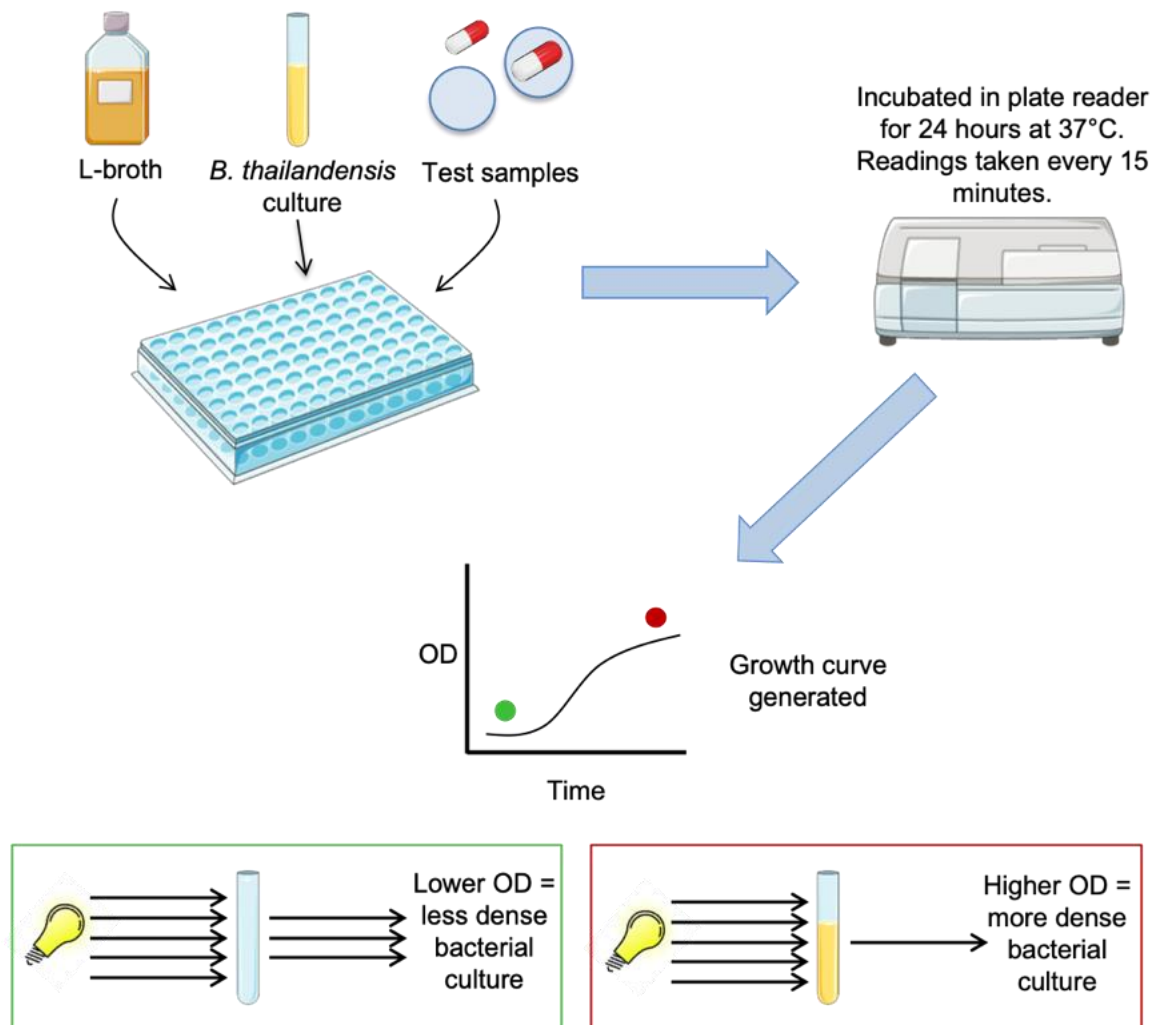


Figure 2.3 – An illustration of the bacterial OD assay setup. Wells were cultured with L-broth, *B. thailandensis* E555 GFP and the antibiotic sample being tested, either free drug or PM loaded, at a range of concentrations. They were incubated for 24 hours in a plate reader, with OD readings being taken every 15 minutes.

2.2.4.1.3 PM-loaded antibiotic and *B. thailandensis* assay

PM-doxycycline and PM-rifampicin were serially diluted to give concentrations ranging between 0 – 7.6 $\mu\text{g}/\text{ml}$ and 0 – 4.25 $\mu\text{g}/\text{ml}$, respectively. Negative controls of L-broth only, and PM-empty, and a positive control of free antibiotic (0.04 – 100 $\mu\text{g}/\text{ml}$) were also included. The filtrate of each PM-antibiotic sample was also tested to determine whether any unencapsulated antibiotic remained within preparations that could contribute to any bacterial growth inhibition observed.

2.2.4.1.4 Broken PM-antibiotic and *B. thailandensis* assay

DMF: PM-antibiotic samples were made and then pelleted as described in sections 2.2.1 and 2.2.2.6, respectively. Supernatant was discarded and the residual pellet volume was resuspended in equivolume DMF. PBS was then added to make the final volume up to 350 μl , to ensure enough

sample for the OD plate assay to be performed in triplicate. The concentration of the 350 μ l starting solution was measured on the NanoDrop 2000c UV-vis spectrophotometer. Control samples included PM-empty nanoparticles, a PBS:DMF vehicle control, free antibiotic and free antibiotic in PBS:DMF at the same ratio as in PM samples.

98°C/65°C heating: PM-doxycycline samples were made and pelleted, as previously. The pellet was resuspended in 400 μ l of PBS and then heated at either 98°C or 65°C for approximately 8 hours. Control samples included PM-empty heated to 98°C/65°C, free doxycycline 0 – 12.5 μ g/ml heated to 98°C/65°C, and free doxycycline 0 – 12.5 μ g/ml unheated. As the PM-doxycycline samples were not measured on the Nanodrop beforehand, starting concentrations were unknown.

2.2.4.2 PM-loaded antibiotic and intracellular *B. thailandensis* assay

RAW 264.7 macrophages were seeded into a 24-well plate at 2.5×10^5 cells/cm² (5×10^5 cells/ml) and left overnight to incubate at 37°C to ensure a cell density of 5×10^5 cells/cm² (1×10^6 cells/ml) by the following day. *B. thailandensis* culture was diluted, using L-15 media, to a concentration of 1×10^7 bacteria/ml. This was added to the cells and left to incubate for 1 hour, to allow bacterial infection of the cells. The media was then removed, and a kanamycin (1 mg/ml)/L-15 solution added to the wells along with the PM-antibiotic preparations. PM-doxycycline was applied corresponding to final concentrations of antibiotic ranging from 0.75 – 4.5 μ g/ml, and PM-rifampicin at 2.6 μ g/ml. PMs were incubated for a period of 3 or 21 hours and then cells were lysed and 100 μ l of lysate plated onto agar plates for quantification of bacterial colony forming units. Negative controls included wells with PM-empty nanoparticles, and wells containing cells only. A positive control of free antibiotic alone was also tested. All control groups contained the same level of PBS as in the PM-antibiotic samples, as a vehicle control to ensure PBS had no effect itself. Agar plates were incubated at 37°C for 48 hours before being counted (Figure 2.4). Intracellular killing bacterial inhibition assays were performed using facilities at DSTL, Porton Down.

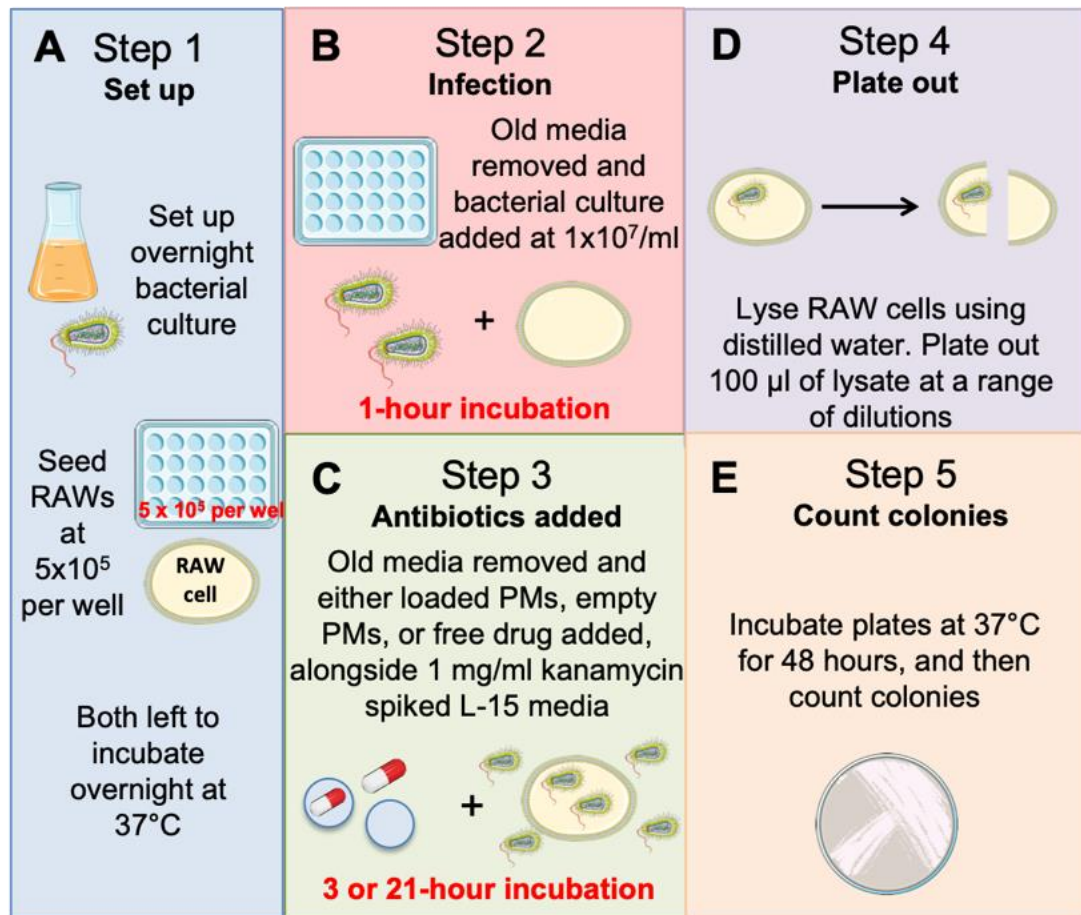


Figure 2.4 – A step-by-step illustration of the intracellular killing assays. (A) An overnight bacterial culture was prepared, and RAW 264.7 macrophage cells were seeded into a 24-well plate at 500,000 cells per well; (B) RAW cells were infected with *B. thailandensis* E555 GFP for 1 hour; (C) antibiotic samples were applied as either free drug, PM-loaded drug, or empty PMs as a control. Kanamycin was present at 1 mg/ml to kill extracellular bacteria; (D) RAW cells were lysed and any persisting intracellular bacteria was plated out onto agar plates; (E) after 48 hours incubating the colonies on the plates were counted to determine how effectively the antibiotic samples were at killing intracellularly.

Chapter 3: Antibiotic selection and encapsulation into polymersomes

Chapter 3: Antibiotic selection and encapsulation into polymersomes

3.1 Introduction

Whilst nanocarriers, such as polymersomes (PMs), possess a range of benefits, a large amount of characterisation must be performed to assess details such as encapsulated payload concentration. Furthermore, to become considered options for medical application, PMs must be able to achieve a stable encapsulation of their payloads. This short introduction will discuss why the antibiotics used were chosen, before moving on to present other examples of how nanoparticles for drug delivery have been formulated and characterised.

B. pseudomallei and *B. thailandensis* are both susceptible to growth inhibition by similar antibiotics. Levofloxacin was an antibiotic chosen for this project because it is an example of one which they are both sensitive to (Judy *et al.*, 2009), and one which is currently already being used for the treatment of melioidosis (Ross *et al.*, 2018). Levofloxacin's ability to treat melioidosis is largely because it can penetrate host cells. Although levofloxacin is effective against *B. pseudomallei* at low concentrations, it lacks potency compared to other antibiotics used in melioidosis treatment. One study investigated the survival of persistent populations of *B. pseudomallei* after antibiotic exposure and found ciprofloxacin to be more potent. Furthermore, the group infected mouse models with *B. pseudomallei*, and found that after 5 or 10 days of levofloxacin treatment colonisation of the lungs, livers, and spleens remained (Ross *et al.*, 2019). The encapsulation of levofloxacin inside PMs could allow better intracellular accumulation of the antibiotic, and the potential for sustained high internal concentrations. These types of dosing may aid in the elimination of hard-to-treat persisting bacterial populations, and prevent relapse of infections in the future.

Rifampicin is a bactericidal antibiotic belonging to the rifamycin class (Chiang and Starke, 2018), and functions by inhibiting bacterial transcription via the blocking of RNA polymerase. It is frequently used for the treatment of the intracellular bacteria *Mycobacterium tuberculosis*; however it can cause unpleasant side effects including gastrointestinal upset and hepatotoxicity (Hassounah *et al.*, 2016). Whilst rifampicin has been shown to have some effectiveness at treating *B. pseudomallei* *in vitro* (Cheng and Currie, 2005), it is not used clinically due to high levels of resistance (Sarovich *et al.*, 2012). By encapsulating rifampicin into PMs, there is the potential to reduce off-target side effects and also to achieve a high and sustained cell drug concentration that may allow issues of resistance to be overcome. It has been demonstrated already within the

literature that rifampicin can be encapsulated within a different type of PM to decrease the level of intracellular *M. tuberculosis* (Rizzello *et al.*, 2017), so this gives good foundations for work with rifampicin in this project.

Doxycycline has a prominent role in the treatment of clinical cases of *B. pseudomallei*. It belongs to the tetracycline class of antibiotics, and so functions by binding to the bacterial ribosomes and inhibiting protein synthesis (Raval *et al.*, 2018). In the treatment of *B. pseudomallei* patients are required to take intravenously administered antibiotics for between two to four weeks, until a clinical response is seen. After this they switch to oral antibiotics to ensure eradication of the infection, for which doxycycline has been frequently used, in combination with other drugs. This oral administration stage can last for at least three to six months (Limmathurotsakul and Peacock, 2011). In recent years doxycycline has been replaced during the eradication phase for co-trimoxazole due to fewer patient side effects being observed (Dance, 2014). A study published in 2014 found that during the oral eradication phase patients receiving a combination of co-trimoxazole and doxycycline suffered more significantly from side effects such as skin rashes and gastrointestinal disorders than patients receiving co-trimoxazole alone (Chetchotisakd *et al.*, 2014). If doxycycline could be packaged within PMs then, similarly to rifampicin, it could reduce such harmful off-target side effects and could be re-considered as a therapy to treat this infection.

Finally, novobiocin is an aminocoumarin antibiotic that works in a bactericidal manner by inhibiting DNA gyrase during bacterial replication, preventing DNA synthesis (Jara *et al.*, 2016). Due to the high levels of resistance often displayed by *B. pseudomallei*, it has been suggested that novel, repurposed, or reformulated antibiotics are necessary in order to provide treatment options. Novobiocin has been shown to display good activity against *B. pseudomallei in vitro* at relatively low concentrations (Thibault *et al.*, 2004), however despite this there is a lack of information surrounding the use of aminocoumarin antibiotics for the treatment of these infections. Within the literature possible explanations for this include their lack of solubility, as well as concerns over the emergence of resistance, and their toxicity to eukaryotic cells (Galm *et al.*, 2004). The encapsulation into nanoparticles may help to alleviate all of these challenges, and as there are no recorded examples of novobiocin being encapsulated within PMs this makes it a new and untapped avenue to explore.

Antibiotics can be loaded into PMs in a variety of ways including passively and actively. Due to their clinical success, a large amount of information exists within the literature on the different methods of loading LMs, however the same techniques can be applied to PMs. In general, passive loading involves the formation of nanoparticles into solutions already containing dissolved

payload, whereas active loading usually involves the driving of payload into preformed nanoparticles. Active loading is usually highly efficient at generating high internal nanoparticle concentrations (Sur *et al.*, 2014), as will be explored further in section 3.3. Despite this, due to the relative simplicity of sample preparation, passive loading is still widely used for nanoparticle drug formulations. For their use as drug delivery vehicles, nanoparticles must achieve the highest encapsulated concentration as possible. Whilst one approach is through active loading methods, another is to increase the concentration of nanoparticles themselves generated during formation to achieve a higher number of particles delivered per dose. One group investigated how altering the sizes of LMs affects their particle concentration, by using DLS and nanoparticle tracking analysis (NTA) as measurement techniques. It was found that LMs with larger sizes had lower particle concentrations. For example at approximately 150 nm particles had concentrations of $2.25 \times 10^{11}/\text{ml}$, versus particles of 500 nm in size having concentrations of $1 \times 10^{11}/\text{ml}$ (Ribeiro *et al.*, 2018). This suggests nanoparticles for drug delivery should be smaller in radius to ensure optimal payload delivery.

Nanoparticle stability is another key characteristic for drug delivery vehicles. PMs are thought to possess better stability than LMs due to their thicker hydrophobic membrane which renders them more impermeable to payload leakage (Discher *et al.*, 1999). One recent study formulated both LMs and PMs and compared the two for their stability, hydrodynamic radius, and their ability to encapsulate both hydrophilic and hydrophobic compounds. Although minimal variation was found in payload encapsulation efficiency of the two formulations, PMs were shown to possess smaller sizes than LMs and, likely as a result of this, experienced better uptake into HeLa cells after a 4-hour incubation. The samples were left to dialyse for a period of 8 weeks at room temperature, and LMs were shown to have a drastically reduced ability to retain payload compared to PMs, with approximately 5% and 70% being retained respectively. This was mirrored in the hydrodynamic size recordings showing PMs retained their initial sizes, whereas LMs significantly increased in size (Aibani *et al.*, 2020). This work highlights the advantages PMs have over other already established drug delivery systems, and how they can be utilised effectively for drug encapsulation.

The nanoparticle polymersomes used for this project were poly(ethylene oxide-b-caprolactone) (PEO-PCL). They were chosen due to each block being individually approved by the FDA for clinical use, thereby giving them a promising chance at bench to clinic translation (Qi *et al.*, 2013). The PMs self-assemble when exposed to an aqueous solution, such as PBS, due to their amphiphilic nature, with PEO being hydrophilic, and PCL hydrophobic (Zhu *et al.*, 2012). The presence of both hydrophilic and hydrophobic regions allows for the encapsulation of both types of drugs, those

which are readily soluble, and those less so. Any pharmaceutical drug must possess some level of water solubility, however close to 40% of drugs currently on the market, and 90% of those still in clinical trials, have poor water solubility (Kalhapure *et al.*, 2019). This makes PMs a good candidate for delivering these hydrophobic drug molecules, as high levels of drug may be packaged within PMs and delivered via this alternative route. Certainly in the case of intracellular bacterial infections there are already examples of relatively poorly water soluble antibiotics being delivered using polymeric nanoparticles (Bodaghabadi *et al.*, 2018).

This chapter will investigate the susceptibility of *B. thailandensis* to the antibiotics chosen for this project, and the encapsulation efficiency of PMs for these antibiotics. The aims of the experiments in this section are:

- To determine the minimum inhibitory concentration (MIC) of the antibiotics needed to inhibit *B. thailandensis*
- To establish a method to disrupt the PMs to enable a more accurate measurement of encapsulated drug concentration
- To assess optimal loading of the antibiotics, and the level of retention by the PMs, if any, using UV-vis and high-performance liquid chromatography (HPLC) techniques
- To assess the sizes of the PMs using both dynamic light scattering (DLS) and transmission electron microscopy (TEM) methods.

3.2 Results

3.2.1 Antibiotic selection using MIC assays

A minimum inhibitory concentration (MIC) assay was performed, as described in section 2.2.4.1.1, to determine the effect of four antibiotics on *B. thailandensis* growth inhibition. Briefly, antibiotics that had been selected as potential choices were added to *B. thailandensis* growing free in culture, at a variety of concentrations ranging from 0.05 – 100 $\mu\text{g/ml}$, and the bacterial growth was then assessed over a period of 24 hours, using optical density (OD) as a growth measurement. The data presented shows the growth levels after 24 hours. The assay was performed once for each antibiotic, but carried out in triplicate.

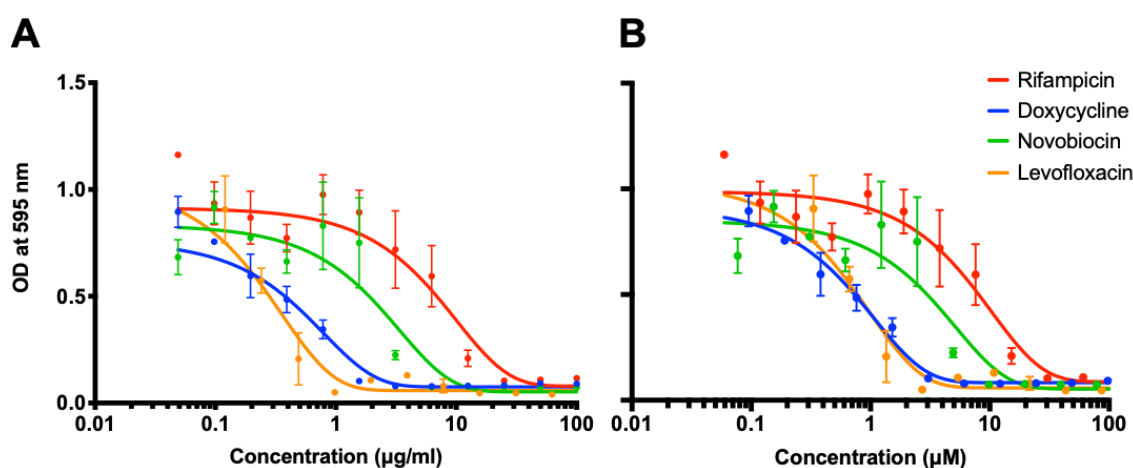


Figure 3.1 – MIC assay to test free antibiotic efficacy on *B. thailandensis* free in culture medium. (A) All four antibiotics were applied to free growing *B. thailandensis* at concentrations ranging from 0.05-100 $\mu\text{g/ml}$ and growth was assessed over 24 hours. Each antibiotic was able to successfully inhibit the growth of the bacteria when applied at the higher concentrations. (B) The same data presented as the molar concentrations to allow better comparison of antibiotic potency. Data, from the 24-hour timepoint, is presented as the mean and SEM of one biological repeat performed in triplicate, $n=1$.

The MIC curves show a dose dependent response, whereby as the concentration of drug increases the level of bacterial density decreases. The point at which the curves flatten at the bottom represents the MIC needed to inhibit the specific bacteria. All four of the antibiotics tested were able to inhibit the growth of *B. thailandensis* after a 24-hour period. Concentrations of 25.0 $\mu\text{g/ml}$ (30.4 μM), 1.56 $\mu\text{g/ml}$ (3.05 μM), 12.5 $\mu\text{g/ml}$ (19.7 μM), and 0.98 $\mu\text{g/ml}$ (2.71 μM) for rifampicin, doxycycline, novobiocin and levofloxacin, respectively, were sufficient to achieve complete growth inhibition on the free growing bacteria (Figure 3.1). This data shows us that these antibiotics are all viable choices for attempting to encapsulate into the PMs.

3.2.2 Antibiotic encapsulation and stability tests

3.2.2.1 *Disrupting the PMs for more accurate payload measurement*

PMs cause a large amount of Rayleigh scattering which can interfere with antibiotic concentration assessments made using UV-vis, if the antibiotic's characteristic peaks are in the lower wavelength regions. For this reason, ways of disrupting the PMs so that the antibiotic could be released and measured directly without this interference was investigated. Multiple techniques were tried including the use of harsh organic solvents and by altering the pH. PMs were loaded with either the antibiotic levofloxacin or a hydrophilic dye, fluorescein, left to dialyse for the usual period and were then treated with one of the test conditions before being analysed on the UV-vis spectrophotometer.

Fluorescein is a fluorescent dye that remains quenched at high concentrations, such as when inside a PM. Upon release from the PMs it begins to fluoresce, and appears a bright yellow/green colour to the eye, which provides an indication that PM structure has been successfully disrupted. PMs were made, either empty or loaded with fluorescein, and then diluted 1:5 with PBS to reduce UV-vis saturation. PM-empty remained colourless, whilst PM-fluorescein displayed its orange, quenched, colour (Figure 3.2A). NanoDrop UV-vis measurements showed the characteristic Rayleigh scattering peaks in both samples, although higher for PM-fluorescein, and also the peak at 491 nm unique to fluorescein absorbance (Figure 3.2B). The pH was adjusted to 4.5 using hydrochloric acid, to represent the acidic conditions found intracellularly due to lysosomal action, and a slight colour change was observed (Figure 3.2C). Although not the bright yellow fluorescence of free fluorescein this colour change eluded to potential disruption of PM structure and release of payload. Despite this, after pH adjustment Rayleigh scattering was still observed when analysed by UV-vis. Samples were measured undiluted and strong scattering peaks were seen, with the characteristic fluorescein peak at 491 nm suffering large interference (Figure 3.2D).

Fluorescence is arguably a better method to use for assessing nanoparticle payloads which possess an intrinsic fluorescence. For this reason, pH treated samples were also measured on a fluorometer. Fluorescein has a characteristic peak at approximately 515 nm wavelength, which can be seen at a neutral pH (Figure 3.2E). PM-fluorescein samples displayed a peak at approximately a 530 nm wavelength, suggesting encapsulation within PMs shifted the fluorescein's peak slightly. Upon acidification to pH 4.5 no signal was detected from either the free fluorescein or PM-fluorescein samples. After neutralising samples the original peaks were once again visible (Figure 3.2E, F). These results suggest that fluorescein's fluorescence is sensitive to low pH levels. Furthermore, it suggests that because the same fluorescence intensity was

observed following neutralisation, that no drug was likely released from the PMs during acidification, in turn showing that PM structure disruption at this pH was ineffective.

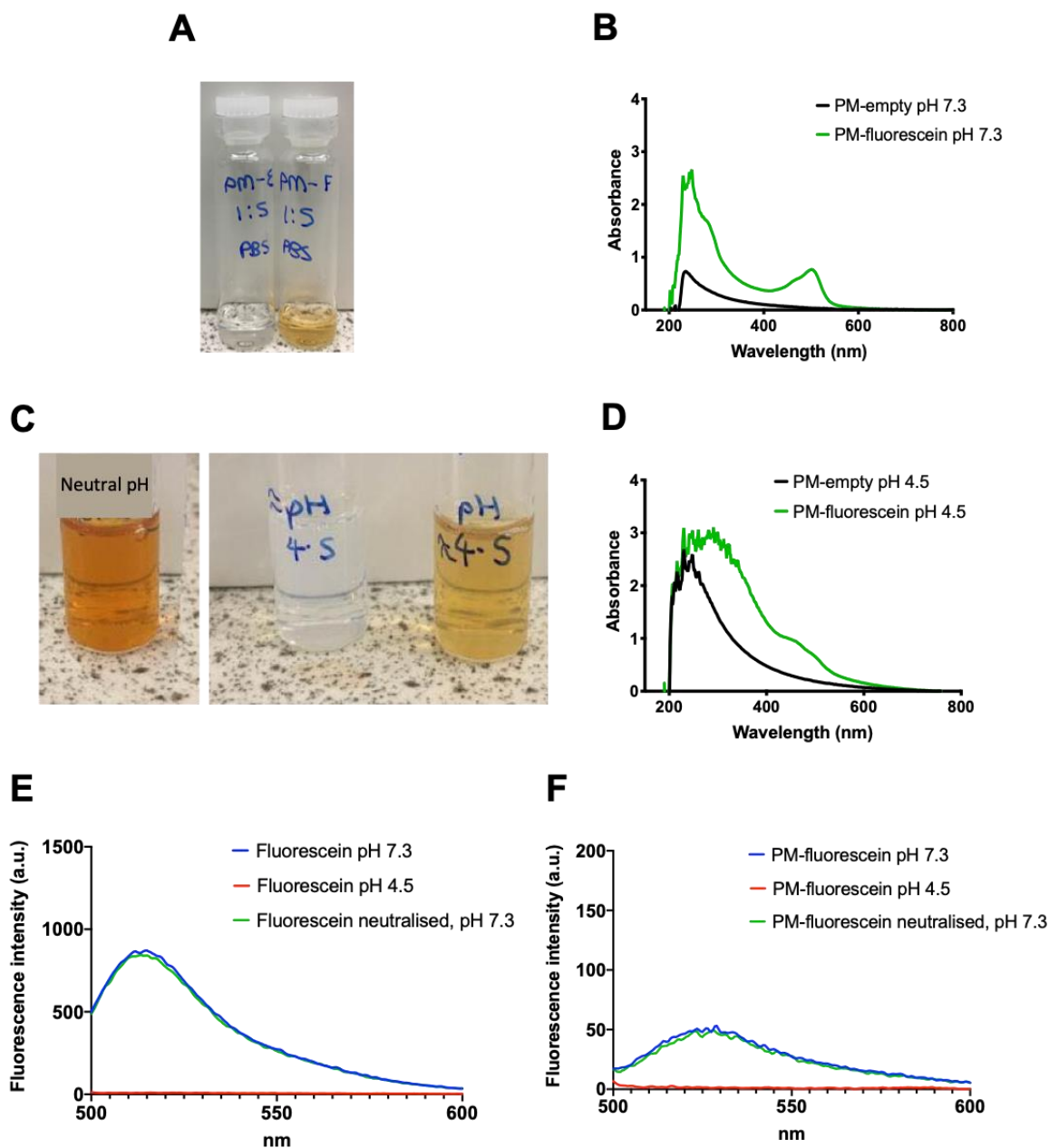


Figure 3.2 – Assessment of PM breaking using altered pH. (A) PM-fluorescein and PM-empty were diluted 1:5 and then (B) measured on the NanoDrop at a neutral pH. Rayleigh scattering was seen in both cases. (C) When the pH was adjusted to 4.5 a slight colour change was seen, however (D) Rayleigh scattering was still observed suggesting PMs were still intact and the pH change had not broken the PMs apart. (E) Fluorescein samples were measured on a fluorometer to assess fluorescence intensity changes in response to low pH. (F) PM-fluorescein samples were assessed in the same way as free fluorescein using a fluorometer. Fluorescein’s fluorescence was shown to be inactivated at these lower pH levels.

Organic solvents were also used to try and disrupt the PM structure. Acetonitrile was tested first by mixing neat solvent with PM-empty nanoparticles at both a 1:2 and 1:5 dilution. In neither case did the Rayleigh scattering disappear, and so this indicated that this solvent was not able to disrupt the PMs (Figure 3.3A). The next solvent tested was dimethylformamide (DMF), which was added to PM-levofloxacin samples at a 1:2 dilution. DMF was chosen as it is used in the PM preparation process to dissolve PEO-PCL polymer, and so there was good rationale it would disrupt the PM's structure once fully formed. There was a very clear reduction in the level of Rayleigh scattering detected (Figure 3.3B), and this suggested that mixing the PMs with DMF at this dilution would be sufficient to disrupt them and measure the antibiotic concentration more accurately. DMF treated PM-levofloxacin revealed a clear peak at approximately 290 nm, which would otherwise have been masked by Rayleigh scattering, and corresponded to levofloxacin's characteristic absorbance spectra, see section 3.2.2.2. Going forward, all future antibiotic concentration assessments made using the NanoDrop involved disrupting the PMs using a minimum of a 1:2 dilution with DMF.

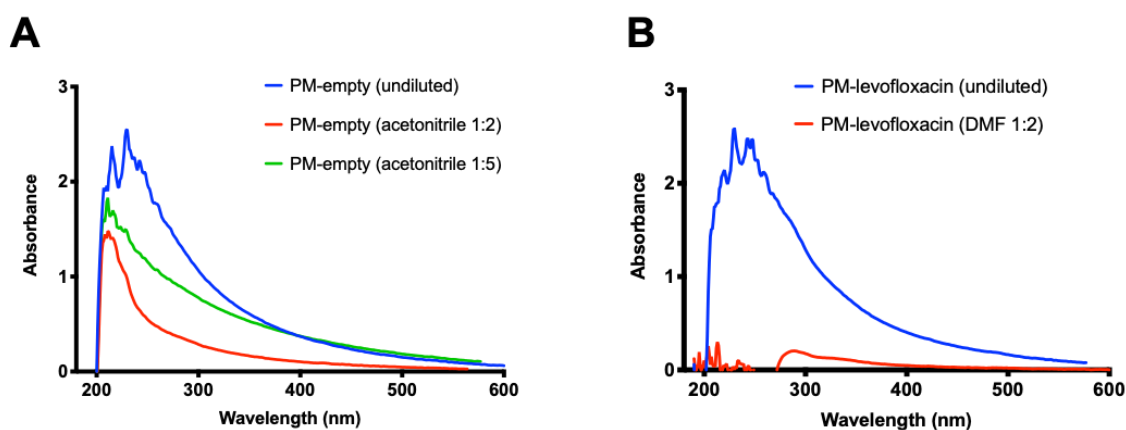


Figure 3.3 – Assessment of PM disruption using different organic solvents. (A) PM-empty samples were mixed with different concentrations of acetonitrile and then assessed for reduction in nanoparticle Rayleigh scattering peak visible at wavelengths less than 300 nm. (B) PM-levofloxacin samples were mixed with DMF at a 1:2 ratio and Rayleigh scattering assessed. DMF applied at an equivolume with PM sample was enough to eliminate Rayleigh scattering, and allowed detection of levofloxacin signal that would otherwise have been masked.

3.2.2.2 Encapsulation of levofloxacin

3.2.2.2.1 Determination of levofloxacin encapsulation using UV-vis analysis

Experiments reported in section 3.2.1 showed four antibiotics inhibited *B. thailandensis* growth, and so these were investigated further for PM encapsulation. It should be noted that the discovery of being able to disrupt the PMs using DMF, as described in section 3.2.2.1 came after the body of work for PM-levofloxacin preparations had been done. For this reason, the data displayed in this section was performed on intact PMs. To begin with, a standard curve was

produced using a series of known concentrations of levofloxacin, dissolved in PBS, ranging from 0 $\mu\text{g/ml}$ to 30 $\mu\text{g/ml}$. Levofloxacin had an absorption spectrum with a peak at 287 nm (Figure 3.4A), which was linear in intensity with respect to concentration, $R^2 = 0.99$ (Figure 3.4B).

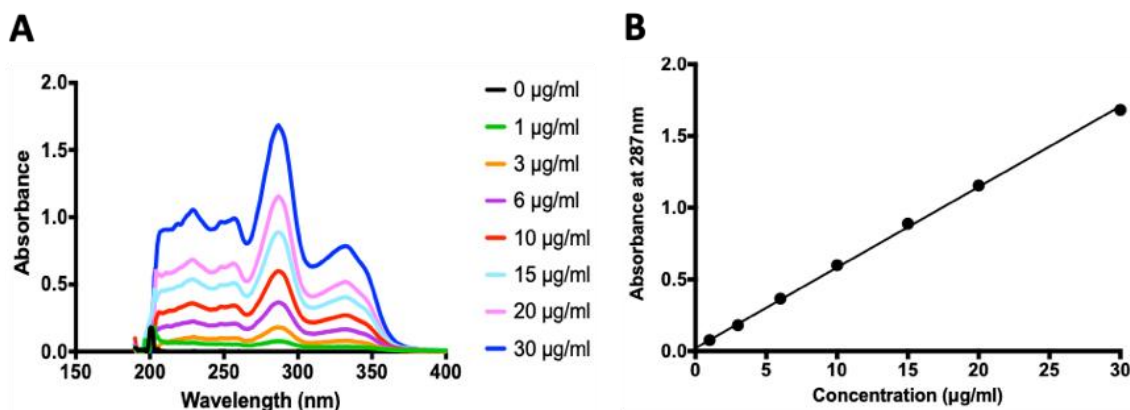


Figure 3.4 – Levofloxacin absorption spectra and standard curve. (A) The absorption spectra of levofloxacin over a range of different known concentrations, 0 $\mu\text{g/ml}$ -30 $\mu\text{g/ml}$. Samples were measured in black-sided quartz cuvettes using the NanoDrop 2000c UV-vis spectrophotometer. (B) The standard curve generated from the known concentrations. Plotted using the absorbance values measured at 287 nm. Standard curve has an $R^2 = 0.99$.

For the assessment of the encapsulation efficiency of PMs, PMs were loaded with 20 mg/ml of the antibiotic, either into their hydrophobic shell, or hydrophilic core – as discussed in section 2.2.1. For each of the PM samples a large peak was seen at approximately 210 nm, and then the spectra in all declined as the wavelength increased (Figure 3.5). No free drug signal was detected, likely due to it having passed through the dialysis membrane and being fully dialysed away. Interestingly, even within PM samples there was no detection of the characteristic peaks displayed by levofloxacin, at 287 nm or 332 nm, as seen earlier in Figure 3.4.

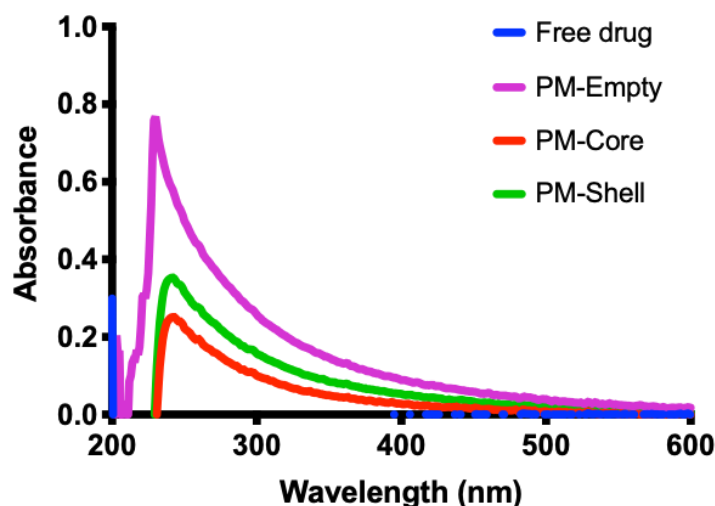


Figure 3.5 – Absorption measurements of levofloxacin loaded PMs. Levofloxacin was loaded into both the core and shell regions of PMs, and dialysed for one week, alongside empty PMs and free levofloxacin as controls. After this, samples were measured on the NanoDrop 2000c UV-vis spectrophotometer at the correct dilutions. The characteristic spectra of levofloxacin was not observed, suggesting it was not present in the samples after one week.

3.2.2.2.2 Determination of levofloxacin encapsulation using HPLC analysis

Due to the lack of levofloxacin signal detected using UV-vis analysis, it was hypothesised that this method may be too insensitive to detect the potentially low concentrations within the PMs. Instead, the more sensitive method of HPLC was employed. These studies were conducted to assess the level of levofloxacin released from the PMs into the dialysate sink over a period of one week. From this initial indirect analysis, the level of antibiotic retained within the PMs could be calculated. A standard curve was constructed, using the HPLC machine, to allow future concentrations to be determined (Figure 3.6). It included a variety of levofloxacin concentrations, diluted in PBS, ranging between 0 $\mu\text{g/ml}$ and 150 $\mu\text{g/ml}$. The absorbance measurements using HPLC were highly linear with respect to concentration of levofloxacin, with an $R^2 = 1.00$ (2 dp). For the HPLC experiment, empty PMs, core loaded PMs (20 mg/ml), shell loaded PMs (20 mg/ml), and free levofloxacin (20 mg/ml) were prepared. The concentration of levofloxacin released from the particles over time, during dialysis, was then assessed, as described in more detail in section 2.2.2.3. The experiment was performed 3 times, with different PM preparations each time. Within each experiment, triplicate repeats were taken for each timepoint on the HPLC machine.

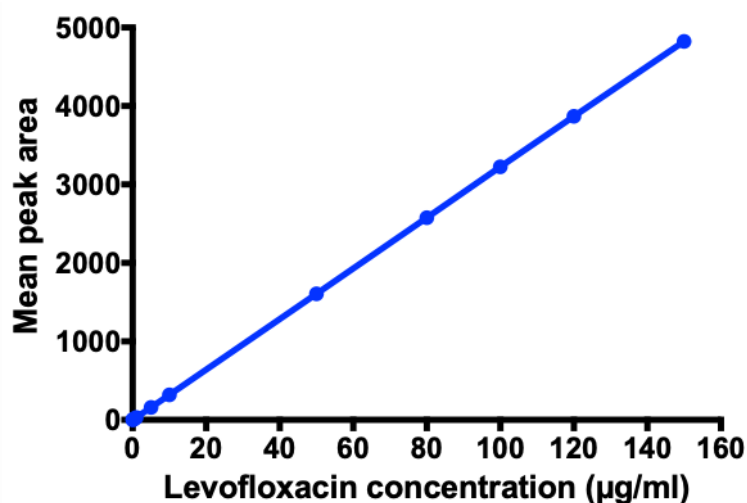


Figure 3.6 - The standard curve for levofloxacin generated using HPLC. Shown is a range of known concentrations spread from 0 µg/ml to 150 µg/ml. Standard curve possessed an $R^2 = 1$.

The PMs and control samples contained 20 mg/ml of levofloxacin. As they were made up to a final volume of 2 ml, this corresponds to 40 mg of levofloxacin present in samples at the start of the experiment. If all the antibiotic were released into the 300 ml PBS sink, it would equate to a concentration of 133.3 µg/ml (1 dp). Figure 3.7 is plotted as a percentage of this amount, i.e. the percentage of levofloxacin released into the dialysate buffer over a one-week period. In all PM samples there was a rapid release of levofloxacin from the dialysis tubes into the PBS buffer sink, with, on average, over 70% of the levofloxacin initially loaded being released by 24 hours. However, the rate of release from the shell loaded PMs was lower than that from either the free antibiotic, or the core loaded PMs. By 24 hours there was a significant difference observed between the release of shell loaded antibiotic versus the free antibiotic ($75.7\% \pm 9.0$ versus $98.3\% \pm 0.8$) ($p = 0.0005$, two-way ANOVA with Tukey's post-hoc test). Based on the amount of antibiotic present in the dialysate, shell loaded PMs were found to retain, i.e. have an encapsulation efficiency of, on average, 23% after 1 week. This corresponds to a concentration of 4.8 mg/ml. No more antibiotic was found in the dialysate for over a week post-formation, suggesting that the shell loaded PMs were able to retain this payload for at least one week (168 hours). In contrast, there was no significant difference observed in the amount of levofloxacin released between free drug and core loaded PMs at any timepoint.

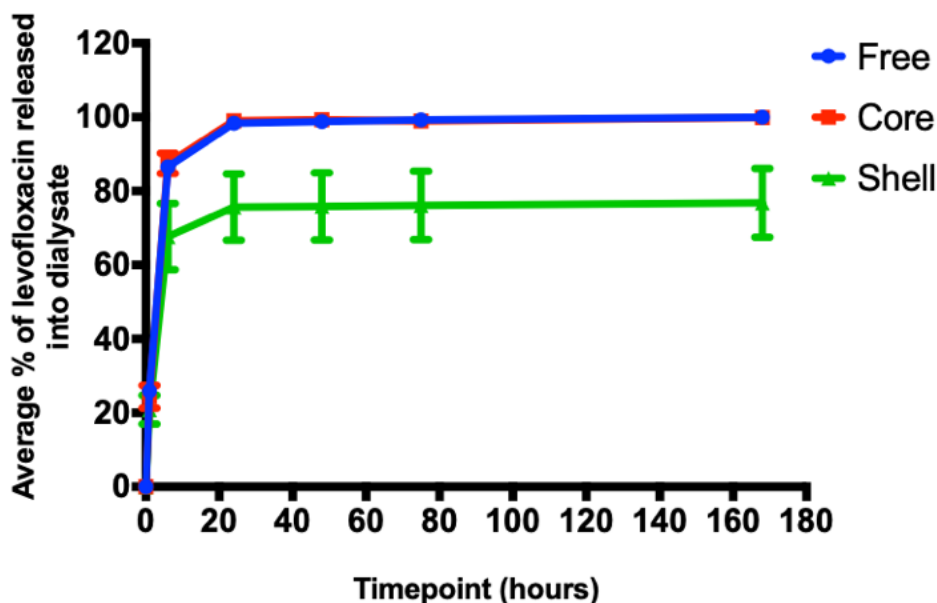


Figure 3.7 – The release of levofloxacin from loaded PMs compared to the free drug control. Results were obtained using HPLC. Rate of levofloxacin release from shell loaded PMs was lower than that from free or core loaded antibiotic. By 24 hours a significant difference was observed between the shell and free samples ($75.7\% \pm 9.0$ versus $98.3\% \pm 0.8$; $p = 0.0005$, two-way ANOVA with Tukey's post-hoc test). In contrast, no significant difference was observed in the amount of levofloxacin released between the free and core samples at any timepoint. Graph shows the averages of the three repeats \pm SD.

3.2.2.2.3 Levofloxacin retained as dead volume in syringe

Despite these seemingly promising results, shortly after this data was collected, at approximately eighteen months into the project, it was discovered that the syringes used in the preparation of the PMs had a dead volume of approximately 100 μ l. Figure 3.8 shows this problem highlighted using a blue dye for visualisation. During the initial set up the polymer and levofloxacin mix would be loaded into the syringe at a volume of 400 μ l, Figure 3.8A. Following stepwise dropping of this into the glass vial, the syringe pumps stalls as the syringe contents is expelled, Figure 3.8B. At this point, even with a blue dye, it is extremely difficult to see any residual volume. The levofloxacin polymer mix is colourless, and so this further adds to visualisation difficulties. It was discovered that if the syringe is removed from the pump and the plunger pulled back, this residual 100 μ l could be seen, Figure 3.8C. Whilst this volume may seem insignificant, 100 μ l out of an initially loaded 400 μ l corresponds to 25% of the sample that has been left and disposed of. It was upon this discovery that it was realised the retention seen in previous HPLC data, was in fact not due to PM retention, but that the sample could not be accounted for as it had been disposed of with the syringe.

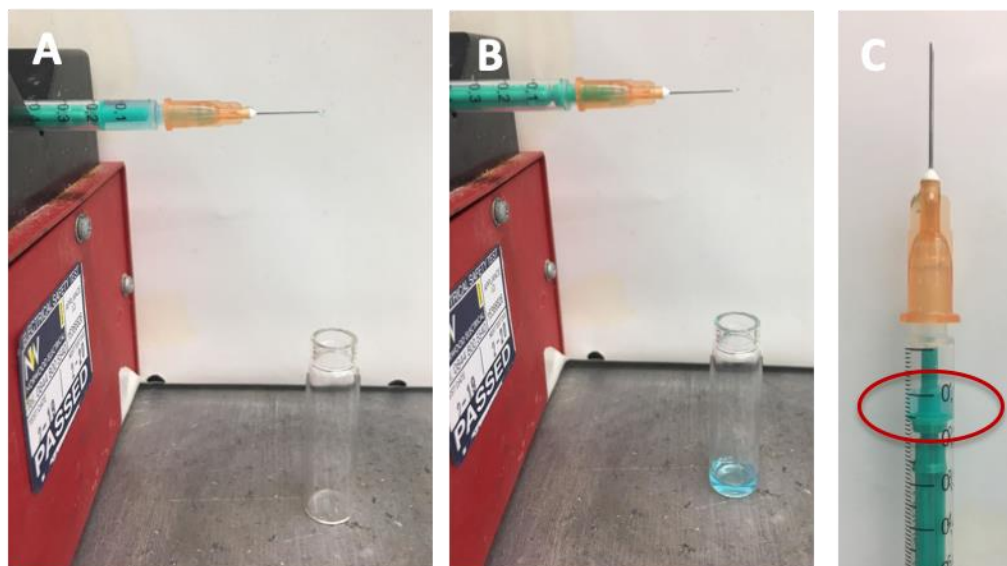


Figure 3.8 – Dead volume within syringe. Norm-ject Tuberkulin syringe retains approximately 20% of the loaded polymer antibiotic volume when being expelled by syringe pump.

3.2.2.3 Encapsulation of novobiocin

Moving on from levofloxacin, and from this point ensuring full syringe expulsion, the next antibiotic tested was novobiocin. To begin with, a series of known concentrations between 1 – 60 $\mu\text{g/ml}$ were made up, with novobiocin dissolved using a 1:1 ratio of DMF:PBS, the same buffer that the PM samples would be in after being disrupted using DMF. Novobiocin displayed a peak at 306 nm (Figure 3.9A) and showed linearity with respect to concentration, R^2 value of 0.99 (Figure 3.9B).

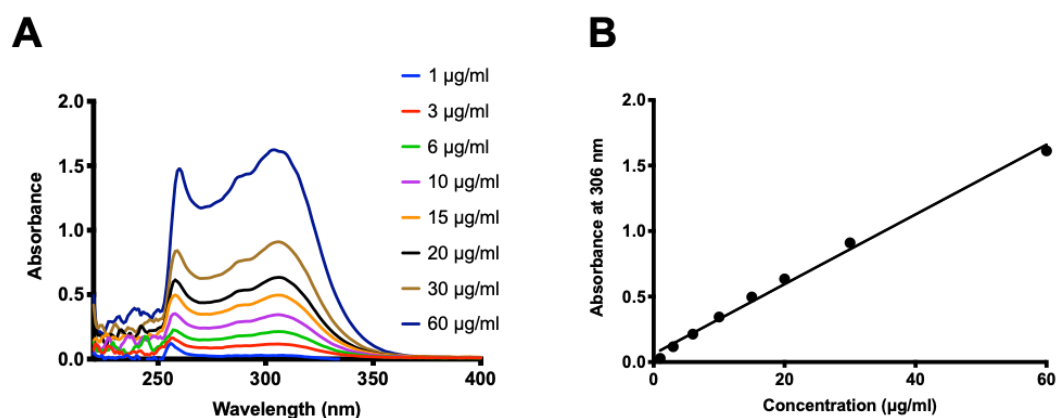


Figure 3.9 – Novobiocin absorption spectra and standard curve. (A) The absorption spectra of novobiocin over a range of concentrations from 1 – 60 $\mu\text{g/ml}$. Samples were measured in black-sided quartz cuvettes using the NanoDrop 2000c UV-vis spectrophotometer. (B) The standard curve generated from the peak at 306 nm, $R^2 = 0.99$.

The novobiocin used in these experiments was, specifically, novobiocin sodium salt, which was soluble in both DMF and PBS. For that reason, PMs were made in both ways with novobiocin loaded at a concentration of 10 mg/ml into either the hydrophobic shell (DMF dissolved), or the hydrophilic core (PBS dissolved), as described in section 2.2.1. A PM-empty sample and a free, unencapsulated novobiocin sample also at 10 mg/ml, were included to act as controls. The samples were all diluted with DMF at a 1:2 dilution before being measured. To further reduce novobiocin signal interference from Rayleigh scattering and absorbance as a result of the polymer, the PM-empty signal was deducted from the PM-novobiocin samples. There was a high level of antibiotic signal detected from both the core and shell loaded PM preparations. There was a small level of signal detected from the free drug control, suggesting dialysis was not yet complete and small concentrations of novobiocin remained un-dialysed (Figure 3.10A). After multiplying by the DMF dilution factor, the concentrations present in the samples corresponded to 63.4 $\mu\text{g/ml}$, 57.5 $\mu\text{g/ml}$, and 5.61 $\mu\text{g/ml}$ for PM-novobiocin (core), PM-novobiocin (shell), and free novobiocin, respectively. These results showed that the PMs were able to retain the antibiotic and prevent it from being removed via dialysis.

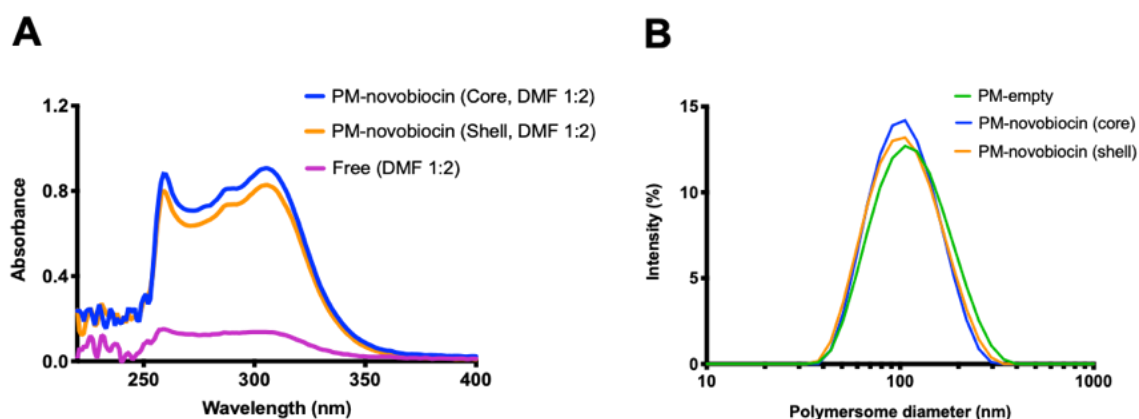


Figure 3.10 – Encapsulation and size characterisation of PM-novobiocin preparations. (A) PM-novobiocin (core) and PM-novobiocin (shell) preparations were shown to be able to retain 63.4 $\mu\text{g/ml}$ and 57.5 $\mu\text{g/ml}$, respectively, whilst the free control retained 5.61 $\mu\text{g/ml}$ after 48 hours of dialysis. (B) DLS size measurements showed no clear differences between the samples, with sizes of 106.4 nm, 97.06 nm, and 96.45 nm for PM-empty, PM-novobiocin (core), and PM-novobiocin (shell), respectively.

The sizes of the PM-novobiocin samples was assessed using DLS (Figure 3.10B). The data for each sample represents one biological repeat. The sizes were as listed in Table 8 below. Pdl values were also recorded, as a measure of how uniform the samples were in size. As the values all fall close to 0 it suggests the PM preparations were relatively monodisperse in size. Together this data

indicates that the addition of novobiocin to the preparations does not likely cause adverse effects such as aggregate formation, or excessive nanoparticle size increase.

Table 8: Sizes and Pdl values for PM-novobiocin and control preparations.

	Hydrodynamic diameter (d. nm)	Polydispersity index (Pdl)
PM-novobiocin (core loaded)	97.06	0.125
PM-novobiocin (shell loaded)	96.45	0.143
PM-empty	106.4	0.178

Although novobiocin sodium salt was found to be soluble in both PBS and DMF, it was slightly more so in DMF, and the level of antibiotic encapsulated was similar in both cases. For this reason, all future work with PM-novobiocin samples was performed using PMs where the antibiotic had been dissolved in the DMF solvent fraction during self-assembly. In order to assess the optimal loading concentrations for PM-novobiocin samples, multiple batches of PMs were made up with novobiocin concentrations ranging from 0 mg/ml – 50 mg/ml. Previously, PM-novobiocin samples had been dialysed for 48 hours, however due to the remnants of free drug control signal seen after this time (Figure 3.10A), samples were dialysed for 54 hours and with extra buffer changes to encourage complete removal of unencapsulated drug. Additionally, after this period samples were spun through a filter spin column to separate the PMs from their PBS buffer, and the filtrate collected was tested to determine if any antibiotic signal was still present, see section 2.2.2.3. PMs were broken using the 1:2 dilution with DMF method and then measured on the NanoDrop. The spectra were recorded, and the PM-empty signals deducted to cancel out interference from polymer signal. Interpolation from the standard curve (Figure 3.9B) was used to calculate the encapsulated concentrations.

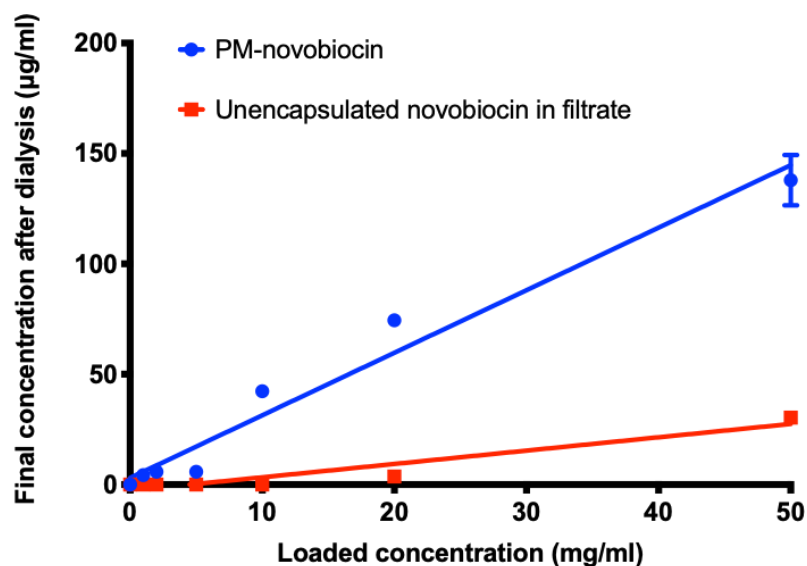


Figure 3.11 – Optimal loading of novobiocin into PMs. There was a positive linear relationship between the loading concentration of novobiocin and the encapsulated concentration within PMs post dialysis. Data is presented as the mean and SEM of one biological repeat performed in triplicate, n=1.

As expected, a positive linear relationship between loading concentration and final encapsulated concentration was observed (Figure 3.11). However, during preparation of these samples it was observed that at the 50 mg/ml loading concentration samples precipitated, suggesting PM saturation had been reached. Nevertheless, dialysis was continued, and the sample measured alongside the rest. Measurements from the filtrate showed that at the higher loading concentrations of 20 mg/ml and 50 mg/ml there was still unencapsulated drug present. For that reason, it was concluded that for the rest of this project any work performed using PM-novobiocin would be carried out using a loading concentration of 10 mg/ml, as this was the highest loading concentration tested that resulted in the maximum encapsulated concentration without significant unencapsulated drug remaining.

After confirming PMs were capable of encapsulating novobiocin, it was next investigated how stable these preparations were, and for how long the payload could be retained. The PM-antibiotic stability assay was performed as described in section 2.2.2.3. It was hypothesised that either a gradual decrease in antibiotic signal over time would be observed, suggesting release from PMs, or that a steady state would be reached where the PMs were able to hold onto the payload and antibiotic signal remain detectable.

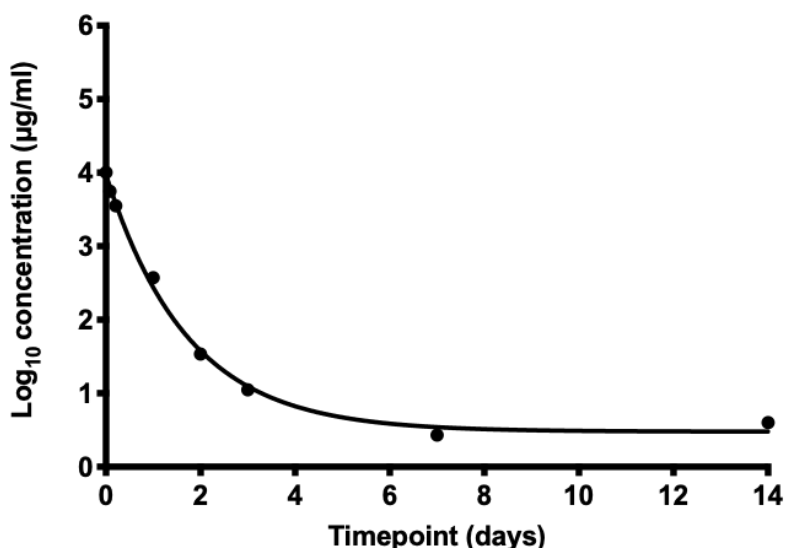


Figure 3.12 – PM-novobiocin stability over 14 days. PM-novobiocin samples were made and left dialysing for 14 days. Repeated concentration measurements were made and the level of release from PMs assessed. Data presented is the average of three repeats, n=3.

In the first 4 days there was a sharp decrease in the level of antibiotic present within the dialysis membrane (Figure 3.12). This was likely due to the dialysis process, where all of the unencapsulated drug present at the time of preparation was removed. The decrease may also include release from the PMs to an extent. However, by day 7 a steady state was reached where the concentration of novobiocin detected remained constant and indicated that it was being successfully retained within the PMs in the dialysis membrane, and not leaching away. By day 14 the PM-novobiocin preparations were found to retain on average $4.00 \mu\text{g/ml} \pm 6.51 \mu\text{g/ml}$. Overall the data from this section display how novobiocin can be successfully encapsulated into PEO-PCL PMs and retained for a period of at least 14 days.

3.2.2.4 Encapsulation of doxycycline

The next antibiotic investigated was doxycycline, a tetracycline clinically used in the treatment of *Burkholderia pseudomallei*. Standards of doxycycline were made up ranging from between 0 – 30 $\mu\text{g/ml}$ in a 1:1 ratio of DMF:PBS. Doxycycline was observed to have peaks at approximately 270 nm and at 372 nm (Figure 3.13A). The peak at 372 nm was used to construct the standard curve as it was furthest away from the lower wavelength regions that are most interfered with by Rayleigh scattering. The curve displayed good linearity, with an R^2 value of 0.99 (Figure 3.13B).

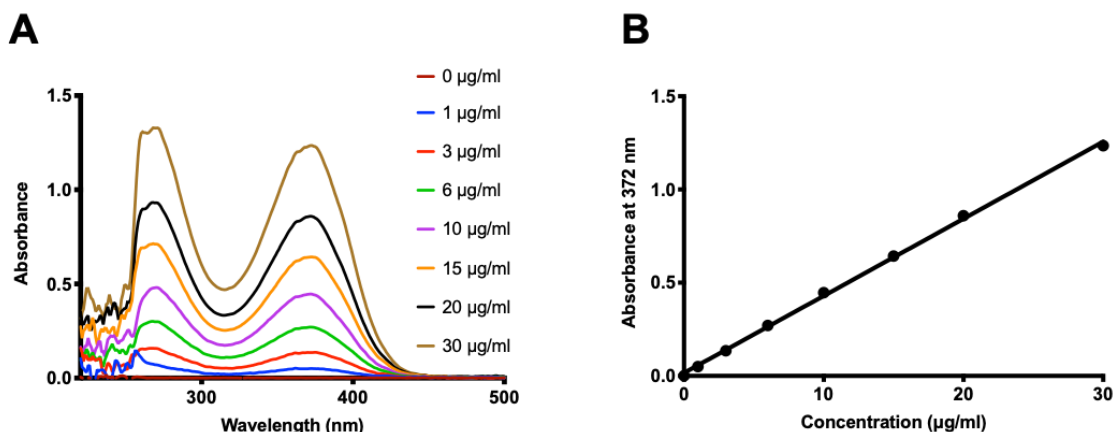


Figure 3.13 – Doxycycline absorption spectra and standard curve. (A) The absorption spectra of doxycycline over a range of concentrations from 0 – 30 µg/ml. Samples were measured in black-sided quartz cuvettes using the NanoDrop 2000c UV-vis spectrophotometer. (B) The characteristic peak at 372 nm was used to construct a standard curve, with an R^2 value of 0.99.

Doxycycline hyclate was incorporated into PMs either by inclusion in the aqueous solvent phase (PBS – ‘core loaded’), or into the organic solvent phase (DMF – ‘shell loaded’), up to concentrations of 50 mg/ml, after which precipitation occurred. It was observed that as the loading concentration of doxycycline increased, the concentration present in the PM preparations after dialysis also increased. An independent, unpaired t-test (two-tailed) confirmed that there was an insignificant difference in loading between the core or shell preparations at a 50 mg/ml loading concentration ($p > 0.1$). PM-doxycycline shell loaded had a final concentration of 12.2 µg/ml whilst PM-doxycycline core loaded had a final concentration of 10.9 µg/ml. For both preparations there was 0.00 µg/ml of free, unencapsulated doxycycline in the filtrate at any loading concentration (Figure 3.14). Therefore, 50 mg/ml was the highest loading concentration tested that gave the best level of drug encapsulation post-dialysis, and that also did not result in sample precipitation, or leave unencapsulated drug in the filtrate.

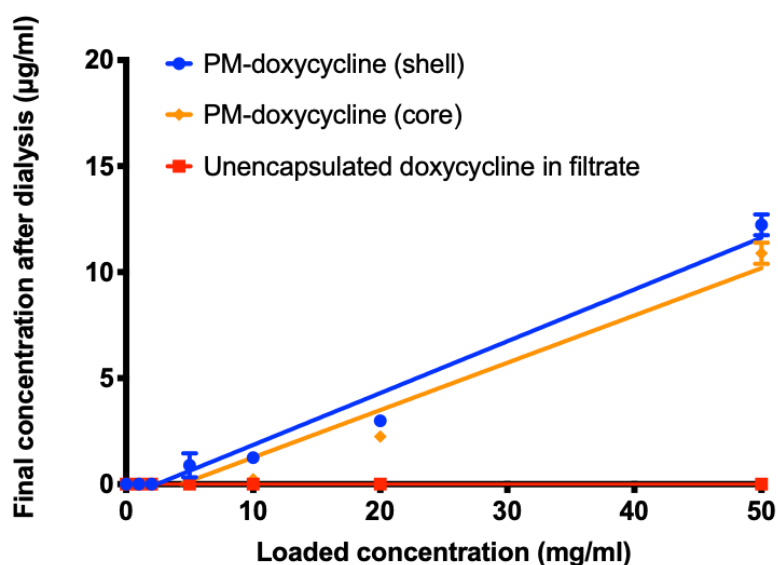


Figure 3.14 – Optimal loading of doxycycline into PMs. As the loading concentration was increased, the higher the level of doxycycline present in PMs after dialysis was measured to be. Data is presented as the mean and SEM of one biological repeat performed in triplicate, n=1.

Due to the lack of significance in doxycycline encapsulated in shell loaded PMs versus core loaded PMs, 50 mg/ml core loaded formulations were used for future assays. This was to ensure a range of both shell and core loaded preparations were used within the project. PM-doxycycline retention studies showed that, as before, in the first 3 days there was a sharp decrease in the level of antibiotic detected, but that by day 4 a steady state had been reached whereby no more antibiotic was being lost from the system, and the antibiotic concentration being measured remained consistent (Figure 3.15A). By day 14 the PM-doxycycline preparations were found to retain on average $15.2 \mu\text{g/ml} \pm 2.19 \mu\text{g/ml}$. Data was normalised to a PM-empty control.

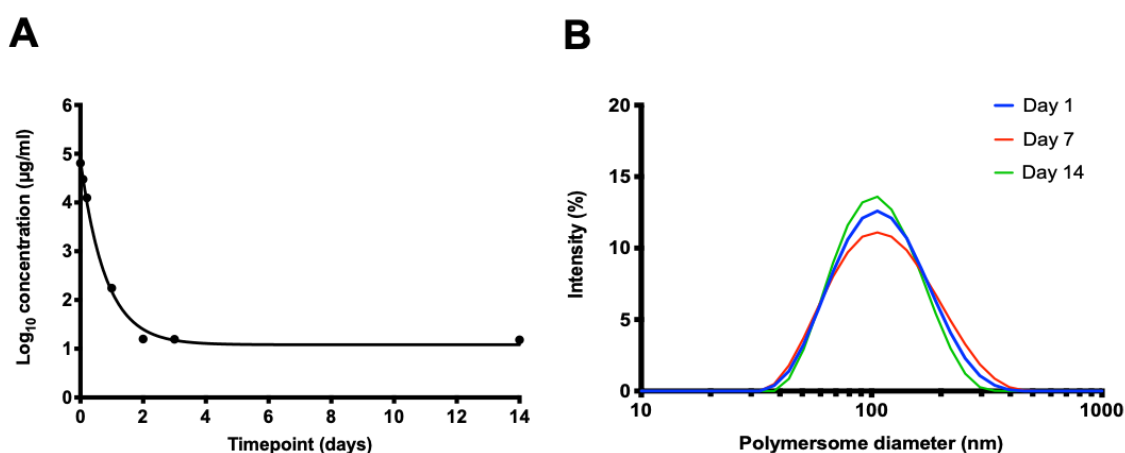


Figure 3.15 – PM-doxycycline stability over 14 days. (A) Samples were dialysed for 14 days with repeated concentration measurements taken to assess the level of antibiotic release. Data presented is the average of three biological repeats, n=3. (B) DLS readings were also taken across the 14-day period to assess any changes in the PM hydrodynamic diameter. Measurements were taken using one batch of PM-doxycycline maintained across the 14 days.

Alongside the release assay the stability of these PMs was tested using DLS as a measure of PM integrity. One batch of PM-doxycycline was kept for a period of 14 days, and the size was tested at days 1, 7, and 14 (Figure 3.15B). The results are also displayed below in Table 9. An independent, unpaired t-test (two-tailed) revealed no significant difference in the PM sizes between day 1 and day 14 ($p > 0.1$). This supported the findings of the release assay as it suggests the PMs are still intact after 14 days, which would help to explain how they are able to retain the antibiotic payload for this period of time. Overall, this data confirms that doxycycline can be successfully encapsulated into PEO-PCL PMs and retained for at least 14 days.

Table 9: Sizes and Pdl values for PM-doxycycline measured over a 14-day period.

	Hydrodynamic diameter (d. nm)	Polydispersity index (Pdl)
Day 1	101.4	0.177
Day 7	104.6	0.210
Day 14	101.0	0.186

3.2.2.5 Encapsulation of rifampicin

The final antibiotic explored was rifampicin, a strongly hydrophobic antibiotic belonging to the rifamycin class. Standards were prepared at concentrations ranging from 0 – 60 $\mu\text{g/ml}$, with the antibiotic dissolved in a 1:1 ratio of DMF:PBS. Rifampicin possesses a characteristic peak at 484 nm, which lies well away from any potential effects of Rayleigh scattering (Figure 3.16A), and so this was used to construct the standard curve, which had an R^2 value of 0.99 (Figure 3.16B).

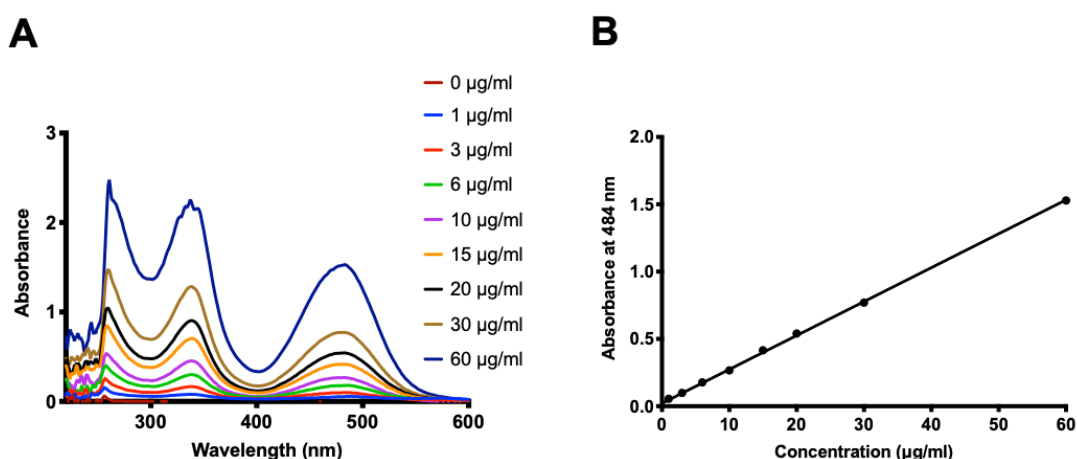


Figure 3.16 – Rifampicin absorption spectra and standard curve. (A) The absorption spectra of rifampicin over a range of concentrations from 0 – 60 $\mu\text{g/ml}$. Samples were measured in black-sided quartz cuvettes using the NanoDrop 2000c UV-vis spectrophotometer. (B) The characteristic peak at 484 nm was used to construct a standard curve, with an R^2 value of 0.99.

Due to its hydrophobic nature, rifampicin was found to be very weakly soluble in PBS. For this reason, these nanoparticles were made only by dissolving the antibiotic into the organic solvent phase of the PMs during self-assembly (shell loaded). To assess the optimal loading of PM-rifampicin particles, a series of different loading concentrations were tested, from 0 mg/ml – 50 mg/ml. Samples were left to dialyse for 72 hours with repeated buffer changes. The 50 mg/ml loaded sample precipitated heavily upon making, leaving a thick, viscous solution that was impossible to work with and so for this reason it was discounted and deemed to be above the saturation level (Figure 3.17A). The remaining samples followed the same patterns as seen with previous antibiotics, in that the higher the loading concentration, the higher the concentration of drug remaining after dialysis. This can be seen easily with rifampicin, without even the need for measuring, due to its bright orange colour. For each increase in loading concentration a much darker orange was seen in the PM samples post-dialysis (Figure 3.17B). After spinning the samples through the filter spin columns it was clear that despite not being able to see any precipitate in the 20 mg/ml sample with the naked eye, that there was still a high amount of unencapsulated drug remaining, with 110.5 $\mu\text{g/ml}$ being detected on the NanoDrop. At a 10 mg/ml loading concentration, 42.9 $\mu\text{g/ml}$ was detected in the PM samples, with only 1.4 $\mu\text{g/ml}$ being detected from the filtrate (Figure 3.17C). For this reason, a 10 mg/ml loading concentration was the one chosen for any future studies using PM-rifampicin preparations.

A final test performed, using PM-rifampicin at 10 mg/ml loading, was to compare the samples to a free drug control at the same concentration. Figure 3.17D shows two dialysis tubes containing 10 mg/ml of rifampicin, one in the presence of PEO-PCL polymer (left), and one without (right). Because rifampicin is bright orange, it was easy to see that in the sample without any polymer a large amount of solid precipitate had formed, seen at the top of the tube. This precipitate was not present in the PM-rifampicin sample. This shows how there was an interaction between this antibiotic and the polymer which stabilised the drug in solution and increased its solubility in comparison to the free drug control.

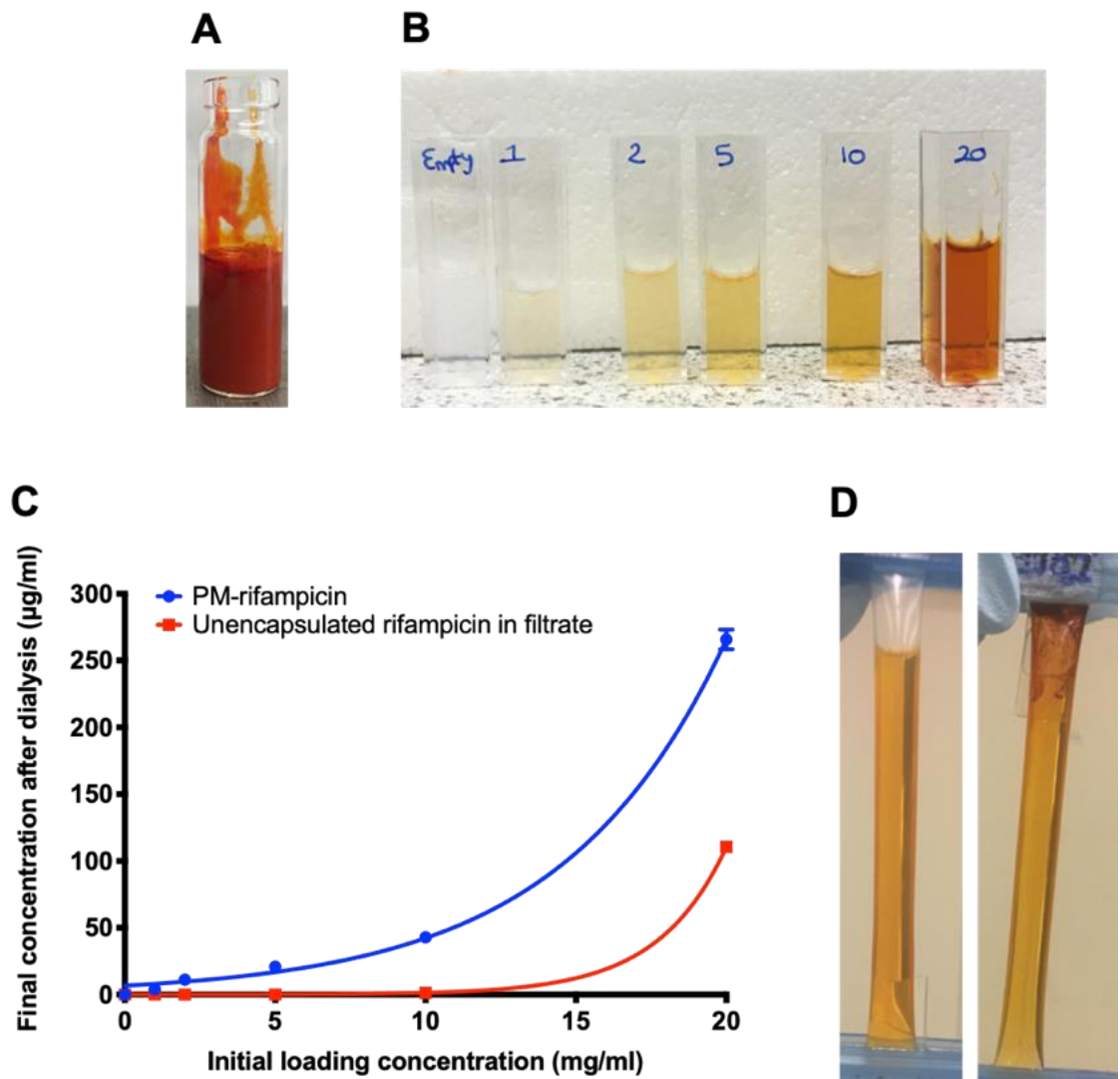


Figure 3.17 – Optimal loading of rifampicin into PMs. (A) An example of a precipitated PM-rifampicin preparation, in this case at a 50 mg/ml loading attempt. (B) The bright orange colour allows the increase in loading achieved to be easily seen, samples shown from PM-empty through to a 20 mg/ml loading concentration. (C) Although with a higher loading concentration a higher encapsulated concentration was seen post-dialysis, loading concentrations greater than 10 mg/ml resulted in a high level of free drug still present in samples. Data is presented as the mean and SEM of one repeat performed in triplicate, $n=1$. (D) Photos showing 10 mg/ml of rifampicin in the presence of PEO-PCL polymer (left), or without (right). Precipitate forms without PMs present, confirming an interaction between rifampicin and PEO-PCL that stabilises the drug and increases its solubility.

Using the 10 mg/ml shell loaded PM-rifampicin nanoparticles, the stability of these PMs and their release of the drug over time was measured. Three separate batches of PMs were made, and the concentration assessed at a series of timepoints across a 14-day period. Similarly to previous results, there was a sharp decrease in antibiotic concentration in the first 3 days, but by day 4 a steady state had been reached and no more rifampicin was being lost from within the dialysis

membrane, and therefore PMs (Figure 3.18A). At day 14 the PM-rifampicin preparations were found to retain on average $8.46 \mu\text{g/ml} \pm 2.41 \mu\text{g/ml}$. Data was normalised to a PM-empty control group. DLS was also used to measure any changes in the PM-rifampicin size over the 14 days (Figure 3.18B), with readings being taken on day 2, day 7, and day 14. The recorded hydrodynamic diameters are displayed in Table 10. An independent, unpaired t-test (two-tailed) revealed a significant difference in sizes between day 2 and day 14 ($p < 0.01$), however it is unlikely that this is a truly biologically significant result. Overall, PM-rifampicin was shown to be another PM-antibiotic preparation that was able to successfully, and stably, encapsulate an antibiotic for at least 14 days.

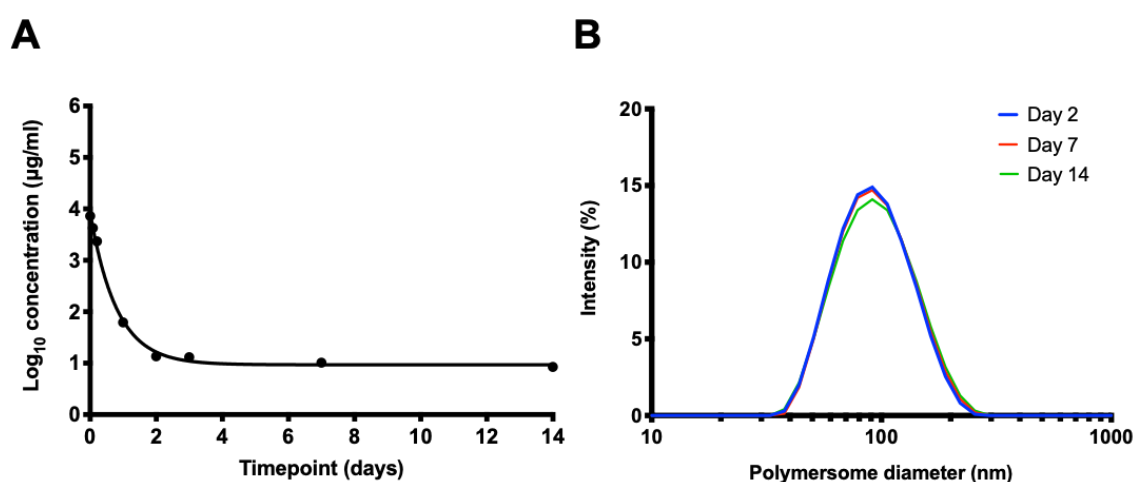


Figure 3.18 – PM-rifampicin stability over 14 days. (A) Samples were left dialysing for 14 days with repeated concentration measurements taken to assess the level of antibiotic release. Data presented is the average of three repeats, $n=3$. (B) DLS readings were also taken across the 14-day period to assess any changes in the PM hydrodynamic diameter. Measurements were taken using one batch of PM-rifampicin maintained across the 14 days.

Table 10: Sizes and Pdl values for PM-rifampicin measured over a 14-day period.

	Hydrodynamic diameter (d. nm)	Polydispersity index (Pdl)
Day 2	86.9	0.129
Day 7	88.3	0.139
Day 14	91.0	0.177

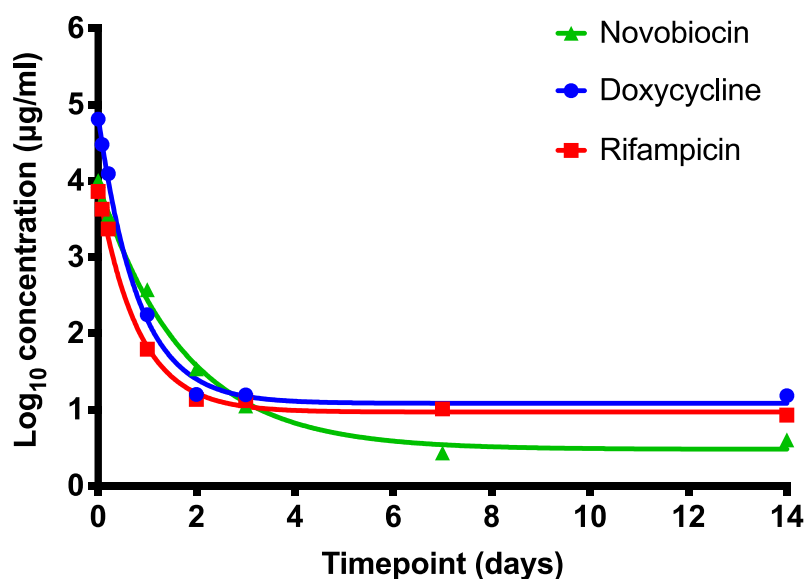
3.2.2.6 Comparison of novobiocin, doxycycline and rifampicin PMs

To recap the findings of this section so far, it has been shown that multiple antibiotics could be successfully encapsulated into PEO-PCL PMs. These were: novobiocin, doxycycline and rifampicin. Although a large body of work was performed with levofloxacin, this antibiotic was not able to be encapsulated and so has been excluded from this comparison section. Data from all of the antibiotic release assays has been compiled into graph format (Figure 3.19A), and then specific analysis based on day 14 results included within the table (Figure 3.19B). The final concentrations retained after a 14-day period were: 4.00 µg/ml, 15.2 µg/ml, and 8.46 µg/ml for PM-novobiocin, PM-doxycycline, and PM-rifampicin, respectively. Their optimal loading concentrations were determined, as discussed in previous sections, and based on this the encapsulation efficiency of antibiotic loading could be determined using the equation below. Efficiencies were as follows: PM-novobiocin (0.04%), PM-doxycycline (0.03%), and PM-rifampicin (0.08%).

$$\frac{\text{Antibiotic mass retained by PMs}}{\text{Initial mass of antibiotic loaded}} \times 100$$

For the ease of workload of future experiments, work with PM-novobiocin preparations was not continued as it had the lowest level of antibiotic encapsulated. Efforts were focused on PM-doxycycline and PM-rifampicin preparations, allowing assessment of one core loaded formulation and one shell loaded, respectively.

A



B

Antibiotic	Initial loading concentration (mg/ml)	Day 14 concentration (µg/ml)	Day 14 concentration (µM)	Encapsulation efficiency (%)
Novobiocin	10	4.00	6.30	0.0400
Doxycycline	50	15.2	29.6	0.0304
Rifampicin	10	8.46	10.3	0.0846

Figure 3.19 – Comparison of PM-antibiotic preparations. (A) Overlay of the PM-antibiotic release curve assays over 14 days. (B) Analysis of the 14-day timepoints, including a measure of the encapsulation efficiency of the antibiotic loading into PMs.

3.2.3 Concentrating the polymersomes to increase drug concentration

This section investigates the difference in retained antibiotic in the ‘bulk’ PM solution versus the ‘local’ concentration. When the PMs are initially made, they are suspended in a buffer with a final volume of 2 ml. All of the concentration assessments presented so far have been on this sample of PMs, the bulk solution (Figure 3.20). However, in this solution the PMs are highly diluted in the PBS buffer, and the PMs themselves only occupy a fraction of the total volume. It is likely that the concentration of antibiotic in the PMs alone, undiluted, is far higher than reported so far. To investigate this, PMs can be pelleted via ultracentrifugation (UCF), as described in section 2.2.2.3, and once the supernatant has been removed the concentration of drug in PMs alone can be measured.

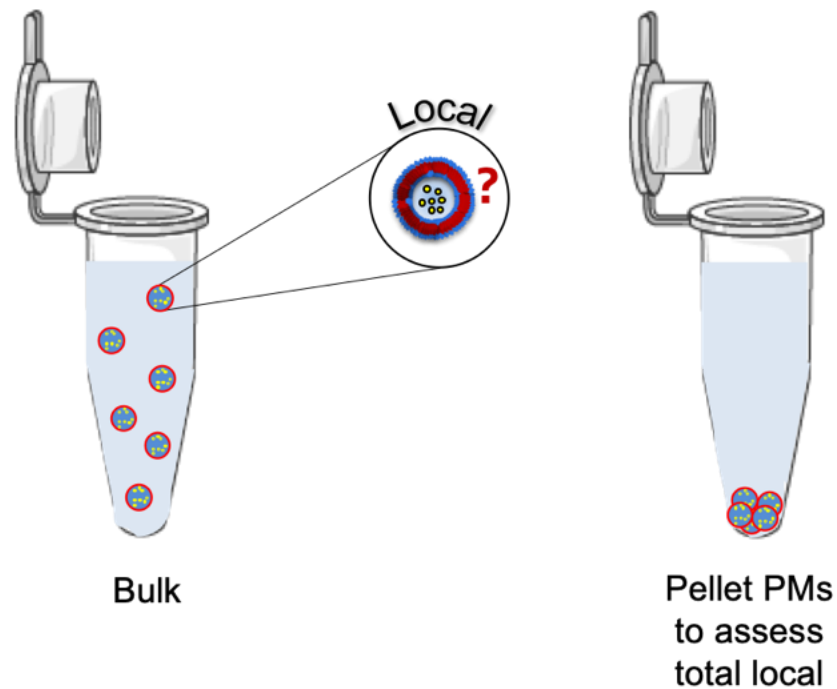


Figure 3.20 – A schematic of the bulk PM solution, versus the PM pellet as a local concentration assessment. PMs can be ultracentrifuged to form a pellet, and once the supernatant has been removed, the antibiotic concentration undiluted can be measured.

It was first tested how susceptible the PMs are to being spun down using UCF, with two key questions in mind: are they all successfully pelleted, and does this method damage the PMs? PMs were made loaded with Dil, a fluorescent lipophilic dye that is bright pink, allowing for easy visuals on whether the PMs have all pelleted or not. The PMs were spun for either 30 minutes, or 2 hours, at a low UCF setting (100,000 x g), or the maximum UCF setting (186,000 x g). 186,000 x g for 2 hours saw the most complete pelleting, but some colour was still seen in the supernatant suggesting that even on the highest setting some PMs would be lost in the supernatant (Figure 3.21A). PMs were also analysed using DLS to test if they were stable at this high UCF setting. After being spun down, a sample was taken from the supernatant and measured, the remaining supernatant discarded, and then the pellet re-suspended and also measured. The supernatant gave a reading suggesting nanoparticles with a diameter of 54.81 nm were present. This supports the visual findings from Figure 3.21A, that even at the highest UCF speed some PMs still remained within the supernatant. The re-suspended PMs recorded a size of 73.39 nm, which was in line with the usual expected size for PEO-PCL PMs (Figure 3.21B).

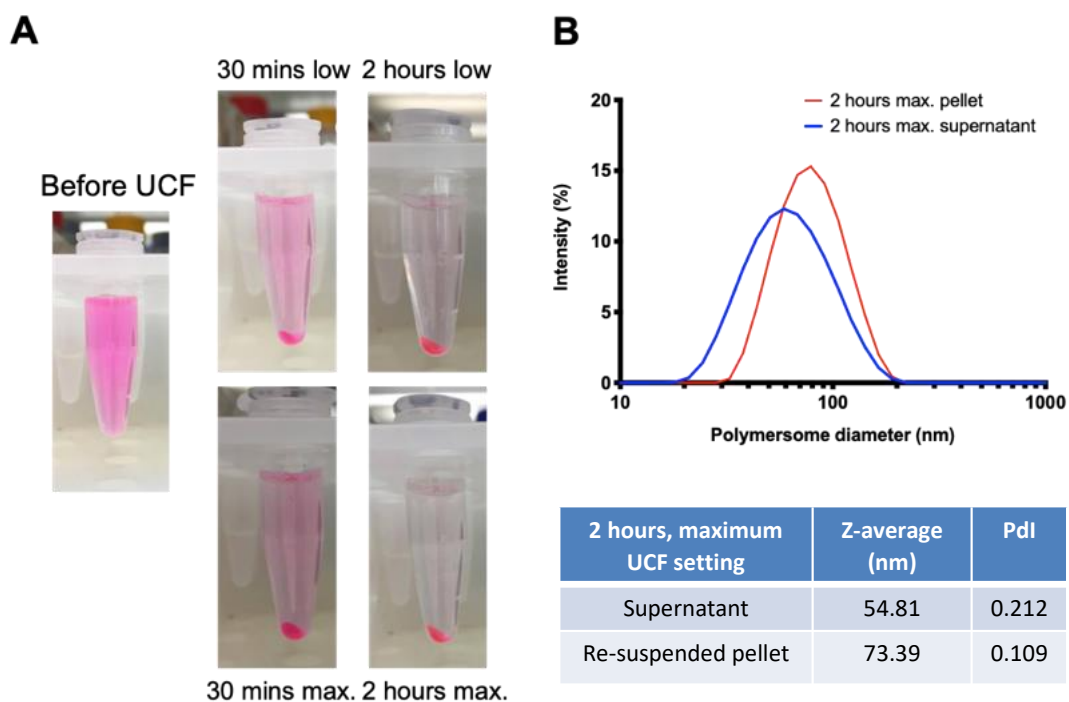

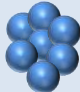




Figure 3.21 – Investigation into UCF speeds on PMs, and their subsequent sizes. (A) PMs loaded with fluorescent Dil were used to assess the efficiency with which PMs pellet during UCF at various settings. (B) DLS measurements for PM-Dil at the maximum UCF setting of 186,000 x g, for 2 hours.

Following this, PM-doxycycline and PM-rifampicin were tested for their local versus bulk concentrations. Samples were made and dialysed as usual, and then bulk concentrations were assessed on the NanoDrop after disrupting PMs with a 1:2 DMF dilution. PM-doxycycline gave a reading of 21.7 $\mu\text{g/ml}$ and PM-rifampicin gave a reading of 31.2 $\mu\text{g/ml}$. From these concentrations, estimations of the local drug concentration expected were calculated and presented in the table on the next page. Certain elements of PM characterisation have been rounded and approximated, to allow only a rough estimation of local concentration.

Table 11: Estimations of the expected local antibiotic concentration within PM-doxycycline and PM-rifampicin formulations.

Step	Description	Calculation	Schematic
1	The volume of one PM	<ul style="list-style-type: none"> $\frac{4}{3} \pi r^3$ $\frac{4}{3} \pi 50^3$ $500,000 \text{ nm}^3$ $5 \times 10^{-16} \text{ ml}$ ($1 \text{ nm}^3 = 1 \times 10^{-21} \text{ ml}$) 	
2	The total volume of PMs in final preparation	<ul style="list-style-type: none"> PMs in final volume = 3×10^{12} Volume occupied = $(5 \times 10^{-16}) \times (3 \times 10^{12}) = 0.0015 \text{ ml}$ 	
3	Local PM-doxycycline	<ul style="list-style-type: none"> PM-doxycycline bulk concentration = $21.7 \mu\text{g/ml}$ Therefore, $43.4 \mu\text{g}$ present in final 2 ml preparations. $43.4 \mu\text{g}$ spun down into PM pellet $43.4 \mu\text{g}$ in 0.0015 ml $28,933 \mu\text{g}$ in 1 ml 28.9 mg/ml (estimated) 	
4	Local PM-rifampicin	<ul style="list-style-type: none"> PM-rifampicin bulk concentration = $31.2 \mu\text{g/ml}$ Therefore, $62.4 \mu\text{g}$ present in final 2 ml preparations. $62.4 \mu\text{g}$ spun down into PM pellet $62.4 \mu\text{g}$ in 0.0015 ml $41,600 \mu\text{g}$ in 1 ml 41.6 mg/ml (estimated) 	

These calculations highlight that the level of drug encapsulated locally, is likely to be within the mg/ml range, as opposed to the $\mu\text{g/ml}$ level that the bulk readings give. To test this theory, the bulk preparations of PM-doxycycline and PM-rifampicin were spun in the UCF for 2 hours at $186,000 \times g$ to pellet the PMs. The supernatant was removed, and the pellets were re-suspended in specific volumes to enable measurement by the NanoDrop. From the standard curve a concentration was determined, which was multiplied by the dilution factor to give the local concentration. For example, a pellet (0.0015 ml) re-suspended in a 1.5 ml volume would have a dilution factor of $\times 1000$. Pellets of PM-doxycycline suggested a local concentration of 29.1 mg/ml , and PM-rifampicin of 38.1 mg/ml (Figure 3.22). These are the mean results of two repeat experiments using different PM batches each time. Results from the experiment align well with the predicted local concentrations estimated in Table 11, and highlight that a mg/ml level of drug is achieved when the PMs are concentrated. This gives potential for future drug delivery work in that high levels of antibiotics could be dosed.

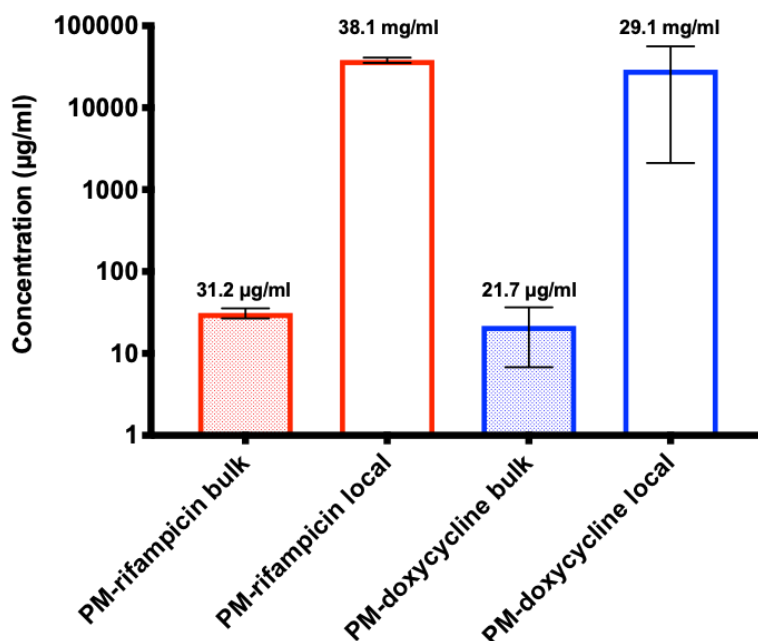


Figure 3.22 – Bulk versus local PM-antibiotic concentrations. PM-rifampicin and PM-doxycycline preparations were assessed for their concentrations in bulk solution, compared to after being pelleted. Results indicate that PMs can be concentrated using ultracentrifugation to achieve far higher antibiotic concentrations. Data is presented as the mean and SD of two repeat experiments.

3.2.4 Sizing of the polymersomes using transmission electron microscopy

Transmission electron microscopy (TEM) was briefly used as a second method to evaluate the sizes of the PEO-PCL polymersomes, using protocols based on Johnston *et al.* 2010. Here, empty PMs stained with ferrocene, prepared as described in section 2.2.2.2, were tested. The PMs did not fare well under the TEM electron beam, and were seen to visibly burst within a matter of seconds before extensive images could be collected. Figure 3.23 shows this happening, giving an example of what one PM looked like initially, Figure 3.23A, through to how it looked just prior to bursting, Figure 3.23D.

Despite TEM not being a viable sizing technique for these PMs, the images that were able to be collected do support the DLS findings to some level, in that the empty PM measured below had a diameter of approximately 100 nm.

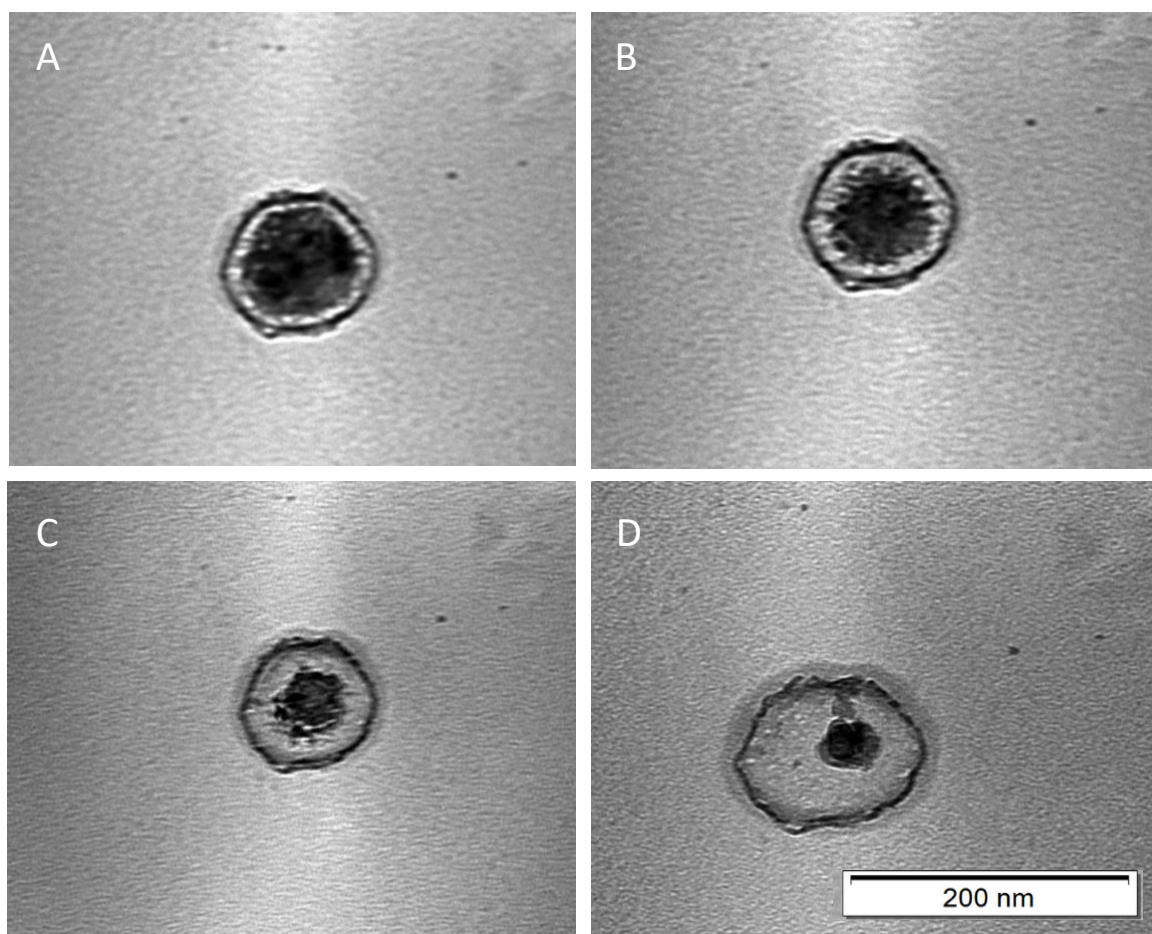


Figure 3.23 – Size characterisation of empty PMs using TEM. Images focus on one PM, and how its appearance change over time from its initial imaging (A), through to its final appearance before bursting under the electron beam (D).

3.3 Discussion

Nanoparticles, in particular polymersomes (PMs), are systems with the potential for drug delivery purposes. This project investigated their use in the delivery of antibiotics to intracellular locations where *Burkholderia spp.* reside. In order for PMs to become viable treatment options, they must be able to demonstrate the ability to encapsulate appropriate drugs to treat such infections, and retain them for a time period long enough to be clinically useful. The experiments conducted in this chapter addressed these topics by showing that:

- The antibiotics doxycycline, rifampicin, levofloxacin and novobiocin are all effective at inhibiting *B. thailandensis* growth, and may be further investigated for PM encapsulation purposes
- PM structure can be disrupted, to allow a more accurate measurement of the payload
- The antibiotics doxycycline, rifampicin and novobiocin can all be optimally loaded into PEO-PCL PMs
- In cases where antibiotics could be loaded, they could also be successfully retained for a period of at least 14 days
- Over the course of the 14 days the PMs maintained a constant hydrodynamic radius, suggesting preserved stability
- PMs may be concentrated, using ultracentrifugation, to achieve a higher antibiotic concentration

Minimum inhibitory concentration (MIC) assays were performed to assess the efficacy of levofloxacin, doxycycline, rifampicin and novobiocin against free-growing *B. thailandensis in vitro*. The MIC is defined as the minimum amount of antibiotic needed to inhibit the growth of bacteria during an overnight period of incubation (Andrews, 2001). The observation that all four of these antibiotics inhibited the growth of the bacteria is supported by a wealth of published evidence. For example, one study performed by Ross *et al.* (2018) determined the MICs for rifampicin, levofloxacin and doxycycline acting upon *B. pseudomallei* to be at concentrations below 50 µg/ml. Another study reported that novobiocin was able to inhibit the growth of 90% of *B. pseudomallei* at concentrations of 8 µg/ml, similar to our reported 12.5 µg/ml (Thibault *et al.*, 2004). Collectively these results all support these antibiotics to be viable treatment options for *B. pseudomallei* and *B. thailandensis* bacterial infections. The fact reasonably low concentrations were sufficient to see growth inhibition is even more promising as it reduces the risk of drug loading capabilities being a limiting factor for this project.

Assessing the level of payload encapsulated by the PMs is a challenging task, made even more difficult by the presence of the polymer, and the interference this can cause to antibiotic concentration readings. Nanoparticles, and other small particles, are capable of scattering light due to Rayleigh scattering. When an incident light hits the particles, it causes a polarisation of the molecule which results in scattering (Fan *et al.*, 2014). A particular feature of Rayleigh scattering is that it causes shorter wavelengths to be scattered more greatly than longer wavelengths (Emery and Camps, 2017). This is problematic when assessing antibiotic payload concentrations using UV-vis absorbance spectra, as if the characteristic peaks being investigated fall at lower wavelengths, interference from the PMs can occur. Multiple different methods were therefore tested in an attempt to disrupt the PMs, and thereby decrease interference from nanoparticle scattering. During uptake into cells, nanoparticles may be trafficked through the endosomal pathway where changes to a more acidic environment may be experienced, due to endosomal vesicle fusion with lysosomes. Here, the pH changes from a neutral level to around pH 6.5 - 4.5 (Hu *et al.*, 2015). It is known that once inside a cell, nanoparticles are able to release their payloads, and in part this may be due to degradation as a result of a pH shift. To assess this the hydrophilic dye fluorescein was utilised which fluoresces only at low concentrations and is quenched at higher concentrations, like when loaded into PMs (Nichols *et al.*, 2012; Scarpa *et al.*, 2016). In an attempt to mimic the internal cellular conditions, the pH of PM-fluorescein preparations was adjusted to 4.5 to see if any fluorescence was detectable, indicating fluorescein release and potential PM breakage. Results from Figure 3.2 suggested that this pH shift was not sufficient to disrupt the PMs, primarily due to a lack of decrease in Rayleigh scattering being seen, but also due to lack of changes in fluorescence intensity.

Upon measurement of the samples using a fluorometer, it was observed that in the more acidic conditions the fluorescence of fluorescein was fully quenched. This result was interesting, as it shows that fluorescence is not a good indicator for PM disruption as a result of pH. Even if the PMs were releasing the dye, this would not be detectable due to fluorescence quenching as a result of the acidic conditions. Similar effects have been documented previously of fluorescein's fluorescence being quenched at low pH levels (Martin and Lindqvist, 1975; Peterson, 2010). It was hypothesised however, that if PM disruption had occurred higher levels of fluorescein should be detected upon pH neutralisation than present originally. This was also not seen, suggesting that no disruption had occurred, and confirming that a pH shift to 4.5 alone was not sufficient to disrupt PMs. Nanoparticles differ in their complexity, with some being specifically designed to hydrolyse at lower pH levels, as discussed in section 1.5.4. However the PEO-PCL PMs in this project do not possess these pH-sensitive cleavage links, and so it is possible changes to pH do not affect their stability as with other PM preparations, hence the lack of degradation observed.

Organic solvents were also investigated in an attempt to break the PMs for more accurate payload concentration assessment. Acetonitrile and dimethylformamide (DMF) were both tried, but with only DMF showing any ability to reduce Rayleigh scattering (Figure 3.3). There are no known reports in the literature of other groups using DMF to disrupt the PMs. This is most likely because DMF is highly toxic to cells, and so using it on the PMs to disrupt them would render them useless if then applied to cells. A study performed by Jamalzadeh *et al.* (2016) showed that out of multiple different organic solvents tested, DMF was the most toxic to RAW 264.7 macrophage cells. Nevertheless, for the purpose of payload concentration assessments alone this is not a factor, as the disrupted PMs would not be applied to cells. Whilst much research has been performed on sophisticated stimuli-responsive PMs, section 1.5.4, there are far fewer examples of groups who have utilised approaches to disrupting PMs purely for concentration measurement accuracy. One group which did use the detergent Triton X-100 to disrupt PMs, allowing for fluorescence measurements to be taken (Bixner *et al.*, 2016). As Triton X-100 was not tested during this project it could be another agent to be tested as part of future work. This being said, there is still evidence for it being cytotoxic to mammalian and murine cell lines (Dayeh *et al.*, 2004), and so it is arguably no better than using DMF. It should be noted that whilst DMF is used in the preparation of the PMs within this thesis, following the rigorous dialysis process there are only trace levels of DMF remaining with the PM samples.

Using these methods of disrupting the PMs to enable a more accurate payload concentration calculation, experiments moved onto assessing the level of encapsulation of antibiotic by the PMs, and how long this could be retained for. It was observed that some antibiotics could be successfully encapsulated, whilst others, such as levofloxacin, could not. A large portion of time within this project was spent attempting to encapsulate levofloxacin into PMs. However, shortly after all of this data was collected, it was discovered the syringes used in the PM preparation retained an approximate volume of 100 μ l, a quarter of what was initially loaded into them (Figure 3.8), section 3.2.2.2.3. As a result, rather than achieving a successful encapsulation efficiency of 20%, as hypothesised from Figure 3.7, this amount was in fact being lost in the disposal of the syringes, and little to no levofloxacin was being encapsulated within the PM preparations. There were no other examples found within the literature providing evidence for levofloxacin being loaded into PMs. One group did however compare the loading capabilities of levofloxacin into either liposomes (LMs) or polymeric nanoparticles made from PEG-PLA, with a view to treating *Pseudomonas aeruginosa* infections in cystic fibrosis patients (Derbali *et al.*, 2019). This team discovered that polymeric nanoparticles achieved much lower drug encapsulation efficiencies compared to LMs, with results showing 1% versus 12%, respectively. Furthermore, *in vitro* drug release assays determined that, upon dialysis, the polymeric

nanoparticles were not able to retain levofloxacin any better than the free levofloxacin control, with 100% of the drug being released after a period of 48 hours, compared to only approximately 30% release from LMs. Contrastingly, other groups have successfully shown levofloxacin encapsulation within polymeric nanoparticles (López-López *et al.*, 2019), suggesting that encapsulation of this particular antibiotic may yield more variable results within polymeric-based nanoparticles.

Despite the disappointing results with levofloxacin, encapsulation was successful to varying degrees with rifampicin, doxycycline and novobiocin. For all of these antibiotics it was found that the level of antibiotic successfully encapsulated post-dialysis could be increased by increasing the amount of drug initially loaded into the PMs (Figures 3.11, 3.14, 3.17). It was observed, unsurprisingly, that in all cases there came a point where no more antibiotic could be encapsulated and held in solution by the PMs, and the sample would precipitate due to saturation. Other groups have investigated how the loading concentrations of drugs can affect the overall payload encapsulated. Danafar *et al.* (2014) researched PMs made from PLA-PEG-PLA triblock co-polymers, and their ability to encapsulate atorvastatin and lisinopril, two drugs used in the treatment of lowering cholesterol and treating high blood pressure. The group found that when the drug:co-polymer ratio was increased from 0.5 to 2, the drug loading percentage could be increased from 8.2% to 28.3% for lisinopril, and 9.5% to 40.9% for atorvastatin. This highlights how the loading of drugs into PMs can be optimised for better encapsulation levels. Similarly, a study performed by Bodaghabadi *et al.* (2018) investigated the optimal loading of rifampicin into mPEG-OA polymeric nanoparticles, for the treatment of intracellular *Brucella melitensis* infection. Rifampicin was loaded at concentrations ranging between 2 – 40 mg/ml, and after filtration, the encapsulated concentrations assessed. It was shown that, as seen within this project, as the loading concentration increased, so did the encapsulated level. However, this study showed nicely that the level of encapsulated drug plateaus, and in this case any increase in loading concentration above 20 mg/ml saw no additional increase in encapsulated concentration, suggesting the PMs had reached the limit of what they could encapsulate. Whilst this study did not elaborate on the visual state of the preparations at these high concentrations, it is likely that precipitation of rifampicin would have been seen, much like within this project.

There have been only a handful of other examples of rifampicin and doxycycline being loaded into PMs. PM-rifampicin preparations have been investigated for tuberculosis therapies (Moretton *et al.*, 2015), and eradication of intracellular parasites within macrophages (Rizzello *et al.*, 2017), whilst PM-doxycycline has been researched for use in treating intracellular bacterial species (Wayakanon *et al.*, 2013). No examples of PM-novobiocin preparations have been reported,

further adding to the novelty of the work performed within this project. It is of interest what factors determine whether or not an antibiotic can be loaded successfully. Hydrophobic molecules are desirable for nanoparticle packaging due to their otherwise poorly soluble nature; however, it has been suggested that due to their hydrophobicity they may precipitate in aqueous solutions, leading to large drug aggregates forming which can lower the drug loading efficiency within nanoparticles (Cai *et al.*, 2015). On the other hand, hydrophilic drugs tend to be able to escape by diffusion through to the external aqueous media in short periods of time, therefore resulting in low encapsulation efficiency also. Furthermore, this issue is exacerbated even more for smaller hydrophilic molecules, such as antibiotics, which are far more likely to be able to diffuse through nanoparticle walls than larger hydrophilic molecules, such as proteins (Huang *et al.*, 2018). Multiple other chemical factors also play a role in which small molecules may be successfully encapsulated, such as drug-polymer interactions due to the presence of functional groups. Drug release from nanoparticles such as PMs occurs either by the breakdown of the nanoparticle, or from diffusion of the drug. If a payload is released faster than the nanoparticle is known to break down naturally, this suggests drug diffusion is occurring. The rate at which this happens may be, in part, a result of how weakly bound and adsorbed a drug is on the surface of nanoparticles (Singh and Lillard, 2009). In the case of the antibiotics used within this project, all of them, with the exception of rifampicin, could be dissolved in either aqueous PBS, or non-aqueous DMF, suggesting the level of hydrophobicity was less of a factor for the encapsulation success rate. It is more likely that complex drug-polymer interactions were occurring which ultimately determined whether or not encapsulation was seen.

Whilst encapsulation of doxycycline, rifampicin and novobiocin was observed in this project, the encapsulation efficiencies remained low, ranging from 0.03% to 0.08% (Figure 3.19). This is a common occurrence for nanoparticle drug loading, and frequently encapsulation efficiencies reported are under 5% (Wang *et al.*, 2015). For example, when Wayakanon *et al.* (2013) loaded doxycycline into PMs they recorded an encapsulation efficiency of between 1-2%. However, there are some examples of highly successful drug loading, with far greater encapsulation efficiencies being achieved, largely as a result of the type of drug loading used at the point of preparation. Generally, the passive method of loading used for this project, nanoprecipitation, is not the most efficient and there are other active loading techniques which may be able to incorporate a higher initial payload. There is a body of research describing the active loading of other types of nanoparticle systems, such as LMs, and it is highly likely these methods could also be applied to PMs. In a study performed by Zhang *et al.* (2009) three different LM loading methods were compared for the highest encapsulation efficiency. These were: thin film, reverse phase evaporation, and remote loading methods by ammonium sulphate gradients. It was found that

the remote loading method achieved a far greater encapsulation efficiency, of $45.6\% \pm 3.3$, compared to the other two passive loading methods. The thin film method and reverse phase evaporation method achieved $23.2\% \pm 3.6$ and $11.2\% \pm 4.3$, respectively. Remote loading via ammonium sulphate gradients usually involves drying the lipids into a thin film, and then hydrating with varying concentrations of ammonium sulphate solution. The resulting LMs are then dialysed into a saline solution over a period of time. During this time the ammonia sulphate gradient is established. Ammonia efflux from the LMs and into the dialysate creates a proton gradient – ammonia is a base and so its removal from the LMs creates a $[H^+]_{liposome} > [H^+]_{dialysate}$. The efflux of ammonia is what drives the influx of the un-protonated drug across the liposomal membrane. The interaction of the drug and the remaining intraliposomal sulphate creates a gel-like precipitate which entraps the drug inside the aqueous core of the LMs (Bolotin *et al.*, 1994).

Another example of a method used to achieve active loading is by generating pH gradients using other types of buffers. The principle of the pH gradient method is for the un-protonated, weakly basic, drugs to move into the acidic PM interiors, where they become protonated. The protonated forms are then no longer membrane permeable, and so unable to pass back out of the PMs, therefore entrapping the drugs efficiently. Choucair *et al.* (2005) looked at loading the anti-cancer drug, doxorubicin, into PMs using the nanoprecipitation method, the same as within this project, however with the introduction of a pH gradient. The co-polymers were dissolved in an organic solvent, and then added dropwise to pH 2.5 water to induce self-assembly. PMs were then dialysed to remove the excess organic solvent, resulting in a sample of unloaded PMs with an aqueous core at pH 2.5. Doxorubicin was then added in solution to the PMs, and the pH of the solution adjusted to 6.3. Therefore, $pH_{inside\ PMs} = 2.5$, $pH_{outside\ PMs} = 6.3$. Control groups were made where doxorubicin was added to PM mixes with no pH gradient. Other groups have performed similar studies, but instead of achieving the intra-PM pH using pH 2.5 water, they have achieved an intra-PM pH of 4 using citrate buffer instead (Nahire *et al.*, 2014). Results from Choucair and colleagues determined that the presence of the pH gradient could enhance the loading of the drug up to 10-fold, compared to samples which were made in the absence of a pH gradient. Overall, multiple different methods are available to load nanoparticles, and many of these can be applied to the production of PMs. This project focused only on passively loading the PMs, but in the context of drug delivery and achieving high drug concentrations, active loading methods should be considered for any continuing future work. The higher the encapsulated antibiotic concentration achieved the more effective a single dose of PMs may be against *B. thailandensis*, and other bacterial species, in theory. This could lead to a reduction in doses and shortening of treatment time when administered clinically. The active loading experiments used by Choucair *et*

al. would be easily replicated using the PMs within this study, and one would predict they would lead to higher encapsulated payloads.

One point for consideration with the data presented in this chapter is the characteristics of an antibiotic which allow it to be successfully encapsulated. As seen, some antibiotics such as levofloxacin are not retained, whereas others such as doxycycline and rifampicin are stably encapsulated by the PMs. The physicochemical properties of all of the antibiotics are listed in Table 4, but do not shed much light as to why these differences might occur, due to similar properties being recorded for all antibiotics. It is likely that more complex chemical interactions are occurring between drug and polymer which are based around the chemical structures of the antibiotics, and the bonds they are capable of forming with PEO-PCL. For example, levofloxacin's structure is relatively simple compared to drugs like doxycycline and rifampicin, and this might affect the numbers, and types, of chemical interactions and bonds formed between the drug and the polymer, causing differences in encapsulation.

The majority of antibiotics tested in this project were soluble in both PBS (for PM aqueous phase 'core' loading) and DMF (for PM solvent phase 'shell' loading). We hypothesised that depending on the PM phase the drugs were initially dissolved into, shell membrane loading or aqueous core loading could be achieved. In reality, this is not certain and so experiments should be performed to confirm whether this differential loading was achieved. Techniques such as nuclear magnetic resonance (NMR) could be investigated as a tool to assess this. NMR is a type of spectroscopy which can fix around a particular atom in a compound and display different signals depending on the environment of this atom, i.e. different signals for an atom in an aqueous environment versus an organic solvent environment. A review published by Darbeau (2006) gives a detailed account of the principles of NMR. In terms of PMs used for drug delivery it may not be of the greatest importance where in the PM the drug is primarily binding to (membrane or core) so long as a high drug encapsulation is achieved, and the PMs are able to inhibit bacterial growth. However, understanding the chemistry behind the loading process is likely essential to exploiting maximum drug encapsulation.

The dynamic light scattering (DLS) results collected within this project showed that the PMs had diameters within the range of 91 – 106 nm, and low Pdl values, suggesting samples were monodisperse and largely uniform in size (Figures 3.10, 3.15, 3.18). Whilst DLS is one of the most commonly used techniques to assess small particle size, it is not without its limitations. One of the key shortfalls to DLS is its susceptibility for size results to be skewed due to larger particles, such as dust or aggregated sample. Even if very small concentrations of these larger particles are

present it can bias characterisation estimations across all size classes (Kim *et al.*, 2019; Malm and Corbett, 2019). An excellent paper by Tomaszewska *et al.* (2013) highlighted this issue by investigating the detection limits of DLS machines. Silver nanoparticles of known sizes, 10 nm and 80 nm, were mixed together in different ratios and measured. The group found that as the ratio of larger particles increased, the signal from the smaller particles decreased, with the peak disappearing altogether when the proportion of 10 nm particles dropped to 95%. The result of this is that the DLS readings would inaccurately suggest a monodisperse sample, with a lower PDI, when in reality there were certainly particles of different sizes present. In terms of results presented in this project, DLS readings repeatedly display only one clean peak, showing that there are indeed PMs present at the expected approximate size. However, of the final nanoparticle sample contents, if only 5% of larger particles is able to conceal smaller particles, it is highly possible that the PM preparations are not as monodisperse as the PDI values suggest, and that many smaller particles may also be present within the sample. This is not necessarily an issue, however it may contribute towards lower drug encapsulation efficiencies if the nanoparticles being formed are largely not of the desired size and structure.

The general consensus in the literature is that most nanoparticle characterisation methods have shortfalls, and the best way to overcome this is to use a selection of sizing methods. For this reason, transmission electron microscopy (TEM) was used in an attempt to obtain PM size readings. It was found that it was extremely challenging to obtain images from the PMs, as they very quickly burst under the electron beam. From the one image that was collected (Figure 3.23), it seems that the PMs had a size of approximately 100 nm, which supports the DLS data, even if loosely. There have been other examples within the literature of PMs being imaged using TEM, one such example even with PEG-PCL PMs, like in this project. Johnston *et al.* (2010) used PEG5K-PCL5K PMs loaded with ferrocene in their membrane as a type of stain, to characterise the sizes of their cores using TEM. Another paper investigated the broad size distributions that can be observed after formation of PEG-PLA PMs, and used both DLS and TEM to monitor size changes when PMs were exposed to different size extrusion techniques. They found that the sizes generated by DLS were larger than those by TEM, and suggested this was due to DLS including the thick hydrophilic PEG corona in its diameter estimation, leading to a size overestimation (Apolinário *et al.*, 2018). This work was supported by Hinterwirth *et al.* (2013) who used gold nanoparticles to compare multiple different sizing techniques, including DLS and TEM. They found that whilst there was good linearity between the diameters determined by both methods, the DLS results were consistently slightly larger than TEM results. Whilst it seems that the DLS measurements collected within this study may be slightly larger than in true reality, the fact that good correlations are seen in the literature between DLS and TEM measurements, and that DLS is

still the most commonly used method, gives confidence that the PMs used here are sized as best as is currently possible.

Whilst encapsulation of antibiotics within PMs has been shown to be possible, the concentrations measured in the bulk solution were relatively low, and as previously discussed, this is not an uncommon problem for drug encapsulation within delivery vehicles. In order to administer clinically relevant concentrations of antibiotic, it is likely that by using bulk PM solutions large volumes would have to be administered. It was hypothesised that if the PMs could be concentrated this might allow for a higher PM-antibiotic concentration to be achieved in a single dose, thereby potentially reducing duration of therapy in future scenarios. PMs were able to be pelleted using ultracentrifugation (UCF), albeit not in entirety and with small levels of PMs remaining in the supernatant, as seen from pink PM-Dil colour in the supernatant and by confirmation with DLS data (Figure 3.21). It is unsurprising that not all PMs were pelleted, as the PMs themselves are made up almost entirely of the same buffer in which they are suspended, meaning there is negligible weight difference which would allow efficient UCF. A study by Robertson *et al.* (2016) investigated methods of purifying PMPC-PDPA PMs made using PBS buffer. They used differential centrifugation to separate out the different structures formed within their PM sample, but what was of note was that even after centrifuging their PMs for 2 hours at 20,000 x g, structures were still seen in the supernatant at approximately 50-60 nm in size, according to DLS measurements. This supports data from this project, which showed that nanoparticle structures measured from the supernatant gave a DLS size reading of 54.8 nm. It is possible that these supernatant nanoparticles are not PMs, but other smaller structures formed during PM preparation, such as micelles, but only TEM analysis would allow this to be confirmed. If the structures are PMs, or other types of nanoparticle containing any antibiotic, it must be understood that by pelleting the sample using ultracentrifugation, some drug may be lost in the supernatant.

The results from the pelleting test yielded good results, showing that locally – i.e. within the PMs alone, concentrations of up to 1000-fold higher than the bulk suspension concentration could be achieved (Figure 3.22). Other groups within the literature have similarly reported the need for concentrating nanoparticles, and one group in particular investigated concentrating polymeric nanospheres. Rather than using UCF, they applied an osmotic stress to nanoparticles entrapped within a dialysis membrane, to encourage movement of water molecules from the inside of the dialysis membrane to the outside, thereby increasing nanoparticle concentration within the bag. Results from this study showed that the greater the osmotic stress applied on the nanospheres, the more efficient the concentrating of the nanoparticles was, with concentration factors of up to

50 achieved in only a few hours. Furthermore, the nanospheres maintained original characteristics and were not damaged by this process. The paper then compared this method with the method used in this project, UCF. They reported that by using UCF concentration factors of 10 were achieved, but that the pellet was difficult to work with, and to re-suspend. Despite this, they confirmed that nanoparticles retained their original characteristics after UCF, showing that at least there was no damage from this process (Vauthier *et al.*, 2008). These findings certainly support observations from within this project, mostly in that the PM pellets after UCF were very challenging to work with due to a 'stickiness' that made efficiently re-suspending them hard. Additionally, due to the fact that not all particles are pelleted from the supernatant effectively, if any future work is to be performed investigating PM concentrating, this method of osmotic stress should be investigated. The method of UCF still gave a better concentration factor than reported by Vauthier *et al.*, but it would be interesting to see if similar results could be obtained using this newly proposed method.

Chapter 4: Internalisation and intracellular
localisation of polymersomes in RAW 264.7
macrophages

Chapter 4: Internalisation and intracellular localisation of polymersomes in RAW 264.7 macrophages

4.1 Introduction

As seen previously in Chapter 3, PMs have the ability to encapsulate a variety of different antibiotics stably. This is key when considering their use as drug delivery vehicles, as in many cases drugs must be retained before reaching a specific target site. However, despite the potential of PMs, it was next assessed whether they were capable of reaching the site of bacterial infection, inside RAW 264.7 macrophages. Therefore, the hypothesis that PMs can be internalised by infected macrophage cells was tested. These tests are key to determining whether these nanoparticles remain viable options for the treatment of intracellular infections.

Whilst much research has been conducted using LMs as drug delivery vehicles, resulting in multiple FDA-approved formulations (Olusanya *et al.*, 2018), the PM field is less advanced with no approved formulations to the best of our knowledge. A large reason for this is the relative lack of information surrounding *in vivo* assessments, including the immunogenicity of particular block copolymer materials and also the pharmacokinetics of PMs within the body. Furthermore, within the literature there is a clear lack of direct performance comparison between well-established LM formulations and PMs. Until clear advantages of using PMs over LMs can be shown, the translation to clinical application may remain slow (Matoori and Leroux, 2020). It is for this reason that the investigation of PM uptake into various cell types is so essential, as it contributes towards extending our understanding of how PMs interact with human host-like environments. Future work related to this project could be to perform assays again alongside LM preparations and assess whether their uptake into macrophage cells was as efficient.

Within this chapter different techniques have been utilised to assess PM uptake, including fluorescence and confocal microscopy, real-time imaging, imaging flow cytometry (IFC), and Coherent anti-Stokes Raman scattering (CARS) imaging, some of which were discussed in Chapter 1. The experimental techniques used within this chapter each offer different benefits, for example fluorescent and confocal microscopy allowed for relatively quick testing to assess PM uptake qualitatively, and real-time imaging allowed a better understanding of the precise speed in which PMs were taken up by macrophages. The IFC, ImageStream, technology allowed uptake to be measured quantitatively and also the co-localisation between PMs and invading *B. thailandensis*

bacteria within macrophages. This investigation is extremely relevant in terms of drug delivery, because as much of the PM payload as possible is desired to collect at the same site as the infection. There are currently no known examples within the literature of IFC being used to assess co-localisation between nanoparticles and an intracellular bacterial infection. This makes the work performed within this chapter not only novel, but of great value when trying to pick apart nanoparticles as delivery vehicles for these types of infection. The majority of nanoparticle uptake research within the literature has relied on the use of labelled nanoparticles, usually fluorescently tagged, to aid cellular uptake tracking. One caveat to this is the potential dissociation of the dye from the nanoparticle leading to inaccuracy in data gathered, and the possible imaging analysis of the dye itself rather than the nanoparticle (Takov *et al.*, 2017; Münter *et al.*, 2018). The CARS method used within this chapter is able to largely overcome this problem by allowing label-free imaging of the PMs, using their internal C-H bond structures to generate signals which can then be image processed (Masihzadeh *et al.*, 2013; Jones *et al.*, 2019).

Other research groups have also investigated nanoparticle cellular uptake using real-time fluorescence microscopy. One group used polymeric micelles labelled with fluorescent doxorubicin to investigate uptake into a human breast adenocarcinoma cell line (MCF-7), and saw a rapid intracellular fluorescence increase in the first 2 hours of incubation, which continued to increase over the 12-hour period tested. This group also went on to show the co-localisation of these polymeric nanoparticles with the cell's early endosomes, highlighting a potential cellular entry pathway for such nanoparticles (Qiu *et al.*, 2014).

IFC has also been previously used for the assessment of nanoparticle uptake into cells. Vranic and colleagues used IFC to differentiate between internalised SiO₂ nanoparticles, and those only adhering to the extracellular membrane of human adenocarcinoma cells (NCI-H292). The group reported that after a 4-hour incubation at 4°C, nanoparticles located predominantly on the cell surface, whereas after a 4-hour incubation at 37°C they had been largely internalised (Vranic *et al.*, 2013). This example highlights the benefit of using IFC over traditional flow cytometry (FC) techniques where the precise nanoparticle localisation, and confirmation of cellular uptake, could not otherwise be definitively reported. In a similar study, Phanse and colleagues used IFC to assess the uptake of either polymeric nanoparticles or *Salmonella enterica* into RAW 264.7 macrophages. They reported that after the addition of cytochalasin-D, an actin polymerisation inhibitor, there was reduced internalisation of both nanoparticles and *S. enterica*, displayed by increased cell surface accumulation (Phanse *et al.*, 2012). This work suggests that the nanoparticles and bacteria are taken up into cells by similar pathways, which is beneficial when

macrophages

considering drug delivery to the exact target site of infection. However, one element this paper lacked was using IFC to image cells that had been jointly exposed to *S. enterica* and polymeric nanoparticles, as opposed to the individual exposure of each. This additional co-exposure data would have allowed the assessment of whether co-localisation was observed between nanoparticles and bacteria. Using IFC for this purpose could fill a gap within the literature and highlight the potential of delivering drug-loaded nanoparticles to the precise intracellular bacterial infection site.

These examples have relied on using labelled nanoparticle formulations, however there have been previous attempts to assess cellular internalisation by label-free methods. One group assessed the uptake of PMPC-PDPA PMs into human oral cells, and oral tumour cell lines, using a mathematical model with *in vitro* assay validation. The model developed considered a range of uptake factors such as PM size, concentration, the level of bonding between cellular receptors and nanoparticles, and the subsequent internalisation recycle rates of these receptors. The group reported that the number of receptors per cell was what contributed most heavily to predicted PM uptake level between different cell types (Sorrell *et al.*, 2014). Label-free assessment of nanoparticle uptake has also been performed using CARS technology. Garrett and colleagues used CARS to monitor polymeric nanoparticle uptake into murine kidney tissue, following oral administration. The perfect drug delivery system would target sites of infection/disease, whilst avoiding organs where the payload is toxic, or build-up in organs such as the kidney. Therefore, being able to utilise CARS as an assessment of nanoparticle localisation within the body has great benefits. Raman spectroscopy is able to detect CH₂ bonds within biological samples at 2840 cm⁻¹, whereas the deuterated equivalent, CD₂, detects at 2100 cm⁻¹, which is considered to be a 'biologically silent' region. Within this study Garrett *et al.* used deuterated nanoparticles to ensure the recovered signal was from their polymeric nanoparticles (Garrett *et al.*, 2015). The success from this group provides a good foundation to this project for using CARS as a method to label-free image the PEO-PCL PMs within macrophage cells, and furthermore adds potential to future methods to investigate the localisation of PMs within mouse models.

This chapter will investigate whether PEO-PCL PMs are able to be successfully taken up by RAW 264.7 macrophage cells, whether healthy or infected with *B. thailandensis*. The aims of the experiments in this section are:

- To determine whether PMs can be taken up into healthy RAW 264.7 cells, using epifluorescence imaging as a measurement

Chapter 4: Internalisation and intracellular localisation of polymersomes in RAW 264.7
macrophages

- To determine whether PMs can be taken up into *B. thailandensis* infected RAW 264.7 cells, using confocal microscopy
- To use ImageStream technology to assess co-localisation between *B. thailandensis* bacteria and internalised PMs
- To use CARS technology to investigate how PMs can be imaged within RAW 264.7 cells without a prior need for labelling.

4.2 Results

4.2.1 Polymersome uptake into healthy RAW 264.7 macrophage cells

4.2.1.1 Epifluorescence

To become a viable option for intracellular drug delivery, PMs must be shown to be able to be taken up by cells of interest, in the case of this project, RAW 264.7 macrophage cells. Dil is a lipophilic membrane dye with a characteristic absorbance peak at 560 nm (Figure 4.1A). The absorbance of known Dil concentrations, unencapsulated and in DMF solution, was used to construct a standard curve (Figure 4.1B), and this was in turn used to assess the level of Dil encapsulation achieved within PMs. PM-Dil samples were made and dialysed as usual, and the samples were additionally spun through a filter to assess whether any unencapsulated Dil remained present within the buffer surrounding PMs (Figure 4.1C). Results confirmed that 6.9 μM of Dil was successfully encapsulated within PMs, and that no signal was detected from the filtrate, confirming efficient dialysis (Figure 4.1D).

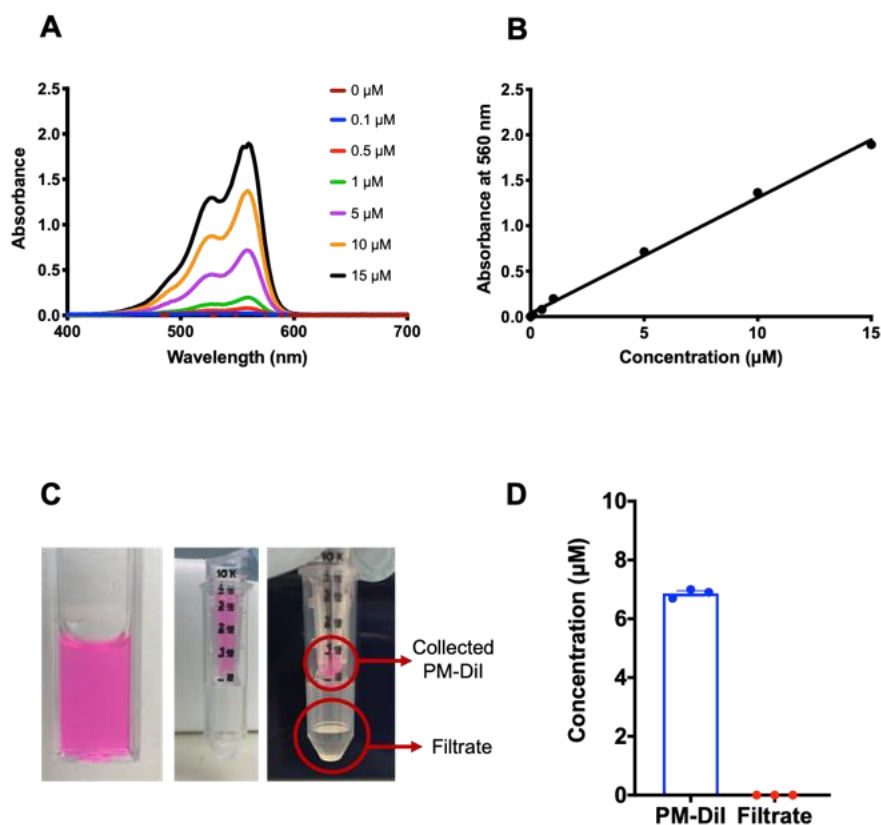


Figure 4.1 – Preparation of Dil-loaded nanoparticles. (A) The varying concentrations used to construct the Dil standard curve, ranging from 0 – 15 μM . Dil standards were prepared in a solution with DMF. The absorbance spectra of Dil possesses a characteristic peak seen at 560 nm. (B) A standard curve of Dil, with an $R^2 = 0.99$. (C) The PM-Dil samples were spun through a filter in order to separate PMs from the surrounding buffer (filtrate). (D) PM-Dil nanoparticles possessed a loaded concentration of 6.9 μM , and upon measuring the filtrate it was confirmed there was no unencapsulated Dil remaining post-dialysis.

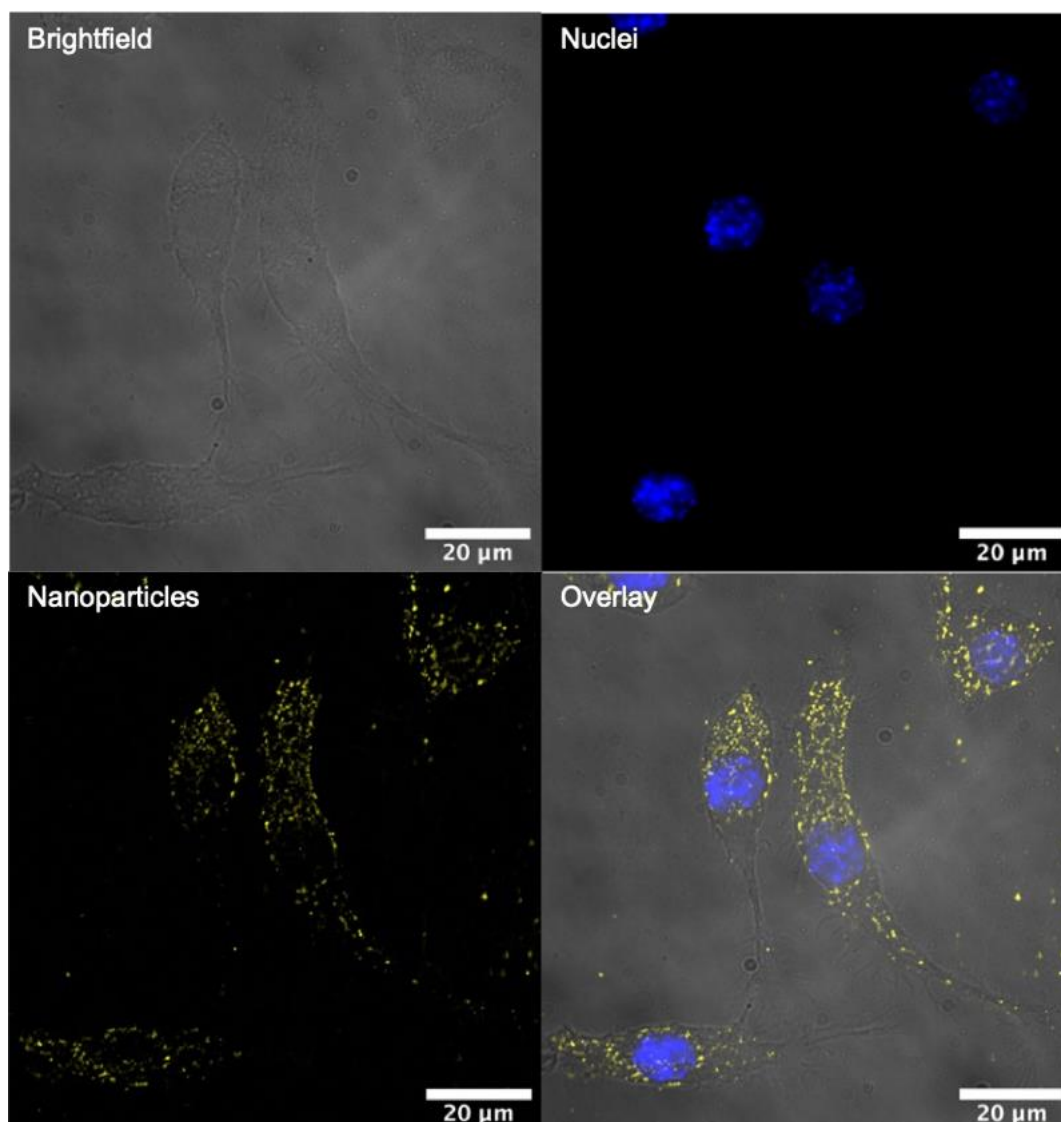


Figure 4.2 – Epifluorescent images showing PM uptake into RAW 264.7 cells after a 4-hour incubation. RAW cells were incubated with Dil-loaded PMs for a period of 4 hours. Following this, cells were stained with Hoechst nuclear dye (1 µg/ml), and then imaged on the Zeiss Axio Imager.M2m epifluorescence microscope.

RAW cells were incubated for 4 hours with PM-Dil nanoparticles, and Hoechst nuclear stain was also applied in order to visualise cell nuclei. Yellow puncta were observed in RAW 264.7 cells, indicating the uptake of Dil-labelled PMs (Figure 4.2). They did not penetrate into the nucleus, as highlighted by the fact the blue nuclear stained region remained separate from the yellow PM puncta.

4.2.1.2 Real-time polymersome uptake into RAW 264.7 cells

To investigate time-dependent uptake of PM-Dil in RAW 264.7 cells, a Nanoimager S super-resolution microscope equipped with a heated environmental chamber was used to image cells exposed to labelled PMs over 27 minutes. Labelled puncta initially appeared to be concentrated at the cell periphery (9 minutes, Figure 4.3A), however at later timepoints puncta were observed within cells. It should be noted that by the 20-minute snapshot shown the Z-position had been shifted to the bottom of the cell, hence the slightly out of focus image shown.

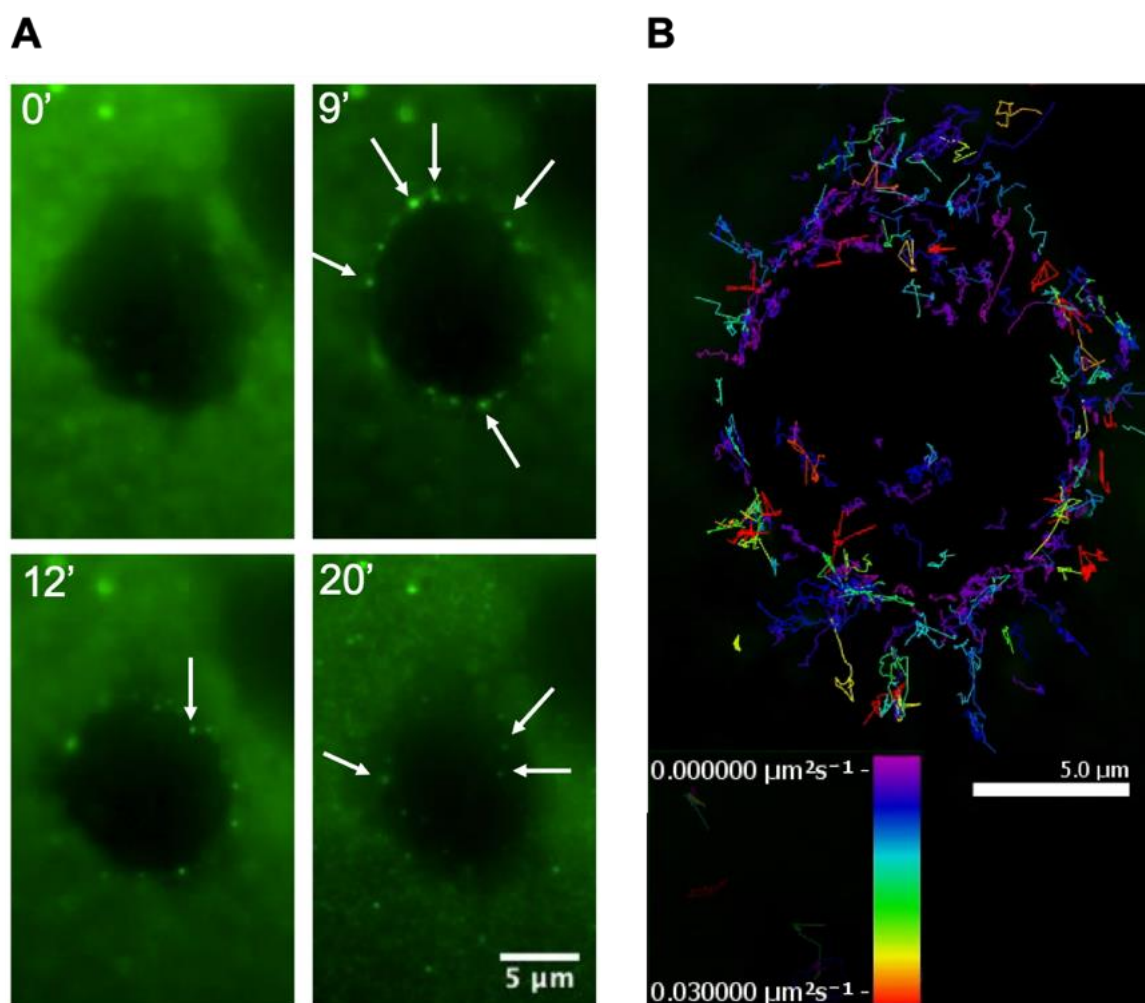


Figure 4.3 – Stills from a time-lapse video of PM-Dil uptake into RAW 264.7 macrophage cells. (A) The progress of PM-Dil uptake can be seen between 0 and 20 minutes. White arrows indicate the position of puncta collecting either at the cell periphery or within cells. (B) Tracking analysis was performed which displayed clear PM tracks within cells by the end of the 27-minute uptake assay. Images were obtained using a Nanoimager S super-resolution microscope.

A tracking algorithm was also applied to these images which allowed the temporal movement of puncta to be visualised by tracks, with their corresponding rate of movement (Figure 4.3B). These tracks are displayed based on their diffusion coefficients shown in the colour key within Figure 4.3B. The data gathered displays the tracks of PMs that have made their way inside the cell, and so supports data from Figure 4.3A that in as little as 27 minutes the PMs are able to make their way inside the cell of interest.

The Nanoimager microscope was also used to assess the degree of co-localisation between PM-Dil nanoparticles and lysotracker dye. Fluorescence images were collected for both PM-Dil (green puncta) and Lysotracker (red puncta), and the images merged to assess co-localisation (orange puncta) (Figure 4.4). Lysotracker stains for lysosome organelles, and so this suggests PM nanoparticle co-localisation with these subcellular structures.

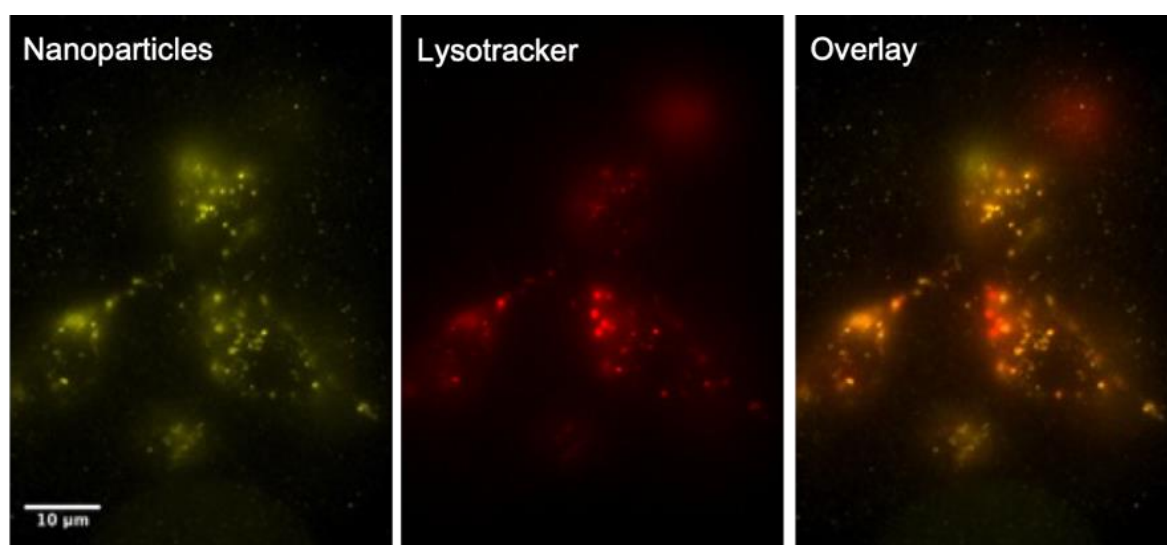


Figure 4.4 – Co-localisation between PM-Dil nanoparticles and lysosomes. Co-localisation between PMs and lysosomes was observed in as little as 27 minutes. The nanoparticles are depicted in green, lysosomes in red, and the spots of orange in the overlay image show the co-localised areas. Images were taken using a Nanoimager S super-resolution microscope.

4.2.1.3 Coherent anti-Stokes Raman scattering (CARS)

A key challenge with using fluorescent membrane stains, such as Dil, as a method to image nanoparticles is the possible dissociation of the stain from the nanoparticle, leading to imaging of the dye itself rather than specifically the nanoparticles. CARS is a technique that allows for label free imaging of PMs by using the polymer's C-H bonds as a marker instead. This allows unambiguously for detection of the PMs, and their presence inside cells, rather than non-specific dyes. RAW 264.7 cells were incubated with PM-doxycycline nanoparticles for a period of 21 hours and then imaged for both a CARS signal and a two-photon fluorescence (TPF) signal. The TPF signal can be obtained due to the intrinsic fluorescence possessed by doxycycline, and is a method to determine whether higher fluorescence is observed intracellularly in PM-delivered doxycycline samples compared to free unencapsulated doxycycline at the same concentration. It was hypothesised that (i) there would be a higher level of polymer CARS spot signal in the PM-treated cells compared to the untreated control, and (ii) that there would be a higher level of TPF signal coming from PM-doxycycline treated cells. Control groups present included cells exposed to PM-empty nanoparticles; untreated; free doxycycline at 4.5 $\mu\text{g/ml}$; free doxycycline at 20 $\mu\text{g/ml}$.

Cell samples were scanned and then nine tile images stitched together using Fiji software (Figure 4.5A). A software package, Ilastik, was used to separate the image background from the cells and construct a binary image (Figure 4.5B). Following this, using Fiji software, this binary image was processed and cleaned to ensure removal of objects smaller than 50 μm^2 , which were categorised as debris (Figure 4.5C). Using the software package Icy, a mask was created over the CARS image (Figure 4.5D) and a spot detector plug-in used to determine the number of CARS spots present within the image, and the total brightness intensity. Each red circle generated represents a spot that was detected by the plug-in (Figure 4.5E).

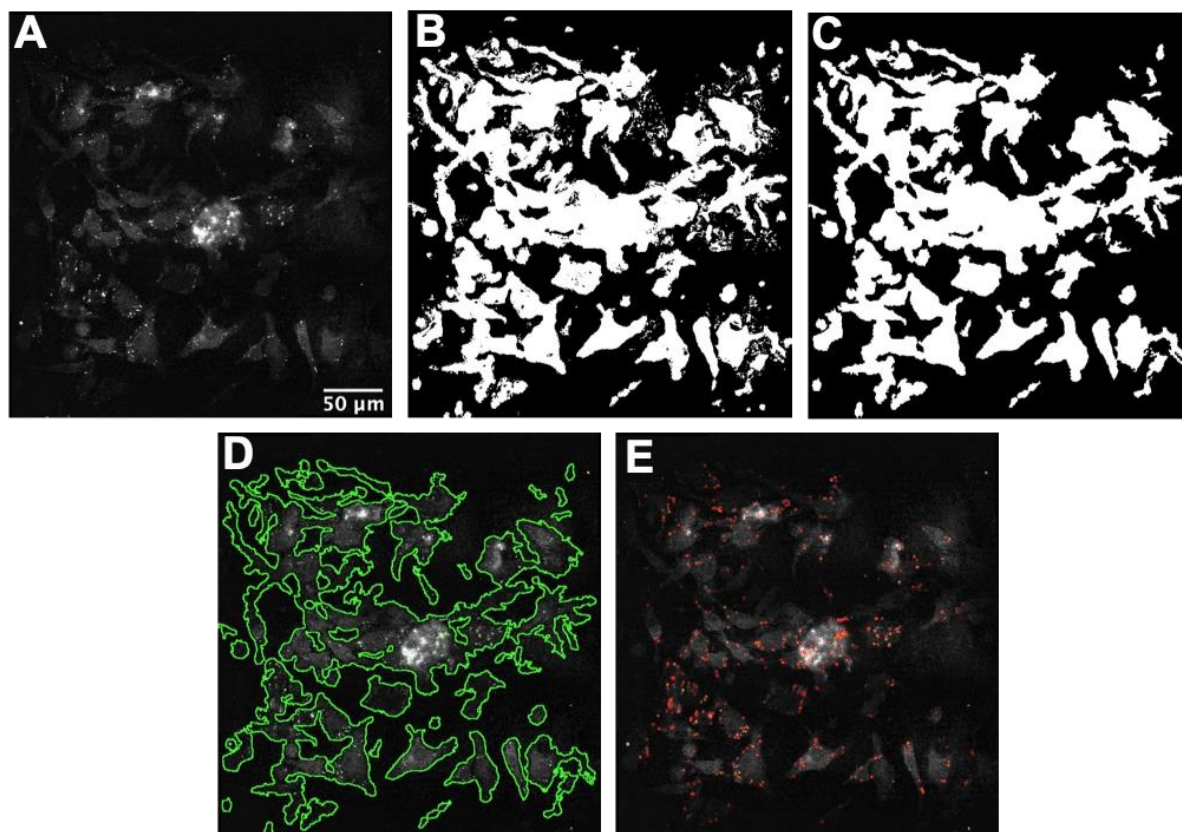


Figure 4.5 – CARS image processing stages. (A) CARS image showing PM-empty nanoparticles within RAW 264.7 macrophages. (B) Images were first processed in Ilastik to convert them to a binary image without background inclusion. (C) The binary images were processed to remove cell debris and background artefacts from inclusion. (D) Software package Icy was used to create a mask over the CARS image. (E) Within Icy a spot detector plug-in was used to perform a spot-count to assess the number and brightness intensity of CARS spot signals detected within cells.

White puncta were observed in the CARS images from cell samples that were treated with either PM-empty or PM-doxycycline (Figure 4.6A). As expected, CARS spots were not visible in the control cells that were either untreated, or exposed to free drug only. This suggests that the white puncta originate from the PM nanoparticles and their C-H bonds. The TPF images showed very little fluorescence detection from any of the samples, with the exception of the free doxycycline 20 $\mu\text{g}/\text{ml}$ positive control, which showed slightly higher visible levels. The CARS and TPF signals were then overlaid into one image.

macrophages

Quantitative analysis was carried out on the images and the level of pixel brightness intensity measured, performed as described previously. There was no significant difference in the level of brightness, i.e. fluorescence, observed between untreated cells and PM-doxycycline treated cells (Figure 4.6B). This does not support the initial hypothesis that there would be a significant increase in the fluorescence level between PM-doxycycline treated cells compared to untreated due to the fluorescence of doxycycline. There was a significant increase in the brightness intensity in the free doxycycline 20 $\mu\text{g/ml}$ positive control compared to the untreated control (one-way ANOVA with a Tukey's post-hoc test, $p < 0.0001$). Image analysis also revealed that on average PM-empty and, surprisingly, free doxycycline at 20 $\mu\text{g/ml}$ treated cells had a significantly higher number of CARS spots detected per μm^2 than untreated cells (one-way ANOVA with a Tukey's post-hoc test; PM-empty $p < 0.001$, free doxycycline 20 $\mu\text{g/ml}$ $p < 0.01$) (Figure 4.6C). Additionally, the mean area of CARS spots per μm^2 was also significantly higher in these samples of cells (PM-empty $p < 0.01$; free doxycycline 20 $\mu\text{g/ml}$ $p < 0.05$) (Figure 4.6D). Overall, the data from this section suggests that - although doxycycline could not be visualised at higher intracellular levels when delivered by PMs compared to control groups - PMs are taken up into RAW 264.7 macrophages due to evidence from CARS microscopy. Importantly, this also highlights the utility of label-free imaging of nanoparticle uptake in cells, and supports earlier results using imaging of fluorescent dye-labelled PMs.

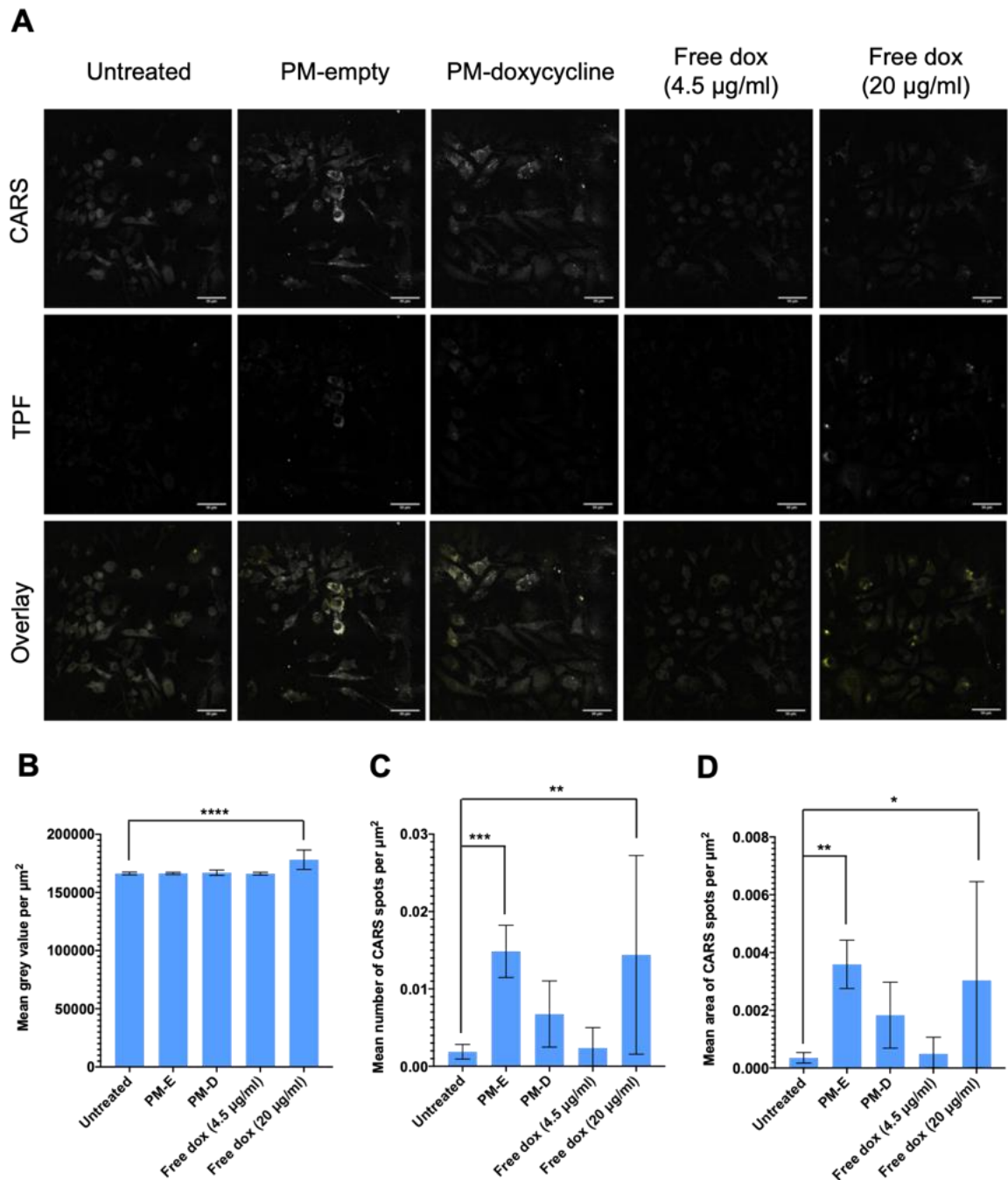


Figure 4.6 – CARS and TPF images alongside quantitative image analysis data. (A) A collection of images taken from cells that had been exposed to either PM-empty, PM-doxycycline, free doxycycline at 4.5 µg/ml, free doxycycline at 20 µg/ml, or untreated. CARS and TPF images were taken separately and then overlaid. TPF excitation was 797.2 nm and emission was 450 nm. Scale bars shown are at 50 µm. (B) The mean grey value per µm². (C) The mean number of CARS spots per µm². (D) The mean area of CARS spots per µm². Data represents the mean and SD of one repeat performed in triplicate. All statistical tests performed were one-way ANOVAs with a Tukey's post-hoc test. * = $p < 0.05$, ** = $p < 0.01$, *** = $p < 0.001$, **** = $p < 0.0001$.

4.2.2 Polymersome uptake into *B. thailandensis* infected RAW 264.7 cells

4.2.2.1 Confocal analysis of uptake

Following confirmation that PMs are taken up by RAW 264.7 macrophage cells, uptake into *B. thailandensis* infected cells was next assessed to ensure a prior bacterial infection does not alter the cellular level of PM uptake. DiD is another lipophilic membrane dye that was utilised within this project. It possesses a characteristic absorbance peak at 649 nm, and using a series of known concentrations, in DMF solution, (Figure 4.7A,B) a standard curve was constructed (Figure 4.7C). Similarly to when using Dil, PM-DiD samples were spun through a filter and the level of unencapsulated DiD remaining, if any, was measured (Figure 4.7D). Throughout the experiments which used PM-DiD, these nanoparticles were applied with an encapsulated concentration of $7.2 \mu\text{M} \pm 0.9$, and no signal was detected from the filtrate, highlighting all dye was bound to the PMs (Figure 4.7E).

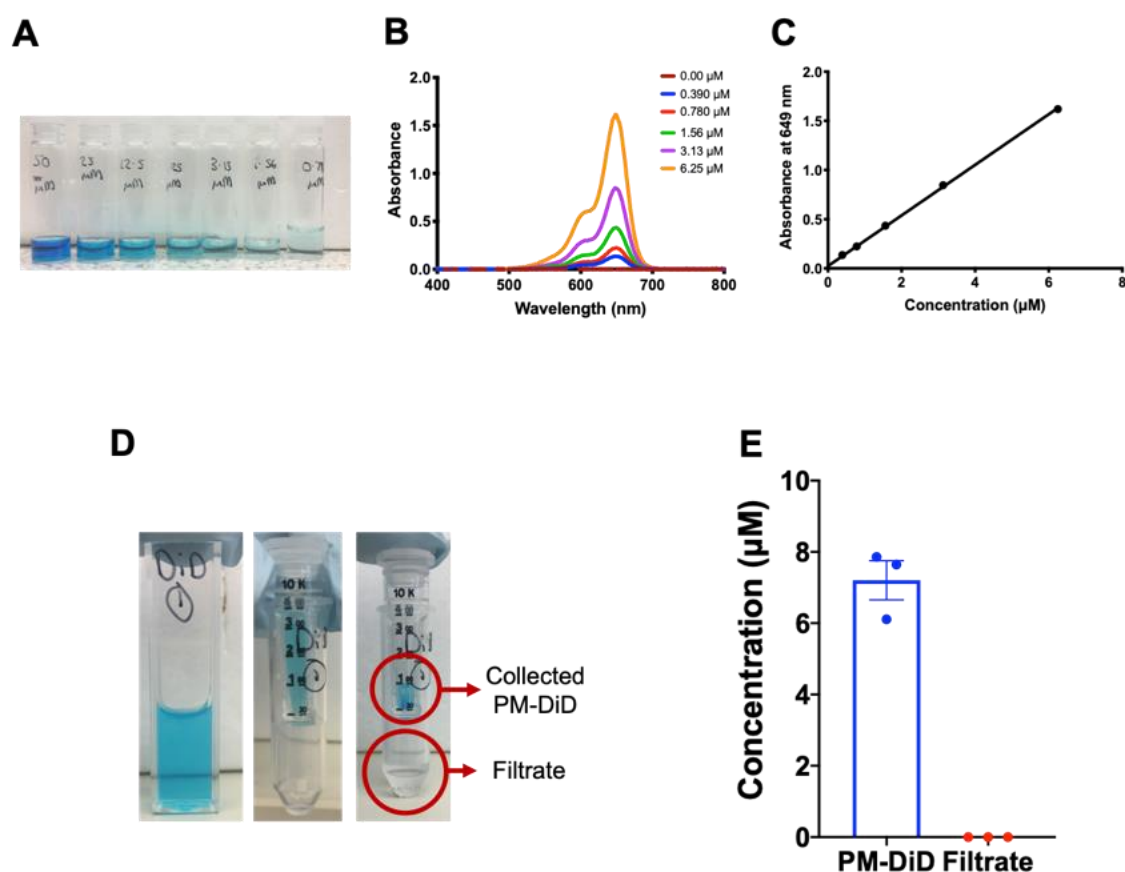


Figure 4.7 – Preparation of DiD-loaded nanoparticles. (A) The varying concentrations used to construct the DiD standard curve, ranging from 0 – $6.25 \mu\text{M}$. DiD was made up in solution with DMF. (B) The absorbance spectra of DiD, with a characteristic peak seen at 649 nm. (C) A standard curve of DiD, with an $R^2 = 0.99$. (D) The PM-DiD samples were spun through a filter in order to separate PMs from the surrounding buffer (filtrate). (E) PM-DiD nanoparticles possessed a loaded concentration of $7.2 \mu\text{M} \pm 0.9$, and upon measuring the filtrate it was confirmed there was no unencapsulated DiD remaining post-dialysis.

RAW cells, infected with *B. thailandensis*, were then incubated with PM-DiD nanoparticles for a period of 3 hours before confocal imaging. *B. thailandensis* is genetically modified with a green fluorescent protein (GFP) tag, which can be seen by the green fluorescence in Figure 4.8. DiD, depicting presence of PMs, is shown in red. Despite the presence of intracellular bacteria, DiD puncta were still present intracellularly after PM incubation, indicating that cellular infection does not qualitatively affect PM uptake.

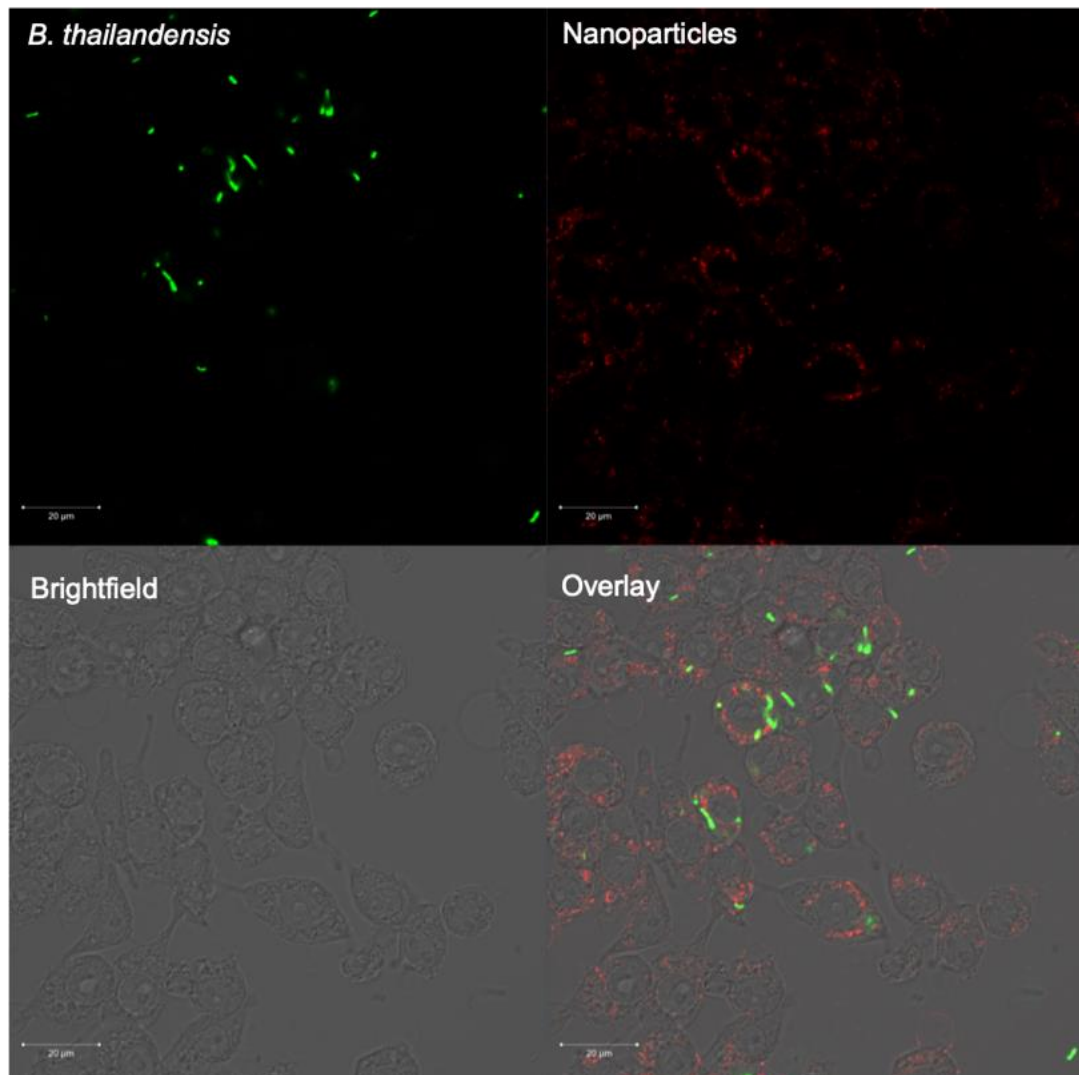


Figure 4.8 – Confocal microscope image of PM-DiD uptake into *B. thailandensis* infected RAW 264.7 macrophage cells. Following a 3-hour incubation with PM-DiD nanoparticles, infected cells showed a good level of uptake, confirming a prior infection does not limit the cell’s abilities to take up nanoparticles. Scale bar is 20 µm.

4.2.2.2 ImageStream analysis of uptake and bacterial co-localisation

In previous sections the uptake of PM nanoparticles into RAW 264.7 macrophage cells has been demonstrated. To further this work, the method of imaging flow cytometry (IFC) was used, using specifically ImageStream technology. IFC is capable of imaging cells on a single cell-by-cell basis, and captures intracellular 'slices' of cells as they pass through the camera. This feature therefore not only allows imaging and quantification of fluorescent molecules passing through the flow, but also for intracellular localisation of the fluorophores within cells. This makes IFC an invaluable tool, as it allows direct assessment of co-localisation between GFP expressing *B. thailandensis*, and fluorescently labelled PM nanoparticles.

Cells were infected with *B. thailandensis* and then incubated with PM-DiD nanoparticles for 3 or 21 hours, and these cells are later referred to as the group '**B.t exposed cells + PMs**'. Control groups were also included, and these were cells incubated with *B. thailandensis* but without the presence of PMs (**B.t exposed cells**), and cells incubated with PMs without the presence of a prior infection (**Control cells + PMs**). IFC data is based on cell population sizes of 10,000. Figure 4.9 illustrates the hierarchical gating process that the cell selection involved. Only in focus (R1) and single cells (R2) were analysed. Examples of images collected on the ImageStream are also included. Channel 01 contains brightfield images of the cells, Channel 02 is of the GFP fluorescence from *B. thailandensis*, and Channel 11 is the DiD fluorophore representing the PM nanoparticles. Table 12 is also included and uses the mean values taken from the '**B.t exposed cells + PMs**' population to highlight numerically the gating process.

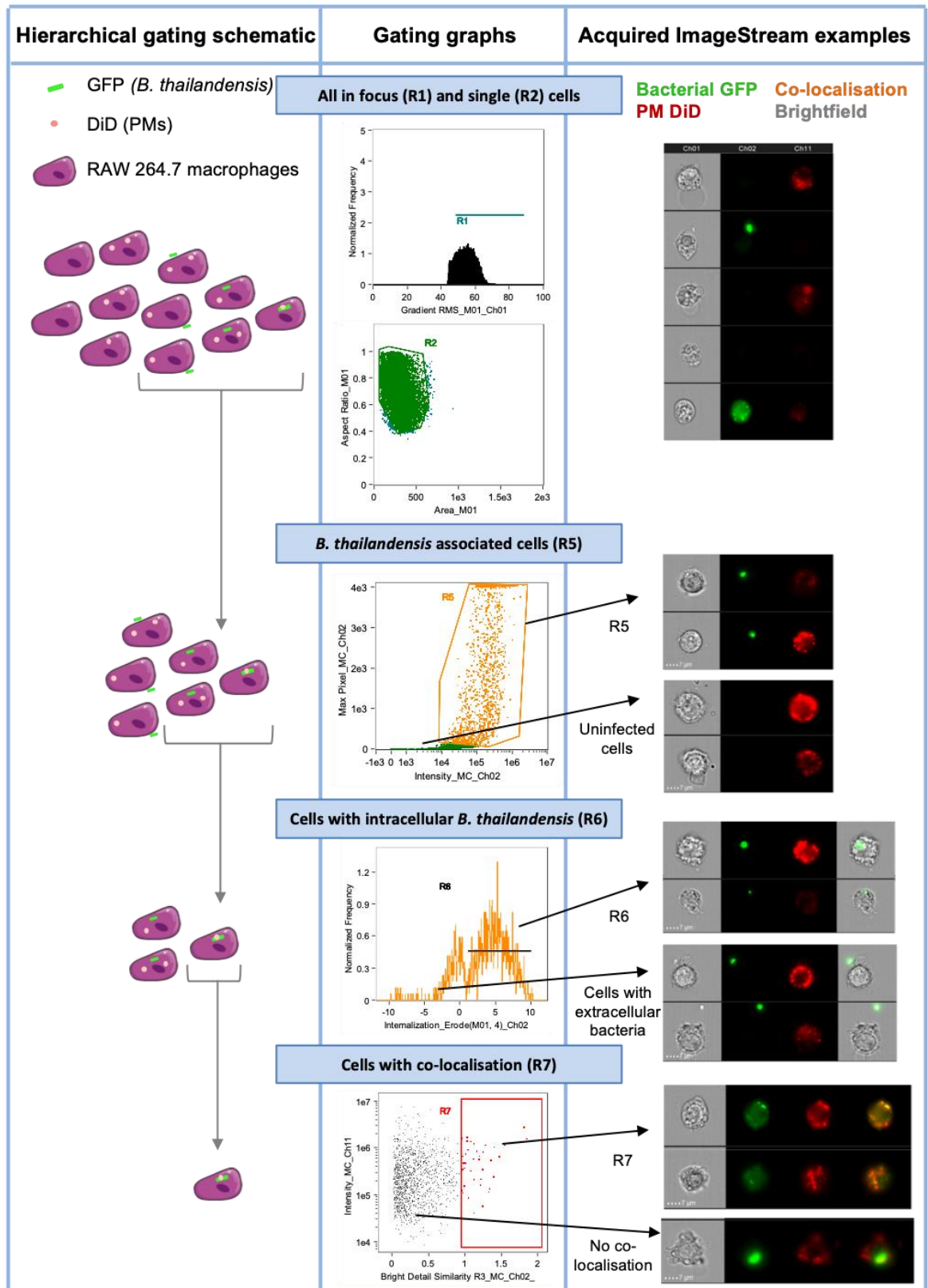


Figure 4.9 – A breakdown of the gating process used to select cells displaying co-localisation, and a visualisation of the detected fluorophores. Of the approximate 10,000 cells acquired, a series of gating regions were added to select desired cells. Quantitative analysis could then be performed on each gated cell population. Examples of the typical ImageStream images collected during this project are also shown. Ch01 represents the brightfield channel where individual cells can be captured; Ch02 is the GFP fluorophore from *B. thailandensis*, and Ch11 is the DiD fluorophore from the labelled PM nanoparticles. Scale bar is at 7 μm .

Table 12: Quantification of PM and *B. thailandensis* co-localisation within RAW 264.7 macrophage cells. Data is taken from the bacteria and PM exposed cell populations at both 3 and 21-hour incubations.

Region	Description	3-hour PM incubation			21-hour PM incubation		
		Cell count	% of total events	% of gated cells (region)	Cell count	% of total events	% of gated cells (region)
R0	All	10,000	100	-	10,000	100	-
R1	In focus	9853	98.5	98.5	9326	93.3	93.3
R2	Single cells	9835	98.4	99.8 (In focus)	9270	92.7	99.4 (In focus)
R5	Cells with associated Bt	2619	26.2	26.6 (Single cells)	6205	62.1	66.9 (Single cells)
R6	Intracellular bacteria	1057	10.6	40.4 (Cells with ass. Bt)	2522	25.2	40.6 (Cells with ass. Bt)
R7	Co-localised	197	2.0	18.6 (Intracellular bacteria)	80	0.80	3.2 (Intracellular bacteria)
R8	% of cells with PMs (taken from R1)	9843	98.4	99.9 (In focus)	9310	93.1	99.8 (In focus)

From the cell images acquired, those which included single and in focus cells were gated (selected for further analysis), and from this population any cells that were also positive for DiD staining were selected. Cells were defined as being PM positive once they fell over a threshold level of fluorescence (Figure 4.10). By this metric, both cells that were exposed to bacteria (***B.t* exposed cells + PMs**) and those that were not (**Control cells + PMs**) were positive for DiD. Within the **Control cell + PMs** group 99.96% of cells contained PMs after 3 hours, compared to 99.94% after 21 hours. Similarly, in the ***B.t* exposed cells + PMs** population 99.90% of cells contained PMs after 3 hours, and 99.83% after 21 hours. There were no significant differences found within groups, indicating increased incubation time did not increase the number of cells containing PMs (Figure 4.11A).

A drawback of analysing cells by percentage positive for PMs (as in Figure 4.11A), is that it generates only a 'positive for PMs' versus 'negative for PMs' result, and gives no information on the intensity of the fluorescence signal detected. To overcome this, mean fluorescence intensity of DiD was used as an indicator of the number of PMs present within PM positive cells. In both populations, '***B.t* exposed cell + PMs**' and '**Control cells + PMs**', there was a significantly higher level of fluorescence measured after 21 hours ($p < 0.0001$, two-way ANOVA with Tukey's post-hoc

test), indicating a greater number of PMs present intracellularly at 21 hours compared to 3 hours. Additionally, by 21 hours the 'Control cells + PMs' showed a significantly higher level of fluorescence than the '*B.t* exposed cells + PMs' cells ($p < 0.0001$, two-way ANOVA with Tukey's post-hoc test). This suggests a prior *B. thailandensis* exposure may limit the number of PMs that can be taken up by the RAW 264.7 cells (Figure 4.11B).

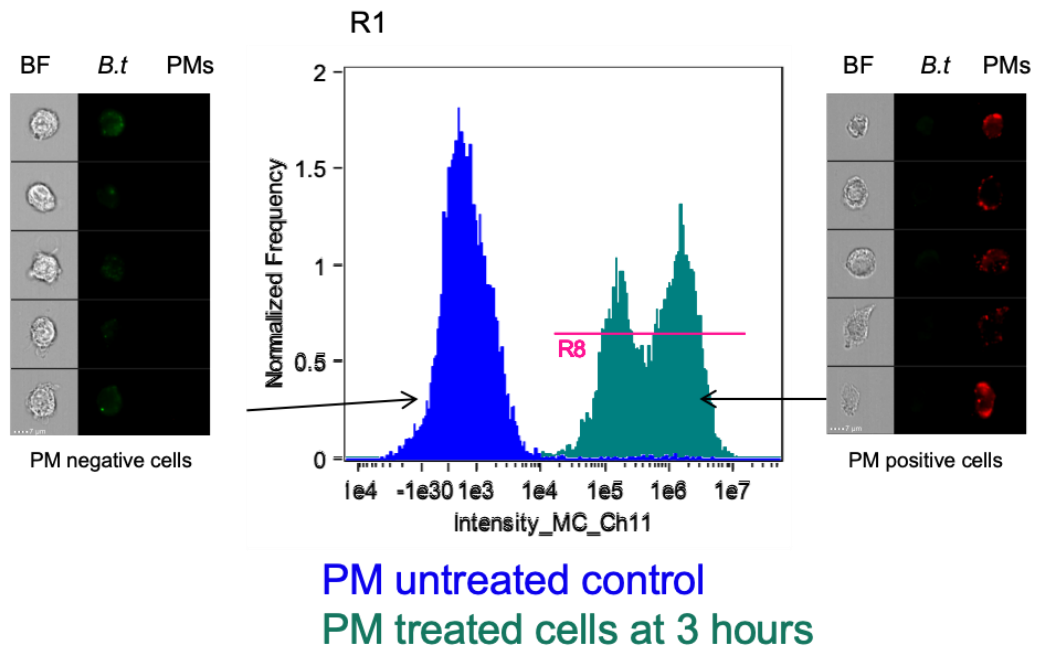


Figure 4.10 – Imaging flow cytometry gating for PM positive cells. Of all the single and in focus cells, cells were considered positive for PMs once the DiD fluorescence reached the threshold fluorescence intensity of 15,000. Untreated control cells exhibited fluorescence intensities below 10,000. The PM positive cells comprised the R8 gated population.

After exposure of RAW 264.7 cells with *B. thailandensis*, there was not a 100% infection of the cells, and so within the '*B.t* exposed cells + PMs' population some uninfected cells remained. It was therefore assessed whether the level of uptake varied between *B. thailandensis* infected cells, and those which remained uninfected post-exposure. The population was therefore gated into '**Uninfected + PMs**' cells and '**Cells with associated bacteria + PMs**'. 'Associated bacteria' includes any bacterial/cell interaction, for example cells with intracellular bacteria; external bacteria touching the cell membrane; or bacteria located in close proximity to the cell. At 21 hours, a significantly higher level of PM uptake was seen from '**Cells with associated bacteria + PMs**' compared to '**Uninfected + PMs**' cells, indicating cells may be primed for uptake due to the prior bacterial infection ($p < 0.0001$, two-way ANOVA with Tukey's post-hoc test) (Figures 4.11C,D). After a 21-hour *B. thailandensis* exposure, 62.1% of cells were associated with bacteria (and of this 40.6% were intracellular), and the remaining 37.9% of cells were not (Table 12).

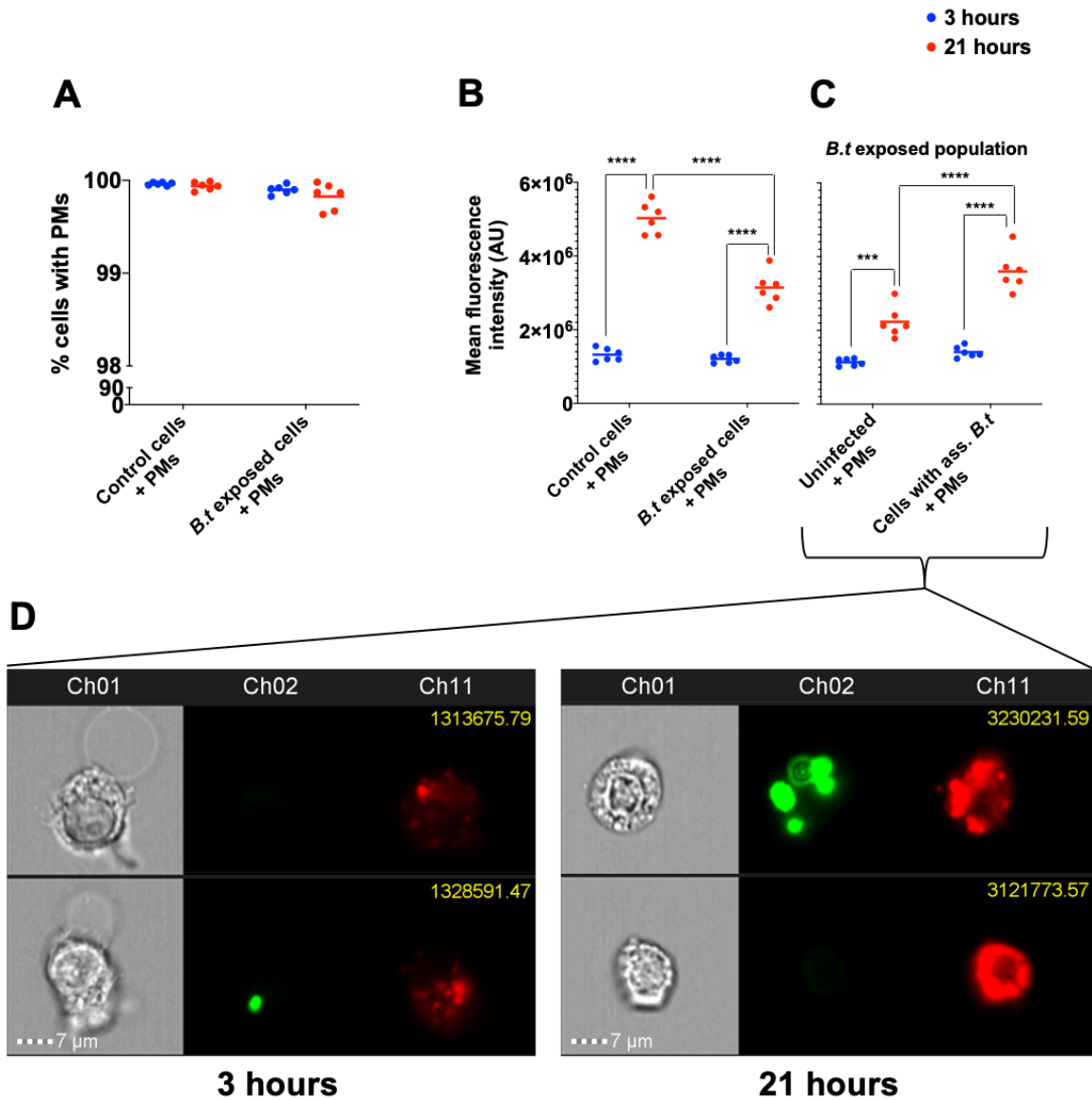


Figure 4.11 – Assessment of PM uptake into RAW 264.7 macrophage cells. (A) A comparison of the percentage of cells showing PM uptake after 3 and 21 hours in *B. thailandensis* exposed cells, or control cells. (B) The mean PM fluorescence intensity in RAW 264.7 macrophage cells after 3 and 21 hours, in *B. thailandensis* exposed cells versus control cells. (C) The population of cells that had been exposed to *B. thailandensis* was further broken down to assess the particular cells responsible for PM uptake. It revealed that *B. thailandensis* associated macrophages were as capable of uptake as macrophages which remained uninfected, even after bacterial exposure. (D) A comparison of DiD (PM) fluorescence (red), at 3 and 21-hour incubations, in both uninfected cells, and cells with a bacterial association (green). Values in yellow show the mean fluorescence intensity of PMs of that individual cell. Scale bars are at 7 μ m. All statistical tests performed were two-way ANOVAs with a Tukey's post-hoc test. * = $p < 0.05$, ** = $p < 0.01$, *** = $p < 0.001$, **** = $p < 0.0001$.

It was next assessed what proportion of cells contained specifically intracellular bacteria (R6). There was a significantly higher percentage of intracellular bacteria after a 21-hour incubation compared to a 3-hour, with an increase from 11.3% to 27.0% for the '**B.t exposed cells**' control group ($p < 0.0001$, two-way ANOVA with Tukey's post-hoc test), and an increase from 10.8% to 27.5% for the '**B.t exposed cells + PMs**' ($p < 0.0001$, two-way ANOVA with Tukey's post-hoc test) (Figure 4.12A). Figure 4.12B shows image examples of the appearance of cell-associated bacteria (top and middle images) compared to intracellular bacteria (bottom images).

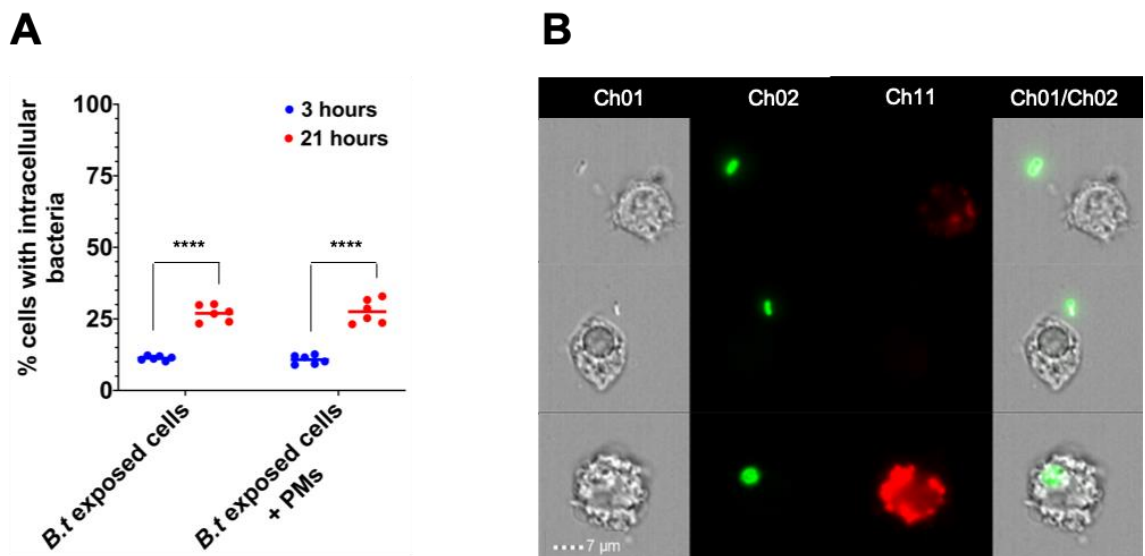


Figure 4.12 – The proportion of cells containing intracellular bacteria from the ImageStream assay. (A) The percentage of cell containing intracellular bacteria at 3 and 21 hours, compared between *B. thailandensis* exposed cells and control cells. (B) ImageStream captured images highlighting the difference between cells with external bacteria (top), external but touching bacteria (middle), and cells with intracellular *B. thailandensis* (bottom). All statistical tests performed were two-way ANOVAs with a Tukey's post-hoc test. **** = $p < 0.0001$.

Finally, of all the cells containing PMs and intracellular bacteria (R6), the level of direct co-localisation between PM-DiD puncta and *B. thailandensis* GFP signal was measured (R7). Co-localisation was calculated by comparing fluorescence signal from both GFP and DiD channels and using Pearson's correlation coefficient to generate a value between 0 and 1, representing no co-localisation or perfect co-localisation, respectively. There was found to be a significantly higher level of co-localisation seen at the 3-hour timepoint, with 18.6% of cells showing co-localisation, compared to the 21-hour timepoint, with only 3.2% of cells showing co-localisation ($p < 0.0001$, unpaired t-test, two-tailed) (Figure 4.13A). Figure 4.13B shows examples of images collected from the ImageStream displaying co-localisation. Areas of orange puncta represents sites of direct co-localisation between the green bacterial GFP, and the red PM-DiD. This data is highly relevant

macrophages

when considering nanoparticles for drug-delivery, as it shows a good level of targeting to the exact infection site.

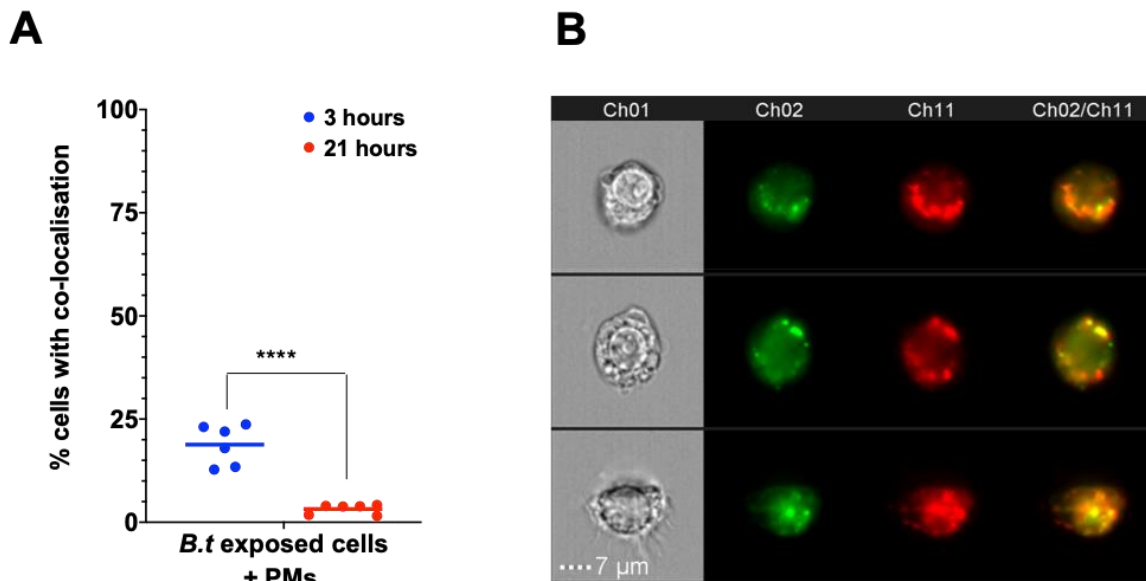


Figure 4.13 – Co-localisation of *B. thailandensis* and PMs. (A) The proportion of cells displaying direct co-localisation between *B. thailandensis* and DiD from the PM nanoparticles. A significantly higher level of co-localisation was observed at the 3-hour timepoint compared to the 21-hour ($p < 0.0001$, unpaired t-test, two-tailed). (B) ImageStream images collected which visually show co-localisation within RAW 264.7 macrophage cells. The orange puncta represent areas of co-localisation.

4.3 Discussion

In the previous chapter it was shown that polymersome (PM) nanoparticles are able to stably encapsulate and retain antibiotics, within either their hydrophobic shell membranes, or their aqueous cores. The work was continued in this chapter by investigating whether PM nanoparticles were able to be taken up by cells of interest for this project, RAW 264.7 macrophages. *B. pseudomallei* primarily resides within macrophage cells of the body, and so it is imperative that the nanoparticles can access these intracellular locations, if they are to be used successfully clinically. The experiments conducted within this chapter addressed these points by showing that:

- PMs labelled with lipophilic membrane dye, DiI, are taken up by RAW 264.7 macrophages
- Label-free imaging of PMs in healthy RAW 264.7 macrophages is possible using Coherent anti-Stokes Raman scattering (CARS) imaging, providing a step towards eliminating the need for labelling of nanoparticles in order to image them
- PMs are taken up by RAW 264.7 macrophage cells pre-infected with *B. thailandensis*, showing that intracellular infection does not inhibit cellular PM uptake
- PMs labelled with lipophilic membrane dye, DiD, directly co-localised with intracellular *B. thailandensis*, assessed using the imaging flow cytometer, ImageStream.

Nanoparticles made from poly(ethylene oxide-b-caprolactone) (PEO-PCL) are a good choice for using in research on drug-delivery vehicles, as each individual polymer block has FDA approval, and so aids in potential for use clinically (Qi *et al.*, 2013). These polymer-based nanoparticles have been widely researched, and those using PEO and PCL components were some of the first systems to be investigated (Gref *et al.*, 1994; Allen *et al.*, 1998), largely due to their biocompatibility. Despite this, the PMs used within this project were far simpler in design than other nanoparticles which possess, for example, targeting moieties (Larson and Ghandehari, 2012; Gao *et al.*, 2014; Dehaini *et al.*, 2016), or the ability to degrade upon exposure to certain environmental stimuli (Meng *et al.*, 2012; Gandhi *et al.*, 2015). This simple system design has advantages and disadvantages in terms of uptake into cells. One obvious potential drawback is the possibility that a lack of active targeting present on the PM's surface, may lead to a lower uptake by the cells of interest. Similarly, once inside a cell, if the PMs do not have properties allowing environmental release in response to pH, for example, this may reduce the ability for payloads to be released and take effect. Ideally, future experiments would be able to take place which could modify the block co-polymer to include these features, and then experiments performed again to allow for a comparison of uptake efficacies. The cells being investigated for PM uptake within this project

macrophages

were RAW 264.7 macrophages. Macrophages by nature take up foreign materials (Gustafson *et al.*, 2015), and so it was hypothesised that PM uptake should likely occur with ease, and without the need for more complex targeting systems. Furthermore, due to the minimal amount of literature on PM drug delivery for intracellular bacterial infections, maintaining simplicity for preliminary *in vitro* tests was considered to be advantageous and the most straightforward starting point.

Dye-labelled PMs were taken up by RAW 264.7 macrophage cells after a 4-hour incubation period (Figure 4.2), and Nanoimager data indicated that this occurs in an even shorter timeframe, with PM-Dil uptake being seen in as little as 27 minutes (Figure 4.3). Although the mechanism of nanoparticle uptake into cells remains unclear, it is known that macrophages are capable of taking up foreign particles, and other materials, via the active process of endocytosis within minutes (Thyberg *et al.*, 1985). Endocytosis comprises both phagocytosis and pinocytosis forms of cell uptake, the former responsible for larger particle uptake, generally 250 nm plus in size, and the latter for smaller nanoscale particles (Foroozandeh and Aziz, 2018). There are other examples within the literature of nanoparticles being taken into cells through mechanisms aside from endocytosis, including passive diffusion across the cell membrane. One particular group showed how quantum dots, with sizes between 1 – 5 nm, were able to increase flexibility of lipid bilayers enough to penetrate without leaving holes in the membrane (Wang *et al.*, 2012). However, it is likely that due to the PMs used in this project being a much larger size than this, that their main mechanism of entry is endocytosis. A possible future experiment that might test this theory would be to block endocytosis pathways in the RAW cells, and to observe whether PM uptake still occurs to the same level, or if it is hindered/fully inhibited. Many different inhibitors of the various endocytic pathways have been reported (Dutta and Donaldson, 2012), all of which could be used to specifically determine which PM uptake mechanism(s) is used. One particular study has done just this, and investigated the effects of blocking macrophage endocytosis on nanoparticle uptake (Kuhn *et al.*, 2014). The group used inhibitors that were specific to each one of the endocytic pathways tested to assess how this hindered nanoparticle uptake. For example, cytochalasin D was used to inhibit actin formation, which both phagocytosis and macropinocytosis rely on, and chlorpromazine hydrochloride to inhibit clathrin-mediated endocytosis (a form of pinocytosis). For all inhibitors tested, uptake of 40 nm polystyrene nanoparticles was found to be partially impeded, with some intracellular particles still detected. This suggests that nanoparticles can be taken up via a number of endocytic routes, and that impeding one does not totally eliminate nanoparticles from entry. The impedance seen strongly shows that phagocytosis,

macropinocytosis and clathrin-mediated endocytosis are key pathways involved in nanoparticle uptake.

One of the significant findings from the Nanoimager data, was that by the end of the 27-minute uptake session, a high degree of co-localisation was observed between the nanoparticles and the lysosomes (Figure 4.4). Other studies have also reported this co-localisation, supporting this project's findings (Nicolete *et al.*, 2011). This could be highly relevant in the context of drug delivery to intracellular infections as when endocytosed by the macrophage cell the usual pathway of bacterial degradation involves endosomal processing resulting in a fusion of the internal vesicle with degradative lysosome organelles (Gruenberg, 2001; Huotari and Helenius, 2011). The co-localisation observed within this project supports the hypothesis that this project's PMs are actively taken up into cells via the endocytic pathway. Therefore, if both the bacteria and the PMs are taken up by the same pathway it suggests that they would be in close proximity to one another, giving antibiotic-loaded PMs great potential to deliver drugs to the desired target location.

There have been other studies which have investigated the uptake of nanoparticles into cells, and one highly relevant paper was published which used fluorescein loaded PEG-PCL PMs, like those used within this study, to assess payload release into mammalian L929 fibroblast cells (Scarpa *et al.*, 2016). Fluorescein is a hydrophilic fluorophore and is quenched at high concentrations, for example when inside PMs. Scarpa *et al.* showed that approximately 15 minutes into incubation with L929 cells, fluorescence was detected, therefore indicating not only PM uptake into the cells, but also intracellular release of the payload in order for fluorescein to become unquenched and fluoresce. This paper directly supports findings from this project that the PEO-PCL PMs are capable of uptake into cells, and also suggests some form of PM degradation once inside cells. The paper does raise some interesting points, as one feature of fluorescein is that its fluorescence is quenched by acidic environments (Martin and Lindqvist, 1975; Peterson, 2010), therefore the visualisation of it after 15 minutes suggests the PMs may have been located within either early endosomes, or the cytoplasm. If the PM payload is able to make its way into the cytoplasm this is highly promising for tackling *B. thailandensis* infections, as this species is able to escape the endosomal vesicles shortly after intracellular entry and reside in the cytoplasm (Cheng and Currie, 2005; Ozanic *et al.*, 2015). Future work for this project would include performing the same assay, with fluorescein loaded PEO-PCL PMs incubated with RAW 264.7 macrophages. It would be highly valuable to show that the simple design PM nanoparticles within this project are capable of intracellular release without the need for complex environmental stimuli modifications as

macrophages

mentioned earlier. Despite this, due to Scarpa *et al.* using the identical PM design to this project, there can be confidence that this intracellular breakdown would be the case within RAW 264.7 macrophages as well.

Although PM-labelling using fluorophores allows good insight into the nanoparticle uptake capabilities, one shortfall is the possible dissociation of the dye from the nanoparticles. This dissociation may cause the lipophilic dyes used (eg DiD/DiI) to transfer to other cell organelles and membranes, which would in turn cause images gathered to potentially display the footprints of where the PMs had been within cells, rather than accurate real-time cellular locations (Takov *et al.*, 2017; Münter *et al.*, 2018). Coherent anti-Stokes Raman scattering (CARS) microscopy was investigated as a method which could overcome this problem, as discussed previously, and was shown to be able to successfully image PM uptake into RAW 264.7 macrophages. Other groups have used CARS for similar purposes, and one such group, as stated in section 4.1, used CARS to measure polymeric nanoparticle uptake into murine kidney tissues (Garrett *et al.*, 2015). Another group used CARS in conjunction with transmission electron microscopy (TEM) to assess nanocrystal uptake into RAW 264.7 macrophages. The group showed that using brightfield imaging the nanoparticles were seen to collect around the cell peripheries following a 6-hour incubation, however CARS imaging confirmed the nanoparticles were inside the cells. The use of TEM alongside these studies revealed the nanocrystals localised to subcellular membrane bound vesicles which showed morphology typical for early endosomes and phagolysosomes. Therefore, once confirmed using CARS as being the nanoparticle of interest, TEM can be used to most precisely confirm cellular localisation and intracellular fate (Saarinen *et al.*, 2019). These two studies both provide excellent direction for the future work of this project, and certainly using CARS to image *ex vivo* murine organs, would provide useful knowledge for the implications of using our PM-antibiotic formulations for a clinical application.

The CARS work performed in this project has not been perfected, and there were still some limitations to the results generated. It is well known that if a cell is exposed to an environmental insult, or perhaps disease, this will elicit a stress response which can sometimes result in the formation of stress granules which form in the cytoplasm or nuclei of the cells (Mahboubi and Stochaj, 2017). It is possible that the effect of PMs on the macrophage cells caused a stress response, leading to the inclusion and visualisation of the granules, alongside the PMs, on the CARS images collected. One study researched stress granule formation in macrophages after a 3-hour arsenite exposure, and the confocal images collected showed similar structures to those seen within this study, although far more sparse and lower in number (Naz *et al.*, 2019). In

contrast, and reassuringly for this work, another group measured stress response in macrophages after exposure to PMs. They applied PMs at a higher concentration than in this project's CARS assay, and found there to be no significant differences in stress-related gene regulation between untreated- and PM-treated macrophages (Fenaroli *et al.*, 2020). Despite this, any future work using CARS for this project should involve repeating this experiment using specially designed deuterated polymer to form the PMs. This would allow fixation around the C-D bond, as opposed to the C-H bond. As these bonds are not present in natural cell structures (Zhang *et al.*, 2019), any signal seen from CARS images would unambiguously show that PMs were present within cells, without any interference from potential stress granules. Nevertheless, the images from this project almost certainly show PM uptake into the cells of interest and, importantly, highlight the potential for label-free imaging of nanoparticles inside cells. Despite its benefits, there are minimal publications using CARS analysis of cellular uptake of nanoparticles. To the best of our knowledge, the work within this project is the first example of PMs being investigated for uptake into macrophage cells.

The next body of work presented in this chapter came from investigating nanoparticle uptake into cells which possessed a prior *B. thailandensis* intracellular infection. Despite infection, cells were observed to take up fluorescently labelled PMs, and furthermore a direct co-localisation occurred between PMs and bacteria. A higher level of intracellular fluorescence was seen after 21 hours, compared to after 3 hours. This trend has been reported before within the literature, where one group looked at the uptake of a fluorescently labelled polymer-drug bioconjugate nanoparticle into RAW 264.7 cells. They found, similarly, that between 0-6 hours there was relatively low uptake, but by 24 hours a significant increase in fluorescence was measured (Abed *et al.*, 2015). It was observed that control cells (which had never been exposed to *B. thailandensis*) achieved the highest level of PM uptake, followed by cells which had been exposed and possessed associated bacteria, and finally with exposed cells which remained uninfected taking up the least amount of PMs (Figure 4.11). These observations were interesting, as they seem conflicting in that in one case the control cells have the highest level of uptake, whilst those exposed but also uninfected possess the least. Despite this, the control group and the uninfected cells from the exposed population are not directly comparable, due to the fact that even the exposed, but uninfected, cells were still subjected to media containing *B. thailandensis*. It is possible the bacteria are responsible for secreting chemical signals which act upon the macrophages and signal them to limit uptake.

macrophages

Macrophage activation, and the possible differences between bacterially exposed versus unexposed populations, may provide an answer for the variations seen in PM uptake in Figure 4.11. It is well known that macrophages can be activated in response to specific stimuli, and there are two routes this priming can take which have traditionally been put forward. Classically activated macrophages (M1) tend to arise as a result of bacterial infection, whereas alternatively activated macrophages (M2) are more immune modulator, anti-inflammatory, types of cells (Reichel *et al.*, 2019). This M1/M2 terminology came as a result of experiments that were performed *in vitro* (Mills *et al.*, 2000). In reality, and certainly within *in vivo* systems, there is likely not such a distinct split, and activated macrophages are able to show a spectrum of phenotypes rather than one extreme polarisation (Hume, 2015). Interestingly, the work reported from multiple papers suggested that polymeric nanoparticles caused an activation in macrophages that represented an M2-like activation over M1 (Bygd *et al.*, 2015; Ye *et al.*, 2016). However, literature is also present showing how polymeric nanoparticles stimulate production of pro-inflammatory cytokines, indicating more of an M1 polarisation (Nicolette *et al.*, 2011). This highlights the complexity of macrophage cell signalling and the effects nanoparticles may have on these cells.

There has been suggestion that *in vitro* M1 type macrophages experience enhanced phagocytosis capabilities (Qie *et al.*, 2016), whereas M2 type macrophages display increased pinocytosis capabilities (Montaner *et al.*, 1999). It is possible, therefore, that in the '**B.t exposed cells + PMs**' cell population, the cells have been M1 activated and primed for enhanced phagocytic uptake, whereas in the '**Control cells + PMs**' they are more M2 activated, and so primed for enhanced pinocytosis. As previously mentioned, phagocytosis usually involves the uptake of larger particles, and pinocytosis smaller nanometre particles, therefore it is not unreasonable to suggest pinocytosis is the primary route of uptake into cells. This could explain why the control group experiences the highest intensity of PM fluorescence. Within the *B. thailandensis* exposed cell population, the uninfected cells show the lowest level of fluorescence (Figure 4.11C) perhaps because they have been primed for phagocytic uptake, but due to a lack of bacteria invading the cells this is happening less effectively, resulting in less PM uptake. One possible future experiment which could determine if this is the case would be to culture cells and bacteria together, spin them out, and apply just the media supernatant along with any signalling factors to fresh cells. One would hypothesise that secreted cell signalling factors would be enough to induce M1-type activation of new cells. This would explain the difference between the uninfected cells in the bacterial exposed population versus the healthy unexposed controls.

The ImageStream data also provided excellent information on the ability of PMs to directly co-localise with intracellular *B. thailandensis*. Other groups have attempted to perform similar studies, and one such paper investigated the co-localisation of actively targeted nanoparticles with intracellular *Staphylococcus aureus*. Peptides which specifically bind to *S. aureus* were shown to display 21.5% co-localisation with intracellular *S. aureus* when analysed by confocal microscopy. The paper then reports that when this peptide was coated onto silver nanoparticles and incubated with RAW 264.7 macrophages, the pattern of localisation of the nanoparticles was in good agreement with the previous confocal data (Hussain *et al.*, 2018). Another group researched co-localisation between fluorescent lysostaphin loaded PMs and intracellular *S. aureus*, and found there to be intracellular co-localisation between the two (Fenaroli *et al.*, 2020). The main limitation to the methods within these papers was the use of confocal techniques as a quantitative readout. The ImageStream has a far higher throughput and is more all-encompassing of the samples being tested. Furthermore, confocal microscopy has the potential to include bias into results as one may search for the best images. Another group showed how Raman scattering can be used to observe co-localisation between silver nanoparticles and *Escherichia coli* (Chaudhari and Pradeep, 2015). This study was, however, an extracellular interaction and not in the presence of cells, making it slightly less relevant in the context of intracellular drug delivery. Another study used fluorescence microscopy to assess co-localisation between polymeric PLGA nanoparticles and *Mycobacterium bovis* BCG within macrophage cells. The paper reported that there was good nanoparticle uptake into cells, but unequivocally no co-localisation with the BCG bacteria. They determined that the vast majority of bacteria were residing within early phagosomes, LysoTracker negative compartments, whereas the nanoparticles were consistently found to co-localise with LysoTracker, suggesting their presence in phagolysosome-like compartments (Kalluru *et al.*, 2013). Whilst this paper doesn't share the co-localisation findings of this project, it does support the Nanoimager data showing PM co-localisation with lysosomes (Figure 4.4). Furthermore, despite Kalluru *et al.* not seeing co-localisation, their rifampicin loaded PLGA nanoparticles were able to effectively clear macrophages of the *M. bovis* infection. This shows that even if co-localisation is not present, or present at extremely low levels, in terms of drug delivery this may not matter. The nanoparticles clearly do not need to be in directly the same compartment in order to achieve bacterial killing. This bodes well for this project, as co-localisation was present, but low. To the best of our knowledge no examples reside within the literature of ImageStream technology being used to assess bacterial-nanoparticle intracellular co-localisation.

macrophages

Overall the results within this chapter show that nanoparticles can be taken up well by RAW 264.7 macrophages. Despite this promising finding, there are many other factors which must be considered when improving PMs for the use of intracellular drug delivery for medical applications. For example, particle size can affect the level of cellular uptake seen in macrophages. It was reported that the optimal particle size for macrophage uptake is in the micrometre range as opposed to nanometre (Hirota and Ter, 2012). Peritoneal macrophages have been shown to display increased rates of clearance with increasing particle diameter, with polystyrene beads 1.1 μm in size being cleared 10 times faster than 100 nm beads, and 70 times faster than 30 nm beads (Pratten and Lloyd, 1986). An excellent review by Bleul *et al.* (2015) reports on how different techniques can be employed to control PM sizes. Future work for this project could involve altering polymer properties prior to the production of PMs, leading to a change in PM size, to see if this might enhance PM uptake into cells further. Similarly, the material of the nanoparticles can affect uptake. It has been seen a great amount within the literature that PEGylation of nanoparticles can hinder uptake into macrophages (Qie *et al.*, 2016; Behzadi *et al.*, 2017). In part PEGylation remains desirable, as if administered *in vivo* it would increase circulation time within the bloodstream and prevent clearance by the body, enabling a longer-lasting effect for drug delivery. However, it is a fine balance between minimising clearance, through PEGylating, and achieving good uptake into macrophage cells where bacterial infections reside, through perhaps a different surface material. Nevertheless, the results from this chapter show that even though PEGylated, the PMs are highly capable of being taken up into macrophage cells, and furthermore are able to exhibit direct co-localisation with *B. thailandensis*, making them a highly viable option for progression to *in vivo* studies.

Chapter 5: Polymersomes for antibiotic delivery and killing of intracellular *Burkholderia thailandensis*

Chapter 5: Polymersomes for antibiotic delivery and killing of *Burkholderia thailandensis*

5.1 Introduction

Work presented in the previous two chapters showed the potential of polymersome (PM) nanoparticles to encapsulate a variety of antibiotics, and that they are taken up by RAW 264.7 macrophage cells infected with *Burkholderia thailandensis*. In order to become viable treatment options for intracellular infections, the PMs must also display the ability to reduce the bacterial burden within infected cells, once taken up. This introduction will discuss some of the challenges associated with the development of antibiotic therapies, how nanoparticles are being utilised for new approaches to drug delivery, and how PEO-PCL PMs might contribute towards this growing area of nanomedicine.

The golden era of antibiotics has been short-lived due to the emergence of antimicrobial resistance (AMR). Global deaths as a result of multidrug resistance are rising, and as of 2019 it was thought that over 33,000 deaths yearly in Europe were a direct consequence of antibiotic resistant infections (da Cunha *et al.*, 2019). Coupled with this is the issue that a new class of antibiotic has not been discovered for 40 years, largely due to reduced economic incentives for this type of research to be performed (Bartlett *et al.*, 2013). One avenue being explored is the attempt to increase the efficacy of certain antibiotics by repackaging them into nanoparticles. In this way, rather than discovering new antibiotics it may be possible to make existing ones work more effectively, for example in an intracellular environment (Schalk, 2018; Dassonville-Klimpt and Sonnet, 2020).

Nanoparticles, specifically liposomes (LMs), have been widely researched for their use in the delivery of cancer therapeutics, and have received FDA-approval for a number of these formulations (Olusanya *et al.*, 2018). This is also now extending to liposomal formulations used for antibiotic delivery purposes, of which some are beginning to receive FDA approval for their clinical use (Fatima *et al.*, 2018). One such product is the FDA-approved liposomal formulation, Arikace[®], which is used to treat patients suffering from *Mycobacterium spp.* related lung infections (Shirley, 2019). The LMs encapsulate the aminoglycoside antibiotic, amikacin, and *in vitro* investigations highlighted that this antibiotic had potent activity against multiple *Mycobacterium* species (Brown-Elliott *et al.*, 2013). Upon encapsulation into LMs, the formulation was able to successfully reduce intracellular counts of *M. avium* and *M. abscessus* from macrophages, and significantly,

was found to do so more effectively than the free drug (Rose *et al.*, 2014). The LMs are administered via the inhalation route, and during nebulisation approximately 70% of the antibiotic payload remains associated with the LMs, and the remaining dose delivered to the lungs as free drug (Griffith *et al.*, 2018). Whilst this highlights a level of stability from these preparations, it is perhaps undesirable to have anything less than 100% stability until the target infection site is reached. Without such stability there is a greater risk of selection pressures for antibiotic resistance arising, and also from off-target side effects of the free drug. For this reason, other nanoparticles which offer greater stability might be able to improve these current drug delivery systems.

Section 1.5.6 covered extensively other examples of LMs used to deliver antibiotics to bacterial infections. However, aside from LMs a number of other types of nanoparticle have also been researched for this application. One example is the use of a polymer-drug conjugate nanoparticle to deliver penicillin to intracellular *S. aureus* residing within RAW 264.7 macrophages. The group engineered penicillin G (Pen G) to covalently link to polyisoprene chains, and furthermore added an environmentally-sensitive linker which would release the antibiotic once inside the macrophages. The group were able to achieve high levels of drug loading with the antibiotic payload comprising between 55 – 62% of the final formulation weight. Whilst these nanoparticles were able to inhibit the growth of *S. aureus* free in culture, minimum inhibitory concentrations of up to 0.156 $\mu\text{g/ml}$ were needed, compared to only 0.03 $\mu\text{g/ml}$ for free Pen G. Interestingly, in conjugates without the presence of the environmentally-sensitive linker no bacterial inhibition was seen, suggesting the antibiotic was well sequestered by the nanoparticles. Similarly, in an intracellular environment, only the nanoparticles containing the environmentally-sensitive linker were able to reduce the bacterial burden, and the conjugates lacking this did not display any significant killing. The group assessed the intracellular drug concentration using cell lysates and HPLC, and found that Pen G was only able to be detected intracellularly using environmentally-sensitive nanoparticles, but that even in the presence of cell efflux inhibitors this concentration reached undetectable levels after 24 hours. Despite this, the use of nanoparticles allowed an intracellular concentration to be achieved that was not possible with free drug, or nanoparticles lacking the sensitive linker, highlighting the benefit of these fine-tuned drug delivery systems (Abed *et al.*, 2015). Whilst this is an excellent example of the direction the field of antibiotic drug delivery using nanoparticles is taking, there are elements which need improving. For example, it would be preferable to be able to develop a drug delivery system that was able to release its payload intracellularly without the need for additional complex linker chemistries. Furthermore, in the case of this example and the previous liposomal formulation, both lack the presence of PEG

which is known to increase circulation time within the body (Sercombe *et al.*, 2015). Therefore, developing nanoparticles with both simple chemistries as well as the possession of PEG, or PEG-like molecules, should be key when considering nanoparticles for clinical use.

PM nanoparticles possess a range of benefits over other nanoparticles, such as LMs, as already discussed in Chapter 1. These include characteristics such as a reduced payload permeability (Discher *et al.*, 1999), longer time in circulation within the body (Allen and Cullis, 2013), and the ability to control their chemical properties to allow them to become responsive to stimuli such as temperature and pH (Du *et al.*, 2005; Lomas *et al.*, 2007; Lee *et al.*, 2010; Gandhi *et al.*, 2015). However, despite these benefits no PM preparations have been given clinical approval for use as a therapy, to the best of our knowledge. This highlights the area the research for this PhD project occupies, and the advances that could be made for this field if the PM-antibiotic preparations were able to inhibit the growth of an intracellular species, such as *B. thailandensis*.

Other research groups have also begun to use PMs for antibiotic drug delivery to intracellular infections. One group has used PMs to encapsulate the antibiotics metronidazole and doxycycline with the aim of delivering them to *Porphyromonas gingivalis* in an attempt to prevent periodontitis (Wayakanon *et al.*, 2013). In a more recent example, pH-sensitive PMs have been used to achieve the intracellular targeting and eradication of *Mycobacterium spp.*, *Staphylococcus aureus* and also show their ability to access TB granulomas (Fenaroli *et al.*, 2020). Much of this work is also similar to that conducted by Lane *et al.* who used pH-sensitive PMs to show effective killing of *B. thailandensis* (Lane *et al.*, 2015). Despite the similarities some of this work shows to this project, the methods mentioned in previous examples rely on complicated polymer chemistry to engineer functionality into their PM systems. Furthermore, they do not incorporate the PEO block which is responsible for preventing opsonisation and immune cell clearance once in the body. Therefore, the simple PM systems used within this project, made completely from FDA-approved materials, offer an attractive alternative and advancement on the PM technology which already exists.

This chapter will investigate whether PEO-PCL PMs loaded with antibiotics are able to inhibit the growth of *B. thailandensis* residing intracellularly within RAW 264.7 macrophage cells. The aims of the experiments in this section are:

- To assess whether antibiotics lose potency during the PM preparation period which could cause a reduction in bacterial growth inhibition

- To assess whether PM-antibiotic preparations are able to inhibit the growth of *B. thailandensis* growing free in culture medium
- To determine whether the PMs could be broken in order to release their antibiotic payloads into medium containing free growing *B. thailandensis*, to prove encapsulation within PMs does not inactivate the antibiotics
- To assess the capabilities of PM-antibiotic preparations to reduce the bacterial burden of intracellular *B. thailandensis*
- To select a variety of poorly intracellularly available antibiotics and determine whether their intracellular efficacy against *B. thailandensis* can be improved through their encapsulation into PMs.

5.2 Results

5.2.1 Comparison of old and new antibiotic efficacies

Before beginning bacterial inhibition investigations, it was first necessary to determine whether there was any loss of antibiotic efficacy over time. The PMs were prepared each time with fresh stock antibiotic, but due to the period of room temperature dialysis which must occur, they were not used immediately. To assess whether this period impacted efficacy, a bacterial growth optical density (OD) assay was performed, as described in section 2.2.4.1. Briefly, free growing *B. thailandensis* were cultured with L-broth and either doxycycline (0 – 6.25 µg/ml) or rifampicin (0 – 50.0 µg/ml), using both freshly made stocks or those stored for a period of 7 days prior to use. The bacteria were left to grow for 24 hours with an OD reading being taken every 15 minutes. There were no significant changes in bacterial growth dependent upon whether fresh or 7-day old stocks were used for either doxycycline (Figure 5.1A), or rifampicin (Figure 5.1B). The results are also presented as 24-hour data only, for clearness, and in this set of results the media only negative control has been subtracted from readings to remove interference (Figure 5.1C). The lack of difference in efficacies implies that if no intracellular inhibition was seen in future experiments by PM-antibiotic preparations, it would not be as the result of the antibiotic time spent at room temperature.

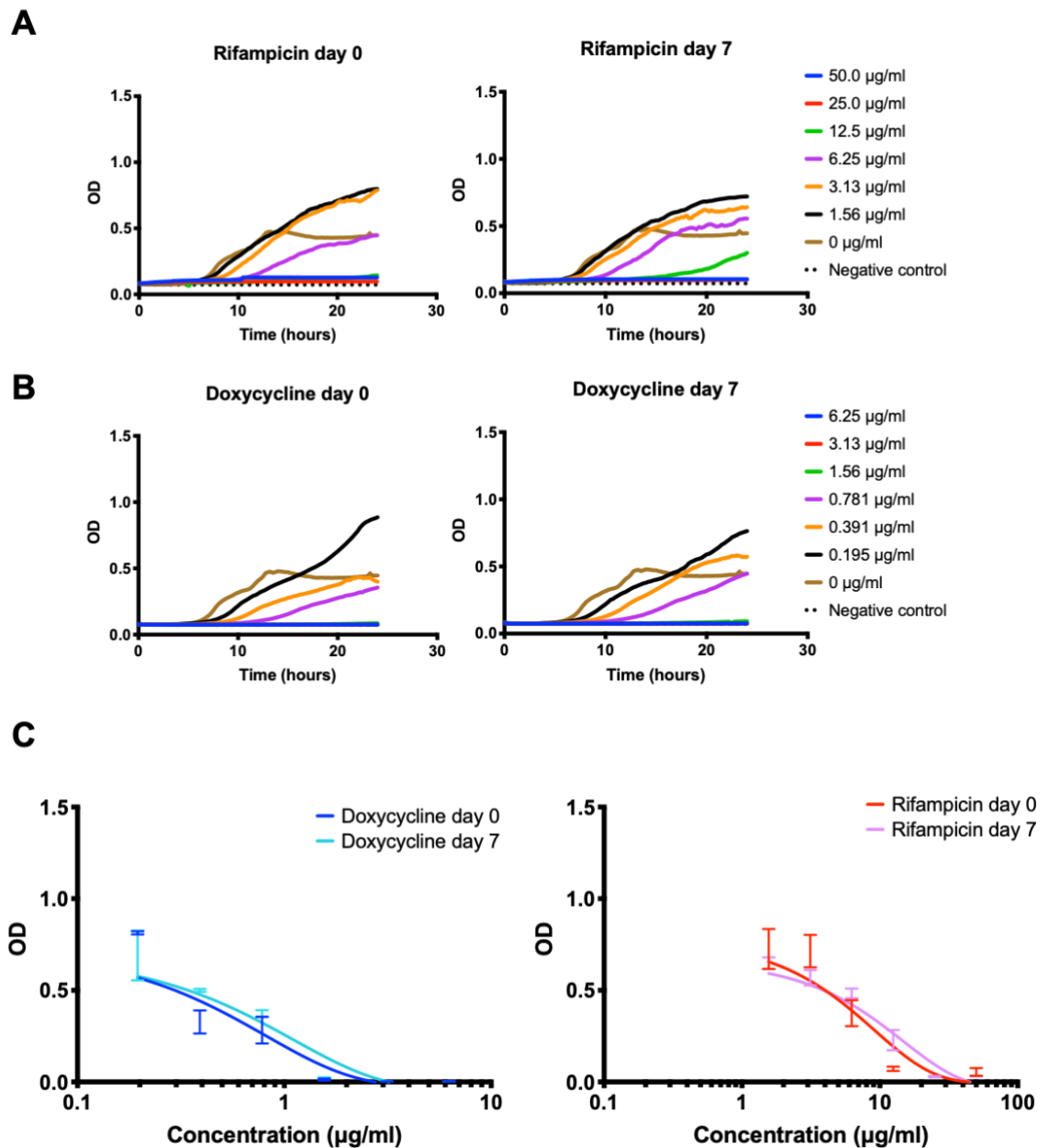


Figure 5.1 – Comparison of doxycycline and rifampicin efficacies at day 0 versus day 7. (A) Growth of free growing *B. thailandensis* over 24 hours when rifampicin was applied at a day 0 or day 7 stock. (B) Growth of free growing *B. thailandensis* over 24 hours when doxycycline was applied at a day 0 or day 7 stock. (C) The 24-hour data from Figures 5.1A and 5.1B. There was no difference in efficacy between new and old antibiotic stocks. Data is taken from one biological repeat performed in triplicate, with the mean and SEM plotted. In this set of results the media only negative control has been subtracted to remove interference.

5.2.2 PM-antibiotic preparations did not inhibit *B. thailandensis* growing free in culture

So far in the project it has already been determined that the antibiotics doxycycline and rifampicin are able to inhibit the bacterial species *B. thailandensis* (section 3.2.1), and that these antibiotics remain stable and effective over a 7-day period of being at room temperature. Furthermore, work reported in Chapter 3 shows how stable encapsulation of these antibiotics into PMs makes them viable drug-delivery systems for treating bacterial pathogens. It was next investigated how the PM-antibiotic preparations affected the growth of *B. thailandensis* free in culture, with no cells present.

An OD assay was performed, as in section 5.2.1, with the only exception that antibiotics were loaded into PMs, not added free/unencapsulated. Samples were applied undiluted, however upon addition of the *B. thailandensis* culture to the plate wells, this resulted in the highest final concentration tested having a dilution factor of 1:2 (concentration dilution factor 0.5). Based on the estimated encapsulated antibiotic concentrations from Chapter 3, this correlated to PM-doxycycline being applied at concentrations ranging from 0 – 7.6 µg/ml, and PM-rifampicin from 0 – 4.2 µg/ml. A PM-empty control was also applied at the same dilution factor to ensure the same number of PMs and PBS vehicle vector were administered. The PM-antibiotic samples were also spun through a filter in order to separate the PM-antibiotic from the surrounding buffer (filtrate). This filtrate was collected and applied to *B. thailandensis*, in the same manner as the rest of the samples.

PM-doxycycline did not significantly reduce bacterial growth inhibition compared to PM-empty samples at any concentration dilution factor tested (two-way ANOVA with Tukey's post-hoc test). Samples of filtrate did not affect bacterial growth, indicating that any unencapsulated antibiotic was not at a sufficient concentration to inhibit growth (Figure 5.2A). This inability to reduce bacterial growth can be seen clearly when the PM-doxycycline group is compared to the free, unencapsulated doxycycline treated *B. thailandensis* control (Figure 5.2B). Similar results were observed with PM-rifampicin samples, where no inhibition from PM-rifampicin was measured, and also none from the filtrate sample. PM-empty samples were able to achieve a significantly lower OD than PM-rifampicin in all cases ($p < 0.01$, two-way ANOVA with Tukey's post-hoc test), except at a concentration dilution factor of 0.5 where there was a significant increase in OD compared to PM-rifampicin samples ($p < 0.05$). This suggests at the most concentrated PM-empty sample tested the nanoparticles increased the level of bacterial growth (Figure 5.2C). Compared

to the free rifampicin control, PM-rifampicin at the same concentration saw no effect on the bacteria (Figure 5.2D). Overall, this assay highlighted that PM encapsulated antibiotics were unable to inhibit bacterial growth compared to their unencapsulated equivalent concentration.

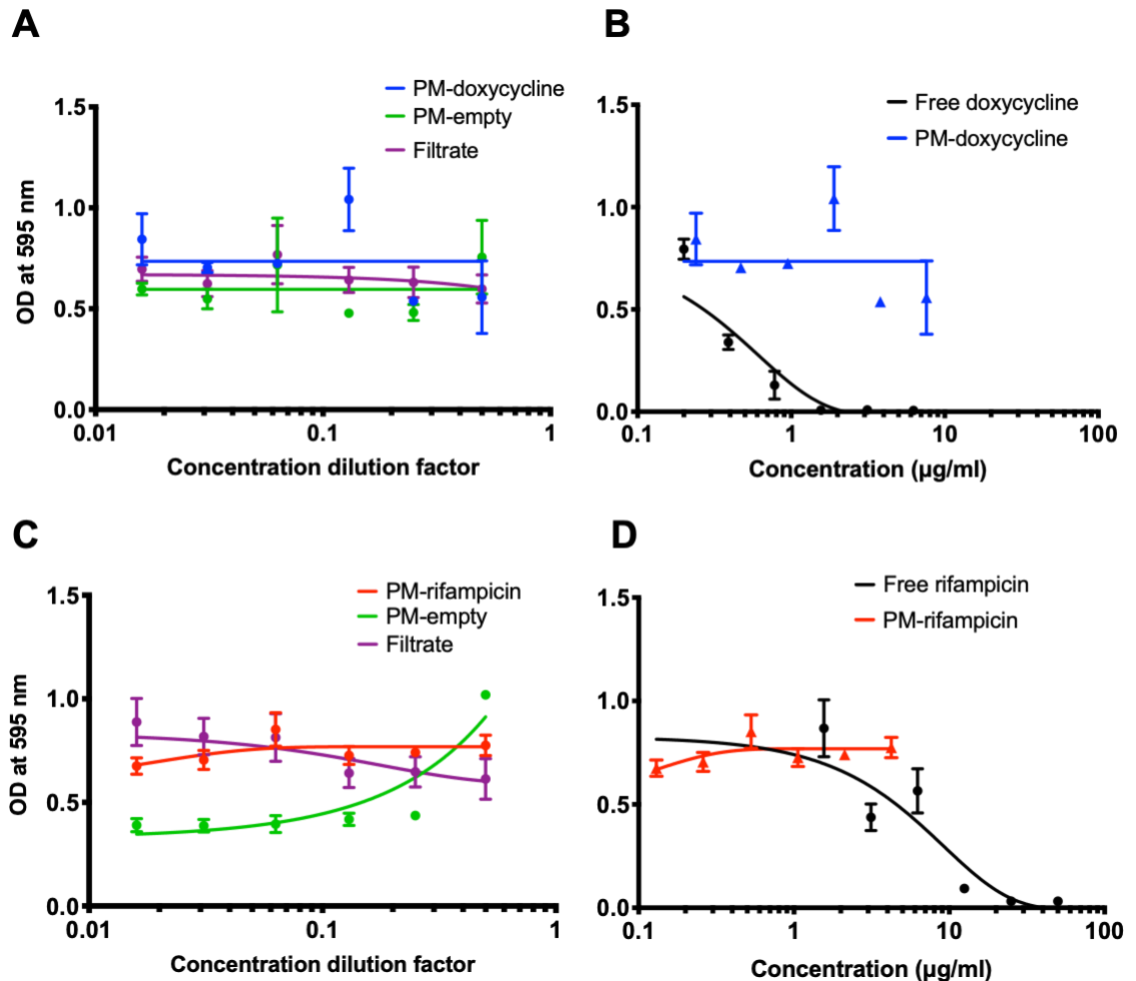


Figure 5.2 – Effect of PM-antibiotics on free growing *B. thailandensis*. (A) PM-doxycycline and control groups display a lack of inhibition on *B. thailandensis*. (B) When compared to the free doxycycline control, PM-doxycycline at the same concentration displays no inhibition. (C) PM-rifampicin and control groups show no inhibition on *B. thailandensis*. (D) Compared to the free rifampicin control the PMs elicit no bacterial inhibition. All graphs display the 24-hour growth data only, and are plotted to a non-linear regression, one-phase decay line of best fit. Data is the mean and SEM of one biological repeat performed in triplicate.

5.2.3 Broken PM-antibiotic effect on *B. thailandensis* growth free in culture

5.2.3.1 PM disruption using DMF

It was hypothesised that the lack of efficacy of PM encapsulated antibiotics in inhibiting bacterial growth could be because the antibiotic was either tightly sequestered by the PMs, and so was not bioavailable, or because the antibiotic had been inactivated during the process of PM encapsulation. The bacterial OD assay provides a good method to test the presence of any free antibiotic, due to the sensitivity of the bacteria. It was therefore hypothesised that if it were possible to disrupt PM structure, and release the internal payload, then if functioning the antibiotic should be able to inhibit growth.

Previously, in Chapter 3, adjusting the pH to an acidity level mirroring an intracellular environment was tested, and found that it did not disrupt PM structure when using Rayleigh scattering as an integrity indicator. Adding DMF to the PMs did appear to disrupt PM integrity however, and so this was one method tested further using the bacterial OD assay. A caveat to using bacterial OD as a readout for PM disruption as a result of DMF application is that DMF is highly toxic to cells and so would likely kill *B. thailandensis*. For this reason, the volume of DMF used had to be kept as minimal as possible, whilst being applied ideally at equivolume to the PM solution, to ensure significant disruption (refer back to Chapter 3, section 3.2.2.1). To achieve this, PM-antibiotic preparations were ultracentrifuged and pelleted, and then this small volume resuspended in DMF. The benefit to this not only allowed minimal DMF to be used, but also allowed the entirety of the PMs to be spun down and included in the assay, ensuring maximum antibiotic was being applied to the *B. thailandensis* culture.

PM-rifampicin was pelleted and DMF applied to give a solution composed of 30 μ l PMs:10 μ l DMF. The volume of the PM pellet was larger than anticipated, and so equivolume of DMF could not be added due to the resultant concentration of DMF being too high for application to *B. thailandensis*. The experiment was nevertheless continued in the hope that even this smaller volume of DMF would be enough to elicit a level of PM breakage and antibiotic release. The solution was made up to 350 μ l using PBS to ensure there was a large enough volume to complete the assay with triplicate technical repeats. This final solution had a DMF dilution of 1:35, which would be reduced to 1:140 after the application of L-broth and *B. thailandensis* culture within the assay. A DMF dilution of 1:100, or more, was desired to limit the effect on the bacteria. The concentration of this final 350 μ l solution of broken PM-rifampicin and DMF was measured on the NanoDrop UV-vis spectrophotometer. Scattering was seen due to the large volume of PBS that

was added to the broken pellet, which likely caused PMs to begin reforming as the aqueous phase now dominated the inorganic DMF phase used to disrupt PMs (Figure 5.3). For rifampicin the peak used to assess concentration is a higher wavelength (484 nm) and without significant interference from the scattered region, however a PM-empty control was included and subtracted from the PM-rifampicin signal regardless. A rifampicin concentration of 83.8 $\mu\text{g/ml}$ was determined. Using this stock solution of broken PMs and DMF, once used within the assay and diluted with L-broth and *B. thailandensis* culture, it was calculated that the highest concentration in the assay would be 20.9 $\mu\text{g/ml}$. This concentration should be high enough to measure bacterial inhibition, as the MIC for rifampicin was 25 $\mu\text{g/ml}$ and so an 'S'-shaped growth curve should be detected if rifampicin is fully released and functioning. A vehicle control was also prepared, using the same ratio of PBS:DMF as in the PM samples, to ensure the effect of DMF on *B. thailandensis* was accounted for.

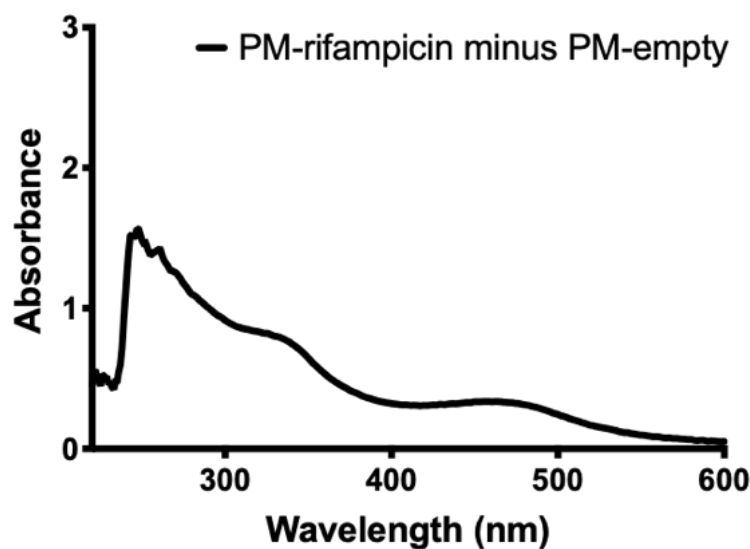


Figure 5.3 – Absorbance spectra of broken PM-rifampicin nanoparticles after DMF disruption. The PMs were made and dialysed as usual, and then pelleted for 2 hours at 186,000 x g. The PM pellet was mixed with DMF to aid PM disruption, resuspended in PBS, and then measured on the NanoDrop to assess the concentration. A PM-empty control was included, and data presented is with this control signal subtracted. The PM pellet/DMF/PBS solution was found to possess a concentration of 83.8 $\mu\text{g/ml}$.

Disrupted PM-rifampicin samples did not inhibit *B. thailandensis* growth at any concentration tested. There was also no significant difference between PM-rifampicin samples and PM-empty. Furthermore, the lack of significance between PM-rifampicin and the PBS:DMF vehicle control highlighted no effect from the presence of DMF (two-way ANOVA with Tukey's post-hoc test). The lack of significance between the free rifampicin dissolved in PBS:DMF, and the free rifampicin in

PBS alone showed that the DMF had no effect on the efficacy of rifampicin (Figure 5.4). Overall, these results support the theory that the antibiotic may become inactivated in some way as a result of the PM production process, as no killing was seen despite DMF being capable of disrupting the structure. That being said, as mentioned earlier an equivolume of DMF was not used in this example, and so it is possible that not all of the PMs were broken. Furthermore, during the resuspension in PBS it is likely that the broken PMs reformed due to the majority of the buffer being aqueous PBS. It is possible the hydrophobic rifampicin then became re-associated with the polymer and therefore remained bio-unavailable when mixed with *B. thailandensis*.

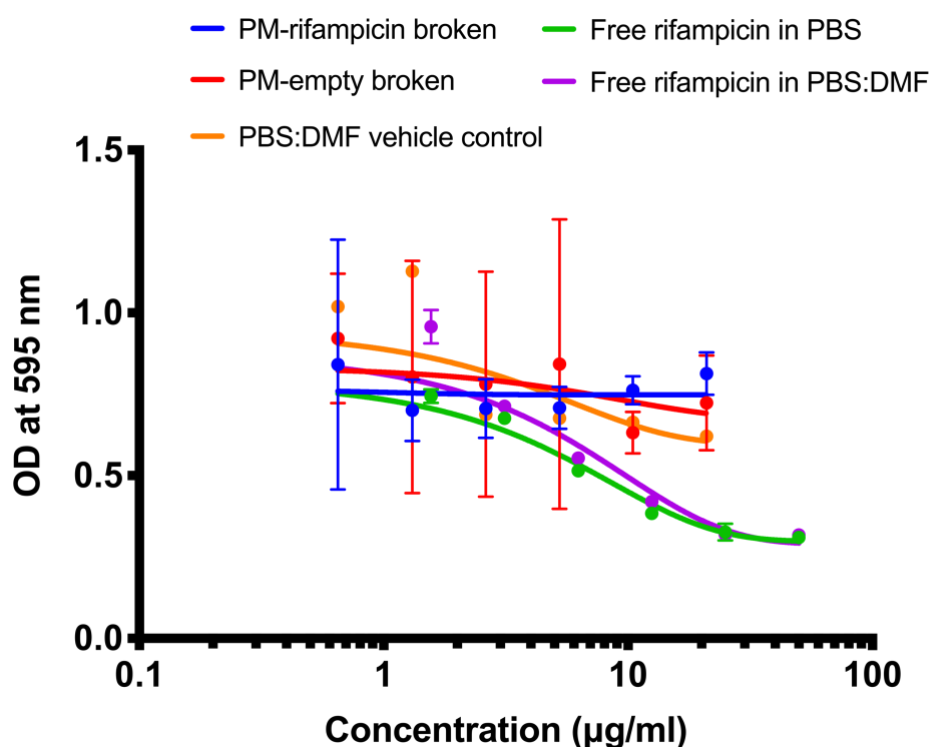


Figure 5.4 – Effect of disrupted PM-rifampicin nanoparticles on the growth of *B. thailandensis*. PMs were broken using DMF and then applied to free growing *B. thailandensis* at concentrations ranging from 0 - 20.9 µg/ml. No growth inhibition was seen at any concentration, and there was no significant difference between the broken PM-rifampicin samples and PM-empty. In addition, no significant difference was seen between PM-rifampicin and the PBS:DMF vehicle control, confirming that the DMF present had no significant effect on bacterial inhibition (two-way ANOVA with Tukey’s post-hoc test). Graph shows the mean and SEM of one biological repeat performed with triplicate technical repeats.

The same experiment was then performed using PM-doxycycline. This time the PM-doxycycline pellet was mixed with a larger volume of DMF, in the ratio 20 µl PMs: 30 µl DMF. This was to ensure PMs were being mixed with enough DMF to fully disrupt them, according to results from

Chapter 3. This mix was then resuspended in PBS, resulting in a final DMF dilution of 1:20. After further dilution in the assay with *B. thailandensis* culture and L-broth, this would result in a 1:80 DMF dilution – slightly more concentrated than desired however the appropriate controls were included, as previously. The broken PM-doxycycline solution was measured on the NanoDrop, with the signal from a broken PM-empty control being subtracted as usual. The concentration of these PMs was found to be 54.8 µg/ml (Figure 5.5A). Using this as a stock solution meant that the broken PM-doxycycline concentrations tested on *B. thailandensis* ranged from 0 – 13.7 µg/ml, which was well above the MIC meaning that a good growth curve should be seen if the doxycycline was released and functioning.

The results from this assay were similar to previously with broken PM-rifampicin samples. Broken PM-doxycycline nanoparticles were unable to inhibit the growth at any concentration tested, and there was no significant difference seen between their effect and that of broken PM-empty nanoparticles, with the exception of the point at 1.7 µg/ml which was considered an outlier and ignored (two-way ANOVA with Tukey's post-hoc test) (Figure 5.5B). Contrastingly from the PM-rifampicin assay a larger than equivolume of DMF was used on the PM pellet, suggesting complete, or near complete, disruption of the PMs should have occurred. Furthermore, as doxycycline is hydrophilic, resuspension in PBS is unlikely to have caused reassociation and sequestration of antibiotic to PEO-PCL polymer, making it bio-unavailable, if this is what occurred with the PM-rifampicin samples.

Overall, the results from this section point towards the hypothesis that the antibiotics may be inactivated during the process of PM production. Based on results from Chapter 3, using DMF causes a loss of Rayleigh scattering, indicative of loss of PM structure, and therefore predicted payload release. As no bacterial growth inhibition was seen it suggests either the DMF is not releasing the payloads as predicted, or the antibiotics are inactivated.

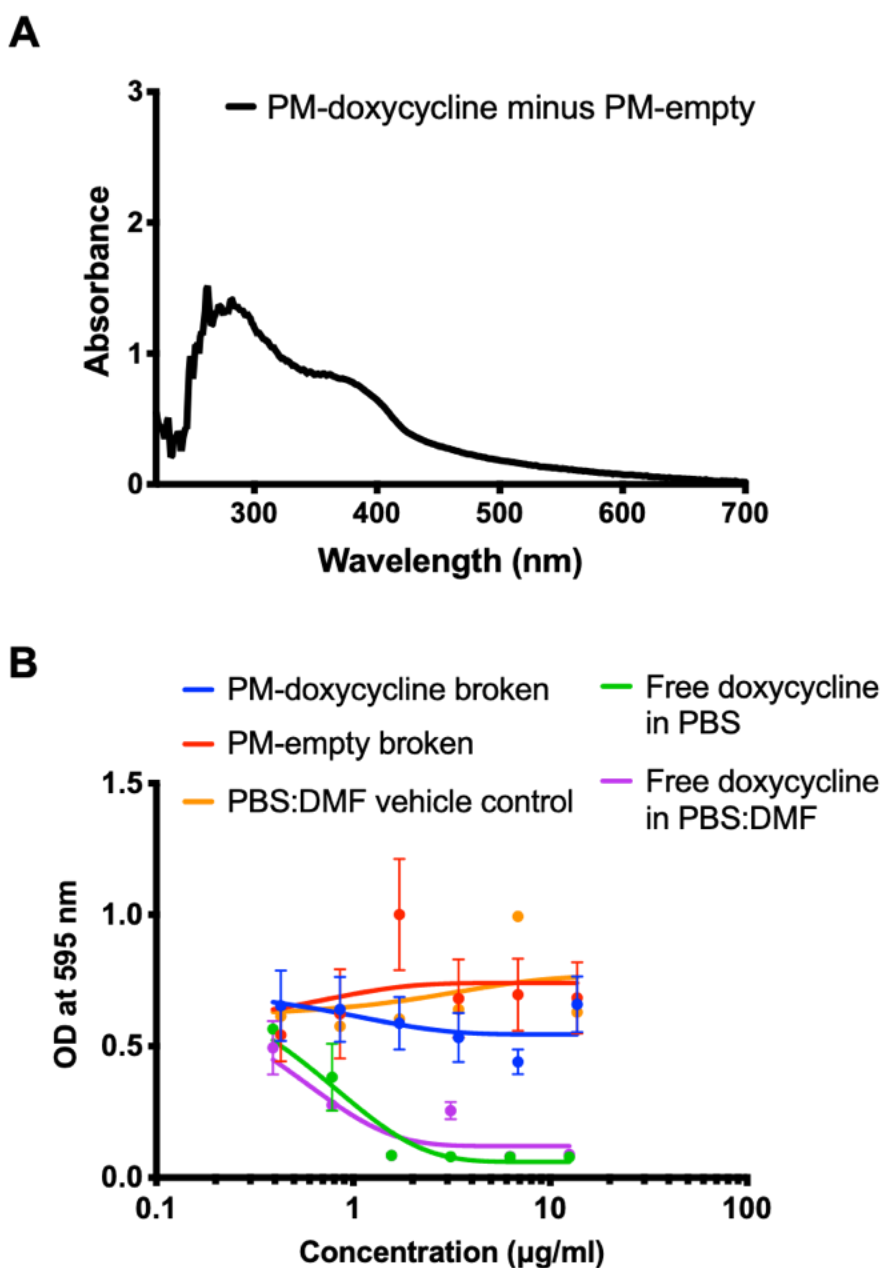


Figure 5.5 – Effect of disrupted PM-doxycycline nanoparticles on the growth of *B. thailandensis*. (A) Absorbance spectra of PM-doxycycline after disruption with DMF. (B) PMs were mixed with DMF in an attempt to break them and release the doxycycline payload, so that the antibiotic could inhibit free growing *B. thailandensis*, if functioning. However, at no concentration tested was a decrease in bacterial growth seen, and there was no significant difference reported between broken PM-doxycycline samples and broken PM-empty, with the exception of the outlier point at 1.7 µg/ml (two-way ANOVA with Tukey’s post-hoc test). Graph shows the mean and SEM of one biological repeat performed with triplicate technical repeats.

5.2.3.2 PM disruption using heat

Heat was next investigated as another method to disrupt the PMs. Based on evidence from the literature, the PEO-PCL polymer blend has a transition melting point of 60°C (Qiu *et al.*, 2003). It was hypothesised that if the PM-antibiotic preparations were heated above this point then the PEO-PCL would melt, the structure lost, and the payloads released. Two temperatures were tested, 65°C and 98°C. Similarly to in section 5.2.3.1, the PMs were pelleted prior to heating so that all PMs and their antibiotic contents could be included within the assays. The pellet was then resuspended in 400 µl of PBS to ensure a large enough volume to complete the assay with triplicate technical repeats. The PM solution was heated at the various temperatures for a period of 8 hours. In both cases, free antibiotic at the same concentration was also heated to the same temperature.

After a period of heating at 98°C for 8 hours, the PM-doxycycline sample did not reduce bacterial growth. There was no significant difference between PM-doxycycline samples and PM-empty samples heated to the same temperature (two-way ANOVA with Tukey's post-hoc test). At this temperature the antibiotic itself was inactivated, as seen from the purple line representing free doxycycline heated to 98°C (Figure 5.6). After the PMs had been heated some residue solid debris remained in the solution. The samples were added to the *B. thailandensis* culture as planned, however the error bars from the OD readings were large, and it is possible this was due to interference from this debris. Nevertheless, heating the PMs to 98°C led to loss of antibiotic activity (compare purple and green plots in Figure 5.6), which precluded testing that payload release could be induced by heating at this temperature.

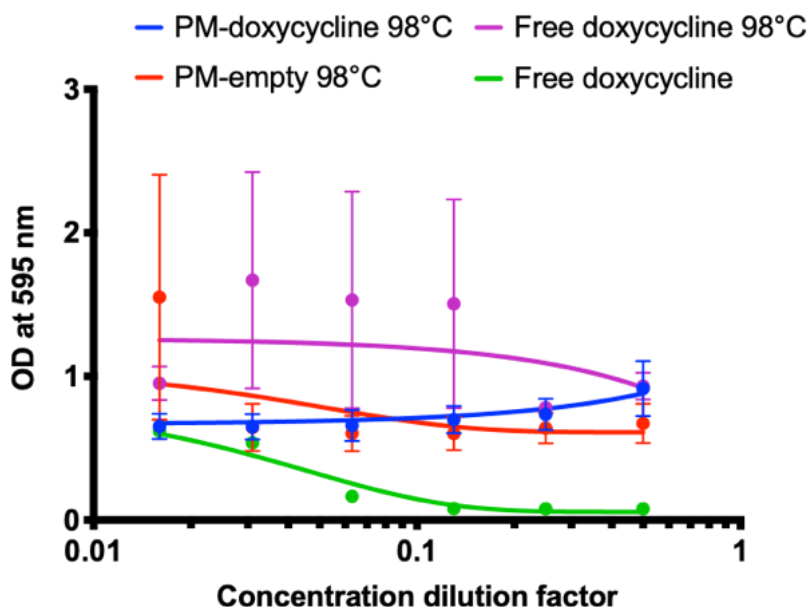


Figure 5.6 – Effect of breaking PM-doxycycline nanoparticles, using 98°C heat, on the growth of *B. thailandensis*. PMs were pelleted and then heated at 98°C for 8 hours before being applied to free growing *B. thailandensis* culture. No bacterial inhibition was seen from the PM-doxycycline samples, and there was no significant difference compared to the PM-empty control (two-way ANOVA with Tukey’s post-hoc test). The free doxycycline control also heated to 98°C revealed that the antibiotic was inactivated at these high temperatures. Graph shows the mean and SEM of one biological repeat performed with triplicate technical repeats.

When the assay was conducted after a period of heating at 65°C for 8 hours a different trend was seen. This time the free doxycycline control heated to 65°C showed the ability to inhibit growth at the highest concentration tested (12.5 µg/ml), showing that at this temperature the antibiotic remained effective (Figure 5.7). Although the doxycycline was able to inhibit growth, there was a reduction in efficacy observed. The MIC from Chapter 3 suggested doxycycline was able to completely inhibit growth at concentrations of 1.56 µg/ml, however anything less than 12.5 µg/ml from the heated sample was unable to achieve this. Despite that, the heated PM-doxycycline samples followed the same inhibition pattern as the free doxycycline control, and at the highest concentration of heated PMs applied, a reduction in bacterial growth was seen. A significant difference was seen between PM-doxycycline samples and PM-empty samples, at the highest concentration tested ($p = 0.0001$, two-way ANOVA with Tukey’s post-hoc test).

These results suggest that antibiotic activity is retained on encapsulation in PMs, and that whilst the antibiotic is sequestered from the bacteria it can be released by moderate heating.

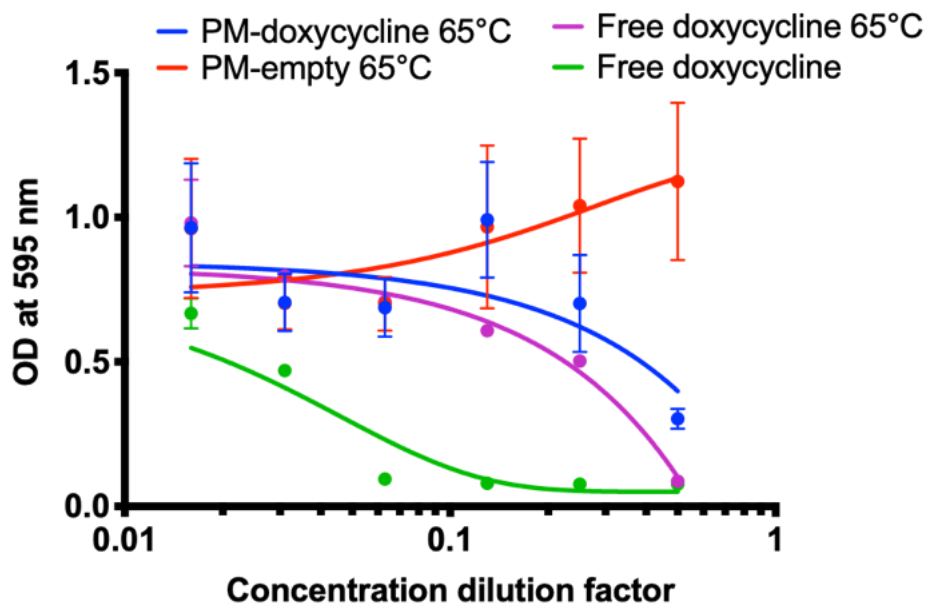


Figure 5.7 – Effect of breaking PM-doxycycline nanoparticles, using 65°C heat, on the growth of *B. thailandensis*. PMs were pelleted and then heated at 65°C for 8 hours before being applied to free growing *B. thailandensis* culture. Bacterial inhibition was seen at the highest concentration dilution factor applied (0.5) from the PM-doxycycline samples, and there was a significant difference compared to the PM-empty control ($p = 0.0001$, two-way ANOVA with Tukey’s post-hoc test). Graph shows the mean and SEM of one biological repeat performed with triplicate technical repeats.

5.2.4 PM-antibiotic preparations are able to successfully kill intracellular *B. thailandensis*

To test the hypothesis that PMs need to be taken up by the host cell in order to be broken down and release their payloads, their effect at killing intracellular *B. thailandensis* residing within RAW 264.7 macrophages was investigated. Initial work was performed using PM-doxycycline preparations, rather than PM-rifampicin, as previous assays suggested doxycycline might be the more potent of the two antibiotics against *B. thailandensis*. PM-doxycycline nanoparticles were initially titrated onto the infected cells at a range of concentrations (0 – 4.56 $\mu\text{g/ml}$), and then incubated for a period of 3 or 21 hours. Cells were then lysed, using distilled water, plated onto agar plates and incubated for 48 hours before the colony forming units (CFU) were used as a readout of bacterial killing. The concentration for the PM-doxycycline stocks was based on the PM stability data presented in Chapter 3, and the conclusion that after their dialysis period the PM-doxycycline preparations contain $15.2 \mu\text{g/ml} \pm 2.19 \mu\text{g/ml}$. A bacteria only control was also

included where the same volume of PBS was added as in each different PM sample, in order to account for any effect of the buffer used.

After a 3-hour PM incubation there was no bacterial killing seen. No significant difference was seen between PM-doxycycline and PM-empty samples (two-way ANOVA with Tukey's post-hoc test), and no significant difference was seen between PM-doxycycline and the bacteria only control (two-way ANOVA with Tukey's post-hoc test) (Figure 5.8A). The free doxycycline control was also unable to eradicate intracellular *B. thailandensis*, even at concentrations tested higher than the MIC. However, after a 21-hour incubation these patterns had changed, and intracellular killing of *B. thailandensis* was observed. There was a significant difference between PM-doxycycline and PM-empty in their ability to kill intracellular bacteria ($p < 0.05$, two-way ANOVA with Tukey's post-hoc test). PM-doxycycline was also able to significantly reduce the bacterial burden compared to the bacteria only control group ($p < 0.05$, two-way ANOVA with Tukey's post-hoc test). One observation was that the PM-empty nanoparticles might cause an increase in bacterial number compared to the control group, however no statistical significance was reported (Figure 5.8B). These results demonstrate that PM-doxycycline inhibit the growth of intracellular *B. thailandensis*.

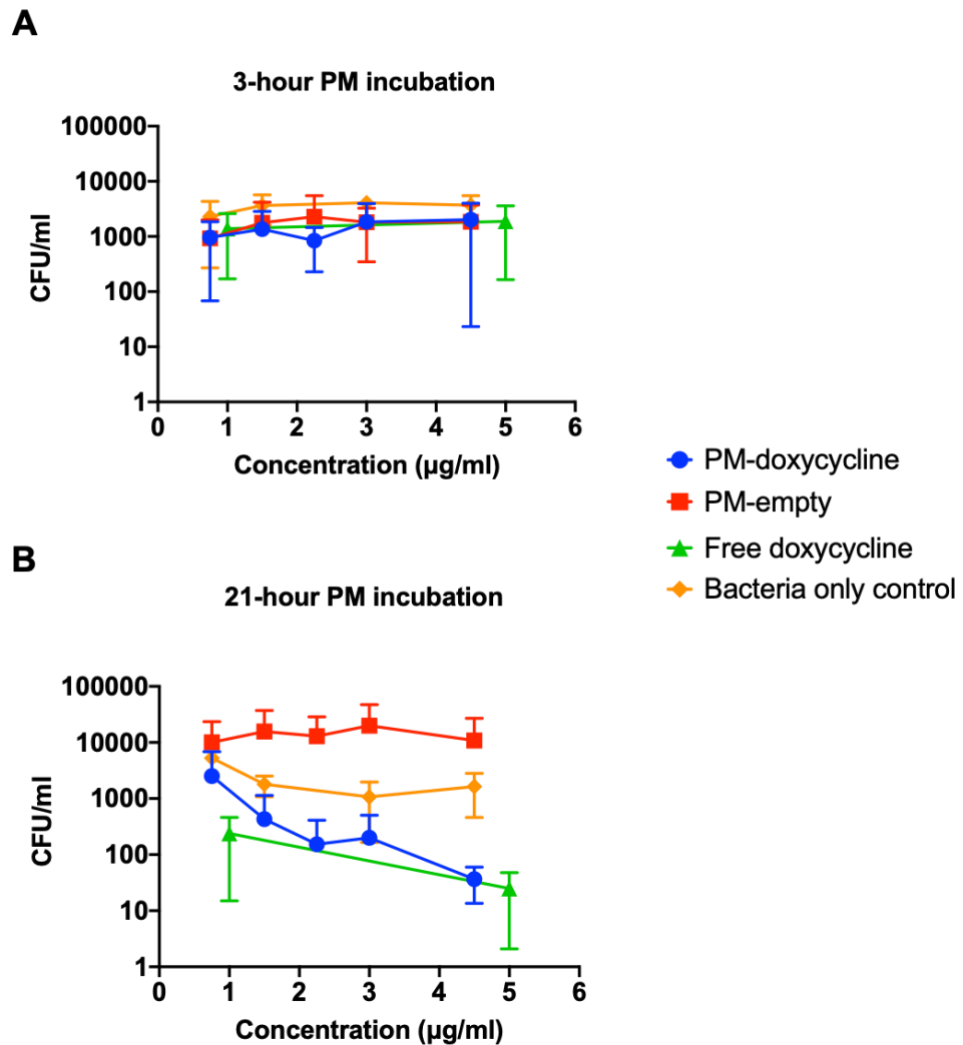


Figure 5.8 – Effect of PM-doxycycline on intracellular *B. thailandensis* at 3 and 21 hours. PM-doxycycline was applied to infected cells at concentrations ranging from 0 – 4.5 $\mu\text{g/ml}$, and then left to incubate for 3 or 21 hours. (A) After a 3-hour incubation, no significant killing was observed. (B) However, after 21 hours PMs were able to significantly reduce the bacterial burden compared to either the no antibiotic control group, or the PM-empty control ($p < 0.05$, two-way ANOVA with Tukey’s post-hoc test). Graph data is presented as the mean and SD of three biological repeats, $n = 3$.

Bacterial counts can vary quite largely from one assay to the next and so it was next tested whether the variation seen previously (Figure 5.8) was from experiment-to-experiment bacterial variation, or variation within the same assays. For the following experiments only the highest PM-doxycycline concentration (4.5 $\mu\text{g/ml}$) and the lowest (0.75 $\mu\text{g/ml}$) were investigated. The same as previously, PMs were incubated for 3 or 21 hours. Within the first repeat no significant bacterial reduction was seen after 3 hours, however after a 21-hour incubation there was a significant level of killing by PM-doxycycline samples at both the high and low concentrations tested, compared to the control ($p < 0.001$, two-way ANOVA with Tukey’s post-hoc test) (Figure 5.9A). At the lower

concentration, 0.75 $\mu\text{g/ml}$, PM-doxycycline reduced the bacterial count to 5500 CFU/ml \pm 3500, compared to the control bacterial count of 78,000 CFU/ml \pm 23,092. At the higher concentration, 4.5 $\mu\text{g/ml}$, a greater degree of killing was achieved with a bacterial count of only 120 CFU/ml \pm 53, versus the control count at 69,000 CFU/ml \pm 22,096. In the second assay repeat there was significant killing observed after 3 hours, although only at the higher concentration tested ($p < 0.01$, two-way ANOVA with Tukey's post-hoc test), with a reduction from 611 CFU/ml \pm 327, to 170 CFU/ml \pm 107. In this repeat there was no statistical significance in the level of bacterial reduction by PM-doxycycline compared to the control after 21 hours. However, at the higher concentration tested there was significantly more killing than from PM-empty samples ($p < 0.05$, two-way ANOVA with Tukey's post-hoc test). Despite the lack of statistical significance compared to the control, at the higher concentration tested PM-doxycycline samples were found to reduce bacterial number from 2183 CFU/ml \pm 208 (control), to only 17 CFU/ml \pm 14 (Figure 5.9B).

The results from these two assays were then averaged and normalised against the control group at the 1:20 dilution (0.75 $\mu\text{g/ml}$ concentration). No significant difference was observed in any of the 3-hour PM incubation samples. After normalisation, at 21-hours the PM-doxycycline applied at the lower concentration achieved a count of 24 CFU/ml \pm 26, compared to the control count of 100 CFU/ml \pm 30 ($p < 0.001$, two-way ANOVA with Tukey's post-hoc test). The higher concentration achieved a count of 0.3 CFU/ml \pm 0.3, compared to the control of 75 CFU/ml \pm 24 ($p < 0.001$, two-way ANOVA with Tukey's post-hoc test) (Figure 5.9C).

Overall, the error within each assay was small. This shows that the PM-doxycycline preparations are able to consistently have the same effect on the bacterial culture they are applied to, and that variation most likely arises from the natural fluctuations which occur in the culture of *B. thailandensis*.

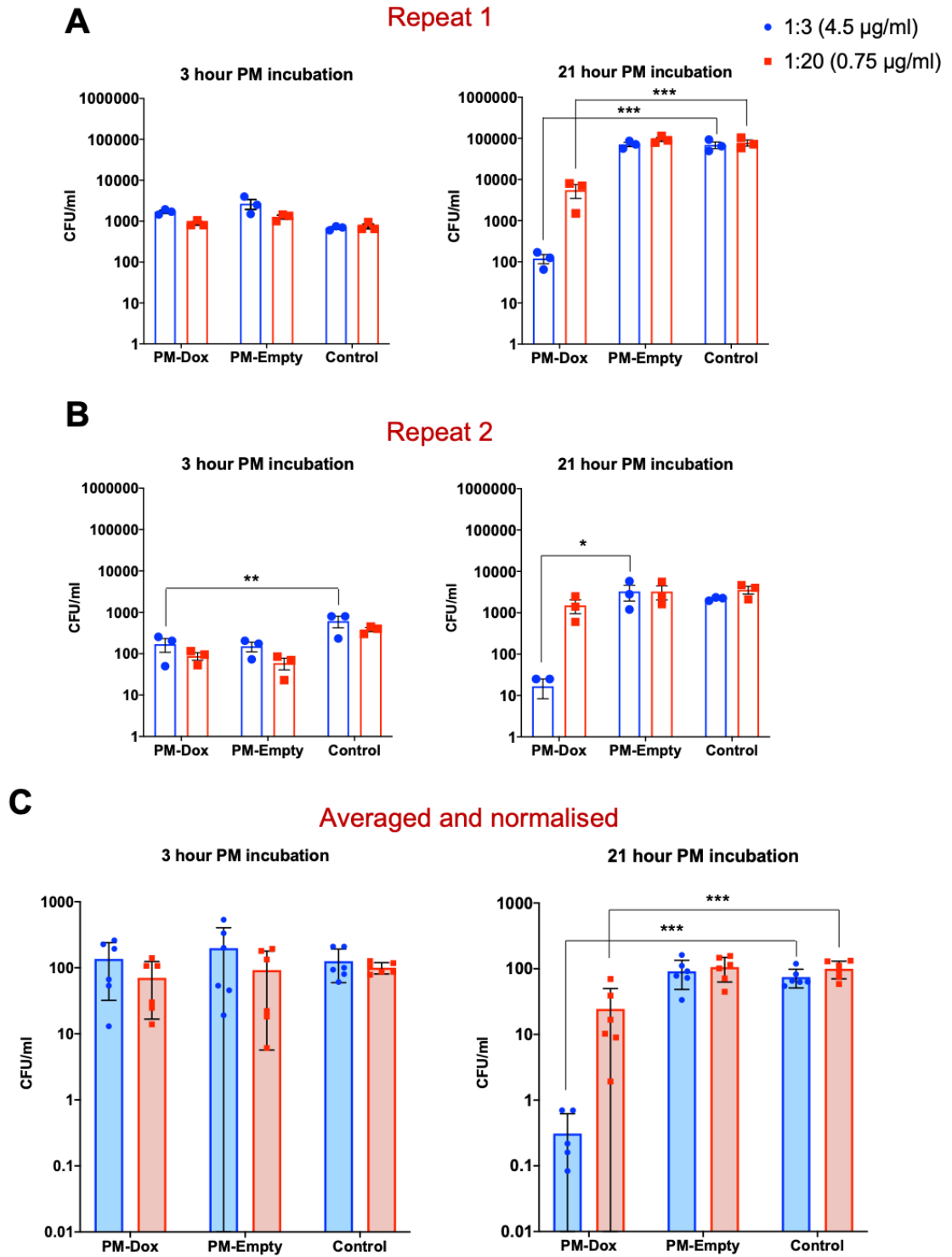


Figure 5.9 – Intraassay variability of PM-doxycycline nanoparticles on intracellular *B. thailandensis*. PM-doxycycline was applied to infected cells at concentrations of 4.5 µg/ml and 0.75 µg/ml, and then left to incubate for either 3 or 21-hours. Each timepoint was performed with triplicate technical repeats. (A) Data from biological repeat 1. Mean and SEM plotted. (B) Data from biological repeat 2. Mean and SEM plotted. (C) Averages from repeats 1 and 2 with data normalised to the control at the 0.75 µg/ml concentration. In all graphs data is presented as the mean and SD. In all cases PM-doxycycline was not able to reduce bacterial burden significantly compared to the control after a 3-hour incubation, however at the 21-hour timepoint significance was seen. Significance was calculated using a two-way ANOVA with Tukey's post-hoc test. * = $p < 0.05$, ** = $p < 0.01$, *** indicates a $p < 0.001$.

Next, the efficacy of PM-antibiotic samples was compared to their equivalent free antibiotic concentrations. PM-antibiotics were applied at concentrations of 4.5 $\mu\text{g/ml}$ for doxycycline assays, and 2.6 $\mu\text{g/ml}$ for rifampicin assays.

PM-doxycycline nanoparticles significantly reduced the intracellular bacterial burden compared to the control group, with a count of 9 CFU/ml \pm 5 versus 1628 CFU/ml \pm 1308, respectively ($p = 0.001$, one-way ANOVA with Tukey's post-hoc test). No significant difference was seen between the PM-doxycycline group and the free doxycycline control applied at the same concentration (Figure 5.10A). PM-rifampicin nanoparticles were also shown, for the first time within this project, to be able to significantly reduce the intracellular *B. thailandensis* burden compared to the control. PM-rifampicin nanoparticles reduced the intracellular count to 161 CFU/ml \pm 48, compared to 1772 CFU/ml \pm 1222 for the control ($p < 0.05$, one-way ANOVA with Tukey's post-hoc test). In this assay the free rifampicin control was able to significantly reduce the bacterial count compared to the encapsulated equivalent concentration ($p < 0.01$, one-way ANOVA with Tukey's post-hoc test) (Figure 5.10B).

Overall results from these assays confirmed that PM-doxycycline samples could work to a similar efficacy level as the free drug, with non-significant differences between the two. Results also demonstrated that a second PEO-PCL-antibiotic preparation, PM-rifampicin, has successfully been developed that can be used to treat intracellular *B. thailandensis*.

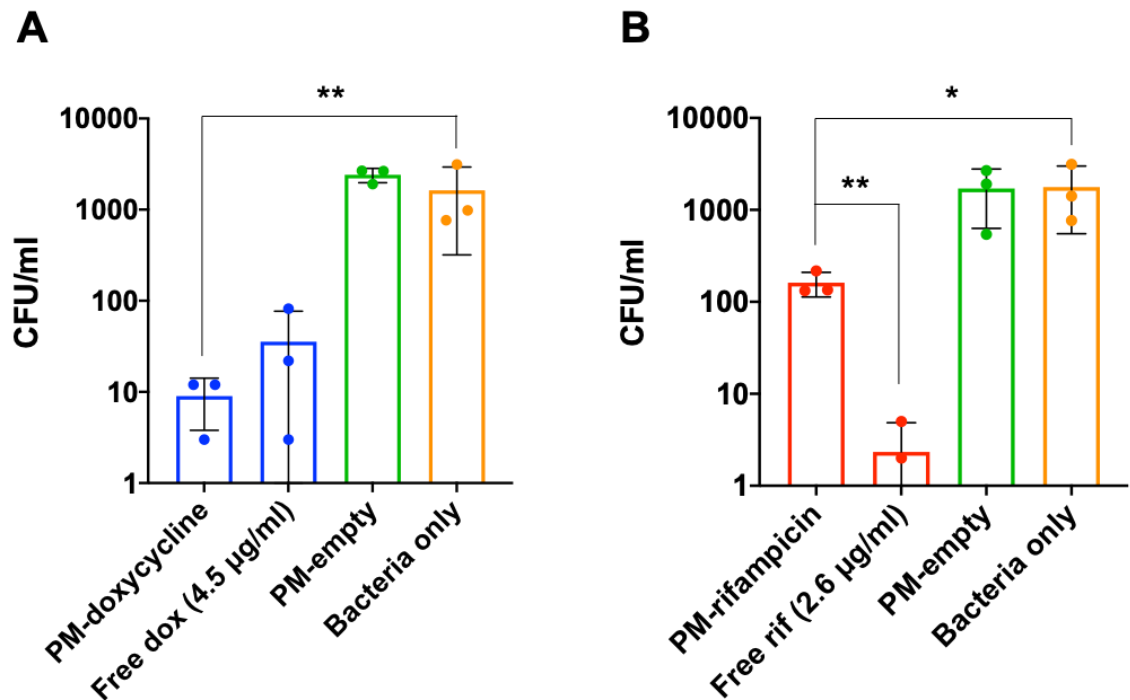


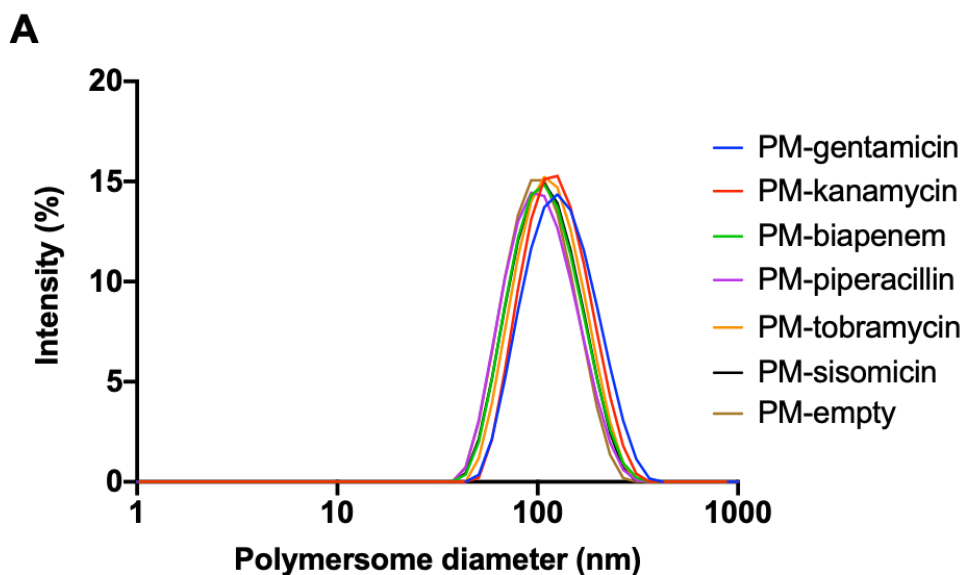
Figure 5.10 - Comparison of PM-antibiotic preparations and their equivalent free drug concentrations on the efficacy against intracellular *B. thailandensis*. (A) PM-doxycycline nanoparticles were able to significantly reduce bacterial burden compared to the control, however no significant difference was found between PMs and the equivalent concentration of free drug. (B) PM-rifampicin nanoparticles were also able to significantly reduce bacterial burden compared to the control, however the free drug equivalent was found to be significantly better at doing so. Graphs represent the mean and SD of three biological repeats, $n = 3$. Significance was calculated using a one-way ANOVA with Tukey's post-hoc test. * = $p < 0.05$, ** = $p < 0.01$.

5.2.5 PM-antibiotic screening assay

Until now, all of the antibiotics used within this project have been ones which are capable of penetrating host cells. The final section of this chapter will focus around testing PM-antibiotic preparations comprising antibiotics which are currently poorly bioavailable to intracellular bacteria. Generally, the two main classes of antibiotic which fit this criterion are the β -lactams, and the aminoglycosides. Therefore a number of antibiotics spanning these classes were chosen, which showed evidence of activity against free growing *B. thailandensis*, but that would work less effectively in an intracellular environment.

Dynamic light scattering (DLS) was used to assess the size distributions of these PMs, as a method of determining whether PMs were forming with the approximate expected sizes, based on previous characterisation of PEO-PCL PMs. All of the PM samples generated DLS curves as expected, with the characteristic PM peak at approximately 100 nm (Figure 5.11A), suggesting

that loading the PMs with these new antibiotics did at least not alter their ability to form PMs of usual structure. The polydispersity index (Pdl) values for all of the sample PMs was reported to be low, showing a good level of monodispersity and a more uniform sample size (Figure 5.11B).



B

Sample	Z-average	Pdl
PM-gentamicin	119.9	0.123
PM-kanamycin	117.3	0.142
PM-biapenem	103.1	0.135
PM-piperacillin	99.1	0.164
PM-tobramycin	106.9	0.123
PM-sisomicin	103.0	0.133
PM-empty	96.6	0.121

Figure 5.11 – DLS sizing data of the new PM-antibiotic preparations. (A) All of the samples tested possessed the characteristic PEO-PCL hydrodynamic diameter of approximately 100 nm. This clear peak and lack of other peaks suggests the PMs form normally even with incorporation of new antibiotics. (B) The Pdl values for each of the preparations remained low, showing good monodispersity in the size of the samples.

It was not possible to use UV-vis as a method for assessing encapsulated concentration for these antibiotics. Some do not possess an absorbance spectrum due to their chemical structures, and others possess characteristic peaks which fall within the lower wavelengths where PM Rayleigh scattering is highest, causing interference and inaccurate measurement. This, alongside time constraints, meant that the usual rigorous PM characterisation could not be performed. Instead, PMs were prepared in the normal way, dialysed, and then applied to infected cells and determined what effects occurred, if any. A 'dialysed free antibiotic' control was included within the assay to ensure that if bacterial killing was seen it could be confirmed that this was not due to un-dialysed antibiotic. The assay was optimised using the aminoglycoside antibiotic, kanamycin. The MIC of kanamycin was determined, using OD, for its effect on free growing *B. thailandensis*, and was found to fully inhibit growth at concentrations greater than 31.6 $\mu\text{g/ml}$ (Figure 5.12).

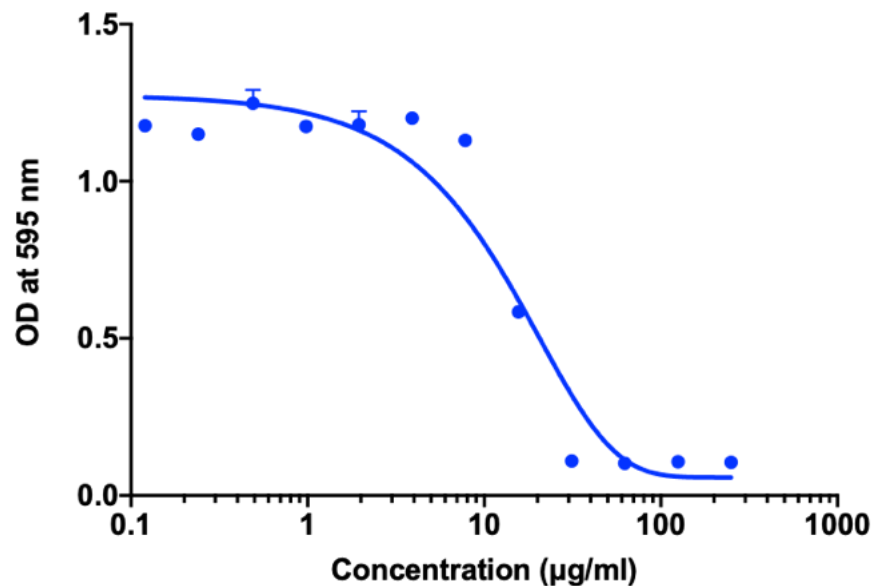


Figure 5.12 – MIC for kanamycin acting on free growing *B. thailandensis*, as determined by using OD. Kanamycin was applied to free growing *B. thailandensis* culture at concentrations ranging from 0 – 250 $\mu\text{g/ml}$. Growth was monitored over a 24-hour period, and the 24-hour timepoint data plotted. Complete growth inhibition was observed at concentrations greater than or equal to 31.6 $\mu\text{g/ml}$. Data is presented as the mean and SEM of three technical repeats, with a non-linear one phase decay line of best fit applied.

PM-kanamycin nanoparticles were unable to reduce the intracellular *B. thailandensis* burden within RAW 264.7 macrophages. Free kanamycin at 200 $\mu\text{g/ml}$ was also found to be non-significant compared to control groups, despite a concentration far greater than the MIC being used, highlighting how poor this antibiotic is at penetrating into host cells. PM-doxycycline nanoparticles were included as a positive killing control, and as expected reduced intracellular *B.*

thailandensis counts significantly ($p < 0.001$, one-way ANOVA with Tukey's post-hoc test). No significant difference was observed between PM-doxycycline and the equivalent concentration of free doxycycline (Figure 5.13).

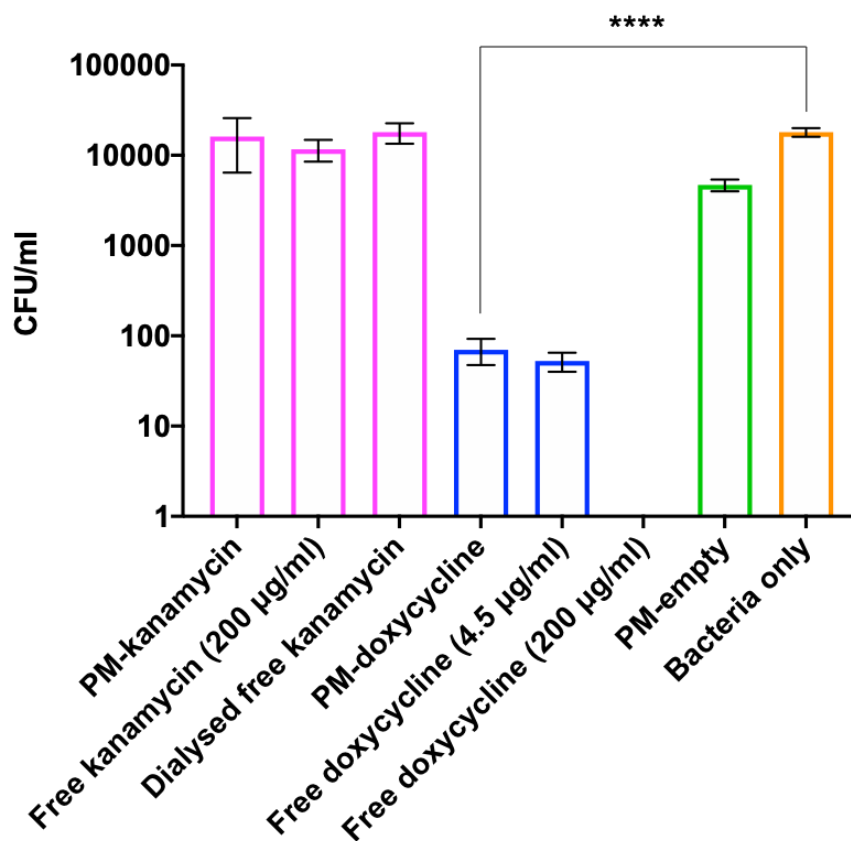


Figure 5.13 – Effect of PM-kanamycin nanoparticles on intracellular *B. thailandensis*. PMs were loaded with 50 mg/ml of kanamycin, dialysed, and then incubated for 21 hours with *B. thailandensis* infected RAW 264.7 macrophages. Neither the PM-kanamycin, nor free kanamycin controls, were able to significantly reduce the bacterial burden of cells. Data is presented as the mean and SEM of one biological repeat performed with triplicate technical repeats. Statistical analysis was performed in the way of a one-way ANOVA with Tukey's post-hoc test. **** indicates a $p < 0.0001$.

Due to the time-consuming nature of these assays with all of the relevant controls, moving forward the aim was to screen as many PM-antibiotic preparations as possible, and if any reduction in *B. thailandensis* numbers was observed, those specific PM-antibiotic preparations would be repeated alongside all of the controls listed in Figure 5.13. Six antibiotics belonging to either the β -lactam or aminoglycoside classes were tested. There was no significant difference between PM-antibiotic samples and the control for any antibiotics, with the exception of PM-sisomicin nanoparticles. PM-sisomicin nanoparticles reduced the intracellular *B. thailandensis*

count to 440 CFU/ml \pm 113 compared to the control level of 989 CFU/ml \pm 161 ($p < 0.01$, unpaired t-test, two-tailed). Referencing Table 4, there are no obvious physicochemical differences between sisomicin and the other antibiotics tested. As before PM-doxycycline also achieved a significant level of bacterial reduction ($p < 0.001$, unpaired t-test, one-tailed) (Figure 5.14).

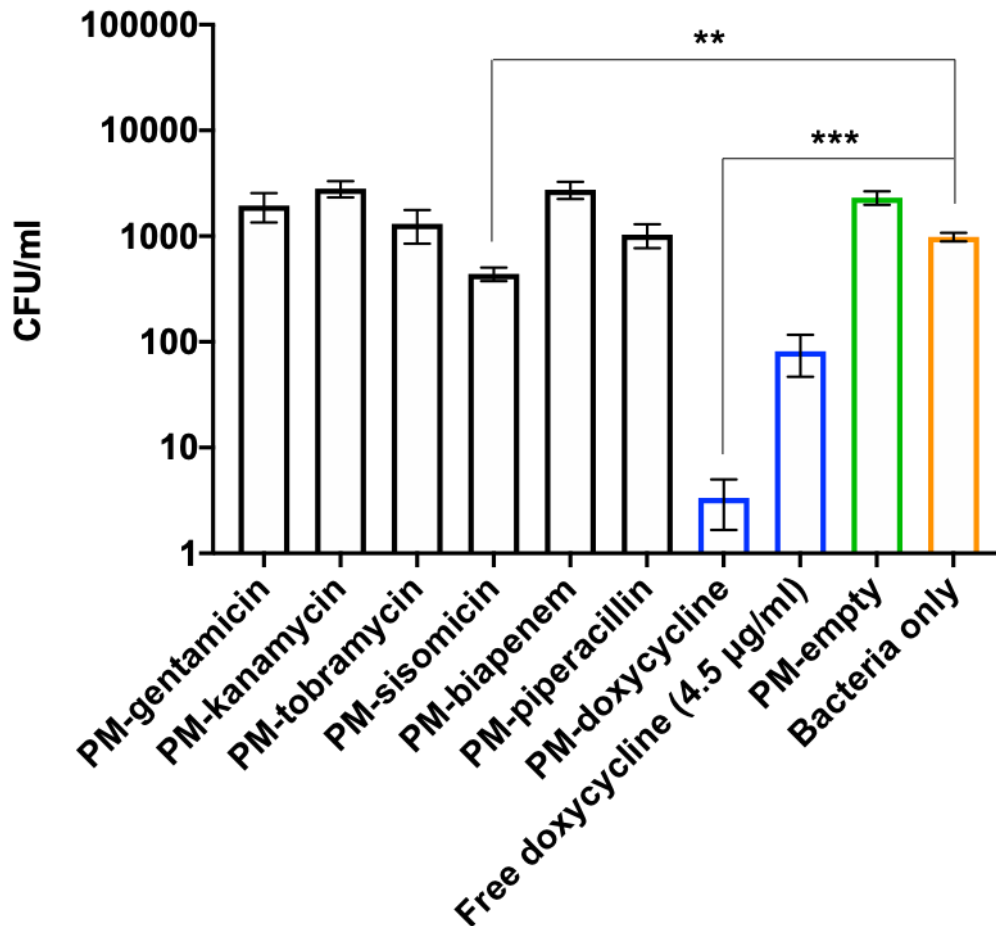


Figure 5.14 – Effect of encapsulated β -lactam or aminoglycoside antibiotics on intracellular *B. thailandensis*. There was no significant level of killing seen for any of the formulations, with the exception of PM-sisomicin nanoparticles ($p < 0.01$, unpaired t-test, two-tailed). PM-doxycycline preparations were also able to significantly reduce *B. thailandensis* numbers ($p < 0.001$, unpaired t-test, one-tailed). Data is presented as the mean and SEM of one biological repeat performed with triplicate technical repeats. *** indicates a $p < 0.001$.

Overall the results from these screening assays could hold highly significant results in the context of antibiotic drug delivery to intracellular infections. They suggest that sisomicin may be an antibiotic that is unable to penetrate the host cell macrophages alone, but when incorporated into PEO-PCL PMs it can achieve a significant level of killing. However, in order to unambiguously make this claim the assay must be repeated again alongside the free sisomicin control to ensure this is not simply one exceptional aminoglycoside that is able to penetrate host cells unaided, and that the PMs do truly make a difference to its delivery.

5.3 Discussion

In Chapters 3 and 4 it has been shown that polymersome (PM) nanoparticles are able to stably encapsulate and retain the antibiotics doxycycline and rifampicin, and that these PMs are successfully taken up by RAW 264.7 macrophage cells. In this chapter work was advanced by assessing the PM-antibiotic preparation's abilities to inhibit the growth of the bacterial species *Burkholderia thailandensis*, which resides primarily within these macrophages. This particular species has limited treatment options which are often highly dosed, causing antibiotic resistance selection pressures and patient off-target side effects. Other treatment options are therefore required, and nanoparticles such as PMs may be able to assist by increasing drug targeting to infection sites, and also by increasing the number of antibiotics available to treat such intracellular infections. The experiments conducted within this chapter aimed to address these points by showing that:

- Antibiotics retained efficacy over a 7-day period, confirming no loss of activity would result from the PM formulation timeline process
- Although PM-antibiotic preparations were unable to inhibit the growth of free growing *B. thailandensis*, significant bacterial killing was observed for intracellular *B. thailandensis*
- PM-antibiotic preparations could be screened to assess the intracellular killing capabilities of antibiotics otherwise bio-unavailable to this space.

During the preparation of antibiotic-loaded PMs, samples were dialysed to ensure the removal of free, unencapsulated antibiotic. This process occurred at room temperature, and meant that at their time of use within an experimental assay, the PM-antibiotic preparations may be up to one week old. It was therefore investigated whether this time spent at room temperature would reduce the antibiotic efficacy. Other reports in the literature show that doxycycline is able to remain stable in aqueous solution for a period of at least 7 days (Redelsperger *et al.*, 2016), and rifampicin for a period of up to 8 weeks (Nahata *et al.*, 1994). However, these studies were based on concentration assessments rather than direct bacterial potency. Therefore, a simple optical density (OD) assay was performed using day 0 and day 7 antibiotic stock preparations. Bacteria growing free in culture grew in the same pattern with antibiotics at either age and were equally as potent as one another, confirming a one-week time period at room temperature would not interfere with efficacy. If, when the intracellular killing assays were performed inhibition was not seen, this test allows confirmation that it is not due to the inactivation of the antibiotics as a result of age.

Upon the addition of PM-antibiotic formulations to *B. thailandensis* growing free in culture however, no inhibition was observed (Figure 5.2) and PMs were unable to reduce growth compared to the control. PM-rifampicin samples had an encapsulated concentration of $8.5 \mu\text{g/ml} \pm 2.4 \mu\text{g/ml}$, however the minimum inhibitory concentration (MIC) for rifampicin on *B. thailandensis*, that was measured in these studies, was $25.0 \mu\text{g/ml}$ for complete inhibition. Furthermore, due to unavoidable dilution of the PMs with *B. thailandensis* culture during the assay, the preparations had a starting concentration of only $4.2 \mu\text{g/ml}$. For this reason, it is unsurprising PM-rifampicin preparations did not inhibit bacterial growth. PM-doxycycline preparations did not share this limitation however; an MIC of $1.56 \mu\text{g/ml}$ was previously recorded, and the starting concentration for the assay was well above this at $7.6 \mu\text{g/ml}$.

It was hypothesised that the antibiotics may remain sequestered inside the PMs, and therefore bio-unavailable to the *B. thailandensis*. Efforts were made to disrupt the structure of PMs as a method to release the encapsulated payloads and allow the antibiotic to take effect, if able to do so. Heating PM-antibiotic preparations to temperatures of 98°C saw no resulting bacterial growth inhibition, and furthermore these high temperatures were found to inactivate doxycycline. This heat inactivation has also been reported within the literature, where one group investigated the effect of heating antibiotics on their MICs. They showed that when doxycycline was heated to 56°C for a period of 30 minutes there was no change in its potency against *S. aureus* and *E. coli* strains. However, when heated to 121°C for only 15 minutes the MIC was drastically altered, and concentrations as much as 32-times greater were needed to inhibit bacterial growth (Traub and Leonhard, 1995). In this project the antibiotics were heated for a considerably longer period than this, ≈ 8 hours at 98°C , and so it is unsurprising no inhibition was seen. Heating PM-antibiotic preparations to temperatures of only 65°C did lead to a reduction in the growth of free *B. thailandensis*, and comparable results to the free doxycycline control. This suggests that the antibiotics are still active within the PMs, and can become potent upon release from the PM's structure.

There have been other examples in the literature of groups researching nanoparticle interaction with bacteria alone, in the absence of cells. Largely these studies have been performed using metal-based nanoparticles, and one in particular reported the ability of silver nanoparticles to induce a pit formation on the *E. coli* bacterial wall, which allowed penetration and ultimately bacterial cell death (Pal *et al.*, 2007). Other factors contribute to the ease of which a nanoparticle may associate with a bacterial cell, including the shape of the particle. It has been suggested that nanoparticles possessing a rod or cube shape bind more easily than spherically shaped

nanoparticles, such as PMs used within this project (Yang *et al.*, 2009; Wang *et al.*, 2014). In addition to these reasons, it has also been suggested that PEGylation of the nanoparticle surface can result in steric hindrance that prevents attachment to the bacterial cells (Yeh *et al.*, 2020). The PMs in this project certainly possess these PEG components, further supporting why inhibition of free growing bacteria was not seen.

Aside from interaction studies using metal nanoparticles, there are also examples of polymeric nanoparticle interactions with bacterial cells. One group used pH-sensitive PLGA-PLH-PEG nanoparticles that would bind to *E. coli* and *S. aureus* bacterial cells under acidic conditions only. They reasoned that due to the higher level of acidity associated with bacterial infection sites, this would aid drug targeting (Radovic-Moreno *et al.*, 2012). Additionally, another paper investigated PMs loaded with rifampicin, and assessed their stability. They discovered that these PM-rifampicin preparations would not release their payload at a neutral pH of 7.4, and that this would only occur upon a drop to at least pH 6 (Fenaroli *et al.*, 2020). This group were also using pH-sensitive stimuli-responsive PMs, whereas the PMs used within this study were simpler and without a pH-sensitive linker. Despite this, in both cases the PMs remained stable and impermeable to antibiotic leaking in a neutral (and in this case 'extracellular') environment, further explaining why no inhibition of free growing *B. thailandensis* was seen.

It has been hypothesised in this study that because the antibiotics remained active within PMs, but were unable to inhibit free growing *B. thailandensis*, that they were tightly sequestered and therefore remained bio-unavailable. It is also believed that the RAW 264.7 macrophage cells would be necessary in order to break down the PMs and release the antibiotics. It is likely that within the cellular environment a whole multiplex of events occur which would result in this breakdown, likely including lower pH and enzymatic activity as the main causes (Behzadi *et al.*, 2017). One future experiment could be to add lysozyme enzymes to the PMs, without the presence of cells, and see if this is able to degrade them. Overall, these results are highly important in the context of drug-delivery to intracellular infection sites, and for reducing off-target side effects and antibiotic resistance selection pressures. Usually, during the course of antibiotic treatment the drugs systemically disseminate across the body, reaching areas such as the gut microflora which are rich in beneficial bacterial species. As a result, these non-target areas experience significant bacterial loss, causing secondary issues and side effects, and most importantly expose all of these bacterial populations to the drug, creating selection pressures for resistance (Zhang *et al.*, 2019). If the PMs are able to keep their payloads sequestered until within a cellular environment, this significantly aids in these challenges.

Intracellular killing assays supported the belief that cellular machinery was needed to release PM payloads, as a significant level of *B. thailandensis* killing was seen compared to control groups when either PM-doxycycline or PM-rifampicin were applied to infected cells. The observation that no significant killing occurred after a 3-hour PM incubation, but was observed after a 21-hour, aligned well with results presented in Chapter 4, where it was shown that cells possess a higher fluorescence intensity for PMs at 21 hours compared to 3 (Figure 4.11). The higher number of PMs present intracellularly at 21 hours suggests a higher concentration of antibiotic payload will have been delivered by this time, compared to at 3 hours.

Another interesting result from the intracellular killing assays came from the PM-rifampicin samples and their efficacy on intracellular *B. thailandensis*. Previous MIC data from Chapter 3 suggested that a rifampicin concentration of 25 $\mu\text{g/ml}$ was needed for a complete inhibition of bacterial growth, based on optical density (OD) readings. When PM-rifampicin samples were applied for 21 hours at a concentration of 2.6 $\mu\text{g/ml}$ a significant level of bacterial killing was seen, resulting in only 161 colony forming units/ml \pm 48 (Figure 5.10B). Although the CFU/ml count was not zero, this small number of bacteria would almost certainly have given an OD reading of close to zero as the machine is less sensitive than a CFU count. This sensitivity variance between methods has also been reported elsewhere in the literature. Udekwu and colleagues investigated the MIC for various antibiotics on cultures of *S. aureus*. In many cases the MIC needed was higher based on CFU/ml data when compared to OD data. For example, they showed a ciprofloxacin MIC of 0.5 mg/L was needed based on OD data, but 1 mg/L was needed based on CFU/ml data (Udekwu *et al.*, 2009). Nevertheless, this shows that being in the presence of cells the antibiotics are somehow more effective at killing the *B. thailandensis*. The free drug control performed the same as the PM-antibiotic samples, and so unfortunately this difference is not due to encapsulation via nanoparticles. However, it is likely that the cell accumulates the antibiotics, thereby increasing the intracellular concentration over time. Another research group showed this with their work, whereby they monitored intracellular macrophage accumulation of antibiotic over time. Human HL-60 cells were differentiated into macrophages and then administered media with a fixed concentration of 25 $\mu\text{g/ml}$ of oritavancin. In as little as 24 hours the intracellular oritavancin concentration had increased 200-fold compared to the extracellular concentration. Similar results were also seen with murine J774 macrophages (Baquir *et al.*, 2012).

Although cells are capable of accumulating drug over time, it is also possible, and likely, that the macrophages possess efflux pumps that pump a level of the antibiotic back out of the cell. This would lower the intracellular antibiotic concentration and reduce the chances of a complete

bacterial killing. A paper by Seral *et al.* (2003) looked into the effects of inhibiting J774 macrophage efflux pumps on the accumulation of the antibiotic azithromycin. Drugs, such as verapamil, are able to inhibit efflux pumps in macrophages such as P-glycoprotein. The paper found that the application of verapamil was able to increase the accumulation of intracellular azithromycin by 2.4-fold. This bodes well for the work in this project, and an interesting future experiment would be to repeat the intracellular killing assays in the presence of a drug such as verapamil. One would expect a lower concentration of drug to be able to elicit the killing of *B. thailandensis*, or a faster rate of killing – perhaps with killing seen at 3 hours rather than just 21 hours, or both. Verapamil is an FDA approved drug (Gupta *et al.*, 2014), and so an interesting idea to develop would be to assess the delivery of both antibiotics and verapamil within PM nanocarriers, as a means to boost their performance further.

In Chapter 4 the use of imaging flow cytometry (IFC) was investigated, using the ImageStream machine, to measure quantitatively nanoparticle uptake into cells, and specifically the co-localisation between GFP-tagged *B. thailandensis* and DiD-labelled PMs. After a 3-hour PM incubation there was a strong level of co-localisation reported, however by 21 hours this rapidly decreased (Figure 4.13). These results were interesting, as one would expect the most bacterial killing to take place during times of high co-localisation, however it was found that it was not until the 21-hour timepoint that intracellular killing was observed. It is possible that a) co-localisation is not required to achieve bacterial killing, b) PMs were hydrolysed by the 21-hour timepoint, and the payload accumulated to levels high enough to achieve killing, c) the DiD fluorophore used to assess PM intracellular localisation had dissociated from the PMs resulting in inaccurate reporting of PM and bacterial co-localisation. In reality, it is likely a combination of these factors contributed to the results seen.

The readout used within this project for intracellular killing was CFU counts. Whilst this technique is widely used, one future experiment could be to utilise the high-throughput capabilities of the ImageStream IFC to assess killing. The *B. thailandensis* strain used within this project possesses a GFP tag, and so it might be possible to use the intensity of GFP fluorescence as a readout for the level of living *B. thailandensis*. One potential limitation to this method, however, is the relatively long half-life that GFP possesses. Within this project, *B. thailandensis* tagged specifically with enhanced GFP (eGFP), a variant of GFP which has a brighter fluorescence allowing easier detection (Zhao *et al.*, 1999), was used. Wild-type GFP has a half-life of approximately 26 hours (Kitsera *et al.*, 2007), and eGFP has been reported to have a half-life of 15 hours (Danhier *et al.*, 2015). This means that even after a bacterial cell has died, the eGFP fluorescence would remain

for a considerable period of time. Therefore, using the fluorescence of eGFP-tagged *B. thailandensis* via IFC would not be the best model for assessing bacterial cell death. There are other groups who have successfully used fluorescence and flow cytometry as a method for assessing bacterial cell death. Hendon-Dunn *et al.* (2018) developed a flow cytometry method that utilised two fluorescent dyes, one a marker for living cells (Calcein violet-AM), and one for dead cells (SYTOX-green). The SYTOX-green marker is able to permeate through damaged bacteria and bind to their DNA. The group used this method as a way to assess *Mycobacterium tuberculosis* viability after exposure to different antibiotics (Hendon-Dunn *et al.*, 2018).

Whilst PMs have been largely researched for their use as drug delivery vehicles for cancer treatments (Sanson *et al.*, 2010; Egli *et al.*, 2011; Meng *et al.*, 2012), their potential for antibiotic drug delivery has also been explored. *B. thailandensis* has also been lightly researched as a species of interest for antibiotic delivery using PMs. In 2015, Lane and colleagues constructed pH-sensitive PMs to deliver the antibiotic ceftazidime to intracellular *B. thailandensis* infections. The PMs were based upon a hydroxyethyl methacrylate (HEMA) and poly(ethylene glycol) methyl ether methacrylate ($FW_{avg} \approx 950$ Da) (O950), or poly(HEMA-O950), copolymer scaffold. RAW 264.7 mouse macrophage cells were cultured with GFP expressing *B. thailandensis*. Cells which were infected, but received no antibiotic treatment, unsurprisingly had large levels of resulting bacteria within cell lysate, in the order of 1.3×10^7 colony forming units per well (CFU/well). Cells treated with 0.2 mg/ml of free ceftazidime displayed reduced bacterial growth, at around 35,000 CFU/well. Cells treated with PM-loaded antibiotic, at a concentration again of 0.2 mg/ml, resulted in undetectable levels of bacteria from the cell lysate (Lane *et al.*, 2015). The results indicate how PMs can be used to deliver antibiotics with greater efficacy than the free drug version. This may be due to the ease of which the free drug is able to cross the cell membrane, and how encapsulation within PMs can aid this process. Additionally, the pH-responsiveness of the PMs allows for drug release only once inside the acidic endosomal pathway compartments, which is likely where bacteria reside, resulting in a greater proportion of the drug in the target location. This paper is key to this project as it delivers PMs to not only the same bacterial model organism, but also to the same cell model of RAW 264.7 macrophages. Success for this research group is encouraging for the work being performed in this study. Future work could be to perform the assays again using pH-responsive PMs to assess whether this increases the bacterial killing seen as a result of increased payload release. It is possible that currently a slow-release, or incomplete release, of drug from the PMs is experienced, hence why an increased efficacy over the free drug was not reported. Despite this, limitations to the Lane *et al.* (2015) paper exist. Although excellent results were presented, the polymers used are yet to have been given FDA approval, unlike the

polymers within this project, and so translation from bench to clinic may not be possible. Additionally, the preparation of these PMs is highly complex in comparison to the simple nanoprecipitation method used in this project. There is a balance that needs to be achieved between using materials which are the best suited to the experiments (perhaps pH-responsive ones like in this paper), and using materials which will easily be applied to real-life scenarios down the line, and that are simple enough to achieve easy reproducibility, relatively quickly.

More recently, another group used pH-sensitive PMPC-PDPA PMs to deliver antibiotics to intracellular *M. tuberculosis*, *M. bovis*, *M. marinum*, and *S. aureus*. They showed the ability of PMs to significantly reduce the intracellular burden both *in vitro*, and *in vivo* using zebrafish as a model organism (Fenaroli *et al.*, 2020). This paper mirrored a lot of the work done within this study, but certainly had limitations. For example, the group confirmed that their PMs were able to retain rifampicin until stimulated to release by a drop in the pH to at least pH 6. Whilst this supports the work presented in this project, that PMs will not release their payloads until taken up by macrophages, Fenaroli *et al.* failed to incubate their PMs with free growing bacteria and confirm their hypothesis remained true in this environment. This project applied the PMs to free growing *B. thailandensis* and confirmed unambiguously there was no release in the absence of macrophages. One particular area where Fenaroli *et al.* achieved desirable results was through their imaging of the PMs. Their PMPC-PDPA PMs were functionalised with a Cy5 fluorophore meaning there could be no dissociation of the dye from the PMs. Despite this, it is still possible that the PMs could break apart and degrade once inside the cells and this would not be distinguishable even from a covalently attached fluorophore. Nevertheless, it is one step beyond simply encapsulating a membrane dye into the PMs, like within this study, and so should be something to consider in future work. Overall, the CARS technology is superior as it allows for completely label-free imaging, and so this is the imaging technique that should be most heavily pursued.

One thing Fenaroli *et al.* achieved, which was not seen in this project, was an increase in the efficacy of PM-loaded antibiotic compared to the free antibiotic alone, both *in vitro* and *in vivo*. This may potentially be due to the fact that the presence of a pH-sensitive linker allows for the complete release of antibiotic payload. Even though results from this PhD did not show an increase in drug efficacy, there are still huge benefits to the antibiotic payload working as effectively but in an encapsulated form. Largely these benefits include the payload being sequestered until inside the cells, and the benefits that come from targeted delivery and reduction of off-target side effects. Furthermore, as stated in the context of the Lane *et al.* (2015)

paper, these pH-sensitive PMs require complex production. The PMs used within Fenaroli and colleagues' study take a minimum of 4 weeks to produce and multiple post-synthesis purification and characterisation steps. Furthermore, of the PMPC-PDPA materials used, only one (PMPC) is FDA approved (Fujiwara *et al.*, 2019), leading to possible delays in using these in a clinical environment. Therefore, whilst these key papers provide reassurance that this project's work is similar and relevant, there are limitations to them that are not present within this study. At the same time however, they do provide some useful direction to where future studies with PEO-PCL PM-antibiotic preparations may go.

It has already been mentioned that intracellular infections are challenging to treat partly due to the poor bioavailability of many antibiotics. There are multiple large groups of antibiotics, for example β -lactams and aminoglycosides, which are largely unable to penetrate the host cell membrane (McOrist, 2000). In many cases these antibiotics are effective at killing the bacteria alone, but once shielded inside the cell they are ineffective. Therefore, a large number of antibiotics have been rendered useless simply due to targeting challenges. Investigations were therefore begun into whether some of these antibiotics may be able to be packaged within PMs as a method to 'Trojan horse' these drugs into the cells. If able to be taken up by cells via the PMs, they would then be released into an intracellular environment more efficiently than they otherwise could have been. If successful, this is a method that could be used to increase the number of antibiotics available to treat an infection. It is a method that repurposes antibiotics by repackaging them.

A number of antibiotics were selected from the β -lactam and aminoglycoside classes that have been shown to display activity against free growing *Burkholderia spp.* (Thibault *et al.*, 2004; Thamlikitkul and Trakulsomboon, 2010; Kovacs-Simon *et al.*, 2019). Sisomicin was chosen due to the minimal published research on its efficacy against *Burkholderia*, and also due to it being one of the cheaper antibiotics to purchase and perform initial tests with. Results showed that none of the PM-antibiotic preparations were able to inhibit intracellular *B. thailandensis* growth, with the exception of sisomicin, which significantly reduced the burden compared to the control group. Due to time constraints it was initially decided to screen many PM-loaded antibiotics, and then of those, any that were effective would be repeated with relevant control groups. However, due to the unforeseen COVID-19 pandemic, it was not possible to perform this repeat with control groups. As a result, one key missing control was free sisomicin. Without this it cannot be confirmed whether the PMs offer the delivery of a drug which would not otherwise be able to penetrate the macrophage and take effect. It also cannot be said for certain that an antibiotic has

successfully been delivered which would otherwise be useless. Future work would certainly involve repeating this assay using the equivalent concentration of free sisomicin. This being said, one group investigated the action of sisomicin on intracellular *Legionella pneumophila* residing within J774A.1 macrophages, and found it to be fully ineffective (Chiaraviglio and Kirby, 2015). The paper did not elaborate as to whether this was due to inability to be taken up by the macrophages, or due to resistance by *L. pneumophila*. To the best of our knowledge, there is no evidence in the literature for sisomicin efficacy on free growing *Legionella spp.* However, another group reported that in a hospital setting only 26% of patients suffering from bronchopneumonias caused by bacterial species sensitive to sisomicin *in vitro* had a favourable response to systemic *in vivo* therapy (Klastersky *et al.*, 1979). This suggests that sisomicin can be effective on free growing bacteria but inhibited by cellular protection. The weight of these results is significant, as if it was possible to show that sisomicin is ineffective when unencapsulated, but able to inhibit *B. thailandensis* when packaged into PMs, that essentially adds another antibiotic therapy to the current available options. Furthermore, there are no known examples in the literature of sisomicin being used to treat *Burkholderia* infections, adding to the novelty of this work.

Overall the results within this chapter display how both PM-doxycycline and PM-rifampicin nanoparticle preparations can be successfully used for the intracellular killing of *B. thailandensis*. Whilst there was no significant killing compared to the free drug controls, there are many benefits that come from the antibiotics simply being packaged within PMs, such as reduced side effects. Results also provide the first example of PMs used from FDA-approved components being used to treat *B. thailandensis* infections, and the translatability to other intracellular infections could be applied with ease. In order to increase the level of killing seen, cellular efflux pump inhibitors should be investigated, as previously mentioned. Furthermore, linking back to Chapter 3 the possibility of actively loading the antibiotics into the PMs may also increase the amount successfully encapsulated. In order to advance this project's findings, and increase their significance, assays should be repeated using *B. pseudomallei*, the category 3 pathogen of which *B. thailandensis* only models. Additionally, rather than using RAW 264.7 cell line macrophages, primary human macrophages should next be investigated, before finally moving onto *in vivo* models, such as the zebrafish model used by Fenaroli and colleagues recently. The groundwork performed within this PhD paves the way for exciting future applications for the PEO-PCL nanoparticles.

Chapter 6: General discussion

Chapter 6: General discussion

6.1 Summary of the main findings of the study

Intracellular bacteria are challenging to treat for multiple reasons, including their increased shielding from host immune responses such as antibody exposure, and furthermore from the poor bioavailability of many antibiotics to the intracellular niche in which they reside. For this reason, current treatments involve lengthy courses of antibiotics which can in turn be problematic due to off-target side effects of these drugs, and the selection pressures for resistance caused by systemic exposure of the human microflora to these drugs. Nanoparticles have been suggested as a solution to these challenges by offering a more targeted approach to drug delivery. With the potential to release payload only at the site of infection, they could aid the creation of high intracellular drug concentrations and simultaneously reduce off-target exposure by sequestering their payloads until within an intracellular environment. The aim of this thesis was to assess the viability of polymersome (PM) nanoparticles for their use as antibiotic drug delivery vehicles. This work has been achieved by:

- Investigating the loading and encapsulation of multiple antibiotics into PMs, and measuring the stability of these preparations over time
- Assessing the uptake of PMs into RAW 264.7 macrophage cells, where many intracellular species reside, and their direct co-localisation with *Burkholderia thailandensis*
- Measuring the ability of the PM-antibiotic preparations to inhibit the growth and reduce intracellular *B. thailandensis* burden within macrophage cells.

The study began with experiments conducted in **Chapter 3** which tested the hypothesis that *PEO-PCL PM nanoparticles can stably encapsulate and retain antibiotics*. The main aim of this chapter was to show that not only could encapsulation of varying antibiotics be achieved, but that the PM-antibiotic association was stable and the payloads would be retained. The results from this section highlighted that PMs could encapsulate the antibiotics novobiocin, rifampicin and doxycycline. A method of disrupting the PM structure was developed, using dimethylformamide (DMF), which allowed antibiotic concentration measurements to be generated without interfering signal from nanoparticle Rayleigh scattering. The initial antibiotic loading experiments confirmed that a cut-off point existed whereby maximal drug had been incorporated into the PMs, and no more could be encapsulated, based on the observation of precipitation of the drug into solution. It was therefore suggested that the optimal loading concentration for each of the antibiotics was the highest level reached before this occurred. In the case of rifampicin it was also shown that in the presence of PEO-PCL polymer the solubility of this drug could be increased, as at a given

concentration precipitation was only present in samples without the polymer. Furthermore, the antibiotics could all be retained over a period of 14 days, with doxycycline and rifampicin showing stable encapsulation over this duration. These PM-antibiotic formulations reached a steady state after 3 days where no more drug was released from the PMs. Finally, it was shown that the PM-antibiotic nanoparticles themselves possessed a high local concentration, much greater than the bulk concentration of PMs in their final buffer solution.

These experiments confirmed that PEO-PCL PMs were viable drug delivery candidates, and so work presented in **Chapter 4** developed this and tested the hypothesis that *PEO-PCL PMs can be taken up intracellularly into cells such as RAW 264.7 macrophages*. The main aim of this chapter was to show that PMs could be taken up into both healthy macrophage cells, but also macrophages that were *B. thailandensis* infected. Fluorescently labelled PMs were produced and both confocal and epifluorescence microscopy used to determine that PMs were able to be taken up by macrophage cells irrespective of whether or not intracellular bacteria were present. Coherent anti-Stokes Raman scattering (CARS) was also used as a method to test PM uptake without the need for prior PM labelling. CARS imaging supported previous findings that PEO-PCL PMs could successfully be taken up by these macrophage cells. Finally, imaging flow cytometry (IFC) was used a method to assess the level of direct co-localisation between fluorescently labelled PMs and *B. thailandensis* bacteria within RAW 264.7 macrophage cells. Co-localisation was detected between the two, with the highest levels being recorded after a 3-hour PM incubation with infected cells. This is the first known example of IFC being used to assess co-localisation between nanoparticles and intracellular bacteria, which highlights the novelty and advance of work within this project compared to other reports within the literature.

The first two chapters confirmed that PMs can be used to encapsulate antibiotics, and that these PMs are compatible with uptake into macrophage cells. The project therefore culminated with the work presented in **Chapter 5** where the hypothesis that *PEO-PCL PMs can inhibit the growth of intracellular B. thailandensis* was tested. The main aim of this chapter was to show, for the first time, how PEO-PCL PMs could be used to reduce the bacterial burden of an intracellular species residing within mammalian cells. PMs did not inhibit the growth of *B. thailandensis* growing free in culture medium. The buffer solution surrounding the PMs also did not inhibit growth, highlighting lack of unencapsulated antibiotic within samples. Attempts to disrupt the PMs and release the antibiotic payloads, using DMF and varying temperatures, were made using bacterial growth inhibition as a readout for success. Only PMs heated to temperatures of 65°C were found to be able to elicit a bacterial growth reduction, and this was hypothesised to be due to PM structure disruption and the release of the otherwise stably sequestered antibiotic. When PMs

were applied to *B. thailandensis* residing intracellularly within RAW 264.7 macrophages, bacterial killing was observed after a 21-hour PM incubation. For both PM-doxycycline and PM-rifampicin preparations a significant level of killing was seen compared to control groups. Finally, it was shown that the developed intracellular bacterial killing assay allowed for the potential screening of many different types of PM-antibiotic formulations. Of those initially selected for these tests, a significant level of killing was observed with one PM-antibiotic formulation, PM-sisomicin, which belongs to a class of antibiotics known to usually have poor intracellular penetration.

6.2 Relevance of the findings

The most relevant and exciting part of this project was the discovery that the PM-doxycycline and PM-rifampicin preparations were able to inhibit the growth of intracellular *B. thailandensis*. Bacterial infections, specifically intracellular infections, pose a threat to modern medicine as their treatment becomes ever more challenging. Intracellular bacteria are capable of surviving and replicating within human host cells, where they are protected from antibody immune responses, and more problematically from many antibiotics which cannot penetrate the cell membrane. This leads to a reduced number of treatment options. Furthermore, current treatment options for these types of infections require lengthy courses of treatment (Abed and Couvreur, 2014), which can cause off-target side effects, and contribute to the increased selection pressure for antibiotic resistance (Dethlefsen and Relman, 2011; Zaman *et al.*, 2017).

The field of nanomedicine is rapidly growing, and the use of vehicles such as PMs has already been utilised, however this has largely been for the delivery of cancer therapeutics. Nanoparticles have been employed with the aim of achieving a more targeted approach, and to enable high and sustained cell drug concentrations, to in turn allow the potential for lower drug doses and/or for shorter treatment periods. Despite their potential for this, only one liposomal nanoparticle formulation has currently received Food and Drug Administration (FDA) approval for clinical antibiotic treatment use (Fatima *et al.*, 2018), and no PM formulations have received this. In part this is due to the complexity of many of the PM preparations currently being researched. Many are made from polymeric materials that do not have FDA approval, and they also require complex chemical pathways to synthesise characteristics such as pH sensitivity. One of the key benefits to the work performed within this project, compared to other groups within the literature, is the simplicity of the PMs. They are made entirely from FDA approved materials, and their formulations are simple and quick to synthesise. This in turn adds to their potential for good clinical translation.

This project focused on targeting the intracellular pathogen *B. thailandensis*. This is the model organism of *B. pseudomallei*, a known biowarfare threat which can cause potentially fatal infections and currently requires treatment lasting up to 6 months (Limmathurotsakul and Peacock, 2011). The PEO-PCL PMs used within this project were shown, for the first time known to be reported, to be able to reduce the intracellular *B. thailandensis* burden significantly compared to control groups. Due to the similarity in antibiotic susceptibilities between *B. thailandensis* and *B. pseudomallei*, this sets good foundations for the technology developed here to be applied to this human pathogen. Furthermore, the PM formulations were shown to stably retain the antibiotic until in an intracellular environment. This is significant when considering their ability to limit off-target side effects to areas such as the gut microbiome, and also gives them the potential to limit selection pressures for antibiotic resistance, due to fewer bacteria being exposed to the PM-sequestered antibiotic.

Overall the work presented in this thesis strongly confirms that PEO-PCL PMs have excellent potential as drug delivery vehicles for the treatment of intracellular bacterial infections. The PM formulations should not be limited to application only to *Burkholderia spp.* as they have the scope to be effective at killing any type of intracellular bacterial infection. *Brucella spp.* have shown susceptibility to both doxycycline and rifampicin, and *Francisella tularensis* to doxycycline (Maurin and Raoult, 2001). These cause the infections brucellosis and tularemia, respectively. Brucellosis is a zoonotic infection which causes detrimental effects on livestock industries and in turn causes socioeconomic challenges in low income communities, particularly in the Middle East. If the disease is left untreated it can become chronic and persist over many years, and may also display complications affecting bones, central nervous system and the heart (Nejad *et al.*, 2020). Tularemia is another example of a zoonotic infection, but also more importantly perhaps, one which has the potential to be used as a bioweapon. It is extremely infectious, and it has been reported that only 10 bacterial cells are required to initiate an infection, via inoculation or inhalation (Dennis *et al.*, 2001). Furthermore, both *Brucella* and *Francisella* infections require undesirable treatments, with brucellosis requiring a lengthy course involving a minimum of a 6-week combined antibiotic therapy, and tularemia requiring the use of a combination of antibiotic classes including aminoglycosides, fluoroquinolones and tetracyclines (Alavi and Alavi, 2013; Caspar and Maurin, 2017). Encapsulation of antibiotics within PMs may reduce treatment time and also limit the chances of resistance arising to such a magnitude of antibiotic classes.

6.3 Limitations and indications for future work

Whilst this project achieved novel and significant findings, there is the potential for improvement and multiple future experiments which could be performed to strengthen the outcomes further. This section will highlight some of the limitations experienced within each chapter, and subsequently discuss how future experiments could overcome these.

In Chapter 3 the encapsulation of various antibiotics into PMs was investigated. The method used to load these drugs was nanoprecipitation, a passive drug-loading process. Generally, this method yields lower encapsulation efficiencies than remote/active-loading processes (Choucair *et al.*, 2005; Zhang *et al.*, 2009). Therefore, one limitation to the work presented in this project was that relatively low encapsulation efficiencies were reported. For nanoparticles that will be used for the purpose of drug delivery, it would be desirable to achieve a loaded concentration as high as possible to ensure the maximal drug delivery per dose. In the context of antibiotic treatment for bacterial infections this would have a greater potential to reduce the need for long treatment courses, in turn limiting side effects and risk of antibiotic resistance. Future work should involve optimising the loading of the PMs using remote loading methods such as ammonium-sulphate gradients, or pH gradients, so that less of the initially added payload is removed via dialysis and more retained within the PMs.

Within the project antibiotics were selected for encapsulation based on their efficacy towards *B. thailandensis*. Furthermore, due to the encapsulated concentration being assessed using UV-vis light spectroscopy, antibiotics were also required to possess a UV-vis absorbance spectrum. For the optimisation of the assays within this project the antibiotics chosen were: levofloxacin, doxycycline, rifampicin and novobiocin. A large limitation to these choices is that these four drugs are all capable of entering a human macrophage cell unaided by nanoparticles. The most ideal outcome from this project would be to achieve the intracellular delivery and functioning of an antibiotic that would not have otherwise had access to the intracellular niche. The main antibiotics which fit this criterion are the aminoglycosides and the β -lactams. However, their use for the work performed in Chapter 3 would have been challenging for multiple reasons. Firstly, in the case of aminoglycosides, they possess little to no absorbance in the UV-vis region, due to a lack of UV chromophores within their structures, making their detection using the NanoDrop technique impossible (Blanchaert *et al.*, 2017). Whilst β -lactams do possess UV-vis spectra, their characteristic peaks tend to fall at very low wavelengths – reported as low as 190 nm (Chen and Swenson, 1969). Peaks within these regions would be heavily interfered with from the PM's Rayleigh scattering signal. Even using DMF to disrupt PM structure and minimise this scattering

interference, it is not fully efficient. This would mean that if low concentrations of β -lactam antibiotics were encapsulated, their detection using UV-vis may be masked by nanoparticle scattering. The ideal antibiotics are those which possess peaks with higher wavelengths, further away from interference to allow unambiguous detection. Without this method of detection it would not be possible to so easily confirm the presence of antibiotics within the PM preparations after the dialysis period.

Another challenge that would have been presented by using these antibiotics is that *B. thailandensis*, and *B. pseudomallei*, usually possess high levels of resistance to these classes (Moore *et al.*, 1999). It was not desired to begin the project by encapsulating antibiotics that would not be effective once inside the infected macrophage cells. However, if more time was to be spent on this project it would certainly be useful to know if these aminoglycoside and β -lactam antibiotics could be encapsulated. This may involve the use of other detection methods, such as mass spectrometry perhaps which would detect the compounds based on their unique chemical structures rather than possession of UV-vis spectra.

In Chapter 4 the uptake of PEO-PCL PMs into RAW 264.7 macrophages was investigated, and it was confirmed that these nanoparticles were capable of penetration into the target cells for this project. Whilst uptake of the nanoparticles is important, another factor which was not considered during this work was the assessment of intracellular release of the payload. Despite the increasing interest in the use of nanoparticles for medical drug delivery applications, there remains little reported on the number of nanoparticles internalised by single cells and subsequently the precise concentration of payload released into cells. One paper by Scarpa *et al.* (2016) developed a method to quantify intracellular release of fluorescein dye from PEO-PCL PMs into mouse fibroblast cells. Fluorescein is a fluorescent dye that is quenched under high concentrations, for example within PMs. Upon release from the nanoparticles the dye fluoresces and can be measured. This group combined fluorescence measurements and flow cytometry to show that approximately 170 PMs were taken up per cell (Scarpa *et al.*, 2016). The work within this project could be progressed by using PM-fluorescein preparations in macrophage cells to confirm that the same pattern of fluorescein release from PMs can be detected. Furthermore, this would provide information on how quickly the fluorescein, and in theory then the antibiotic, is released from the PMs. To advance this work even further antibiotics conjugated with a fluorescent dye could be used to give a direct readout of payload release, concentration and location. Within Chapter 4 the IFC data collected assessed PM location within macrophage cells and their co-localisation to the green fluorescent protein (GFP)-tagged *B. thailandensis*. This was achieved using PMs loaded with a fluorescent dye, DiD, however the caveat to this was that all fluorescence detected was from

the dye and not specifically the PMs. Using a fluorescently labelled antibiotic could allow for more specific tracking of the PMs and their payloads, and also allow accurate assessment of the intracellular antibiotic concentration on a single cell level. Another possible method to track PMs intracellularly could be to use PEO-PCL polymer that had been covalently labelled with a fluorophore, as this would also provide direct assessment of PM intracellular localisation, rather than relying on indirect dye fluorescence readouts.

Using polymer or antibiotic covalently tagged with a fluorescent marker might be one method to assess uptake into macrophages, however an avenue pursued in this project was to remove the need for labelling PMs altogether. This was achieved using coherent anti-Stokes Raman scattering (CARS) imaging. CARS allowed the visualisation of PMs within macrophages due to the Raman spectra that could be obtained from the many C-H bonds possessed by the polymer. Although this work successfully showed significant differences in the level of CARS signal detected from untreated cells compared to PM-empty treated cells, one element that could not be ruled out was the visualisation of stress granule formation, as opposed to PMs, as a result of a cell stress response to nanoparticle exposure (Mahboubi and Stochaj, 2017). Future work should include repeating these CARS experiments using deuterated PEO-PCL polymer. This would allow fixation around C-D bonds instead of C-H, which is beneficial as the deuterated C-D bonds are not present in natural structures such as stress granules (Zhang *et al.*, 2019). This would provide results that unambiguously reported label-free PM imaging inside macrophage cells.

Following on from the work performed to assess PM uptake into macrophage cells, the final chapter investigated whether the PM-antibiotic preparations were able to reduce the intracellular bacterial burden of *B. thailandensis* in RAW 264.7 macrophages. RAW 264.7 macrophages are a murine cell line and were chosen to begin with due to being recognised as an appropriate model for macrophages, and their ease of culture, with stability being shown up until passage numbers as high as 30 (Taciak *et al.*, 2018). However, there are limitations to using a murine cell line as the model for infection rather than, for example, primary human macrophage cells. One paper compared the cytokine response of RAW 264.7 macrophages and human leukocytes to shark cartilage. The results revealed that there were significant differences in the level of TNF α produced by the cells, and furthermore that the primary human leukocytes upregulated IL-1 β production whilst the RAW 264.7 cells showed no such response (Merly and Smith, 2017). Although little has been reported in the literature as to whether differences exist between RAWs and primary human macrophages in terms of rate and efficiency of phagocytosis, if there are known differences in their immune responses it would be more ideal to use primary human cells

in any future assays. This would also make the work more translatable and give a better basis for progressing onto potential mouse model studies.

A similar direction for future work should be the use of the end goal pathogen, *B. pseudomallei*, as opposed to the model organism initially used, *B. thailandensis*. Although *B. thailandensis* is not a recognised human pathogen, the two species share 85% of their genetic information, are found in similar environments, and have very similar intracellular survival mechanisms (Majerczyk *et al.*, 2014). Due to the success of the work presented within this PhD, the next natural step would be to confirm that the same results are observed using RAW 264.7 macrophages infected with *B. pseudomallei*. As mentioned previously, primary human macrophages infected with *B. pseudomallei* would follow.

The final body of work within the project began to investigate the screening of different antibiotics, currently with poor bioavailability, for their incorporation into PMs and delivery to intracellular *B. thailandensis*. The aim of this project was to encapsulate antibiotics that could be used to treat intracellular infections, and whilst this was achieved the results could be advanced through choice of antibiotics encapsulated. As already discussed, certain classes of antibiotics such as the aminoglycosides and β -lactams are very poor at penetrating into an intracellular niche (McOrist, 2000). This therefore reduces the number of antibiotics available to treat such infections. Although there are many benefits to encapsulating any antibiotic, the benefits to encapsulating and delivering an aminoglycoside or β -lactam would be enormous, as it essentially repurposes an antibiotic which could otherwise not have been used for intracellular treatment. Rather than creating and discovering new antibiotics, packaging in nanoparticles is a method of making pre-existing antibiotics work more effectively, and increases the number available for use.

This project began to investigate the loading of some of the antibiotics from within these two classes, however due to time constraints and the onset of COVID-19, experimental time fell short. Some promising results were seen with one antibiotic tested, sisomicin, where a significant reduction in intracellular bacterial burden was seen compared to the control. However, this assay should be repeated with relevant controls to ensure free, unencapsulated sisomicin was definitely unable to penetrate cells and that the PMs were showing genuine improvement of antibiotic efficacy. Future work should also include expanding on these assays to test a wider range of antibiotics currently possessing poor intracellular bioavailability. The benefit these results could make to the project and to the application of PMs for antibiotic delivery are substantial.

Although it has already been stated that these PMs have huge potential for clinical translatability, there would need to be a large body of work performed in order to progress the PM-antibiotic formulations to the point of clinical use. As already mentioned, the assays conducted within this project would need to be advanced onto testing against *B. pseudomallei*, and ideally in primary human macrophages. Past this, and animal models would need to be implemented. There is already published literature showing the use of PEO-PCL micelles for drug delivery using mouse models (Ukawala *et al.*, 2012; Kao *et al.*, 2013). Additionally, other unpublished work performed within this research group at the University of Southampton has successfully used PEO-PCL PMs to inject mice with a particular payload. In both examples, the micelles or PMs were injected intravenously into the tail veins of the mice and found to be tolerated with no notable toxic side effects. Although work performed within this project showed that PM-antibiotic formulations were capable of greatly reducing *in vitro* intracellular bacterial burdens, this may change in an *in vivo* environment. Work, potentially using animal models, could be performed to assess how infections representative of a clinical manifestation could be treated using PMs. Before being used within patients it must be known the upper limit to the number of PMs which could be administered before potentially toxic effects occurred. Furthermore, in patients with more advanced infection, higher doses of PM-antibiotic formulations may be required, all of which must be tested as safe.

Another avenue which should be explored before reaching clinical use is the dissemination of PMs within the body, and where they might accumulate. Although macrophages are often the target cells for intracellular infections, other cells within the body will likely be capable of uptake. *In vivo* imaging techniques can be used to visualise the accumulation of fluorescently labelled nanoparticles within the body. One group used PEO-PCL micelles and an *in vivo* imaging system (IVIS) to show that these nanoparticles located primarily to the lungs, spleen and livers of mice after only 1 hour post-injection, and that strong fluorescence was seen in the livers and spleens even after 48 hours (Asem *et al.*, 2016). This work also supports the previously mentioned work from the research group at the University of Southampton, where after injection of PEO-PCL PMs into mice tail veins, PMs were found to strongly localise within the livers and spleens. Although this may not necessarily have long-term side effects on patients, it should be considered how long the PMs may reside within the body before being broken down and excreted. Furthermore, it should be considered how to increase the nanoparticle time spent at the target site, rather than accumulation within off-target organs such as the liver.

6.4 Conclusions

The work within this project is the first example of PEO-PCL PMs being used to successfully encapsulate antibiotics for the treatment of intracellular *B. thailandensis*. The results described in this thesis demonstrate that PMs are able to stably encapsulate the antibiotics doxycycline and rifampicin, that the PMs themselves are capable of being taken up into RAW 264.7 macrophage cells, and that the PM-antibiotic preparations possess enough antibiotic payload to kill residing *B. thailandensis* infections. Overall, the study provides excellent foundations for PMs to be investigated further for their use as viable antibiotic drug delivery vehicles.

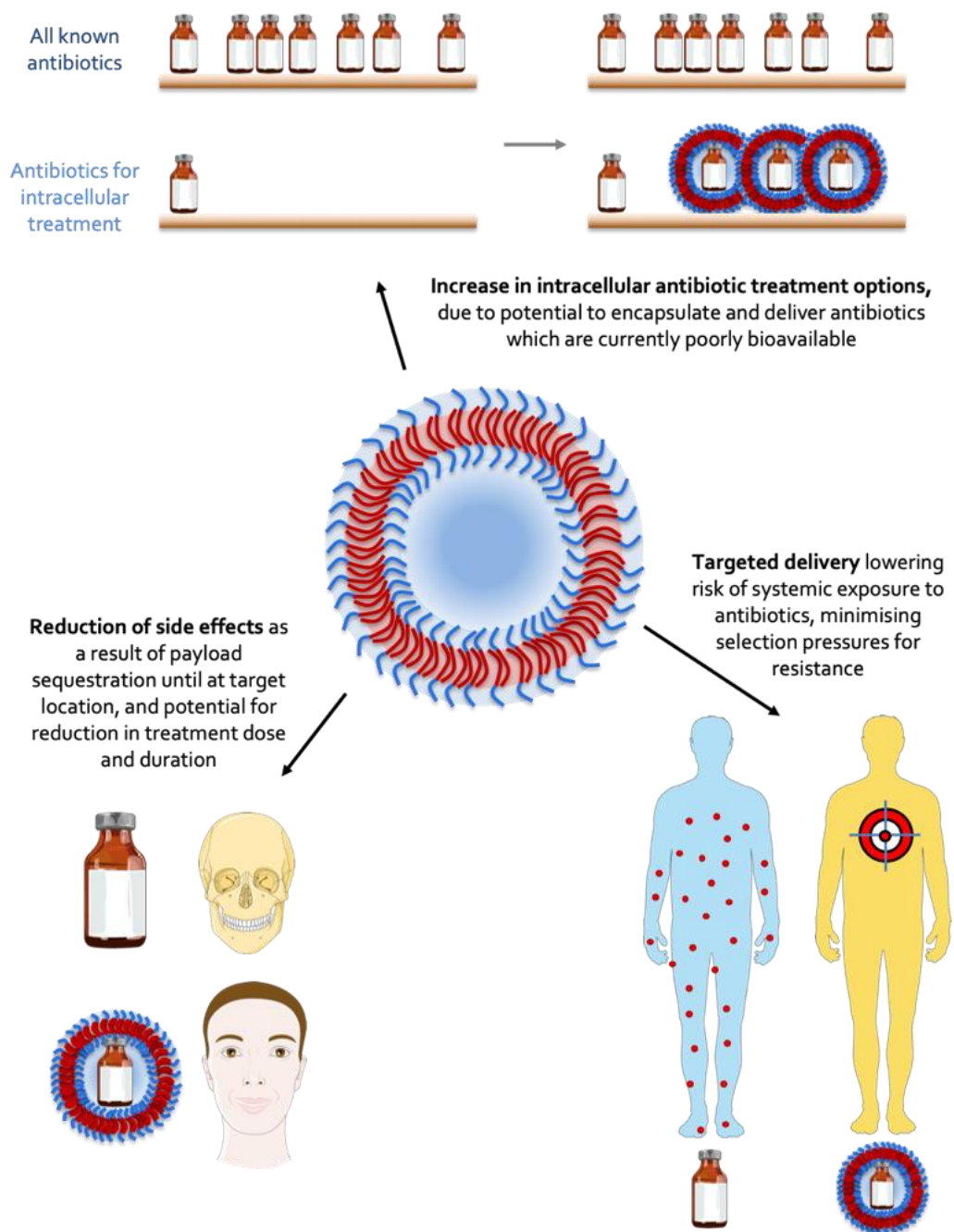


Figure 6.1 – Polymersomes for intracellular antibiotic delivery. An illustration highlighting the potential benefits to antibiotic drug delivery PMs can bring.

List of References

- Abed, N. and Couvreur, P. (2014) 'Nanocarriers for antibiotics: a promising solution to treat intracellular bacterial infections.', *International journal of antimicrobial agents*. Netherlands, 43(6), pp. 485–496.
- Abed, N., Saïd-Hassane, F., Zouhiri, F., Mougin, J., Nicolas, V., Desmaële, D., Gref, R. and Couvreur, P. (2015) 'An efficient system for intracellular delivery of beta-lactam antibiotics to overcome bacterial resistance', *Scientific Reports*. Nature Publishing Group, 5(1), p. 13500.
- Adan, A., Alizada, G., Kiraz, Y., Baran, Y. and Nalbant, A. (2017) 'Flow cytometry: basic principles and applications', *Critical Reviews in Biotechnology*, 37(2), pp. 163–176.
- Aguilar, M.-I. (2004) 'Reversed-phase high-performance liquid chromatography', 251, pp. 9–23.
- Aibani, N., Khan, T. N. and Callan, B. (2020) 'Liposome mimicking polymersomes; A comparative study of the merits of polymersomes in terms of formulation and stability', *International Journal of Pharmaceutics: X*. Elsevier, 2(July 2019), p. 100040.
- Alavi, S. M. and Alavi, L. (2013) 'Treatment of brucellosis: A systematic review of studies in recent twenty years', *Caspian Journal of Internal Medicine*, 4(2), pp. 636–641.
- Alberts, B., Johnson, A., Lewis, J., Raff, M., Roberts, K., and Walter, P. (2002) *Molecular Biology of the Cell*. 4th Edition. New York: Garland Science. Available from: <http://www.ncbi.nlm.nih.gov/books/NBK26884/>
- Alizadeh, H., Salouti, M. and Shapouri, R. (2013) 'Intramacrophage antimicrobial effect of silver nanoparticles against *Brucella melitensis* 16M', *Scientia Iranica*. Elsevier B.V., 20(3), pp. 1035–1038.
- Allen, C., Yu, Y., Maysinger, D. and Eisenberg, A. (1998) 'Polycaprolactone-b-poly(ethylene oxide) block copolymer micelles as a novel drug delivery vehicle for neurotrophic agents FK506 and L-685,818', *Bioconjugate Chemistry*, 9(5), pp. 564–572.
- Allen, H. K., Donato, J., Wang, H. H., Cloud-Hansen, K. A., Davies, J., and Handelsman, J. (2010) 'Call of the wild: Antibiotic resistance genes in natural environments', *Nature Reviews Microbiology*. Nature Publishing Group, 8(4), pp. 251-259.

List of References

- Allen, T. M. and Cullis, P. R. (2013) 'Liposomal drug delivery systems : From concept to clinical applications ☆', *Advanced Drug Delivery Reviews*. Elsevier B.V., 65(1), pp. 36–48.
- Allwood, E. M., Devenish, R. J., Prescott, M., Adler, B. and Boyce, J. D. (2011) 'Strategies for intracellular survival of *Burkholderia pseudomallei*', *Frontiers in Microbiology*, 2(AUG), pp. 1–19.
- Aminov, R. I. (2010) 'A brief history of the antibiotic era: Lessons learned and challenges for the future', *Frontiers in Microbiology*, 1(DEC), pp. 1–7.
- Andrews, J. M. (2001) 'Determination of minimum inhibitory concentrations', *Journal of Antimicrobial Chemotherapy*, 48(suppl_1), pp. 5–16.
- Angelakis, E., Merhej, V. and Raoult, D. (2013) 'Related actions of probiotics and antibiotics on gut microbiota and weight modification', *The Lancet Infectious Diseases*. Elsevier Ltd, 13(10), pp. 889–899.
- Anselmo, A. C. and Mitragotri, S. (2019) 'Nanoparticles in the clinic: An update', *Bioengineering & Translational Medicine*, 4(3), pp. 1–16.
- Apolinário, A. C., Magoń, M. S., Pessoa, A. and Rangel-Yagui, C. de O. (2018) 'Challenges for the self-assembly of poly(Ethylene glycol)-poly(lactic acid) (PEG-PLA) into polymersomes: Beyond the theoretical paradigms', *Nanomaterials*, 8(6).
- Asem, H., Zhao, Y., Ye, F., Barrefelt, Å., Abedi-Valugerdi, M., El-Sayed, R., El-Serafi, I., Abu-Salah, K. M., Hamm, J., Muhammed, M. and Hassan, M. (2016) 'Biodistribution of biodegradable polymeric nano-carriers loaded with busulphan and designed for multimodal imaging', *Journal of Nanobiotechnology*. BioMed Central, 14(1), pp. 1–16.
- Ashida, H., Mimuro, H., Ogawa, M., Kobayashi, T., Sanada, T., Kim, M. and Sasakawa, C. (2011) 'Cell death and infection: A double-edged sword for host and pathogen survival', *Journal of Cell Biology*, 195(6), pp. 931–942.
- Aslam, B., Wang, W., Arshad, M. I., Khurshid, M., Muzammil, S., Rasool, M. H., Nisar, M. A., Alvi, R. F., Aslam, M. A., Qamar, M. U., Salamat, M. K. F. and Baloch, Z. (2018) 'Antibiotic resistance: a rundown of a global crisis', *Infection and Drug Resistance*, 11, pp. 1645–1658.
- Bakker-woudenberg, I. A. J. M. and Lokerse, A. F. (1985) 'Free Versus Liposome-Entrapped Ampicillin in Treatment of Infection Due to *Listeria monocytogenes* in Normal and Atbymic (Nude) Mice', 151(5), pp. 917–924.

- Baquir, B., Lemaire, S., Van Bambeke, F., Tulkens, P. M., Lin, L. and Spellberg, B. (2012) 'Macrophage killing of bacterial and fungal pathogens is not inhibited by intense intracellular accumulation of the lipoglycopeptide antibiotic oritavancin', *Clinical Infectious Diseases*, 54(SUPPL. 3), pp. 229–232.
- Barteneva, N. S., Fasler-Kan, E. and Vorobjev, I. A. (2012) 'Imaging Flow Cytometry: Coping with Heterogeneity in Biological Systems', *Journal of Histochemistry and Cytochemistry*, 60(10), pp. 723–733.
- Bartlett, J. G., Gilbert, D. N. and Spellberg, B. (2013) 'Seven ways to preserve the Miracle of antibiotics', *Clinical Infectious Diseases*, 56(10), pp. 1445–1450.
- Bassetti, M., Vena, A., Croxatto, A., Righi, E. and Guery, B. (2018) 'How to manage *Pseudomonas aeruginosa* infections', *Drugs in Context*, 7, pp. 1–18.
- Beeching, N. J., Dance, D. A. B., Miller, A. R. O. and Spencer, R. C. (2002) 'Biological warfare and bioterrorism', *BMJ*, 324(7333), pp. 336–339.
- Behzadi, S., Serpooshan, V., Tao, W., Hamaly, M. A., Alkawareek, M. Y., Dreaden, E. C., Brown, D., Alkilany, A. M., Farokhzad, O. C. and Mahmoudi, M. (2017) 'Cellular uptake of nanoparticles: Journey inside the cell', *Chemical Society Reviews*. Royal Society of Chemistry, 46(14), pp. 4218–4244.
- Benitez, J. A. and Silva, A. J. (2016) 'Vibrio cholerae hemagglutinin(HA)/protease: An extracellular metalloprotease with multiple pathogenic activities', *Toxicon*. Elsevier Ltd, 115, pp. 55–62.
- Bhavsar, A. P., Guttman, J. a and Finlay, B. B. (2007) 'Manipulation of host-cell pathways by bacterial pathogens.', *Nature*, 449(7164), pp. 827–834.
- Binkley, C. E., Cinti, S., Simeone, D. M. and Colletti, L. M. (2002) 'Bacillus anthracis as an agent of bioterrorism: a review emphasizing surgical treatment.', *Annals of surgery*, 236(1), pp. 9–16.
- Bixner, O., Kurzhals, S., Virk, M. and Reimhult, E. (2016) 'Triggered release from thermoresponsive polymersomes with superparamagnetic membranes', *Materials*, 9(1), pp. 1–14.
- Blair, J. M. A., Webber, M. A., Baylay, A. J., Ogbolu, D. O., & Piddock, L. J. V. (2014) 'Molecular mechanisms of antibiotic resistance.', *Nature Reviews Microbiology*. Nature Publishing Group, 13(1), pp. 42–51.

List of References

Blanazs, A., Armes, S. P. and Ryan, A. J. (2009) 'Self-assembled block copolymer aggregates: From micelles to vesicles and their biological applications', *Macromolecular Rapid Communications*, 30(4–5), pp. 267–277.

Blanchaert, B., Huang, S., Wach, K., Adams, E. and Van Schepdael, A. (2017) 'Assay development for aminoglycosides by HPLC with direct UV detection', *Journal of Chromatographic Science*, 55(3), pp. 197–204.

Bleul, R., Thiermann, R. and Maskos, M. (2015) 'Techniques To Control Polymersome Size', *Macromolecules*. American Chemical Society, 48(20), pp. 7396–7409.

Bodaghabadi, N., Hajigholami, S., Malekshahi, Z. V., Entezari, M., Najafi, F., Shirzad, H. and Sadeghizadeh, M. (2018) 'Preparation and evaluation of rifampicin and co-trimoxazole-loaded nanocarrier against *Brucella melitensis* infection', *Iranian Biomedical Journal*, 22(4), pp. 275–282.

Bolotin, E. M., Cohen, R., Bar, L. K., Emanuel, N., Ninio, S., Barenholz, Y. and Lasic, D. D. (1994) 'Ammonium sulfate gradients for efficient and stable remote loading of amphipathic weak bases into liposomes and ligandoliposomes', *Journal of Liposome Research*, 4(1), pp. 455–479.

Bonifacio, E., Warncke, K., Winkler, C., Wallner, M. and Ziegler, A. G. (2011) 'Cesarean section and interferon-induced helicase gene polymorphisms combine to increase childhood type 1 diabetes risk', *Diabetes*, 60(12), pp. 3300–3306.

Brown, L., Wolf, J. M., Prados-Rosales, R., and Casadevall, A. (2015) 'Through the wall: extracellular vesicles in Gram-positive bacteria, mycobacteria and fungi', *Nature Reviews Microbiology*, Nature Publishing Group, 13(10), pp. 620-630.

Brown-Elliott, B. A., Iakhiaeva, E., Griffith, D. E., Woods, G. L., Stout, J. E., Wolfe, C. R., Turenne, C. Y. and Wallace, R. J. (2013) 'In vitro activity of amikacin against isolates of mycobacterium avium complex with proposed MIC breakpoints and finding of a 16S rRNA gene mutation in treated isolates', *Journal of Clinical Microbiology*, 51(10), pp. 3389–3394.

Bygd, H. C., Forsmark, K. D. and Bratlie, K. M. (2015) 'Altering in vivo macrophage responses with modified polymer properties', *Biomaterials*, 56, pp. 187–197.

Cai, K., He, X., Song, Z., Yin, Q., Zhang, Y., Uckun, F. M., Jiang, C. and Cheng, J. (2015) 'Dimeric Drug Polymeric Nanoparticles with Exceptionally High Drug Loading and Quantitative Loading Efficiency', *Journal of the American Chemical Society*, 137(10), pp. 3458–3461.

- Campbell, E. a. E. A., Korzheva, N., Mustaev, A., Murakami, K., Nair, S., Goldfarb, A. and Darst, S. A. S. a. (2001) 'Structural mechanism for rifampicin inhibition of bacterial rna polymerase.', *Cell*, 104(6), pp. 901–12.
- Caño-muñiz, S., Anthony, R., Niemann, S. and Alffenaar, J. C. (2018) 'New Approaches and Therapeutic Options for Mycobacterium', *Clinical microbiology reviews*, 31(1), pp. 1–13.
- Carlsson, F. and Brown, E. J. (2006) 'Actin-based motility of intracellular bacteria, and polarized surface distribution of the bacterial effector molecules', *Journal of Cellular Physiology*.
- Cash, H. L. and Hooper, L. V. (2005) 'Commensal bacteria shape intestinal immune system development', *ASM news*, 71(2), pp. 77–83.
- Caspar, Y. and Maurin, M. (2017) 'Francisella tularensis susceptibility to antibiotics: A comprehensive review of the data obtained In vitro and in animal models', *Frontiers in Cellular and Infection Microbiology*, 7(APR).
- Celli, J. and Zahrt, T. C. (2013) 'Mechanisms of Francisella tularensis intracellular pathogenesis.', *Cold Spring Harbor perspectives in medicine*, 3(4), pp. 1–14.
- Chaudhari, K. and Pradeep, T. (2015) 'In vitro colocalization of plasmonic nano-biolabels and biomolecules using plasmonic and Raman scattering microspectroscopy', *Journal of Biomedical Optics*, 20(04), p. 1.
- Chen, C. Y.-S. and Swenson, C. A. (1969) 'Ultraviolet absorption spectra of lactams', *The Journal of Physical Chemistry*. American Chemical Society, 73(6), pp. 1642–1647.
- Cheng, A. and Currie, B. (2005) 'Meloidosis: epidemiology, pathophysiology, and management', *Clinical microbiology reviews*, 18(2), pp. 383–416.
- Chetchotisakd, P., Chierakul, W., Chaowagul, W., Anunnatsiri, S., Phimda, K., Mootsikapun, P., Chaisuksant, S., Pilaikul, J., Thinkhamrop, B., Phiphitaporn, S., Susaengrat, W., Toondee, C., Wongrattanacheewin, S., Wuthiekanun, V., Chantratita, N., Thaipadungpanit, J., Day, N. P., Limmathurotsakul, D. and Peacock, S. J. (2014) 'Trimethoprim-sulfamethoxazole versus trimethoprim-sulfamethoxazole plus doxycycline as oral eradication treatment for melioidosis (MERTH): A multicentre, double-blind, non-inferiority, randomised controlled trial', *The Lancet*. Chetchotisakd et al. Open Access article distributed under the terms of CC BY, 383(9919), pp. 807–814.

List of References

Chiang, S. S. and Starke, J. R. (2018) *Mycobacterium tuberculosis*. Fifth Edit, *Principles and Practice of Pediatric Infectious Diseases*. Fifth Edit. Elsevier Inc.

Chiaraviglio, L. and Kirby, J. E. (2015) 'High-throughput intracellular antimicrobial susceptibility testing of *Legionella pneumophila*', *Antimicrobial Agents and Chemotherapy*, 59(12), pp. 7517–7529.

Choucair, A., Soo, P. L. and Eisenberg, A. (2005) 'Active loading and tunable release of doxorubicin from block copolymer vesicles', *Langmuir*, 21(20), pp. 9308–9313.

Christian, M. D. (2013) 'Biowarfare and Bioterrorism', *Critical Care Clinics*. Elsevier Inc, 29(3), pp. 717–756.

Clancy, J. P., Dupont, L., Konstan, M. W., Billings, J., Fustik, S., Goss, C. H., Lymp, J., Minic, P., Quittner, A. L., Rubenstein, R. C., Young, K. R., Saiman, L., Burns, J. L., Govan, J. R. W., Ramsey, B. and Gupta, R. (2013) 'Phase II studies of nebulised Arikace in CF patients with *Pseudomonas aeruginosa* infection.', *Thorax*, 68(9), pp. 818–25.

'Community-associated methicillin-resistant *Staphylococcus aureus* infection among healthy newborns--Chicago and Los Angeles County, 2004.' (2006) *MMWR. Morbidity and mortality weekly report*. United States, 55(12), pp. 329–332.

Cruz, M. E. M., Gaspar, M. M., Martins, M. B. F. and Corvo, M. L. (2005) 'Liposomal superoxide dismutases and their use in the treatment of experimental arthritis', *Methods in Enzymology*, 391(SPEC. ISS.), pp. 395-413.

da Cunha, B. R., Fonseca, L. P. and Calado, C. R. C. (2019) 'Antibiotic discovery: Where have we come from, where do we go?', *Antibiotics*, 8(2).

Currie, B. J., Fisher, D. A., Howard, D. M., Burrow, J. N. C., Selvanayagam, S., Snelling, P. L., Anstey, N. M. and Mayo, M. J. (2000) 'The epidemiology of melioidosis in Australia and Papua New Guinea', *Acta Tropica*, 74(2–3), pp. 121–127.

Currie, B. J., Ward, L. and Cheng, A. C. (2010) 'The epidemiology and clinical spectrum of melioidosis: 540 cases from the 20 year darwin prospective study', *PLoS Neglected Tropical Diseases*, 4(11).

Damgé, C., Vranckx, H., Balschmidt, P. and Couvreur, P. (1997) 'Poly(alkyl cyanoacrylate) nanospheres for oral administration of insulin', *Journal of Pharmaceutical Sciences*, 86(12), pp. 1403–1409.

- Danafar, H., Rostamizadeh, K., Davaran, S. and Hamidi, M. (2014) 'PLA-PEG-PLA copolymer-based polymersomes as nanocarriers for delivery of hydrophilic and hydrophobic drugs: Preparation and evaluation with atorvastatin and lisinopril', *Drug Development and Industrial Pharmacy*, 40(10), pp. 1411–1420.
- Dance, D. (2014) 'Treatment and prophylaxis of melioidosis', *International Journal of Antimicrobial Agents*. Elsevier B.V., 43(4), pp. 310–318.
- Danhier, P., Krishnamachary, B., Bharti, S., Kakkad, S., Mironchik, Y. and Bhujwala, Z. M. (2015) 'Combining Optical Reporter Proteins with Different Half-lives to Detect Temporal Evolution of Hypoxia and Reoxygenation in Tumors', *Neoplasia*. Nencki Institute of Experimental Biology, Polish Academy of Sciences, 17(12), pp. 871–881.
- Darbeau, R. (2006) 'Nuclear magnetic resonance (NMR) spectroscopy: A review and a look at its use as a probative tool in deamination chemistry', *Applied Spectroscopy Reviews*, 41(4), pp. 401–425.
- Dassonville-Klimpt, A. and Sonnet, P. (2020) 'Advances in 'Trojan horse' strategies in antibiotic delivery systems', *Future medicinal chemistry*, 12(11), pp. 983–986.
- Davies, J. and Davies, D. (2010) 'Origins and Evolution of Antibiotic Resistance', *Microbiol. Mol. Biol. Rev.*, 74(3), pp. 417–433.
- Dayeh, V. R., Chow, S. L., Schirmer, K., Lynn, D. H. and Bols, N. C. (2004) 'Evaluating the toxicity of Triton X-100 to protozoan, fish, and mammalian cells using fluorescent dyes as indicators of cell viability', *Ecotoxicology and Environmental Safety*, 57(3), pp. 375–382.
- Dehaini, D., Fang, R. H. and Zhang, L. (2016) 'Biomimetic strategies for targeted nanoparticle delivery', (February), pp. 30–46.
- Dennis, D. T., Inglesby, T. V., Henderson, D. a, Bartlett, J. G., Ascher, M. S., Eitzen, E., Fine, a D., Friedlander, a M., Hauer, J., Layton, M., Lillibridge, S. R., McDade, J. E., Osterholm, M. T., O'Toole, T., Parker, G., Perl, T. M., Russell, P. K. and Tonat, K. (2001) 'Tularemia as a biological weapon: medical and public health management.', *JAMA : the journal of the American Medical Association*, 285(21), pp. 2763–2773.
- Derbali, R. M., Aoun, V., Moussa, G., Frei, G., Tehrani, S. F., Del'Orto, J. C., Hildgen, P., Roullin, V. G. and Chain, J. L. (2019) 'Tailored Nanocarriers for the Pulmonary Delivery of Levofloxacin against *Pseudomonas aeruginosa*: A Comparative Study', *Molecular Pharmaceutics*, 16(5), pp. 1906–1916.

List of References

Dethlefsen, L. and Relman, D. A. (2011) 'Incomplete recovery and individualized responses of the human distal gut microbiota to repeated antibiotic perturbation.', *Proceedings of the National Academy of Sciences of the United States of America*, (Suppl 1), pp. 4554–61.

Dickson, J. S. and Koohmaraie, M. (1989) 'Cell Surface Charge Characteristics and Their Relationship to Bacterial Attachment to Meat Surfaces', pp. 832–836.

Discher, B. M., Won, Y.-Y., Ege, D. S., Lee, J. C.-M., Bates, F. S., Discher, D. E. and Hammer, D. A. (1999) 'Polymersomes: Tough Vesicles Made from Diblock Copolymers', *Science*, 284(5417), pp. 1143 LP – 1146.

Du, J., Tang, Y., Lewis, A. L. and Armes, S. P. (2005) 'pH-Sensitive Vesicles Based on a Biocompatible Zwitterionic Diblock Copolymer', pp. 17982–17983.

Dutta, D. and Donaldson, J. G. (2012) 'Search for inhibitors of endocytosis', *Cellular Logistics*, 2(4), pp. 203–208.

Egli, S., Nussbaumer, M. G., Balasubramanian, V., Chami, M., Bruns, N., Palivan, C. and Meier, W. (2011) 'Biocompatible Functionalization of Polymersome Surfaces : A New Approach to Surface Immobilization and Cell Targeting Using Polymersomes', pp. 4476–4483.

Eloy, J. O., Petrilli, R., Topan, J. F., Antonio, H. M. R., Barcellos, J. P. A., Chesca, D. L., Serafini, L. N., Tiezzi, D. G., Lee, R. J. and Marchetti, J. M. (2016) 'Co-loaded paclitaxel/rapamycin liposomes: Development, characterization and in vitro and in vivo evaluation for breast cancer therapy', *Colloids and Surfaces B: Biointerfaces*. Elsevier B.V., 141, pp. 74–82.

Ember, K. J. I., Hoeve, M. A., McAughtrie, S. L., Bergholt, M. S., Dwyer, B. J., Stevens, M. M., Faulds, K., Forbes, S. J. and Campbell, C. J. (2017) 'Raman spectroscopy and regenerative medicine: a review', *npj Regenerative Medicine*. Springer US, 2(1).

Emery, W. and Camps, A. (2017) *Basic Electromagnetic Concepts and Applications to Optical Sensors, Introduction to Satellite Remote Sensing*.

Ensign, L. M., Cone, R. and Hanes, J. (2012) 'Oral drug delivery with polymeric nanoparticles: The gastrointestinal mucus barriers', *Advanced Drug Delivery Reviews*. Elsevier B.V., 64(6), pp. 557–570.

Ernst, R. K., Guina, T. and Miller, S. I. (1999) 'How Intracellular Bacteria Survive: Surface Modifications That Promote Resistance to Host Innate Immune Responses', *The Journal of Infectious Diseases*, 179(s2), pp. S326–S330.

- Fan, X., Zheng, W. and Singh, D. J. (2014) 'Light scattering and surface plasmons on small spherical particles', *Light: Science and Applications*, 3(March), pp. 1–14.
- Fatima, M. T., Islam, Z., Ahmad, E., Barreto, G. E. and Md Ashraf, G. (2018) 'Ionic gradient liposomes: Recent advances in the stable entrapment and prolonged released of local anesthetics and anticancer drugs', *Biomedicine and Pharmacotherapy*. Elsevier, 107(April), pp. 34–43.
- Fenaroli, F., Robertson, J. D., Scarpa, E., Gouveia, V. M., Di Guglielmo, C., De Pace, C., Elks, P. M., Poma, A., Evangelopoulos, D., Canseco, J. O., Prajsnar, T. K., Marriott, H. M., Dockrell, D. H., Foster, S. J., McHugh, T. D., Renshaw, S. A., Martí, J. S., Battaglia, G. and Rizzello, L. (2020) 'Polymersomes Eradicating Intracellular Bacteria', *ACS Nano*.
- Fierer, J., Hatlen, L., Lin, J. P., Estrella, D., Mihalko, P. and Yau-Young, A. (1990) 'Successful treatment using gentamicin liposomes of Salmonella dublin infections in mice', *Antimicrobial Agents and Chemotherapy*, 34(2), pp. 343–348.
- Flynn, J. L. and Chan, J. (2001) 'Tuberculosis : Latency and Reactivation MINIREVIEW Tuberculosis : Latency and Reactivation Downloaded from <http://iai.asm.org/> on April 8 , 2013 by UNIVERSITY OF PENNSYLVANIA LIBRARY', 69(7), pp. 4195–4201.
- Foroozandeh, P. and Aziz, A. A. (2018) 'Insight into Cellular Uptake and Intracellular Trafficking of Nanoparticles', *Nanoscale Research Letters*. Nanoscale Research Letters, 13.
- Fossum, S., Crooke, E. and Skarstad, K. (2007) 'Organization of sister origins and replisomes during multifork DNA replication in Escherichia coli', *The EMBO Journal*, 26(21), pp. 4514–4522.
- Francino, M. P. (2016) 'Antibiotics and the human gut microbiome: Dysbioses and accumulation of resistances', *Frontiers in Microbiology*, 6(JAN), pp. 1–11.
- Fujiwara, N., Yumoto, H., Miyamoto, K., Hirota, K., Nakae, H., Tanaka, S., Murakami, K., Kudo, Y., Ozaki, K. and Miyake, Y. (2019) '2-Methacryloyloxyethyl phosphorylcholine (MPC)-polymer suppresses an increase of oral bacteria: a single-blind, crossover clinical trial', *Clinical Oral Investigations*. Clinical Oral Investigations, 23(2), pp. 739–746.
- Galm, U., Dessoy, M. A., Schmidt, J., Wessjohann, L. A. and Heide, L. (2004) 'In vitro and in vivo production of new aminocoumarins by a combined biochemical, genetic, and synthetic approach', *Chemistry & Biology*, 11(2), pp. 173–183.

List of References

- Gandhi, A., Paul, A., Sen, S. O. and Sen, K. K. (2015) 'Studies on thermoresponsive polymers : Phase behaviour , drug delivery and biomedical applications', *Asian Journal of Pharmaceutical Sciences*. Elsevier Ltd, 10(2), pp. 99–107.
- Gannon, C. J., Patra, C. R., Bhattacharya, R., Mukherjee, P. and Curley, S. A. (2008) 'Intracellular gold nanoparticles enhance non-invasive radiofrequency thermal destruction of human gastrointestinal cancer cells', *Journal of Nanobiotechnology*, 6, pp. 1–9.
- Gao, W., Thamphiwatana, S., Angsantikul, P. and Zhang, L. (2014) 'Nanoparticle approaches against bacterial infections', *Wiley Interdisciplinary Reviews: Nanomedicine and Nanobiotechnology*.
- Garrett, N. L., Godfrey, L., Lalatsa, A., Serrano, D. R., Uchegbu, I. F., Schatzlein, A. and Moger, J. (2015) 'Detecting polymeric nanoparticles with coherent anti-stokes Raman scattering microscopy in tissues exhibiting fixative-induced autofluorescence', *Multiphoton Microscopy in the Biomedical Sciences XV*, 9329(0), p. 932922.
- George, T. C., Basiji, D. A., Hall, B. E., Lynch, D. H., Ortyu, W. E., Perry, D. J., Seo, M. J., Zimmerman, C. A. and Morrissey, P. J. (2004) 'Distinguishing modes of cell death using the ImageStream® multispectral imaging flow cytometer', *Cytometry Part A*, 59(2), pp. 237–245.
- Gilad, J., Harary, I., Dushnitsky, T., Schwartz, D. and Amsalem, Y. (2007) 'Burkholderia mallei and Burkholderia pseudomallei as bioterrorism agents: National aspects of emergency preparedness', *Israel Medical Association Journal*, 9(7), pp. 499–503.
- Gilad, J., Schwartz, D. and Amsalem, Y. (2007) 'Clinical features and laboratory diagnosis of infection with the potential bioterrorism agents burkholderia mallei and burkholderia pseudomallei.', *International journal of biomedical science : IJBS*, 3(3), pp. 144–52.
- Ginsberg, A. M. and Spigelman, M. (2007) 'Challenges in tuberculosis drug research and development.', *Nature medicine*, 13(3), pp. 290–294.
- Goldberg, M. B. (2001) 'Actin-Based Motility of Intracellular Microbial Pathogens Actin-Based Motility of Intracellular Microbial Pathogens', *Microbiology and Molecular Biology Reviews*, 65(4), pp. 595–626.
- Gref, R., Minamitake, Y., Peracchia, M. T., Trubetskoy, V., Torchilin, V. and Langer, R. (1994) 'Biodegradable long-circulating polymeric nanospheres', *Science*, 263(5153), pp. 1600–1603.

- Griffith, D. E., Eagle, G., Thomson, R., Aksamit, T. R., Hasegawa, N., Morimoto, K., Addrizzo-Harris, D. J., O'Donnell, A. E., Marras, T. K., Flume, P. A., Loebinger, M. R., Morgan, L., Codecasa, L. R., Hill, A. T., Ruoss, S. J., Yim, J. J., Ringshausen, F. C., Field, S. K., Philley, J. V., Wallace, R. J., Van Ingen, J., Coulter, C., Nezamis, J. and Winthrop, K. L. (2018) 'Amikacin liposome inhalation suspension for treatment-refractory lung disease caused by Mycobacterium avium complex (CONVERT) a prospective, open-label, randomized study', *American Journal of Respiratory and Critical Care Medicine*, 198(12), pp. 1559–1569.
- Gruenberg, J. (2001) 'The endocytic pathway: A mosaic of domains', *Nature Reviews Molecular Cell Biology*, 2(10), pp. 721–730.
- Gupta, S., Cohen, K. A., Winglee, K., Maiga, M., Diarra, B. and Bishai, W. R. (2014) 'Efflux inhibition with verapamil potentiates bedaquiline in mycobacterium tuberculosis', *Antimicrobial Agents and Chemotherapy*, 58(1), pp. 574–576.
- Gustafson, H. H., Holt-Casper, D., Grainger, D. W. and Ghandehari, H. (2015) 'Nanoparticle Uptake: The Phagocyte Problem Graphical Abstract HHS Public Access', *Nano Today*, 10(4), pp. 487–510.
- Hassounah, I. A., Shehata, N. A., Kimsawatde, G. C., Hudson, A. G., Sriranganathan, N., Joseph, E. G. and Mahajan, R. L. (2016) *Designing and testing single tablet for tuberculosis treatment through electrospinning, Fabrication and Self-Assembly of Nanobiomaterials: Applications of Nanobiomaterials*. Elsevier Inc.
- Heemskerk, D., Caws, M., Marais, B. and Farrar, J. (2015) *Tuberculosis in Adults and Children*.
- Hendon-Dunn, C. L., Thomas, S. R., Taylor, S. C. and Bacon, J. (2018) 'A Flow Cytometry Method for Assessing M. tuberculosis Responses to Antibiotics', in Gillespie, S. H. (ed.) *Antibiotic Resistance Protocols*. New York, NY: Springer New York, pp. 51–57.
- Hinterwirth, H., Wiedmer, S. K., Moilanen, M., Lehner, A., Allmaier, G., Waitz, T., Lindner, W. and Lämmerhofer, M. (2013) 'Comparative method evaluation for size and size-distribution analysis of gold nanoparticles', *Journal of Separation Science*, 36(17), pp. 2952–2961.
- Hirota, K. and Ter, H. (2012) 'Endocytosis of Particle Formulations by Macrophages and Its Application to Clinical Treatment', *Molecular Regulation of Endocytosis*.
- Hu, Y. B., Dammer, E. B., Ren, R. J. and Wang, G. (2015) 'The endosomal-lysosomal system: From acidification and cargo sorting to neurodegeneration', *Translational Neurodegeneration*. *Translational Neurodegeneration*, 4(1), pp. 1–10.

List of References

Huang, W., Tsui, C. P., Tang, C. Y. and Gu, L. (2018) 'Effects of Compositional Tailoring on Drug Delivery Behaviours of Silica Xerogel/Polymer Core-shell Composite Nanoparticles', *Scientific Reports*. Springer US, 8(1), pp. 1–13.

Hume, D. A. (2015) 'The many alternative faces of macrophage activation', *Frontiers in Immunology*, 6(JUL), pp. 1–10.

Huotari, J. and Helenius, A. (2011) 'Endosome maturation', *EMBO Journal*. Nature Publishing Group, 30(17), pp. 3481–3500.

Hussain, S., Joo, J., Kang, J., Kim, B., Braun, G. B., She, Z., Kim, D., Mann, A. P., Mölder, T., Teesalu, T., Carnazza, S., Guglielmino, S., Sailor, M. J. and Ruoslahti, E. (2018) 'HHS Public Access', 2(2), pp. 95–103.

Imbuluzqueta, E., Gamazo, C., Lana, H., Campanero, M. Á., Salas, D., Gil, A. G., Elizondo, E., Ventosa, N., Veciana, J. and Blanco-Prieto, M. J. (2013) 'Hydrophobic gentamicin-loaded nanoparticles are effective against *Brucella melitensis* infection in mice', *Antimicrobial Agents and Chemotherapy*, 57(7), pp. 3326–3333.

Jacobs, R. F. and Wilson, C. B. (1983) 'Intracellular penetration and antimicrobial activity of antibiotics.', *The Journal of antimicrobial chemotherapy*. England, 12 Suppl C, pp. 13–20.

Jamalzadeh, L., Ghafoori, H., Sariri, R., Rabuti, H., Nasirzade, J., Hasani, H. and Aghamaali, M. R. (2016) 'Cytotoxic Effects of Some Common Organic Solvents on MCF-7, RAW-264.7 and Human Umbilical Vein Endothelial Cells', *Avicenna Journal of Medical Biochemistry*. Hamadan University of Medical Sciences, In press(In press), pp. 10–33453.

Janeway, C. A., Travers, P., Walport, M., and Shlomchik, M. J. (2001) *Immunobiology: The Immune System in Health and Disease*. 5th Edition. New York: Garland Science. Available from: <https://ncbi.nlm.nih.gov/books/NBK27090/>

Jantratid, E., Strauch, S., Becker, C., Dressman, J. B., Amidon, G. L., Junginger, H. E., Kopp, S., Midha, K. K., Shah, V. P., Stavchansky, S. and Barends, D. M. (2010) 'Biowaiver monographs for immediate release solid oral dosage forms: Doxycycline hyclate.', *Journal of pharmaceutical sciences*. United States, 99(4), pp. 1639–1653.

Jara, L. M., Pérez-Varela, M., Corral, J., Arch, M., Cortés, P., Bou, G., Aranda, J. and Barbé, J. (2016) 'Novobiocin inhibits the antimicrobial resistance acquired through DNA damage-induced mutagenesis in *Acinetobacter baumannii*', *Antimicrobial Agents and Chemotherapy*, 60(1), pp. 637–639.

- Johnston, A. H., Dalton, P.D., Newman, T. A. (2010) 'Polymersomes , smaller than you think : ferrocene as a TEM probe to determine core structure', *Journal of Nanoparticle Research*, 12(6), pp. 1997–2001.
- Jones, R. R., Hooper, D. C., Zhang, L., Wolverson, D. and Valev, V. K. (2019) 'Raman Techniques: Fundamentals and Frontiers', *Nanoscale Research Letters*. *Nanoscale Research Letters*, 14(1).
- De Jong, W. H. and Borm, P. J. a (2008) 'Drug delivery and nanoparticles:applications and hazards.', *International journal of nanomedicine*, 3(2), pp. 133–149.
- Judy, B. M., Whitlock, G. C., Torres, A. G. and Estes, D. M. (2009) 'Comparison of the in vitro and in vivo susceptibilities of *Burkholderia mallei* to Ceftazidime and Levofloxacin', *BMC Microbiology*, 9, pp. 1–7.
- Kalhapure, R. S., Bolla, P. K., Boddu, S. H. and Renukuntla, J. (2019) 'Evaluation of Oleic Acid and Polyethylene Glycol Monomethyl Ether Conjugate (PEGylated Oleic Acid) as a Solubility Enhancer of Furosemide', *Processes*, 7(8), p. 520.
- Kalluru, R., Fenaroli, F., Westmoreland, D., Ulanova, L., Maleki, A., Roos, N., Madsen, M. P., Koster, G., Egge-Jacobsen, W., Wilson, S., Roberg-Larsen, H., Khuller, G. K., Singh, A., Nyström, B. and Griffiths, G. (2013) 'Poly(lactide-co-glycolide)-rifampicin nanoparticles efficiently clear *Mycobacterium bovis* BCG infection in macrophages and remain membrane-bound in phago-lysosomes', *Journal of Cell Science*, 126(14), pp. 3043–3054.
- Kao, H. W., Chan, C. J., Chang, Y. C., Hsu, Y. H., Lu, M., Shian-Jy Wang, J., Lin, Y. Y., Wang, S. J. and Wang, H. E. (2013) 'A pharmacokinetics study of radiolabeled micelles of a poly(ethylene glycol)-block-poly(caprolactone) copolymer in a colon carcinoma-bearing mouse model', *Applied Radiation and Isotopes*. Elsevier, 80, pp. 88–94.
- Kim, A., Ng, W. B., Bernt, W. and Cho, N. J. (2019) 'Validation of Size Estimation of Nanoparticle Tracking Analysis on Polydisperse Macromolecule Assembly', *Scientific Reports*. Springer US, 9(1), pp. 1–14.
- Kitsera, N., Khobta, A. and Epe, B. (2007) 'Destabilized green fluorescent protein detects rapid removal of transcription blocks after genotoxic exposure', *BioTechniques*, 43(2), pp. 222–227.
- Klustersky, J., Carpentier-Meunier, F., Kahan-Coppens, L. and Thys, J. P. (1979) 'Endotracheally administered antibiotics for gram-negative bronchopneumonia', *Chest*, 75(5), pp. 586–591.

List of References

- Kohanski, M. A., Dwyer, D. J. and Collins, J. J. (2010) 'How antibiotics kill bacteria: from targets to networks.', *Nature reviews. Microbiology*, 8(6), pp. 423–35.
- Kovacs-Simon, A., Hemsley, C. M., Scott, A. E., Prior, J. L. and Titball, R. W. (2019) 'Burkholderia thailandensis strain E555 is a surrogate for the investigation of Burkholderia pseudomallei replication and survival in macrophages', *BMC Microbiology*. *BMC Microbiology*, 19(1), pp. 1–16.
- Kuhn, D. A., Vanhecke, D., Michen, B., Blank, F., Gehr, P., Petri-Fink, A. and Rothen-Rutishauser, B. (2014) 'Different endocytotic uptake mechanisms for nanoparticles in epithelial cells and macrophages', *Beilstein Journal of Nanotechnology*, 5(1), pp. 1625–1636.
- Kumamoto, Y., Harada, Y., Takamatsu, T. and Tanaka, H. (2018) 'Label-free molecular imaging and analysis by Raman spectroscopy', *Acta Histochemica et Cytochemica*, 51(3), pp. 101–110.
- Ladavière, C. and Gref, R. (2015) 'Toward an Optimized Treatment of Intracellular Bacterial Infections: Input of Nanoparticulate Drug Delivery Systems', *Nanomedicine*, 10(19), pp. 3033–3055.
- Lane, D. D., Su, F. Y., Chiu, D. Y., Srinivasan, S., Wilson, J. T., Ratner, D. M., Stayton, P. S. and Convertine, A. J. (2015) 'Dynamic intracellular delivery of antibiotics via pH-responsive polymersomes', *Polymer Chemistry*, Royal Society of Chemistry, 6(8), pp. 1255–1266.
- Langdon, A., Crook, N. and Dantas, G. (2016) 'The effects of antibiotics on the microbiome throughout development and alternative approaches for therapeutic modulation.', *Genome medicine*. *Genome Medicine*, 8(1), p. 39.
- Larsen, J. C. and Johnson, N. H. (2009) 'Pathogenesis of Burkholderia pseudomallei and Burkholderia mallei.', *Military medicine*. England, 174(6), pp. 647–651.
- Larson, N. and Ghandehari, H. (2012) 'Polymeric conjugates for drug delivery', *Chemistry of Materials*, pp. 840–853.
- Lee, J. S. and Feijen, J. (2012) 'Polymersomes for drug delivery: Design, formation and characterization', *Journal of Controlled Release*. Elsevier B.V., 161(2), pp. 473–483.
- Lee, J. S., Zhou, W., Meng, F., Zhang, D., Otto, C. and Feijen, J. (2010) 'Thermosensitive hydrogel-containing polymersomes for controlled drug delivery', *Journal of Controlled Release*. Elsevier B.V., 146(3), pp. 400–408.

- Leon-Sicairos, N., Reyes-Cortes, R., Guadrón-Llanos, A. M., Madueña-Molina, J., Leon-Sicairos, C. and Canizalez-Román, A. (2015) 'Strategies of intracellular pathogens for obtaining iron from the environment', *BioMed Research International*, 2015.
- Li, Q., Fang, Y., Zhu, P., Ren, C. Y., Chen, H., Gu, J., Jia, Y. P., Wang, K., Tong, W. de, Zhang, W. jun, Pan, J., Lu, D. shui, Tang, B. and Mao, X. hu (2015) 'Burkholderia pseudomallei survival in lung epithelial cells benefits from miRNA-mediated suppression of ATG10', *Autophagy*, 11(8), pp. 1293–1307.
- Lim, J. Y., Yoon, J. and Hovde, C. J. (2010) 'A brief overview of Escherichia coli O157:H7 and its plasmid O157.', *Journal of microbiology and biotechnology*, 20(1), pp. 5–14.
- Lim, J., Yeap, S. P., Che, H. X. and Low, S. C. (2013) 'Characterization of magnetic nanoparticle by dynamic light scattering', *Nanoscale Research Letters*. *Nanoscale Research Letters*, 8(1), pp. 1–14.
- Limmathurotsakul, D. and Peacock, S. J. (2011) 'Meloidosis: A clinical overview', *British Medical Bulletin*, 99(1), pp. 125–139.
- Lomas, H., Canton, I., MacNeil, S., Du, J., Armes, S. P., Ryan, A. J., Lewis, A. L. and Battaglia, G. (2007) 'Biomimetic pH sensitive polymersomes for efficient DNA encapsulation and delivery', *Advanced Materials*, 19(23), pp. 4238–4243.
- Longmire, M., Choyke, P. L. and Kobayashi, H. (2008) 'Clearance properties of nano-sized particles and molecules as imaging agents: considerations and caveats.', *Nanomedicine (London, England)*, 3(5), pp. 703–17.
- López-López, M., Fernández-Delgado, A., Moyá, M. L., Blanco-Arévalo, D., Carrera, C., de la Haba, R. R., Ventosa, A., Bernal, E. and López-Cornejo, P. (2019) 'Optimized Preparation of Levofloxacin Loaded Polymeric Nanoparticles.', *Pharmaceutics*, 11(2).
- Mahboubi, H. and Stochaj, U. (2017) 'Cytoplasmic stress granules: Dynamic modulators of cell signaling and disease', *Biochimica et Biophysica Acta - Molecular Basis of Disease*. Elsevier B.V., 1863(4), pp. 884–895.
- Majerczyk, C. D., Brittnacher, M. J., Jacobs, M. A., Armour, C. D., Radey, M. C., Bunt, R., Hayden, H. S., Bydalek, R. and Greenberg, E. P. (2014) 'Cross-species comparison of the Burkholderia pseudomallei, Burkholderia thailandensis, and Burkholderia mallei quorum-sensing regulons', *Journal of Bacteriology*, 196(22), pp. 3862–3871.

List of References

- Malm, A. V. and Corbett, J. C. W. (2019) 'Improved Dynamic Light Scattering using an adaptive and statistically driven time resolved treatment of correlation data', *Scientific Reports*. Springer US, 9(1), pp. 1–11.
- Martin, M. M. and Lindqvist, L. (1975) 'The pH dependence of fluorescein fluorescence', *Journal of Luminescence*, 10(6), pp. 381–390.
- Masihzadeh, O., Ammar, D. A., Kahook, M. Y. and Lei, T. C. (2013) 'Coherent anti-stokes raman scattering (CARS) microscopy: A novel technique for imaging the retina', *Investigative Ophthalmology and Visual Science*, 54(5), pp. 3094–3101.
- Matoori, S. and Leroux, J. C. (2020) 'Twenty-five years of polymersomes: Lost in translation?', *Materials Horizons*. Royal Society of Chemistry, 7(5), pp. 1297–1309.
- Mattern, M. R. and Scudiero, D. A. (1981) 'Dependence of mammalian DNA synthesis on DNA supercoiling. III. Characterization of the inhibition of replicative and repair-type DNA synthesis by novobiocin and nalidixic acid.', *Biochimica et biophysica acta*. Netherlands, 653(2), pp. 248–258.
- Maurin, M. and Raoult, D. (2001) 'Use of aminoglycosides in treatment of infections due to intracellular bacteria', *Antimicrobial Agents and Chemotherapy*, 45(11), pp. 2977–2986.
- McKinnon, K. M. (2018) 'Flow cytometry: An overview', *Current Protocols in Immunology*, 2018, pp. 5.1.1-5.1.11.
- McOrist, S. (2000) 'Obligate intracellular bacteria and antibiotic resistance', *Trends in Microbiology*, 8(11), pp. 483–486.
- Meng, F., Cheng, R., Deng, C. and Zhong, Z. (2012) 'Intracellular drug release nanosystems In order to elicit therapeutic effects , many drugs including small molecule', *Materials Today*. Elsevier Ltd, 15(10), pp. 436–442.
- Merly, L. and Smith, S. L. (2017) 'Murine RAW 264.7 cell line as an immune target: are we missing something?', *Immunopharmacology and Immunotoxicology*, 39(2), pp. 55–58.
- Messenger, L., Gaitzsch, J., Chierico, L., and Battaglia, G. (2014) 'Novel aspects of encapsulation and delivery using polymersomes', *Current Opinion in Pharmacology*, 18(1), pp. 104-111.
- Mills, C. D., Kincaid, K., Alt, J. M., Heilman, M. J. and Hill, A. M. (2000) 'M-1/M-2 macrophages and the Th1/Th2 paradigm.', *Journal of immunology (Baltimore, Md. : 1950)*. United States, 164(12), pp. 6166–6173.

- Mitragotri, S., Burke, P. A. and Langer, R. (2014) 'Overcoming the challenges in administering biopharmaceuticals: formulation and delivery strategies.', *Nature reviews. Drug discovery*. Nature Publishing Group, 13(9), pp. 655–72.
- Montaner, L. J., Silva, R. P., Sun, J., Sutterwala, S., Hollinshead, M., Vaux, D. and Gordon, S. (1999) 'Luis J. Montaner, 2 * Rosangela P. da Silva, † Junwei Sun,* Shaheen Sutterwala,* Michael Hollinshead, † David Vaux, † and Siamon Gordon †', *Cell*.
- Monteiro, N., Martins, A., Reis, R. L. and Neves, N. M. (2014) 'Liposomes in tissue engineering and regenerative medicine', *Journal of The Royal Society Interface*, 11(101).
- Moore, R. A., Deshazer, D., Reckseidler, S., Weissman, A. and Woods, D. E. (1999) 'Efflux-mediated aminoglycoside and macrolide resistance in *Burkholderia pseudomallei*', *Antimicrobial Agents and Chemotherapy*, 43(3), pp. 465–470.
- Moretton, M. A., Cagel, M., Bernabeu, E., Gonzalez, L. and Chiappetta, D. A. (2015) 'Nanopolymersomes as potential carriers for rifampicin pulmonary delivery', *Colloids and Surfaces B: Biointerfaces*. Elsevier B.V., 136, pp. 1017–1025.
- Mu, H., Tang, J., Liu, Q., Sun, C., Wang, T. and Duan, J. (2016) 'Potent Antibacterial Nanoparticles against Biofilm and Intracellular Bacteria', *Scientific Reports*. Nature Publishing Group, 6(June 2015), pp. 1–9.
- Münter, R., Kristensen, K., Pedersbæk, D., Larsen, J. B., Simonsen, J. B. and Andresen, T. L. (2018) 'Dissociation of fluorescently labeled lipids from liposomes in biological environments challenges the interpretation of uptake studies', *Nanoscale*. Royal Society of Chemistry, 10(48), pp. 22720–22724.
- Nahata, M. C., Morosco, R. S. and Hipple, T. F. (1994) 'Stability of rifampin in two suspensions at room temperature', *Journal of Clinical Pharmacy and Therapeutics*, 19(4), pp. 263–265.
- Nahire, R., Haldar, M. K., Paul, S., Ambre, A. H., Meghnani, V., Layek, B., Katti, K. S., Gange, K. N., Singh, J., Sarkar, K. and Mallik, S. (2014) 'Multifunctional polymersomes for cytosolic delivery of gemcitabine and doxorubicin to cancer cells', *Biomaterials*. Elsevier Ltd, 35(24), pp. 6482–6497.
- Naz, S., Battu, S., Khan, R. A., Afroz, S., Giddaluru, J., Vishwakarma, S. K., Satti, V., Habeeb, M. A., Khan, A. A. and Khan, N. (2019) 'Activation of integrated stress response pathway regulates IL-1 β production through posttranscriptional and translational reprogramming in macrophages', *European Journal of Immunology*, 49(2), pp. 277–289.

List of References

- Nejad, R. B., Krecek, R. C., Khalaf, O. H., Hailat, N. and Arenas-Gamboa, A. M. (2020) 'Brucellosis in the middle east: Current situation and a pathway forward', *PLoS Neglected Tropical Diseases*, 14(5), pp. 1–17.
- Nguyen, H. A., Grellet, J., Paillard, D., Dubois, V., Quentin, C. and Saux, M. C. (2006) 'Factors influencing the intracellular activity of fluoroquinolones: A study using levofloxacin in a *Staphylococcus aureus* THP-1 monocyte model', *Journal of Antimicrobial Chemotherapy*, 57(5), pp. 883–890.
- Nichols, J. J., King-Smith, P. E., Hinel, E. A., Thangavelu, M. and Nichols, K. K. (2012) 'The use of fluorescent quenching in studying the contribution of evaporation to tear thinning', *Investigative Ophthalmology and Visual Science*, 53(9), pp. 5426–5432.
- Nicolete, R., Santos, D. F. D. and Faccioli, L. H. (2011) 'The uptake of PLGA micro or nanoparticles by macrophages provokes distinct in vitro inflammatory response', *International Immunopharmacology*. Elsevier B.V., 11(10), pp. 1557–1563.
- Oliver, A., Canton, R., Campo, P., Baquero, F., Blázquez, J., Cantón, R., Campo, P., Baquero, F. and Blázquez, J. (2000) 'High Frequency of Hypermutable *Pseudomonas aeruginosa* in Cystic Fibrosis Lung Infection', *Science*, 288(5469), pp. 1251–1253.
- Oltra, N. S., Praful, N., and Discher, D. E. (2014) 'From Stealthy Polymersomes and Filomicelles to "Self" Peptide-Nanoparticles for Cancer Therapy', *Annual Review of Chemical and Biomolecular Engineering*, 5, pp. 281–299.
- Olusanya, T. O. B., Ahmad, R. R. H., Ibegbu, D. M., Smith, J. R. and Elkordy, A. A. (2018) 'Liposomal drug delivery systems and anticancer drugs', *Molecules*, 23(4), pp. 1–17.
- Otto, M. (2009) 'Staphylococcus epidermidis—the 'accidental' pathogen', *Nature Reviews Microbiology*, 7(8), pp. 555–567.
- Ozanic, M., Marecic, V., Abu Kwaik, Y. and Santic, M. (2015) 'The Divergent Intracellular Lifestyle of *Francisella tularensis* in Evolutionarily Distinct Host Cells', *PLoS Pathogens*, 11(12), pp. 1–8.
- Pal, S., Tak, Y. K. and Song, J. M. (2007) 'Does the antibacterial activity of silver nanoparticles depend on the shape of the nanoparticle? A study of the gram-negative bacterium *Escherichia coli*', *Applied and Environmental Microbiology*, 73(6), pp. 1712–1720.

- Payne, D. J., Gwynn, M. N., Holmes, D. J. and Pompliano, D. L. (2007) 'Drugs for bad bugs: confronting the challenges of antibacterial discovery', *Nature Reviews Drug Discovery*, 6(1), pp. 29–40.
- Peterson, C. (2010) 'PH dependence and unsuitability of fluorescein dye as a tracer for pesticide mobility studies in acid soil', *Water, Air, and Soil Pollution*, 209(1–4), pp. 473–481.
- Phanse, Y., Ramer-Tait, A. E., Friend, S. L., Carrillo-Conde, B., Lueth, P., Oster, C. J., Phillips, G. J., Narasimhan, B., Wannemuehler, M. J. and Bellaire, B. H. (2012) 'Analyzing cellular internalization of nanoparticles and bacteria by multi-spectral imaging flow cytometry', *Journal of Visualized Experiments*, (64), pp. 1–6.
- Photos, P. J., Bacakova, L., Discher, B., Bates, F. S. and Discher, D. E. (2003) 'Polymer vesicles in vivo : correlations with PEG molecular weight', 90, pp. 323–334.
- Picard, C., Fioramonti, J., Francois, A., Robinson, T., Neant, F. and Matuchansky, C. (2005) 'Review article: Bifidobacteria as probiotic agents - Physiological effects and clinical benefits', *Alimentary Pharmacology and Therapeutics*, 22(6), pp. 495–512.
- Pieters, J. (2008) 'Mycobacterium tuberculosis and the Macrophage: Maintaining a Balance', *Cell Host and Microbe*, 3(6), pp. 399–407.
- Pinto-Alphandary, H., Andremont, A. and Couvreur, P. (2000) 'Targeted delivery of antibiotics using liposomes and nanoparticles: research and applications', *International Journal of Antimicrobial Agents*, 13(3), pp. 155–168.
- Pratten, M. K. and Lloyd, J. B. (1986) 'Pinocytosis and phagocytosis: the effect of size of a particulate substrate on its mode of capture by rat peritoneal macrophages cultured in vitro', *BBA - General Subjects*, 881(3), pp. 307–313.
- Qi, W., Ghoroghchian, P. P., Li, G., Hammer, D. A. and Therien, M. J. (2013) 'Aqueous self-assembly of poly(ethylene oxide)-block-poly(ϵ -caprolactone) (PEO-b-PCL) copolymers: disparate diblock copolymer compositions give rise to nano- and meso-scale bilayered vesicles', *Nanoscale*, 5(22), p. 10908–10915.
- Qie, Y., Yuan, H., Von Roemeling, C. A., Chen, Y., Liu, X., Shih, K. D., Knight, J. A., Tun, H. W., Wharen, R. E., Jiang, W. and Kim, B. Y. S. (2016) 'Surface modification of nanoparticles enables selective evasion of phagocytic clearance by distinct macrophage phenotypes', *Scientific Reports*, 6(January), pp. 1–11.

List of References

- Qiu, F., Wang, D., Zhu, Q., Zhu, L., Tong, G., Lu, Y., Yan, D. and Zhu, X. (2014) 'Real-time monitoring of anticancer drug release with highly fluorescent star-conjugated copolymer as a drug carrier', *Biomacromolecules*, 15(4), pp. 1355–1364.
- Qiu, Z., Ikehara, T. and Nishi, T. (2003) 'Miscibility and crystallization of poly(ethylene oxide) and poly (ϵ -caprolactone) blends', *Polymer*, 44(10), pp. 3101–3106.
- Radovic-Moreno, A. F., Lu, T. K., Puscasu, V. A., Yoon, C. J., Langer, R. and Farokhzad, O. C. (2012) 'Surface charge-switching polymeric nanoparticles for bacterial cell wall-targeted delivery of antibiotics', *ACS Nano*, 6(5), pp. 4279–4287.
- Ragland, S. A. and Criss, A. K. (2017) 'From bacterial killing to immune modulation: Recent insights into the functions of lysozyme', *PLoS Pathogens*, 13(9), pp. 1–22.
- Raval, J. P., Chejara, D. R., Ranch, K. and Joshi, P. (2018) *Development of injectable in situ gelling systems of doxycycline hyclate for controlled drug delivery system, Applications of Nanocomposite Materials in Drug Delivery*. Elsevier Inc.
- Ray, K., Marteyn, B., Sansonetti, P. J., and Tang, C. M. (2009) 'Life on the inside: the intracellular lifestyle of cytosolic bacteria', *Nature Reviews Microbiology*, 7(5), pp. 333-340.
- Reckseidler-zenteno, S. L., Devinney, R. and Woods, D. E. (2005) 'The Capsular Polysaccharide of', *Infection and Immunity*, 73(2), pp. 1106–1115.
- Redelsperger, I. M., Taldone, T., Riedel, E. R., Lepherd, M. L., Lipman, N. S. and Wolf, F. R. (2016) 'Stability of doxycycline in feed and water and minimal effective doses in tetracycline-inducible systems', *Journal of the American Association for Laboratory Animal Science*, 55(4), pp. 467–474.
- Reece, J. B., Urry, L. A., Cain, M. L., Wasserman, S. A., Minorsky, P. V., and Jackson, R. B. (2011) *Campbell Biology. 9th Edition*. Pearson International Edition, Pages 976-990.
- Reichel, D., Tripathi, M. and Perez, J. M. (2019) 'Biological effects of nanoparticles on macrophage polarization in the tumor microenvironment', *Nanotheranostics*, 3(1), pp. 66–88.
- Renwick, M. J., Simpkin, V. and Mossialos, E. (2016) 'Targeting innovation in antibiotic drug discovery and development', *Targeting innovation in antibiotic drug discovery and development: The need for a One Health – One Europe – One World Framework*.

- Ribeiro, L. N. D. M., Couto, V. M., Fraceto, L. F. and De Paula, E. (2018) 'Use of nanoparticle concentration as a tool to understand the structural properties of colloids', *Scientific Reports*, 8(1), pp. 1–8.
- Ribet, D. and Cossart, P. (2015) 'How bacterial pathogens colonize their hosts and invade deeper tissues', *Microbes and Infection*. Elsevier Masson SAS, 17(3), pp. 173–183.
- Rizzello, L., Robertson, J. D., Elks, P. M., Poma, A., Daneshpour, N., Prajsnar, T. K., Evangelopoulos, D., Canseco, J. O., Yona, S., Marriott, H. M., Dockrell, D. H., Foster, S., Geest, B. De, Koker, S. De, McHugh, T., Renshaw, S. A. and Battaglia, G. (2017) 'Targeting mononuclear phagocytes for eradicating intracellular parasites', *bioRxiv*, p. 119297.
- Robertson, J. D., Rizzello, L., Avila-Olias, M., Gaitzsch, J., Contini, C., Magoń, M. S., Renshaw, S. A. and Battaglia, G. (2016) 'Purification of Nanoparticles by Size and Shape', *Scientific Reports*, 6(1), p. 27494.
- Roduit, C., Scholtens, S., De Jongste, J. C., Wijga, A. H., Gerritsen, J., Postma, D. S., Brunekreef, B., Hoekstra, M. O., Aalberse, R. and Smit, H. A. (2009) 'Asthma at 8 years of age in children born by caesarean section', *Thorax*, 64(2), pp. 107–113.
- Rose, S. J., Neville, M. E., Gupta, R. and Bermudez, L. E. (2014) 'Delivery of aerosolized liposomal amikacin as a novel approach for the treatment of nontuberculous mycobacteria in an experimental model of pulmonary infection', *PLoS ONE*, 9(9), pp. 1–7.
- Ross, B. N., Micheva-Viteva, S., Hong-Geller, E. and Torres, A. G. (2019) 'Evaluating the role of *Burkholderia pseudomallei* K96243 toxins BPSS0390, BPSS0395, and BPSS1584 in persistent infection', *Cellular Microbiology*, 21(12).
- Ross, B. N., Myers, J. N., Muruato, L. A., Tapia, D. and Torres, A. G. (2018) 'Evaluating New Compounds to Treat *Burkholderia pseudomallei* Infections', *Frontiers in Cellular and Infection Microbiology*, 8(June), pp. 1–8.
- Saarinen, J., Gütter, F., Lindman, M., Agopov, M., Fraser-Miller, S. J., Scherließ, R., Jokitalo, E., Santos, H. A., Peltonen, L., Isomäki, A. and Strachan, C. J. (2019) 'Cell-Nanoparticle Interactions at (Sub)-Nanometer Resolution Analyzed by Electron Microscopy and Correlative Coherent Anti-Stokes Raman Scattering', *Biotechnology Journal*, 14(4), pp. 1–10.
- Sanson, C., Schatz, C., Meins, J. Le, Soum, A., Thévenot, J., Garanger, E. and Lecommandoux, S. (2010) 'A simple method to achieve high doxorubicin loading in biodegradable polymersomes', *Journal of Controlled Release*. Elsevier B.V., 147(3), pp. 428–435.

List of References

Sarovich, D. S., Price, E. P., von Schulze, A. T., Cook, J. M., Mayo, M., Watson, L. M., Richardson, L., Seymour, M. L., Tuanyok, A., Engelthaler, D. M., Pearson, T., Peacock, S. J., Currie, B. J., Keim, P. and Wagner, D. M. (2012) 'Characterization of ceftazidime resistance mechanisms in clinical isolates of burkholderia pseudomallei from Australia', *PLoS ONE*, 7(2).

Scarpa, E., Bailey, J. L., Janeczek, A. A., Stumpf, P. S., Johnston, A. H., Oreffo, R. O. C., Woo, Y. L., Cheong, Y. C., Evans, N. D. and Newman, T. A. (2016) 'Quantification of intracellular payload release from polymersome nanoparticles', *Scientific Reports*. Nature Publishing Group, 6(July), pp. 1–13.

Schalk, I. J. (2018) 'A Trojan-Horse Strategy Including a Bacterial Suicide Action for the Efficient Use of a Specific Gram-Positive Antibiotic on Gram-Negative Bacteria', *Journal of Medicinal Chemistry*. American Chemical Society, 61(9), pp. 3842–3844.

Seleem, M. N., Munusamy, P., Ranjan, A., Alqublan, H., Pickrell, G. and Sriranganathan, N. (2009) 'Silica-antibiotic hybrid nanoparticles for targeting intracellular pathogens', *Antimicrobial Agents and Chemotherapy*, 53(10), pp. 4270–4274.

Sender, R., Fuchs, S. and Milo, R. (2016) 'Revised Estimates for the Number of Human and Bacteria Cells in the Body', *PLoS Biology*, 14(8), pp. 1–14.

Seral, C., Carryn, S., Tulkens, P. M. and Van Bambeke, F. (2003) 'Influence of P-glycoprotein and MRP efflux pump inhibitors on the intracellular activity of azithromycin and ciprofloxacin in macrophages infected by *Listeria monocytogenes* or *Staphylococcus aureus*', *Journal of Antimicrobial Chemotherapy*, 51(5), pp. 1167–1173.

Sercombe, L., Veerati, T., Moheimani, F., Wu, S. Y. and Hua, S. (2015) 'Advances and Challenges of Liposome Assisted Drug Delivery', 6(December), pp. 1–13.

Shen, Y., Tang, H., Radosz, M., Van Kirk, E. and Murdoch, W. J. (2008) 'PH-responsive nanoparticles for cancer drug delivery', *Methods in Molecular Biology*, 437, pp. 183–216.

Shi, J., Votruba, A. R., Farokhzad, O. C. and Langer, R. (2010) 'Nanotechnology in drug delivery and tissue engineering: From discovery to applications', *Nano Letters*, 10(9), pp. 3223–3230.

Shirley, M. (2019) 'Amikacin Liposome Inhalation Suspension: A Review in Mycobacterium avium Complex Lung Disease', *Drugs*. Springer International Publishing, 79(5), pp. 555–562.

Singh, R. and Lillard, J. W. (2009) 'Nanoparticle-based targeted drug delivery', *Experimental and Molecular Pathology*. Elsevier Inc., 86(3), pp. 215–223.

- Sorrell, I., Shipley, R. J., Hearnden, V., Colley, H. E., Thornhill, M. H., Murdoch, C. and Webb, S. D. (2014) 'Combined mathematical modelling and experimentation to predict polymersome uptake by oral cancer cells', *Nanomedicine: Nanotechnology, Biology, and Medicine*. Elsevier Inc., 10(2), pp. 339–348.
- Spencer, R. C. (2003) 'Bacillus anthracis', *Journal of clinical pathology*, 56(3), pp. 182–187.
- Steele, S., Brunton, J. and Kawula, T. (2015) 'The role of autophagy in intracellular pathogen nutrient acquisition', *Frontiers in Cellular and Infection Microbiology*, 5(June), pp. 1–11.
- Stetefeld, J., McKenna, S. A. and Patel, T. R. (2016) 'Dynamic light scattering: a practical guide and applications in biomedical sciences', *Biophysical Reviews*. Biophysical Reviews, 8(4), pp. 409–427.
- Stevens, M. P., Stevens, J. M., Jeng, R. L., Taylor, A. L., Wood, M. W., Hawes, P., Monaghan, P., Welch, M. D. and Galyov, E. E. (2005) 'Identification of a bacterial factor required for actin-based motility of Burkholderia pseudomallei', *Molecular Microbiology*, 56(1), pp. 40–53.
- Stevens, M. P., Friebel, A., Taylor, L. A., Wood, M. W., Brown, P. J., Hardt, W. D. and Galyov, E. E. (2003) 'A Burkholderia pseudomallei type III secreted protein, BopE, facilitates bacterial invasion of epithelial cells and exhibits guanine nucleotide exchange factor activity', *Journal of Bacteriology*, 185(16), pp. 4992–4996.
- Stevens, M. P., Wood, M. W., Taylor, L. A., Monaghan, P., Hawes, P., Jones, P. W., Wallis, T. S. and Galyov, E. E. (2002) 'An Inv/Mxi-Spa-like type III protein secretion system in Burkholderia pseudomallei modulates intracellular behaviour of the pathogen', *Molecular Microbiology*, 46(3), pp. 649–659.
- Sur, S., Fries, A. C., Kinzler, K. W., Zhou, S. and Vogelstein, B. (2014) 'Remote loading of preencapsulated drugs into stealth liposomes', *Proceedings of the National Academy of Sciences of the United States of America*, 111(6), pp. 2283–2288.
- Taciak, B., Białasek, M., Braniewska, A., Sas, Z., Sawicka, P., Kiraga, Ł., Rygiel, T. and Król, M. (2018) 'Evaluation of phenotypic and functional stability of RAW 264.7 cell line through serial passages', *PLoS ONE*, 13(6), pp. 1–13.
- Takov, K., Yellon, D. M. and Davidson, S. M. (2017) 'Confounding factors in vesicle uptake studies using fluorescent lipophilic membrane dyes', *Journal of Extracellular Vesicles*. Taylor & Francis, 6(1), pp. 1–15.

List of References

- Tenover, F. C. (2006) 'Mechanisms of antimicrobial resistance in bacteria', *American Journal of Infection Control*, 34(5), pp. S3–S10.
- Thamlikitkul, V. and Trakulsomboon, S. (2010) 'In vitro activity of biapenem against *Burkholderia pseudomallei*', *International Journal of Infectious Diseases*, 14(Icid), p. e193.
- Thammana, M. (2016) 'A Review on High Performance Liquid Chromatography (HPLC)', *Research & Reviews: Journal of Pharmaceutical Analysis RRJPA*, 5(2), pp. 22–28.
- Thibault, F. M., Hernandez, E., Vidal, D. R., Girardet, M. and Cavallo, J. D. (2004) 'Antibiotic susceptibility of 65 isolates of *Burkholderia pseudomallei* and *Burkholderia mallei* to 35 antimicrobial agents', *Journal of Antimicrobial Chemotherapy*, 54(6), pp. 1134–1138.
- Thyberg, J., Hedin, U. and Stenseth, K. (1985) 'Endocytic pathways and time sequence of lysosomal transfer of macromolecules in cultured mouse peritoneal macrophages - Double-labeling experiments with horseradish peroxidase and ferritin', *Cell and Tissue Research*, 241(2), pp. 299–303.
- Tomaszewska, E., Soliwoda, K., Kadziola, K., Tkacz-Szczesna, B., Celichowski, G., Cichomski, M., Szmaja, W. and Grobelny, J. (2013) 'Detection limits of DLS and UV-Vis spectroscopy in characterization of polydisperse nanoparticles colloids', *Journal of Nanomaterials*, 2013.
- Toti, U. S., Guru, B. R., Hali, M., McPharlin, C. M., Wykes, S. M., Panyam, J. and Whittum-Hudson, J. A. (2011) 'Targeted delivery of antibiotics to intracellular chlamydial infections using PLGA nanoparticles', *Biomaterials*. Elsevier Ltd, 32(27), pp. 6606–6613.
- Traub, W. H. and Leonhard, B. (1995) 'Heat stability of the antimicrobial activity of sixty-two antibacterial agents', *Journal of Antimicrobial Chemotherapy*, 35(1), pp. 149–154.
- Udekwi, K. I., Parrish, N., Ankomah, P., Baquero, F. and Levin, B. R. (2009) 'Functional relationship between bacterial cell density and the efficacy of antibiotics', *Journal of Antimicrobial Chemotherapy*, 63(4), pp. 745–757.
- Ukawala, M., Rajyaguru, T., Chaudhari, K., Manjappa, A. S., Pimple, S., Babbar, A. K., Mathur, R., Mishra, A. K. and Murthy, R. S. R. (2012) 'Investigation on design of stable etoposide-loaded PEG-PCL micelles: Effect of molecular weight of PEG-PCL diblock copolymer on the in vitro and in vivo performance of micelles', *Drug Delivery*, 19(3), pp. 155–167.

- Van Bambeke, F., Michot, J. M. and Tulkens, P. M. (2003) 'Antibiotic efflux pumps in eukaryotic cells: Occurrence and impact on antibiotic cellular pharmacokinetics, pharmacodynamics and toxicodynamics', *Journal of Antimicrobial Chemotherapy*, 51(5), pp. 1067–1077.
- Vandal, O. H., Pierini, L. M., Schnappinger, D., Nathan, C. F. and Ehrt, S. (2008) 'A membrane protein preserves intrabacterial pH in intraphagosomal *Mycobacterium tuberculosis*', *Nature Medicine*, 14(8), pp. 849–854.
- Vauthier, C., Cabane, B. and Labarre, D. (2008) 'How to concentrate nanoparticles and avoid aggregation?', *European Journal of Pharmaceutics and Biopharmaceutics*, 69(2), pp. 466–475.
- Ventola, C. L. (2015) 'The antibiotic resistance crisis: part 1: causes and threats.', *P&T: A peer-reviewed journal for formulary management (2015)*, 40(4), pp. 277–83.
- Vitas, A. I., Diaz, R., and Gamazo, C. (1997) 'Protective Effect of Liposomal Gentamicin against Systemic Acute Murine Brucellosis.', *Chemotherapy*, 43(3), pp. 204–210.
- Voronin, D. V., Kozlova, A. A., Verkhovskii, R. A., Ermakov, A. V., Makarkin, M. A., Inozemtseva, O. A. and Bratashov, D. N. (2020) 'Detection of rare objects by flow cytometry: Imaging, cell sorting, and deep learning approaches', *International Journal of Molecular Sciences*, 21(7).
- Vranic, S., Boggetto, N., Contremoulins, V., Mornet, S., Reinhardt, N., Marano, F., Baeza-squiban, A. and Boland, S. (2013) 'Deciphering the mechanisms of cellular uptake of engineered nanoparticles by accurate evaluation of internalization using imaging flow cytometry', *Particle and Fibre Toxicology*, 10(2), pp. 1–16.
- Wang, H., Agarwal, P., Zhao, S., Yu, J., Lu, X. and He, X. (2015) 'A biomimetic hybrid nanoplatform for encapsulation and precisely controlled delivery of therasnostic agents', *Nature Communications*, 6.
- Wang, L., He, H., Yu, Y., Sun, L., Liu, S., Zhang, C. and He, L. (2014) 'Morphology-dependent bactericidal activities of Ag/CeO₂ catalysts against *Escherichia coli*', *Journal of Inorganic Biochemistry*. Elsevier Inc., 135, pp. 45–53.
- Wang, Q., Wang, G., Xie, S., Zhao, X. and Zhang, Y. (2019) 'Comparison of high-performance liquid chromatography and ultraviolet-visible spectrophotometry to determine the best method to assess Levofloxacin released from mesoporous silica microspheres/nano-hydroxyapatite composite scaffolds', *Experimental and Therapeutic Medicine*, pp. 2694–2702.

List of References

- Wang, T., Bai, J., Jiang, X. and Nienhaus, G. U. (2012) 'Cellular uptake of nanoparticles by membrane penetration: A study combining confocal microscopy with FTIR spectroelectrochemistry', *ACS Nano*, 6(2), pp. 1251–1259.
- Wayakanon, K., Thornhill, M. H., Douglas, C. W. I., Lewis, A. L., Warren, N. J., Pinnock, A., Armes, S. P., Battaglia, G., Murdoch, C. and Porphyromon-, T. (2013) 'Polymersome-mediated intracellular delivery of antibiotics to treat Porphyromonas gingivalis -infected oral epithelial cells', 27(11), pp. 4455–4465.
- Wiersinga, W. J., van der Poll, T., White, N. J., Day, N. P. and Peacock, S. J. (2006) 'Melioidosis: Insights into the pathogenicity of Burkholderia pseudomallei', *Nature Reviews Microbiology*, 4(4), pp. 272–282.
- Wiersinga, W. J., Virk, H. S., Torres, A. G., Currie, B. J., Shoron, J., Dance, D. A. B., Limmathurotsakul, D., Hospital, R. D., Diseases, T., Wellcome, L. H., Republic, D. and Health, G. (2018) 'HHS Public Access', *Nature Reviews Disease Primers*.
- Willcocks, S. J., Denman, C. C., Atkins, H. S. and Wren, B. W. (2016) 'Intracellular replication of the well-armed pathogen Burkholderia pseudomallei', *Current Opinion in Microbiology*. Elsevier Ltd, 29, pp. 94–103.
- Von Wintersdorff, C. J. H., Penders, J., Van Niekerk, J. M., Mills, N. D., Majumder, S., Van Alphen, L. B., Savelkoul, P. H. M. and Wolffs, P. F. G. (2016) 'Dissemination of antimicrobial resistance in microbial ecosystems through horizontal gene transfer', *Frontiers in Microbiology*, 7(FEB).
- Xie, S., Yang, F., Tao, Y., Chen, D., Qu, W., Huang, L., Liu, Z., Pan, Y. and Yuan, Z. (2017) 'Enhanced intracellular delivery and antibacterial efficacy of enrofloxacin-loaded docosanoic acid solid lipid nanoparticles against intracellular Salmonella', *Scientific Reports*. Nature Publishing Group, 7(January), pp. 1–9.
- Yang, H., Liu, C., Yang, D., Zhang, H. and Xi, Z. (2009) 'Comparative study of cytotoxicity, oxidative stress and genotoxicity induced by four typical nanomaterials: The role of particle size, shape and composition', *Journal of Applied Toxicology*, 29(1), pp. 69–78.
- Ye, L., Zhang, Y., Yang, B., Zhou, X., Li, J., Qin, Z., Dong, D., Cui, Y. and Yao, F. (2016) 'Zwitterionic-Modified Starch-Based Stealth Micelles for Prolonging Circulation Time and Reducing Macrophage Response', *ACS Applied Materials and Interfaces*, 8(7), pp. 4385–4398.

- Yeh, Y. C., Huang, T. H., Yang, S. C., Chen, C. C. and Fang, J. Y. (2020) 'Nano-Based Drug Delivery or Targeting to Eradicate Bacteria for Infection Mitigation: A Review of Recent Advances', *Frontiers in Chemistry*, 8(April), pp. 1–22.
- Zaman, S. Bin, Hussain, M. A., Nye, R., Mehta, V., Mamun, K. T. and Hossain, N. (2017) 'A Review on Antibiotic Resistance: Alarm Bells are Ringing', *Cureus*, 9(6).
- Zhang, J., Leifer, F., Rose, S., Chun, D. Y., Thaisz, J., Herr, T., Nashed, M., Joseph, J., Perkins, W. R. and DiPetrillo, K. (2018) 'Amikacin liposome inhalation suspension (ALIS) penetrates non-tuberculous mycobacterial biofilms and enhances amikacin uptake into macrophages', *Frontiers in Microbiology*, 9(MAY), pp. 1–12.
- Zhang, L., Shi, L., Shen, Y., Miao, Y., Wei, M., Qian, N., Liu, Y. and Min, W. (2019) 'Spectral tracing of deuterium for imaging glucose metabolism', *Nature Biomedical Engineering*. Springer US, 3(5), pp. 402–413.
- Zhang, S., Chen, D. C. and Chen, L. M. (2019) 'Facing a new challenge: The adverse effects of antibiotics on gut microbiota and host immunity', *Chinese Medical Journal*, 132(10), pp. 1135–1138.
- Zhang, X., Sun, P., Bi, R., Wang, J., Zhang, N. and Huang, G. (2009) 'Targeted delivery of levofloxacin-liposomes for the treatment of pulmonary inflammation.', *Journal of drug targeting*, 17(5), pp. 399–407.
- Zhao, H.-F., Boyd, J., Jolicoeur, N. and Shen, S.-H. (2003) 'A coumermycin/novobiocin-regulated gene expression system.', *Human gene therapy*. United States, 14(17), pp. 1619–1629.
- Zhao, X., Duong, T., Huang, C. C., Kain, S. R. and Li, X. (1999) 'Comparison on enhanced green fluorescent protein and its destabilized form as transcription reporters', *Methods in Enzymology*, 302(1992), pp. 32–38.
- Zhu, X., Fryd, M., Tran, B. D., Ilies, M. A. and Wayland, B. B. (2012) 'Modifying the hydrophilic-hydrophobic interface of PEG-b-PCL to increase micelle stability: Preparation of PEG-b-PBO-b-PCL triblock copolymers, micelle formation, and hydrolysis kinetics', *Macromolecules*, 45(2), pp. 660–665.
- Zuba-Surma, E. K., Kucia, M., Abdel-Latif, A., Lillard, J. W. and Ratajczak, M. Z. (2007) 'The ImageStream system: A key step to a new era in imaging', *Folia Histochemica et Cytobiologica*, 45(4), pp. 279–290.